DEFINING STRESS RESISTANCE AND PERSISTENCE PROPERTIES OF UROPATHOGENIC *E. COLI*

by

Jordan Paul Norton

A dissertation submitted to the faculty of
The University of Utah
in partial fulfillment of the requirements for the degree of

Doctor of Philosophy

in

Microbiology and Immunology

Department of Pathology

The University of Utah

December 2013

The University of Utah Graduate School

STATEMENT OF DISSERTATION APPROVAL

The dissertation of **Jordan Paul Norton**

has been approved by the following supervisory committee members:

Matthew A. Mulvey	, Chair	**08/01/13** Date Approved
Janis J. Weis	, Member	**08/01/13** Date Approved
Kael F. Fischer	, Member	**08/01/13** Date Approved
Sherwood R. Casjens	, Member	**08/01/13** Date Approved
Costa Georgopoulos	, Member	**08/01/13** Date Approved

and by **Peter E. Jensen** , Chair of the Department of **Pathology**

and by David B. Kieda, Dean of The Graduate School.

ABSTRACT

Uropathogenic *Escherichia coli* (UPEC) cause the overwhelming majority of community-acquired urinary tract infections (UTI) worldwide. A particularly problematic aspect of UPEC-associated UTI is the rate of recurrent infections—one in four UTIs will recur within six months of the initial infection. In the majority of cases, the strain responsible for the primary infection is identical to the strain causing the recurrent infection. Usually, the urinary tract is maintained as a sterile environment by an array of host defenses. Some of the genetic mechanisms by which UPEC cope with or subvert host defenses in order to colonize and persist within the urinary tract is the primary focus of this thesis. I start by exploring the effects of global metabolic and stress response transcriptional regulation on the virulence potential of UPEC within the murine urinary tract. Therein, I better define the metabolic and stress response limitations affecting UPEC colonization of this niche. I then address the advantages of chromosomally encoded toxin-antitoxin systems in allowing for niche-specific colonization of the urinary tract and explore how these small genetic elements can specifically affect the stress resistance and antibiotic persistence of UPEC. This work, specifically, identifies a novel target for chemotherapeutic agents that would theoretically home in on and hinder only uropathogenic subsets of *E. coli*, combating UTI while leaving commensal *E. coli*

unphazed. Lastly, I attempt to better understand the generation of UPEC stress resistance by studying the evolutionarily conserved genomic rearrangement of chromosomally encoded toxin-antitoxin *hicAB* within these pathogens. I found that constructing this evolutionarily conserved *hicAB* truncation within the ancestral *E. coli* MG1655 promotes serum resistance and survival of this characteristically nonpathogenic strain of *E. coli* within the blood of a murine host. Furthermore, ancestral strains carrying this truncated allele are, in general, more resistant to stress than their unevolved counterparts. In total, this body of work better defines the stress resistance and persistence capacities of UPEC.

TABLE OF CONTENTS

LIST OF FIGURES

LIST OF TABLES

LIST OF ABBREVIATIONS

ASN ..... acidified sodium nitrite
BMDM ..... bone marrow derived macrophage
cAMP ..... cyclic adenosine monophosphate
CFU ..... colony forming units
clm^R ..... chloramphenicol resistance
CNF1 ..... cytotoxic necrotizing factor 1
CRP ..... cyclic adenosine monophosphate receptor protein
CV ..... circulation valley
DNA ..... deoxyribonucleic acid
EPEC ..... enteropathogenic *Escherichia coli*
ExPEC ..... extraintestinal pathogenic *Escherichia coli*
GI ..... genomic island
H_2O_2 ..... hydrogen peroxide
HlyA ..... α-hemolysin
hpf ..... hours postfertilization
hpi ..... hours postinoculation
IPTG ..... isopropyl-β-Dthiogalactopyranoside
kan^R ..... kanamycin resistance
Kbp ..... kilobase pairs
LB ..... Luria-Bertani
LGT ..... lateral gene transfer
LPS ..... lipopolysaccharide
MES-LB ..... morpholineethanesulfonic acid-buffered Luria broth
MIC ..... minimal inhibitory concentration
MV ..... methyl viologen
neaT ..... nomadically evolved acyltransferase
NO ..... nitric oxide
PasTI ..... persistence and stress-resistance toxin and immunity
PBS ..... phosphate buffered saline
PC ..... pericardial cavity
PCR ..... polymerase chain reaction
RNA ..... ribonucleic acid
RNI ..... reactive nitrogen intermediates
RT-PCR ..... reverse transcription polymerase chain reaction
RTX ..... repeats in toxin
Sat ..... secreted autotransporter toxin
TA ..... toxin-antitoxin

TCA .....tricarboxylic acid
THP .....Tamm-Horsfall protein
TLR.....Toll-like receptor
UPEC ..... uropathogenic *Escherichia coli*
UTI.....urinary tract infection
WT..... wild type

ACKNOWLEDGEMENTS

I am most grateful to my mentor, Dr. Matthew Mulvey, for always being excited about basic research and for providing a nurturing, positive environment to work. Also, thank you for allowing me the freedom to pursue my own avenues of research, guiding me along that path, and above all, trusting in me to finish the job. I owe a debt of gratitude to the graduate students of the Mulvey Lab who helped me hone my skills as a scientist and invested many hours focused on my research, whether debating appropriate experiments or assisting in the analysis of results. Specifically, I must acknowledge Bijaya Dhakal and Travis Wiles for their mentoring efforts. You taught me science is—and always should be—a collaborative venture. Lastly, to Shellie, for your patience and love. Thank you for standing by my side, supporting me, and helping me to understand my potential.

CHAPTER 1

INTRODUCTION

Molecular mechanisms of urinary tract infections

Escherichia coli is a Gram-negative bacterium most commonly associated with the gastrointestinal tract of warm-blooded vertebrates. Nonpathogenic strains of *E. coli* maintain a commensal relationship with their host, providing necessary vitamins (i.e., vitamin K and B-complex vitamins) and promoting gastrointestinal homeostasis. The *E. coli* species, however, is extremely heterogeneic [1]. Aside from the nonpathogenic commensals, there are a variety of pathogenic strain groups that cause a wide range of diseases. Enterohemorrhagic *E. coli*—best known for the O157:H7 serotypes found on contaminated food—along with enteropathogenic *E. coli* infections typically cause serious diarrhea and are the most widely publicized *E. coli* subgroups to cause pathology within the gastrointestinal tract. Fortunately, the disease caused by these pathogens is generally self-limiting and isolated solely within the gastrointestinal tract. These *E. coli* pathogens can be juxtaposed with a separate subset of pathogenic *E. coli*—extraintestinal pathogenic *E. coli* (ExPEC)—that lead a seemingly innocuous existence within the gastrointestinal tract but cause disease when given access to alternative niches such as the bloodstream, nervous system, or urinary tract.

ExPEC are the leading cause of Gram-negative sepsis and are, most notably, the most common etiologic agent of urinary tract infections (UTI). A UTI—defined as a microbial infection of the urethra (urethritis), bladder (cystitis), or kidney (pyelonephritis)—is one of the most common bacterial infections worldwide. In the United States alone, UTIs account for 8 million infections each

year with an estimated annual cost exceeding $2.14 billion [2,3]. This disease occurs most commonly among otherwise healthy women, and it is estimated that one in three women will suffer from a UTI by the age of twenty-four with 50% of women experiencing a UTI during their lifetime [4,5]. The gender bias observed in UTI epidemiology can mostly be attributed to differences in genitourinary anatomy. Women possess a significantly shorter urethra than men, which greatly reduces the distance traversed by infectious microbes from urethral opening to bladder lumen. Furthermore, colonization of the vaginal introitus by UTI-competent bacteria—likely as a result of fecal contamination—can increase the likelihood of UTI by increasing the proximity and abundance of infectious microbes [6,7].

As alluded to earlier, ExPEC strains are the most common bacterial cause of UTI. To be more precise, a subset of ExPEC called uropathogenic *E. coli* (UPEC) is the causative agent of disease in more than 80% of uncomplicated community-acquired UTI [4,5,8,9]. A distinct hallmark of UPEC-associated UTI is a high rate of recurrent infection. Of any individual experiencing UTI, there is a 25% chance the infection will recur within six months of the initial infection, and in the majority of cases, the strain responsible for the recurrent infection is identical to the strain causing the incident infection [10-12]. Unfortunately, the molecular mechanisms of recurrent UTI have not been definitively characterized. Previous research has been focused more generally on the virulence factors involved in UPEC pathogenesis within the urinary tract and possible ways by which UPEC may persist within the urinary tract. In an effort to design effective therapeutics

for combating UTI and preventing recurrent UTI, we must understand how UPEC cope with the inherent stresses of host-associated niches and by what molecular mechanisms they can persist in these environments. Some of the previously identified factors that influence UPEC colonization and virulence within the urinary tract include iron acquisition systems, secreted toxins, and adhesins.

Iron acquisition systems

Pathogenic *E. coli* must survive and replicate in order to persist within the urinary tract. Fitness factors such as iron acquisition systems play a large role in allowing survival and replication of *E. coli* in this niche. Ferric iron (Fe^{+3}) is an important element for the proper functioning of many cellular and bacterial proteins, but it is a limited and carefully guarded resource *in vivo* [13]. Importantly, ferric iron is insoluble, necessitating constant association with an iron transport protein. This presents a dilemma to pathogenic bacteria. They must acquire iron in order to replicate and survive *in vivo,* but available iron is already bound to host proteins. UPEC circumvent this problem by producing iron scavenging proteins known as siderophores, and the most common siderophore produced by UPEC is a protein called enterobactin. Enterobactin has a much stronger affinity for iron ($K_d = 10^{-49}$) than the mammalian iron transport protein transferrin ($K_d = 10^{-20}$), allowing it to outcompete host proteins for iron binding [14]. Enterobactin is a common siderophore found in many commensal and pathogenic *E. coli*, and its widespread use is likely what provided the evolutionary pressure for host variation of iron acquisition. Instead of increasing the binding affinity for iron to

outcompete bacterial siderophores, the host protein lipocalin 2 binds directly to enterobactin and prevents its reuptake into bacterial cells. By importing enterobactin-bound lipocalin 2, the host regains its previously pilfered iron [15]. Some UPEC have developed a countermeasure to host lipocalin 2 sequestration of enterobactin. The bacterial gene *iroA* glucosylates enterobactin—forming the siderophore salmochelin—preventing lipocalin 2 binding yet still maintaining a high affinity for iron [16]. In addition to enterobactin and salmochelin, UPEC often encode additional iron acquisition systems [17]. This increases their efficiency at acquiring iron necessary for growth and survival within the host.

Secreted toxins

In some cases, virulence factors may not confer an observable fitness advantage to the infectious microbe but can, instead, impact disease severity. UPEC secreted toxins such as cytotoxic necrotizing factor 1 (CNF1), secreted autotransporter toxin (Sat), and α-hemolysin (HlyA) are examples of virulence factors that affect UTI severity, but their role in bacterial fitness or colonization of the urinary tract is less well defined. In fact, of the three secreted toxins listed, CNF1 is the only toxin that is linked with a possible fitness advantage within the urinary tract [18]. Other aforementioned toxins may offer distinct fitness advantages *in vivo*, but the current model systems used to investigate UTI in the laboratory may not have the resolution required to define these traits. Researchers have, however, been able to discern some of the molecular mechanisms of toxin activity within host cells. CNF1 interacts with a laminin precursor protein on the

surface of the urothelial cell, inducing its endocytosis. Upon release in the host cytoplasm, CNF1 changes glutamine residues in the catalytic domains of Rho family GTPases to glutamate, effectively switching the Rho GTPases to a constitutively active state [19]. This has many downstream effects on the host cell, including filopodia formation, membrane ruffling, and apoptosis [20-23].

Sat is a UPEC secreted toxin that promotes host tissue damage during infection. Cell culture-based experiments have shown that Sat triggers vacuolation in bladder and kidney cells, and histological analysis of *in vivo* infections show Sat-dependent damage primarily to glomeruli and proximal tubule epithelial cells within the kidney [24]. Sat causes extensive damage to host cells—especially during pyelonephritis—and can significantly affect patient morbidity during infection.

HlyA is a prototypic member of the RTX (**R**epeats in **T**o**X**in) protein family. RTX toxins are largely recognized for their ability to form pores within eukaryotic host cell membranes. Unlike other RTX toxins, HlyA exhibits an affinity for a range of target cells that includes leukocytes and epithelial cells [25-28]. The consequence of HlyA pore-formation is dichotomous. If the response made by host cells to repair porous lesions is outpaced by pore-formation (e.g., at high toxin concentrations), intoxication culminates in cytolysis [29]. On the other hand, at sublytic toxin concentrations—which is posited to be more physiology relevant during infection—HlyA elicits a range of physiological alterations that include modulation of immune signaling and cytoloskeletal rearrangements [30]. Although the *hlyA* gene is carried by approximately 50% of UPEC isolates and there has

yet to be a fitness advantage directly attributed to expression of this toxin, it is agreed that its polyergic properties drastically influence the qualitative nature of the host-pathogen interface.

Incidence of severe, highly inflammatory UTI in humans is correlated with HlyA-producing UPEC isolates [31,32]. The histological basis for this relationship was recently described in a murine UTI model system. Smith *et al.*, (2008) observed that HlyA deficient UPEC do not evoke the same level of hemorrhaging and urothelial exfoliation as a wild type, HlyA containing parent strain [33]. UPEC expressing HlyA within the urinary tract leads to increased leukocyte influx and edema, possibly due to widespread tissue damage [27]. The precise mechanism by which HlyA induces such injury could be explained by its cytolytic function; however, it is becoming appreciated that sublytic concentrations of this toxin may in fact be contributing equally to disease outcome. For example, it was recently found that at low concentrations, HlyA activates serine proteases including mesotrypsin within the murine urothelium and cultured human bladder epithelial cells [30]. This unchecked protease activity leads to selected degradation of proteins involved in immune signaling such as the RelA subunit of the transcription factor NFkB and regulatory components of the cytoskeleton such as paxillin. An attractive model for HlyA induced exfoliation, which requires further experimental support, involves the directed manipulation of host urothelial signaling and structural components by this toxin that initiate tissue-wide pathologies—in contrast to general, rampant cytolysis. The duality of HlyA intoxication may afford UPEC a tunable ability to alter the outcome of infection.

Taken together, manipulation of the host cell by secreted toxins may contribute to the persistent, recurrent nature of UPEC infections within the urinary tract.

Adhesins

Adherence is an important step in the colonization and pathogenesis of UPEC, a process that is mediated by a number of adhesive organelles called pili (also known as fimbriae). By adhering to cells within the urinary tract, bacteria can withstand the shear flow of urine and avoid being flushed out during micturation. Type 1 pili mediate adherence of UPEC within the bladder and have been shown to be indispensible for colonization and pathogenesis within the murine urinary tract [34-36], but there is conflicting evidence as to the necessity of this organelle for full virulence during human UTI [37,38]. Superficial bladder epithelial cells produce a set of at least four proteins known as uroplakins that assemble into hexagonal complexes that are further arrayed into plaques that cover most of the luminal surface of the bladder. From electron microscopic observations it seems that the adhesive tip of type 1 pili (FimH) directly interacts with the central depression formed by the hexagonal uroplakin complex to negotiate binding of UPEC with the bladder epithelium [39]. *In vitro* assays have determined UP1a—a component of the uroplakin plaques—as one of the many receptors for type 1 pili. In general, type 1 pili adhere to N-linked oligomannose glycoproteins, which include UP1a, CD48, type I and IV collagen, fibronectin, laminin, and $\alpha_3\beta_1$ integrins [40-45]. Exogenous, soluble D-mannose or any soluble glycoprotein with mannose rich residues can act as a receptor decoy to inhibit

adherence of type 1 piliated UPEC within the urinary tract. This is exemplified in mammals where Tamm-Horsfall protein—a glycoprotein produced to high concentrations within the urinary tract—can act as a receptor decoy for type 1 piliated uropathogens to combat adhesion of UPEC to uroepithelial cells [46,47].

There are other adheins that are important for UPEC pathogenesis. Epidemiological data from human studies show that 90% of UPEC causing pyelonephritis and 100% of UPEC causing bacteremia encode the P pili [48,49]. In this case, epidemiological data correlate with experimental evidence that bacteria encoding P pili have increased adherence to uroepithelial cells [50]. A human study characterizing the importance of P pili in adherence and immune system activation showed that P pili expressing bacteria adhered better to uroepithelial cells and upregulated the recruitment of inflammatory cells to the urinary tract [51]. Complementing this study, intravital microscopy of UPEC-induced pyelonephritis in rats showed that UPEC expressing P pili were better able to adhere to renal cells than their counterparts lacking P pili [52].

Murine models of UTI demonstrated that P pili are not necessary for fulminate pyelonephritis, yet similar studies, along with human epidemiological data, suggest that the P pilus is an important virulence factor for UPEC pathogenesis, specifically adherence [49,50]. The binding of UPEC to the host kidney urothelium is dependent upon the P fimbrial adhesion protein PapG, and a few classes of PapG adhesins have been identified, which seem to provide P pili expressing UPEC with a certain amount of tissue tropism. The PapGII allele is associated with human pyelonephritis and bacteremia, whereas the PapGIII

allele correlates with human cystitis [49,53-55]. All variants bind to Galα(1-4)Galβ moieties present on glycosphingolipids but differ in specificity based upon the total number of N-acetylgalactosamine moieties or sialic acid residues attached to the Galα(1-4)Galβ backbone [56].

Other pili expressed by UPEC include the F1C, S, and Dr/Afa adhesins, and each of these adhesins bind distinct epitopes within the urinary tract. Briefly, F1C pili bind lactosylceramide-containing receptors; S pili are specific for α-sialyl-2,3-β galactoside-containing receptors; and Dr/Afa pili adhere to CD55 (alternatively referred to as complement decay-accelerating factor), $\alpha_5\beta_1$ integrins, and type-IV collagen [27,57]. Notably, Dr/Afa pili are associated with pyelonephritis in pregnant women, which may be related to elevated expression of CD55 in the urinary tract of gestational women [58,59]. Dr/Afa adhesins are also necessary for the establishment of chronic pyelonephritis within rat and mouse models [60]. However, these data have yet to be correlated with human chronic pyelonephritis, and the importance of Dr/Afa adhesins in the pathogenesis of UPEC leading to acute uncomplicated pyelonephritis is not well characterized. Overall, adhesins play a major role in the colonization and pathogenesis of UPEC within the urinary tract.

UPEC invasion

Traditionally, virulent strains of *E. coli* have been considered extracellular pathogens. However, UPEC have been shown to invade and live transiently within host epithelial cells. UPEC are competent to invade many urothelial cells,

including the epithelial cells of the bladder as well as the proximal tubule epithelial cells and collecting duct cells of the kidney [61-63]. Cell culture assays have verified a bacterial adhesive organelle—the type 1 pilus— as both necessary and sufficient for UPEC invasion of urothelial cells [64]. UPEC adherence to the cell surface via type 1 pili induces a signaling cascade within urothelial cells that causes localized rearrangements of the actin cytoskeleton, ultimately resulting in the engulfment of the adherent bacteria by the host plasma membrane through a zipper-like process. Both focal adhesion kinase and phosphoinositide-3 kinase are involved in host actin cytoskeletal rearrangements and are absolutely required for UPEC invasion. Furthermore, it seems that lipid rafts provide important signaling clusters to promote the endocytosis of adherent UPEC. [61,65-68]. Type I piliated UPEC can also affect their internalization in a clathrin-dependent manner through binding $\alpha_3\beta_1$ integrins on the surface of urothelial cells. In total, type 1 pili serve as both an important mediator of adherence and promote the invasion of urothelial cells by UPEC.

The flagellum—a bacterial motility organelle—is necessary for ascending UTI and likely doubles as a UPEC invasin. Flagellar expression occurs concomitant with and is required for UPEC ascension of the urinary tract, and upon entering the kidney, flagellated UPEC can interact with and invade collecting duct cells in an actin-dependent manner [69,70]. Together, these data suggest that UPEC utilize flagella as a motility organelle in order to ascend the ureters to the kidney but may also use the flagella as an invasin to mediate entry into collecting duct cells.

Once internalized, invasive UPEC can replicate, forming a biofilm-like cluster known as an intracellular bacterial community. Most of the normally rod-shaped *E. coli* growing within an intracellular bacterial community (IBC) have been reported to take on a more coccoid morphology within hours after invasion, while a subset is filamentous, stretching as long as 50 μm. These long, filamentous UPEC can extrude through the epithelial cell and potentially mediate invasion of a neighboring bladder epithelial cell while protecting itself from neutrophil phagocytosis [71-73]. In some instances, the IBC ruptures, spilling its contents within the bladder lumen to potentiate further rounds of intracellular bacterial community formation. Conversely, invading UPEC may remain quiescent within LAMP-1 positive endosomes, enmeshed within an actin cage, and this subset of quiescent bacteria is thought to make up a reservoir population capable of seeding recurrent infections [27,74].

UPEC invasion and temporary quiescence within the bladder epithelium may contribute to the high rate of recurrent infections. Up to 90% of community-acquired, uncomplicated recurrent UTI is caused by the same strain of bacteria as the index infection [11,12]. Below is a hypothetical model for how invasion of urothelial cell provides a mechanism for recurrent UTI. Upon entry into the bladder lumen, UPEC can secrete toxins like CNF-1 and α-hemolysin to cause exfoliation of bladder epithelial cells, exposing undifferentiated bladder cells. These underlying cells retain cell surface receptors, such as $\alpha_3\beta_1$ integrins, that allow UPEC to bind and be subsequently internalized within endosomal compartments enmeshed with actin filaments. The internalized bacterium

remains in a quiescent, nonreplicative state until the immature bladder epithelial cell undergoes differentiation into a superficial umbrella cell weeks to months later. The process of differentiation involves active actin cytoskeletal rearrangements, releasing the imprisoned UPEC from its actin cage. The freed bacterium can now grow intracellularly, form an intracellular bacterial community, rupture, and release a hoard of UPEC into the bladder lumen. These events culminate in a recurrent infection by the same strain that was caused the initial infection.

Host response to UTI

The mammalian urinary tract is meant to be a sterile system, and there are many host-associated components that promote sterility and combat infection within the urinary tract. Antimicrobial peptide production is paramount in maintaining a sterile urinary tract, and two antimicrobial peptides classes, namely cathelicidins and defensins, play a pivotal role in this process. Cathelicidins can be expressed by myeloid cells—especially neutrophils—as well as by epithelial cells all over the body, including those of the gastrointestinal tract, skin, lungs, epididymis, and urinary tract. They are constitutively made at low levels by bladder epithelial cells and proximal tubule epithelial cells, with additional activation and release minutes after the detection of microbes within the urinary tract [75,76]. The human gene *Camp* encodes the cathelicidin propeptide that is processed into two α-helical, amphipathic peptides, LL-37 and cathelin. These antimicrobial peptides bind negatively charged groups on the outer leaflet of

bacterial membranes and insert into the membrane to form a pore, neutralizing the microbe. Incidentally, UPEC strains causing pyelonephritis are significantly more resistant to LL-37 than cystitis causing strains, and murine studies show that *Camp*$^{-/-}$ mice are significantly more prone to acute pyelonephritis [76]. Two major types of defensins, α and β, are synthesized in response to infection. Neutrophils produce α-defensin, and epithelial cells in the loop of Henle, distal tubules, and collecting duct cells manufacture β-defensin. Both subsets of defensins are thought to kill by forming pores in the bacterial membrane—similar to cathelicidin-mediated bacterial killing—though the mechanism of defensin-mediated bacterial killing is an active area of research. Both cathelicidins and defensins are made as a component of the innate defense to maintain a sterile urinary tract.

Another protein made in defense of UTI is the Tamm-Horsfall protein (THP). This glycoprotein is synthesized in abundance within the loop of Henle and distributed to the downstream urinary tract via the urine and is the most abundant protein in healthy mammalian urine. THP is heavily glycosylated and contains an evolutionarily conserved mannose-rich side chain. At physiologically relevant concentrations, THP acts as a soluble receptor for type 1 pili to prevent bacterial adherence to mannose-rich host cell receptors via type 1 pili [47]. Because adherence is such a critical step in the pathogenesis of UPEC within the urinary tract, THP is a potent innate factor of host defense to bacterial infection. This is exemplified in murine studies of UTI where *Thp*$^{-/-}$ mice have higher bacterial titers from infection with type-1-pili-positive UPEC [46].

In addition to secreting proteins that frustrate bacterial infection, host cells of the urinary tract can also respond to the presence of invasive bacteria by producing toxic chemicals like nitric oxide, peroxynitrite, and nitrosothiols—collectively referred to as reactive nitrogen intermediates (RNI). Hours after infection, the levels of nitric oxide in the urine can reach up to 50 times more than that of an uninfected control [77]. RNIs can be deleterious to bacterial growth, damaging their nucleic acids, proteins, and lipids. Some resistance mechanisms to RNIs within UPEC have been previously characterized, including the production of polyamines, but it is theorized that many genes contribute to UPEC resistance to RNIs [78].

Toll-like receptors (TLRs) are another important mediator of host innate immunity. In general, TLRs recognize conserved bacterial motifs and signal the associated cell to produce a proinflammatory response through cytokine and chemokine production. This response alerts, attracts, and activates host innate immune responders like neutrophils to promote the clearance of invasive microbes. In mouse models, the most relevant TLRs in the defense against UTI are TLR4 and TLR11 [45,79,80]. TLR4 recognizes the bacterial endotoxin lipopolysaccharide, which is an integral part of the outer membrane of Gram-negative bacteria. Recognition and response to UPEC in symptomatic UTI seems dependent upon functional TLR4 expression. Murine and human studies show that reduced expression of TLR4 promotes asymptomatic bacteriuria, and humans with specific promoter or coding region single nucleotide polymorphisms have an increased frequency of asymptomatic bacteriuria [81,82].

The ligands for TLR11 include the apicomplexan profiling protein of the parasite *Toxoplasma gondii* and the flagellin subunit of *Salmonella* Typhi [83,84]. Although the UPEC specific ligand has yet to be identified, once activated during UPEC infection of the urinary tract, TLR11 signals through a MyD88-dependent pathway to elicit a potent IL-12 response [80]. Murine studies indicate TLR11 potently reduces the severity and extent of renal colonization as *Tlr11*$^{-/-}$ mice have a significantly higher bacterial load in the kidneys [80]. However, the effects of TLR11 activation in human acute pyelonephritis are questionable because a premature stop codon in the human TLR11 gene likely precludes its expression in humans.

Although TLR11 may not have a direct impact on susceptibility to acute pyelonephritis in humans, there are other known genes (e.g., Irf3 and CXCR1) that increase patient susceptibility to acute pyelonephritis. Both human and murine studies show that transcription factor Irf3 is an important determinant of acute pyelonephritis susceptibility. P-piliated UPEC can signal specifically through TLR4 via glycosphingolipid-dependent ceramide release to activate transcription factor Irf3. Decreased promoter activity of Irf3 is coincident with increased susceptibility to acute pyelonephritis, and the specific polymorphisms seen in human populations leading to an increased susceptibility to acute pyelonephritis were experimentally validated in the murine model of UTI. In the absence of Irf3 signaling, neutrophils recruited to infected tissues within the urinary tract were incapable of effectively clearing the infiltrating bacteria,

demonstrating that cellular Irf3 expression must be regulated appropriately for the crucial downstream activation events necessary for limiting UTI [85].

Human studies have correlated reduced expression of the IL-8 receptor CXCR1 with an increased risk of acute pyelonephritis. IL-8 is a major mediator of neutrophils chemotaxis during the proinflammatory response to infection, and appropriate levels of CXCR1 on neutrophils are crucial for proper chemotaxis to the site of infection. Recruited neutrophils eliminate infiltrating microbes through phagocytosis and are necessary for microbial clearance within the urinary tract. Unsurprisingly, many studies have highlighted the importance of functional CXCR1 in neutrophil recruitment and action within the urinary tract [86-89]. In particular, it has been shown that acute pyelonephritis-prone patient populations exhibit intronic and coding region single nucleotide polymorphisms that reduce expression of CXCR1, correlating with decreased numbers of recruited neutrophils during infection and an overall increase in susceptibility to acute pyelonephritis [90]. CXCR1 and Irf3 expression are only two factors that influence UTI susceptibility in humans. An elegant elaboration of other human genes associated with asymptomatic bacteriuria, cystitis, and pyelonephritis is reviewed by Ragnarsdóttir *et al*., 2011 [45].

The host immune system plays a crucial role in preventing and fighting UTI caused by UPEC, but it can also inadvertently contribute to the pathology of the disease. The majority of kidney scarring that results from chronic pyelonephritis is mediated by the host immune system. Constant neutrophil recruitment to the infected site results in an aggregation of innate immune cells,

and recruited macrophages form foam cells within the renal tissue—likely as a result of frustrated efforts to remove the over-abundant neutrophils from the tissue. Macrophages can also contribute to tissue damage by spewing lysosomal contents into the extracellular milieu, damaging both host cells and pathogenic microbes alike.

Ironically, a few innate immune system components can actually facilitate bacterial adherence and entry into renal cells. For example, complement component C3 and TLR4 can catalyze adherence and invasion. Canonically, activated complement opsonizes bacteria to promote its clearance from the host, and TLR4 activation leads to inflammation and the influx of professional phagocytes. However, the association of complement component C3 with UPEC is sufficient to enhance UPEC adherence to renal epithelial cells, likely through binding of opsonized UPEC to host C3 receptor Crry. Consequently, there is an increase in the colonization of UPEC within the upper urinary tract [62]. Additionally, the downregulation of TLR4 in cell culture assays drastically reduced the frequency of bacterial invasion, suggesting TLR4 may facilitate UPEC invasion of renal collecting duct cells [63]. The utilization of host innate immune defenses to increase bacterial adherence or invasion illustrates the complexity of host-pathogen interactions that may take place during UTI.

This dissertation was aimed at acquiring a better understanding of the UPEC-encoded genes that promote resistance to the stresses associated with infecting the urinary tract and persisting within that hostile niche. In Chapter 2, we examine the effects of global metabolic and stress response transcriptional

regulation on the virulence potential of UPEC within the murine urinary tract. Therein, we are able to better define the metabolic and stress response limitations affecting UPEC colonization of the urinary tract. In Chapter 3, we address the advantages of chromosomally encoded toxin-antitoxin systems in allowing for niche-specific colonization of the urinary tract and how they can specifically affect the stress resistance and antibiotic persistence of UPEC. This work specifically identifies a novel target for chemotherapeutic agents that would theoretically hone in on and hinder only uropathogenic subsets of *E. coli*, combating UTI while leaving commensal *E. coli* unphazed. Lastly, we attempt to better understand the evolutionary generation of UPEC stress resistance by studying the conserved genomic reduction of chromosomally encoded toxin-antitoxin *hicAB* within these pathogens. We are able to show that the construction of the evolutionarily conserved *hicAB* truncation within the inferred ancestral *E. coli* strain MG1655 increases survival within envelope stressing conditions and imparts some measure of resistance to human serum complement. In total, this dissertation adds significant contributions to our fundamental understanding of UPEC stress resistance and persistence.

References

1 Touchon, M. *et al.* Organised genome dynamics in the *Escherichia coli* species results in highly diverse adaptive paths. *PLoS Genet* **5**, e1000344, (2009).

2 Foxman, B. Epidemiology of urinary tract infections: incidence, morbidity, and economic costs. *Dis Mon* **49**, 53-70, (2003).

3 Brown, P., Ki, M. & Foxman, B. Acute pyelonephritis among adults: cost of illness and considerations for the economic evaluation of therapy. *Pharmacoeconomics* **23**, 1123-1142, (2005).

4 Foxman, B. Recurring urinary tract infection: incidence and risk factors. *Am J Public Health* **80**, 331-333 (1990).

5 Foxman, B. Epidemiology of urinary tract infections: incidence, morbidity, and economic costs. *Am J Med* **113 Suppl 1A**, 5S-13S, (2002).

6 Rosen, D. A., Hooton, T. M., Stamm, W. E., Humphrey, P. A. & Hultgren, S. J. Detection of intracellular bacterial communities in human urinary tract infection. *PLoS Med* **4**, e329, (2007).

7 Weichhart, T., Haidinger, M., Horl, W. H. & Saemann, M. D. Current concepts of molecular defence mechanisms operative during urinary tract infection. *Eur J Clin Invest* **38 Suppl 2**, 29-38, (2008).

8 Zhang, L. & Foxman, B. Molecular epidemiology of *Escherichia coli* mediated urinary tract infections. *Front Biosci* **8**, e235-244 (2003).

9 Colgan, R., Williams, M. & Johnson, J. R. Diagnosis and treatment of acute pyelonephritis in women. *Am Fam Physician* **84**, 519-526, (2011).

10 Ikaheimo, R. *et al.* Recurrence of urinary tract infection in a primary care setting: analysis of a 1-year follow-up of 179 women. *Clin Infect Dis* **22**, 91-99 (1996).

11 Russo, T. A., Stapleton, A., Wenderoth, S., Hooton, T. M. & Stamm, W. E. Chromosomal restriction fragment length polymorphism analysis of *Escherichia coli* strains causing recurrent urinary tract infections in young women. *J Infect Dis* **172**, 440-445 (1995).

12 Foxman, B. *et al.* Virulence characteristics of *Escherichia coli* causing first urinary tract infection predict risk of second infection. *J Infect Dis* **172**, 1536-1541 (1995).

13 Andrews, S. C., Robinson, A. K. & Rodriguez-Quinones, F. Bacterial iron homeostasis. *FEMS Microbiol Rev* **27**, 215-237 (2003).

14 Fischbach, M. A., Lin, H., Liu, D. R. & Walsh, C. T. How pathogenic bacteria evade mammalian sabotage in the battle for iron. *Nat Chem Biol* **2**, 132-138 (2006).

15 Goetz, D. H. *et al.* The neutrophil lipocalin NGAL is a bacteriostatic agent that interferes with siderophore-mediated iron acquisition. *Mol Cell* **10**, 1033-1043 (2002).

16 Bister, B. *et al.* The structure of salmochelins: C-glucosylated enterobactins of Salmonella enterica. *Biometals* **17**, 471-481 (2004).

17 Hacker, J. & Kaper, J. B. Pathogenicity islands and the evolution of microbes. *Annu Rev Microbiol* **54**, 641-679, (2000).

18 Rippere-Lampe, K. E., O'Brien, A. D., Conran, R. & Lockman, H. A. Mutation of the gene encoding cytotoxic necrotizing factor type 1 (cnf(1)) attenuates the virulence of uropathogenic *Escherichia coli*. *Infect Immun* **69**, 3954-3964, (2001).

19 Aktories, K. Rho proteins: targets for bacterial toxins. *Trends Microbiol* **5**, 282-288, (1997).

20 Schmidt, G. *et al.* Gln 63 of Rho is deamidated by *Escherichia coli* cytotoxic necrotizing factor-1. *Nature* **387**, 725-729 (1997).

21 Flatau, G. *et al.* Toxin-induced activation of the G protein p21 Rho by deamidation of glutamine. *Nature* **387**, 729-733 (1997).

22 Lerm, M. *et al.* Deamidation of Cdc42 and Rac by *Escherichia coli* cytotoxic necrotizing factor 1: activation of c-Jun N-terminal kinase in HeLa cells. *Infect Immun* **67**, 496-503 (1999).

23 Mills, M., Meysick, K. C. & O'Brien, A. D. Cytotoxic necrotizing factor type 1 of uropathogenic *Escherichia coli* kills cultured human uroepithelial 5637 cells by an apoptotic mechanism. *Infect Immun* **68**, 5869-5880 (2000).

24 Guyer, D. M., Radulovic, S., Jones, F. E. & Mobley, H. L. Sat, the secreted autotransporter toxin of uropathogenic *Escherichia coli*, is a vacuolating cytotoxin for bladder and kidney epithelial cells. *Infect Immun* **70**, 4539-4546 (2002).

25 Gadeberg, O. V., Orskov, I. & Rhodes, J. M. Cytotoxic effect of an alpha-hemolytic *Escherichia coli* strain on human blood monocytes and granulocytes in vitro. *Infect Immun* **41**, 358-364 (1983).

26 Keane, W. F., Welch, R., Gekker, G. & Peterson, P. K. Mechanism of *Escherichia coli* alpha-hemolysin-induced injury to isolated renal tubular cells. *Am J Pathol* **126**, 350-357 (1987).

27 Wiles, T. J., Kulesus, R. R. & Mulvey, M. A. Origins and virulence mechanisms of uropathogenic *Escherichia coli*. *Exp Mol Pathol* **85**, 11-19, (2008).

28 Cavalieri, S. J., Bohach, G. A. & Snyder, I. S. *Escherichia coli* alpha-hemolysin: characteristics and probable role in pathogenicity. *Microbiol Rev* **48**, 326-343 (1984).

29 Wiles, T. J. & Mulvey, M. A. The RTX pore-forming toxin alpha-hemolysin of uropathogenic *Escherichia coli*: progress and perspectives. *Future Microbiol* **8**, 73-84, (2013).

30 Dhakal, B. K. & Mulvey, M. A. The UPEC pore-forming toxin alpha-hemolysin triggers proteolysis of host proteins to disrupt cell adhesion, inflammatory, and survival pathways. *Cell Host Microbe* **11**, 58-69, (2012).

31 Dudgeon, L. S. Acute infection of the urinary tract due to a special group of haemolytic bacilli. *J Hyg (Lond)* **22**, 348-354 (1924).

32 Dudgeon, L. S. & Pulvertaft, R. J. On slow lactose fermenting *B. coli* in urinary and intestinal infections. *J Hyg (Lond)* **26**, 285-304 (1927).

33 Smith, Y. C., Rasmussen, S. B., Grande, K. K., Conran, R. M. & O'Brien, A. D. Hemolysin of uropathogenic *Escherichia coli* evokes extensive shedding of the uroepithelium and hemorrhage in bladder tissue within the first 24 hours after intraurethral inoculation of mice. *Infect Immun* **76**, 2978-2990, (2008).

34 Snyder, J. A. *et al.* Transcriptome of uropathogenic *Escherichia coli* during urinary tract infection. *Infect Immun* **72**, 6373-6381 (2004).

35 Connell, I. *et al.* Type 1 fimbrial expression enhances *Escherichia coli* virulence for the urinary tract. *Proc Natl Acad Sci U S A* **93**, 9827-9832 (1996).

36 Hultgren, S. J., Porter, T. N., Schaeffer, A. J. & Duncan, J. L. Role of type 1 pili and effects of phase variation on lower urinary tract infections produced by *Escherichia coli*. *Infect Immun* **50**, 370-377 (1985).

37 Hagan, E. C., Lloyd, A. L., Rasko, D. A., Faerber, G. J. & Mobley, H. L. *Escherichia coli* global gene expression in urine from women with urinary tract infection. *PLoS Pathog* **6**, e1001187, (2010).

38 Bergsten, G., Wullt, B., Schembri, M. A., Leijonhufvud, I. & Svanborg, C. Do type 1 fimbriae promote inflammation in the human urinary tract? *Cell Microbiol* **9**, 1766-1781, (2007).

39 Mulvey, M. A., Schilling, J. D., Martinez, J. J. & Hultgren, S. J. Bad bugs and beleaguered bladders: interplay between uropathogenic *Escherichia coli* and innate host defenses. *Proc Natl Acad Sci U S A* **97**, 8829-8835, (2000).

40 Kukkonen, M. *et al.* Basement membrane carbohydrate as a target for bacterial adhesion: binding of type 1 fimbriae of *Salmonella enterica* and *Escherichia coli* to laminin. *Molecular Microbiology* **7**, 229-237 (1993).

41 Sokurenko, E. V., Courtney, H. S., Ohman, D. E., Klemm, P. & Hasty, D. L. FimH family of type 1 fimbrial adhesins: functional heterogeneity due to minor sequence variations among *fimH* genes. *J. Bacteriol.* **176**, 748-755 (1994).

42 Sokurenko, E. V. *et al.* Pathogenic adaptation of *Escherichia coli* by natural variation of the FimH adhesin. *Proc Natl Acad Sci U S A* **95**, 8922-8926 (1998).

43 Sokurenko, E. V., Courtney, H. S., Maslow, J., Siitonen, A. & Hasty, D. L. Quantitative differences in adhesiveness of type 1 fimbriated *Escherichia coli* due to structural differences in *fimH* genes. *J Bacteriol* **177**, 3680-3686 (1995).

44 Pouttu, R. *et al.* Amino acid residue Ala-62 in the FimH fimbrial adhesin is critical for the adhesiveness of meningitis-associated *Escherichia coli* to collagens. *Mol Microbiol* **31**, 1747-1757 (1999).

45 Ragnarsdottir, B., Lutay, N., Gronberg-Hernandez, J., Koves, B. & Svanborg, C. Genetics of innate immunity and UTI susceptibility. *Nat Rev Urol* **8**, 449-468, (2011).

46 Raffi, H. S., Bates, J. M., Jr., Laszik, Z. & Kumar, S. Tamm-horsfall protein protects against urinary tract infection by proteus mirabilis. *J Urol* **181**, 2332-2338, (2009).

47 Pak, J., Pu, Y., Zhang, Z. T., Hasty, D. L. & Wu, X. R. Tamm-Horsfall protein binds to type 1 fimbriated *Escherichia coli* and prevents *E. coli* from binding to uroplakin Ia and Ib receptors. *J Biol Chem* **276**, 9924-9930, (2001).

48 Stapleton, A. Novel mechanism of P-fimbriated *Escherichia coli* virulence in pyelonephritis. *J Am Soc Nephrol* **16**, 3458-3460, (2005).

49 Otto, G., Sandberg, T., Marklund, B. I., Ulleryd, P. & Svanborg, C. Virulence factors and pap genotype in *Escherichia coli* isolates from

women with acute pyelonephritis, with or without bacteremia. *Clin Infect Dis* **17**, 448-456 (1993).

50 Lane, M. C. & Mobley, H. L. Role of P-fimbrial-mediated adherence in pyelonephritis and persistence of uropathogenic *Escherichia coli* (UPEC) in the mammalian kidney. *Kidney Int* **72**, 19-25, (2007).

51 Bergsten, G. *et al.* PapG-dependent adherence breaks mucosal inertia and triggers the innate host response. *J Infect Dis* **189**, 1734-1742, (2004).

52 Melican, K. *et al.* Uropathogenic *Escherichia coli* P and Type 1 fimbriae act in synergy in a living host to facilitate renal colonization leading to nephron obstruction. *PLoS Pathog* **7**, e1001298, (2011).

53 Johnson, J. R., Russo, T. A., Brown, J. J. & Stapleton, A. papG alleles of *Escherichia coli* strains causing first-episode or recurrent acute cystitis in adult women. *J Infect Dis* **177**, 97-101 (1998).

54 Johanson, I. M., Plos, K., Marklund, B. I. & Svanborg, C. Pap, papG and prsG DNA sequences in *Escherichia coli* from the fecal flora and the urinary tract. *Microb Pathog* **15**, 121-129, (1993).

55 Johnson, J. R. papG alleles among *Escherichia coli* strains causing urosepsis: associations with other bacterial characteristics and host compromise. *Infect Immun* **66**, 4568-4571 (1998).

56 Stromberg, N., Nyholm, P. G., Pascher, I. & Normark, S. Saccharide orientation at the cell surface affects glycolipid receptor function. *Proc Natl Acad Sci U S A* **88**, 9340-9344 (1991).

57 Bower, J. M., Eto, D. S. & Mulvey, M. A. Covert operations of uropathogenic *Escherichia coli* within the urinary tract. *Traffic* **6**, 18-31 (2005).

58 Goluszko, P. *et al.* Dr operon-associated invasiveness of *Escherichia coli* from pregnant patients with pyelonephritis. *Infect Immun* **69**, 4678-4680, (2001).

59 Hart, A. *et al.* Ampicillin-resistant *Escherichia coli* in gestational pyelonephritis: increased occurrence and association with the colonization factor Dr adhesin. *J Infect Dis* **183**, 1526-1529, (2001).

60 Goluszko, P. *et al.* Development of experimental model of chronic pyelonephritis with *Escherichia coli* O75:K5:H-bearing Dr fimbriae:

mutation in the dra region prevented tubulointerstitial nephritis. *J Clin Invest* **99**, 1662-1672, (1997).

61 Dhakal, B. K., Kulesus, R. R. & Mulvey, M. A. Mechanisms and consequences of bladder cell invasion by uropathogenic *Escherichia coli*. *Eur J Clin Invest*, (2008).

62 Springall, T. *et al.* Epithelial secretion of C3 promotes colonization of the upper urinary tract by *Escherichia coli*. *Nat Med* **7**, 801-806, (2001).

63 Chassin, C. *et al.* TLR4 facilitates translocation of bacteria across renal collecting duct cells. *J Am Soc Nephrol* **19**, 2364-2374, (2008).

64 Martinez, J. J., Mulvey, M. A., Schilling, J. D., Pinkner, J. S. & Hultgren, S. J. Type 1 pilus-mediated bacterial invasion of bladder epithelial cells. *Embo J* **19**, 2803-2812 (2000).

65 Eto, D. S. & Mulvey, M. A. Flushing bacteria out of the bladder. *Nat Med* **13**, 531-532, (2007).

66 Martinez, J. J. & Hultgren, S. J. Requirement of Rho-family GTPases in the invasion of Type 1-piliated uropathogenic *Escherichia coli*. *Cell Microbiol* **4**, 19-28 (2002).

67 Shoelson, S. E. *et al.* Specific phosphopeptide binding regulates a conformational change in the PI 3-kinase SH2 domain associated with enzyme activation. *Embo J* **12**, 795-802 (1993).

68 Yin, H. L. & Janmey, P. A. Phosphoinositide regulation of the actin cytoskeleton. *Annu Rev Physiol* **65**, 761-789 (2003).

69 Lane, M. C., Alteri, C. J., Smith, S. N. & Mobley, H. L. Expression of flagella is coincident with uropathogenic *Escherichia coli* ascension to the upper urinary tract. *Proc Natl Acad Sci U S A* **104**, 16669-16674, (2007).

70 Pichon, C. *et al.* Uropathogenic *Escherichia coli* AL511 requires flagellum to enter renal collecting duct cells. *Cell Microbiol* **11**, 616-628, (2009).

71 Mulvey, M. A., Schilling, J. D. & Hultgren, S. J. Establishment of a persistent *Escherichia coli* reservoir during the acute phase of a bladder infection. *Infect Immun* **69**, 4572-4579 (2001).

72 Horvath, D. J., Jr. *et al.* Morphological plasticity promotes resistance to phagocyte killing of uropathogenic *Escherichia coli*. *Microbes Infect* **13**, 426-437, (2011).

73 Justice, S. S., Hunstad, D. A., Seed, P. C. & Hultgren, S. J. Filamentation by *Escherichia coli* subverts innate defenses during urinary tract infection. *Proc Natl Acad Sci U S A* **103**, 19884-19889, (2006).

74 Eto, D. S., Sundsbak, J. L. & Mulvey, M. A. Actin-gated intracellular growth and resurgence of uropathogenic *Escherichia coli*. *Cell Microbiol* **8**, 704-717 (2006).

75 Kai-Larsen, Y. *et al.* Uropathogenic *Escherichia coli* modulates immune responses and its curli fimbriae interact with the antimicrobial peptide LL-37. *PLoS Pathog* **6**, e1001010, (2010).

76 Chromek, M. *et al.* The antimicrobial peptide cathelicidin protects the urinary tract against invasive bacterial infection. *Nat Med* **12**, 636-641, (2006).

77 Poljakovic, M. *et al. Escherichia coli*-induced inducible nitric oxide synthase and cyclooxygenase expression in the mouse bladder and kidney. *Kidney Int* **59**, 893-904 (2001).

78 Bower, J. M. & Mulvey, M. A. Polyamine-mediated resistance of uropathogenic *Escherichia coli* to nitrosative stress. *J Bacteriol* **188**, 928-933, (2006).

79 Vandewalle, A. Toll-like receptors and renal bacterial infections. *Chang Gung Med J* **31**, 525-537, (2008).

80 Zhang, D. *et al.* A toll-like receptor that prevents infection by uropathogenic bacteria. *Science* **303**, 1522-1526, (2004).

81 Hawn, T. R. *et al.* Toll-like receptor polymorphisms and susceptibility to urinary tract infections in adult women. *PLoS ONE* **4**, e5990, (2009).

82 Hawn, T. R. *et al.* Genetic variation of the human urinary tract innate immune response and asymptomatic bacteriuria in women. *PLoS ONE* **4**, e8300, (2009).

83 Yarovinsky, F. *et al.* TLR11 activation of dendritic cells by a protozoan profilin-like protein. *Science* **308**, 1626-1629, (2005).

84 Mathur, R. *et al.* A mouse model of salmonella typhi infection. *Cell* **151**, 590-602, (2012).

85 Fischer, H. *et al.* Pathogen specific, IRF3-dependent signaling and innate resistance to human kidney infection. *PLoS Pathog* **6**, e1001109, (2010).

86 Godaly, G. *et al.* Role of fimbriae-mediated adherence for neutrophil migration across *Escherichia coli*-infected epithelial cell layers. *Mol Microbiol* **30**, 725-735 (1998).

87 Otto, G., Burdick, M., Strieter, R. & Godaly, G. Chemokine response to febrile urinary tract infection. *Kidney Int* **68**, 62-70, (2005).

88 Godaly, G. *et al.* Neutrophil recruitment, chemokine receptors, and resistance to mucosal infection. *J Leukoc Biol* **69**, 899-906 (2001).

89 Frendeus, B. *et al.* Interleukin 8 receptor deficiency confers susceptibility to acute experimental pyelonephritis and may have a human counterpart. *J Exp Med* **192**, 881-890 (2000).

90 Lundstedt, A. C. *et al.* A genetic basis of susceptibility to acute pyelonephritis. *PLoS ONE* **2**, e825, (2007).

CHAPTER 2

ADENYLATE CYCLASE AND THE CYCLIC AMP RECEPTOR PROTEIN MODULATE STRESS RESISTANCE AND VIRULENCE CAPACITY OF UROPATHOGENIC *ESCHERICHIA COLI*

81, 2013, 249-258, doi:10.1128/IAI.00796-12

IAI Journals.ASM.org

Adenylate Cyclase and the Cyclic AMP Receptor Protein Modulate Stress Resistance and Virulence Capacity of Uropathogenic *Escherichia coli*

Grant T. Donovan, J. Paul Norton, Jean M. Bower,* Matthew A. Mulvey

Division of Microbiology and Immunology, Pathology Department, University of Utah School of Medicine, Salt Lake City, Utah, USA

In many bacteria, the second messenger cyclic AMP (cAMP) interacts with the transcription factor cAMP receptor protein (CRP), forming active cAMP-CRP complexes that can control a multitude of cellular activities, including expanded carbon source utilization, stress response pathways, and virulence. Here, we assessed the role of cAMP-CRP as a regulator of stress resistance and virulence in uropathogenic *Escherichia coli* (UPEC), the principal cause of urinary tract infections worldwide. Deletion of genes encoding either CRP or CyaA, the enzyme responsible for cAMP synthesis, attenuates the ability of UPEC to colonize the bladder in a mouse infection model, dependent on intact innate host defenses. UPEC mutants lacking cAMP-CRP grow normally in the presence of glucose but are unable to utilize alternate carbon sources like amino acids, the primary nutrients available to UPEC within the urinary tract. Relative to the wild-type UPEC isolate, the *cyaA* and *crp* deletion mutants are sensitive to nitrosative stress and the superoxide generator methyl viologen but remarkably resistant to hydrogen peroxide (H_2O_2) and acid stress. In the mutant strains, H_2O_2 resistance correlates with elevated catalase activity attributable in part to enhanced translation of the alternate sigma factor RpoS. Acid resistance was promoted by both RpoS-independent and RpoS-dependent mechanisms, including expression of the RpoS-regulated DNA-binding ferritin-like protein Dps. We conclude that balanced input from many cAMP-CRP-responsive elements, including RpoS, is critical to the ability of UPEC to handle the nutrient limitations and severe environmental stresses present within the mammalian urinary tract.

Under homeostatic conditions, the mammalian urinary tract is maintained as a sterile environment through the production of antimicrobial peptides and other toxic compounds, the bulk flow of urine, innate immune cell surveillance mechanisms, and nutrient limitations (1–5). However, select microbial pathogens are capable of colonizing and infecting this normally inhospitable niche. Uropathogenic *Escherichia coli* (UPEC) is the major cause of urinary tract infections (UTI) worldwide, affecting millions and requiring billions of dollars for diagnosis and treatment annually (6). To overcome host defenses and effectively colonize the urinary tract, UPEC employs a variety of virulence factors and stress resistance mechanisms, including adhesive and motility organelles that mediate attachment to and invasion of host cells, toxins that disarm innate immune responses, and multiple iron-scavenging proteins (1, 7–9). The ability to sense and prioritize the use of limited carbon sources within the nutrient-poor environment of the urinary tract is also likely critical to the success of UPEC, but our understanding of the impact that bacterial metabolic pathways have on the establishment and progression of a UTI is incomplete.

Within the urinary tract, UPEC relies largely on the catabolism of small peptides and amino acids for survival and growth (4). UPEC strains that are defective in peptide and carbohydrate transport systems, the tricarboxylic acid (TCA) cycle, and gluconeogenesis are unable to effectively colonize the urinary tract (10, 11). Of note, many UPEC isolates are able to utilize the gluconeogenic amino acid D-serine, which is typically present in urine (12, 13). D-Serine not only provides substrates for the TCA cycle and gluconeogenesis but also serves as an environmental cue that can regulate UPEC virulence. Interplay between bacterial metabolism and virulence is also evident by analysis of the QseBC two-component regulatory system, which was recently shown to modulate carbon flux through key metabolic pathways as well as the expression of UPEC-associated virulence factors like type 1 pili and flagella (14, 15). It is likely that numerous other systems help coordinate the expression of virulence and stress resistance factors with the ability of UPEC to sense and respond to the various carbon sources encountered within the host.

Although *E. coli* strains are generalists with the capacity to metabolize myriad metabolites, they preferentially utilize glucose as a primary carbon source. Transitioning into glucose-limiting conditions triggers the activation of the adenylate cyclase CyaA, producing high levels of the second messenger molecule cyclic AMP (cAMP) (16). Binding of cAMP to the transcription factor cAMP receptor protein (CRP) forms the active cAMP-CRP complex, which directly regulates expression of genes necessary for utilization of alternative carbon sources. However, not all genes that are regulated by cAMP-CRP function in bacterial metabolism (17, 18). Disruption of cAMP signaling within the prominent pathogens *Vibrio cholerae*, *Mycobacterium tuberculosis*, *Salmonella enterica* serovar Typhimurium, and *Pseudomonas aeruginosa* atten-

Received 27 July 2012 **Returned for modification** 25 August 2012
Accepted 24 October 2012
Published ahead of print 31 October 2012
Editor: S. M. Payne

Address correspondence to Matthew A. Mulvey, mulvey@path.utah.edu.

* Present address: Jean M. Bower, Biotechnology Department, Salt Lake Community College, West Jordan, Utah, USA.

G.T.D. and J.P.N. contributed equally to this article.

doi:10.1128/IAI.00796-12

TABLE 1 Bacterial strains and plasmids

Strain or plasmid	Description	Source
Strains		
UTI89	UPEC strain (cystitis isolate, O18:K1:H7)	25
UTI89Δ*cyaA*	UTI89*cyaA*::Clm^r (pKD3)	This study
UTI89Δ*crp*	UTI89*crp*::Clm^r (pKD3)	This study
UTI89Δ*dps*	UTI89*dps*::Kan^r (TT23691)	This study
UTI89Δ*fimH*	UTI89*fimH*::Clm^r (pKD3)	83
UTI89Δ*otsBA*	UTI89*otsBA*::Kan^r (pKD4)	This study
UTI89Δ*rpoS*	UTI89*rpoS*::Kan^r (TT23691)	This study
UTI89Δ*cyaA*Δ*otsBA*	UTI89*cyaA*::Clm^r (pKD3) *otsBA*::Kan^r (pDK4)	This study
UTI89Δ*crp*Δ*rpoS*	UTI89*crp*::Clm^r (pKD3) *rpoS*::Kan^r (TT23691)	This study
UTI89Δ*crp*Δ*dps*	UTI89*crp*::Clm^r (pKD3) *dps*::Kan^r (TT23691)	This study
TT23691	Strain with Kan^r cassette flanked by universal primer sites	84
Plasmids		
pRR48	Amp^r cloning plasmid containing an IPTG-inducible P*tac* promoter upstream of the MCS	26
pKM208	Amp^r plasmid; encodes IPTG-inducible lambda red recombinase	27
pKD3	Template plasmid for gene disruption; contains FRT[a]-flanked Clm^r cassette	28
pKD4	Template plasmid for gene disruption; contains FRT-flanked Kan^r cassette	28
p*crp*	Amp^r plasmid; *crp* (from UTI89) cloned into PstI, KpnI sites of pRR48	This study
p*cyaA*	Amp^r plasmid; *cyaA* (from UTI89) cloned into PstI, KpnI sites of pRR48	This study
p*dps*	Amp^r plasmid; IPTG-inducible expression of *E. coli* Dps	55
p*rpoS*	Amp^r plasmid; *rpoS* (from UTI89) cloned into PstI, HindIII sites of pRR48	This study

[a] FRT, FLP recombination target.

uates virulence through the misregulation of key virulence genes (18–22). Within pathogenic subsets of *E. coli*, the cAMP-CRP complex has been shown to modulate the expression of type 1 pili, major facilitators of bacterial colonization of the bladder mucosa (23). However, the cumulative effects of cAMP-CRP on the virulence potential of UPEC within the urinary tract remain to be elucidated.

Here, we report that the deletion of genes encoding either CyaA or CRP within the UPEC reference strain UTI89 does not affect growth in the presence of glucose but mutants with these deletions are unable to utilize amino acids as the sole carbon source. Furthermore, these mutants are significantly attenuated in the ability to colonize the bladders of mice, dependent upon the presence of intact innate host defenses. In broth culture assays, the *cyaA* and *crp* mutants are both sensitive to reactive nitrogen species and superoxide radicals generated by methyl viologen but highly resistant to hydrogen peroxide (H_2O_2) and acid stress. Resistance of the mutants to H_2O_2 and acid stress is in part attributable to increased translation of the alternate sigma factor RpoS (σ^S) and RpoS-regulated gene products that include catalases and the DNA-binding, iron storage protein Dps. In total, these data indicate that balanced input from cAMP-CRP is critical to the ability of UPEC to catabolize amino acids and appropriately handle harsh environmental stresses, characteristics that are pertinent to bacterial fitness and survival within the urinary tract.

MATERIALS AND METHODS

Bacterial strains and plasmids. All bacterial strains and plasmids are listed in Table 1. The human cystitis isolate UTI89 has been described previously (24, 25). Expression constructs were made using standard molecular biology techniques with the plasmid pRR48 (26). Where indicated, gene expression from the P*tac* promoter in the pRR48 backbone was induced by addition of 0.5 or 1 mM isopropyl-β-D-thiogalactopyranoside (IPTG). Primers used to construct all plasmids are indicated in Table 2, along with primers used to verify each clone by sequencing. Antibiotics (50 μg/ml kanamycin, 20 μg/ml chloramphenicol, or 100 μg/ml ampicillin) were added to plates and growth media to select for mutants and to maintain plasmids when necessary. Targeted gene knockouts were generated in UTI89 using the lambda Red-mediated linear transformation system (27, 28). Briefly, an antibiotic resistance cassette was amplified from pKD3, pKD4, or the template strain TT23691 with 40-bp overhangs specific to sites at the 5′ and 3′ ends of each target gene. PCR products were introduced via electroporation into UTI89 carrying pKM208, which encodes an IPTG-inducible lambda Red recombinase. Knockouts were confirmed by PCR using primers listed in Table 2.

Mouse infections. Seven- to 9-week-old female CBA/J or C3H/HeJ mice (Jackson Laboratory) were used in accordance with IACUC-approved protocols as previously described (29). Mice were anesthetized using isoflurane inhalation and inoculated via transurethral catheterization with 50 μl of a bacterial suspension containing approximately 1×10^7 bacteria. For these noncompetitive infection assays, UTI89 and isogenic knockout mutants were grown statically for 24 h in Luria-Bertani (LB) broth, pelleted by spinning at 10,000 × *g* for 8 min, and resuspended in phosphate-buffered saline (PBS) prior to inoculation. Bladders were recovered at 6 h or 3 days postinoculation, weighed, and homogenized in 1 ml PBS containing 0.025% Triton X-100. Homogenates were serially diluted and plated on LB agar plates to determine the number of bacteria per gram of tissue. Mouse experiments were repeated at least twice, and the total combined data from at least 11 animals are presented.

Growth assays. Bacteria were grown from frozen stocks at 37°C with shaking overnight in 5 ml of LB broth, 100 mM morpholineethanesulfonic acid (MES)-buffered LB broth (MES-LB broth; pH 5.0), or modified M9 minimal medium (6 g/liter Na_2HPO_4, 3 g/liter KH_2PO_4, 1 g/liter NH_4Cl, 0.5 g/liter NaCl, 1 mM $MgSO_4$, 0.1 mM $CaCl_2$, 0.1% glucose, 0.0025% nicotinic acid, 16.5 μg/ml thiamine, and 0.2% casein amino acids). Bacteria were then diluted 1:100 into the appropriate corresponding medium with or without additives as indicated. Growth of quadruplicate 200-μl samples in shaking 100-well honeycomb plates was assessed at 37°C using a Bioscreen C instrument (Growth Curves USA). Stocks of methyl viologen (MV) (also known as paraquat), acidified sodium nitrite (ASN), trehalose, and H_2O_2 were prepared fresh prior to addition to LB or MES-LB broth cultures. Where indicated, IPTG was added to cultures to

TABLE 2 Primer sequences

Primer	Sequence
crp KO[a]	
Forward	GCGCATGGTGCTTGGCAAACCGCAAACAGACCCGACTCTCTGTGTAGGCTGGAGCTGCTTCG
Reverse	CGCGCTACCAGGTAACGCGCCACTCTGACGGGATTAACGACATATGAATATCCTCCTTAG
crp KO confirmation	
Forward	GTATGCAAAGGACGCCACAT
Reverse	TTCGCCAAGCATTAACCCAA
cyaA KO	
Forward	GCGGAATCACAGTCATGACGGGTAGCAAATCAGGCGATACTGTGTAGGCTGGAGCTGCTTCG
Reverse	TACTGCTGCAACAGCGGCGCGTCATGCTCCTGATTGGCAGCATATGAATATCCTCCTTAG
cyaA KO confirmation	
Forward	AACCAGGCGCGAAAAGTGGT
Reverse	CTGAAAGGCGACGAGTGGAT
otsBA KO	
Forward	ATGTCTGTAAAGCGCGTTCTGCGCAACACAATAAGAAATGTGTAGGCTGGAGCTGCTTCG
Reverse	CTACGCAAGCTTAGGAAAGGTAGCAACTTTATCGCGCTGCCATATGAATATCCTCCTTAG
otsBA KO confirmation	
Forward	AGCGAAACGCACTGTCTGAT
Reverse	TTGCCTACGGTGAGTTAAGC
dps KO	
Forward	TTATTCGATGTTAGACTCGATAAACCACAGGAATTTATCCAGGTCGCGAGCACCAAACACCCCCCAAAACC
Reverse	GTGATAGGAACAGCCAGAATAGCGGAACACATAGCTGGTGCTATACTTAGCACACAACCACACCACACCAC
dps KO confirmation	
Forward	GATAGCAGATGGATGCACTA
Reverse	TGACAGTACGCAAAGAGAGC
rpoS KO	
Forward	CCAGCCTCGCTTGAGACTGGCCTTTCTGACAGATGCTTACCACCAAACACCCCCCAAAACC
Reverse	TGCCGCAGCGATAAATCGGCGGAACCAGGCTTTTGCTTGACACACAACCACACCACACCAC
rpoS KO confirmation	
Forward	AATGATGATTGCCGAATGTGACGCTG
Reverse	GCATTGTGTCGTTATGGGCGTAGG
p*crp*	
Forward	CCCCC CTGCAG ATGGTGCTTGGCAAACCGCA
Reverse	CCCCC GGTACC TTAACGAGTGCCGTAAACGA
p*cyaA*	
Forward	CCCCC CTGCAG TTGTACCTCTATATTGAGAC
Reverse	CCCCC GGTACC TCACGAAAAATACTGCTGCA
p*rpoS*	
Forward	CATTC CTGCAG ATGTTCCGTCAAGGGATCA
Reverse	AGTGC AAGCTT TTATTCGCGGAACAGCGCT
pRR48 sequencing primer	
Forward	CTGCTGAAGAGTACTTTGG
Reverse	CCAAAGCTGAAGACATCCAG

[a] KO, knockout.

induce high-level expression of recombinant proteins from p*dps* or p*rpoS*. MacConkey agar and other reagents used in these assays were obtained from Sigma-Aldrich.

Western blots. UTI89, UTI89Δ*cyaA*, and UTI89Δ*crp* were diluted 1:50 from overnight cultures into fresh LB broth and grown with shaking at 37°C until an optical density at 600 nm (OD_{600}) of 0.4 was reached. One milliliter of each culture was pelleted, resuspended in 200 μl B-PER lysis reagent (Thermo Scientific) containing 1 mM phenylmethylsulfonyl fluoride and protease inhibitor cocktail (Roche), and incubated for 15 min at room temperature. Protein concentrations within the lysates were determined using the BCA reagent system (Pierce), and equivalent protein amounts were resolved by SDS-PAGE and transferred to an Immobilon

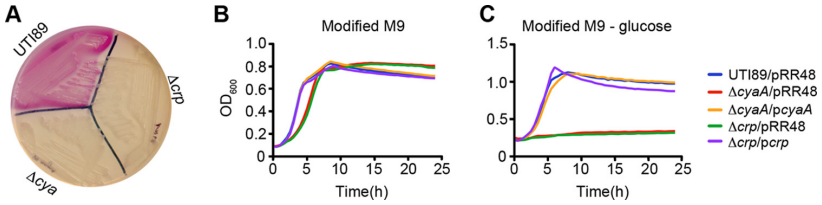

FIG 1 Impaired use of alternative carbon sources by UTI89Δ*cyaA* and UTI89Δ*crp*. (A) MacConkey agar plate streaked with UTI89, UTI89Δ*cyaA*, and UTI89Δ*crp*. Growth of UTI89, UTI89Δ*cyaA*, UTI89Δ*crp*, and complemented mutants in modified M9 medium (B) and modified M9 medium lacking glucose (C). Mutant strains were complemented by uninduced expression of *cyaA* or *crp* from a P*tac* promoter. Strains transformed with the empty vector pRR48 served as controls. Each curve reflects the means of results from a single experiment and is representative of at least three independent experiments performed in quadruplicate.

PVDF-FL membrane (Millipore). Blots were probed using anti-RpoS (Neoclone) and anti-*E. coli* antibodies (Biodesign International) and visualized using enhanced chemiluminescence as previously described (30).

pH stress resistance assays. Bacterial strains from overnight cultures were diluted 1:100 in fresh LB broth and grown with shaking at 37°C for 3 h. LB broth containing 100 μg/ml ampicillin and 0.5 mM IPTG was used for strains carrying plasmids pRR48, p*dps*, or p*rpoS*. Strains were subjected to acid stress (pH 3.5) by the addition of concentrated HCl for 30 min. Bacteria in 1 ml of culture were pelleted at 14,000 × *g* for 5 min and washed in PBS. Surviving bacteria were enumerated by plating serial dilutions on LB agar.

Catalase assays. Overnight bacterial cultures were diluted 1:100 in LB broth and grown with shaking at 37°C to an OD_{600} of 1.0. UTI89/p*rpoS* was grown in broth containing 1 mM IPTG. Bacteria in 1 ml of culture were pelleted, resuspended in 200 μl B-PER lysis reagent (Thermo Scientific), and incubated at room temperature for 15 min. Catalase activity present in the lysates was determined using a Fluoro Catalase kit (Cell Technology) and a Synergy HT multidetection microplate reader (BioTek Instruments, Inc.) according to instructions from the manufacturer.

Trehalose analysis. Chemicals and reagents were purchased from Sigma-Aldrich, except for MSTFA [*N*-methyl-*N*-(trimethylsilyl) trifluoroacetamide], which was purchased from Thermo Scientific, and methoxyamine hydrochloride, which was purchased from MP Biomedicals. Bacterial cultures were grown in modified M9 medium to an OD_{600} of 1.0, pelleted by centrifugation, and frozen. Pellets were suspended in 5 ml of boiling 75% ethanol (EtOH) (aqueous), vortexed, and then incubated at 90°C for 5 min. Cell debris was removed by centrifugation at 5,000 × *g* for 3 min. Supernatants were transferred to new tubes and dried *in vacuo*. Gas chromatography-mass spectrometry (GC-MS) analysis was performed using a Waters GCT Premier mass spectrometer fitted with an Agilent 6890 gas chromatograph and a Gerstel MPS2 autosampler. Dried samples were suspended in 40 μl of a pyridine solution containing 40 mg/ml O-methoxylamine hydrochloride and incubated for 1 h at 30°C. Twenty microliters of each sample was transferred to an autosampler vial and incubated with MSTFA for 30 min at 37°C with shaking. One microliter of sample was injected into the inlet at a 75:1 split ratio. The injector temperature was held at 250°C. The gas chromatograph was obtained using an initial temperature of 95°C for 1 min followed by a 40°C/min ramp up to 110°C, with a hold time of 2 min. This was followed by a second 5°C/min ramp up to 250°C and then a third ramp up to 350°C, with a final hold time of 3 min. A 30-m Restek Rxi-5 MS column with a 5-m-long guard column was employed for analysis. Data were collected using MassLynx 4.1 software. To determine trehalose concentrations specifically, an external calibration curve was developed by performing a 2-fold dilution series starting at 10 μg/μl trehalose in pyridine. This series was analyzed to determine the linear range of analysis, the upper and lower limits of detection and quantitation, and the fragment ion to be utilized for analysis. For quantification, the fragment ion of 331 *m/z* was monitored and the linear range for analysis was determined to be from 100 to 1,000 μg/μl.

Metal stress assay. UTI89/pRR48, UTI89Δ*dps*/pRR48, and UTI89Δ*dps*/p*dps* were grown with shaking overnight at 37°C in LB broth containing 100 μg/ml ampicillin. Nine hundred microliters of each overnight culture was added to a sterile microcentrifuge tube, followed by 100 μl of 0.5 M $CuSO_4$. Tubes were then incubated for 15 min at room temperature, and surviving bacteria were pelleted at 14,000 × *g* for 5 min, washed in PBS, and enumerated by plating serial dilutions on LB agar.

Statistics. Results from *in vivo* mouse assays were analyzed by Mann-Whitney two-tailed *t* tests. Results from the catalase and survival assays were analyzed using two-tailed unpaired *t* tests. Data analysis was performed using Prism 5.0c (GraphPad Software, Inc.). *P* values of less than 0.05 are considered significant.

RESULTS

cAMP-CRP is necessary for lactose and amino acid catabolism by UPEC. Carbon catabolite repression—the preferential use of a carbon source like glucose instead of other secondary carbon sources—is regulated by the generation of cAMP-CRP (16). In the classic example, decreased glucose levels result in enhanced production of cAMP-CRP, which in turn activates the expression of genes needed to catabolize alternate carbon sources like lactose. Using MacConkey agar plates, we established that wild-type UTI89 could consume lactose in the absence of glucose, creating lactic acid and causing the pH indicator neutral red present in the agar to produce a pink color (Fig. 1A). In contrast, the isogenic *cyaA* and *crp* deletion mutants UTI89Δ*cyaA* and UTI89Δ*crp* could not utilize lactose and instead had to ferment available peptone, producing basic ammonia and turning the pH indicator yellow. The ability of the Δ*cyaA* and Δ*crp* mutants to use lactose in these assays was restored by complementation with plasmids p*cyaA* and p*crp*, respectively (data not shown).

Within the urinary tract, UPEC cells are mostly dependent on the catabolism of small peptides and amino acids (10, 12, 13). In modified M9 media containing both glucose and amino acids, wild-type UTI89, UTI89Δ*cyaA*, and UTI89Δ*crp* grew with similar kinetics (Fig. 1B). However, in modified M9 media containing only amino acids as a carbon source, the Δ*cyaA* and Δ*crp* mutants failed to grow unless appropriately complemented with plasmid p*cyaA* or p*crp* (Fig. 1C). The inability of UTI89Δ*cyaA* and UTI89Δ*crp* to catabolize amino acids and other secondary carbon sources such as lactose may affect the fitness of these mutants within the urinary tract.

CRP and CyaA promote UPEC colonization of the bladder. To assess the contribution of cAMP-CRP to UPEC pathogenicity, wild-type UTI89, UTI89Δ*cyaA*, and UTI89Δ*crp* were individually inoculated via transurethral catheterization into adult female

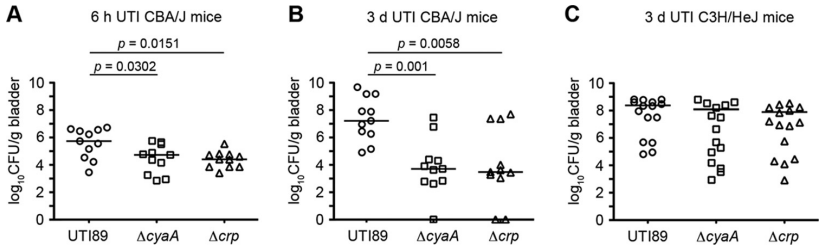

FIG 2 UPEC requires functional cAMP-CRP for virulence in the murine urinary tract. Adult female CBA/J mice (A, B) or C3H/HeJ mice (C) were infected via catheterization with 1×10^7 CFU of wild-type UTI89 or isogenic mutants lacking *cyaA* or *crp*. Graphs show bacterial titers present in the bladder at 6 h (A) and 3 days (B, C) postinoculation. Bars indicate median values for each group; $n \geq 11$ mice. *P* values were determined using Mann-Whitney U tests.

CBA/J mice. In comparison with wild-type UTI89, significantly reduced numbers of both the Δ*cyaA* and Δ*crp* mutants were recovered from bladders at 6 h and 3 days postinoculation (Fig. 2A and B). Interestingly, differences between wild-type UTI89 and the Δ*cyaA* and Δ*crp* mutants were blunted in C3H/HeJ mice (Fig. 2C). Due to defects in Toll-like receptor 4 (TLR4) and possibly other host factors, C3H/HeJ mice have attenuated inflammatory responses and are consequently hypersensitive to UTIs (31–36). In total, these data indicate that cAMP-CRP is critical to the fitness of UPEC within the urinary tract of immunocompetent animals, probably due to regulatory effects of cAMP-CRP on factors that control bacterial resistance to stresses generated by stimulation of host inflammatory cascades. These results prompted us to investigate further potential interplay between cAMP-CRP and stress response mechanisms in UPEC.

UTI89Δ*cyaA* and UTI89Δ*crp* are sensitive to nitrosative stress and methyl viologen but resistant to H_2O_2. Key stresses encountered by UPEC during the course of a UTI include damage elicited by reactive oxygen and nitrogen radicals that can be produced by both host and bacterial cells (37–42). To test the sensitivity of UTI89Δ*cyaA* and UTI89Δ*crp* to nitrosative and oxidative stresses, we utilized acidified sodium nitrite (ASN) and the superoxide generator methyl viologen (MV), respectively (Fig. 3). In these assays, the addition of sodium nitrite to MES-LB broth (pH 5.0) to create ASN results in the production of nitrous acid, NO, and other reactive nitrogen intermediates (43). In MES-LB broth, the Δ*cyaA* and Δ*crp* mutants grew like the wild-type strain, but in the presence of ASN growth of the mutants was markedly attenuated (Fig. 3A and B). Likewise, the addition of MV to LB broth severely impeded growth of both UTI89Δ*cyaA* and UTI89Δ*crp* (Fig. 3D and E). Of note, the mutant cultures did not attain the same optical density as the wild-type pathogen when grown with shaking in nutrient-rich LB broth, but in stationary cultures the mutant and wild-type strains reached equivalent bacterial titers, consistent with results using laboratory K-12 strains (reference 44 and data not shown). While MV impaired growth of UTI89Δ*cyaA* and UTI89Δ*crp*, the same mutants grew remarkably better than the wild-type strain in the presence of H_2O_2 (Fig. 3C). This effect was observed in both MES-LB and regular LB broth cultures, though results were more variable in the latter. Complementation of UTI89Δ*cyaA* and UTI89Δ*crp* with plasmids p*cyaA* and p*crp*, respectively, caused the mutant strains to behave like wild-type UTI89, rendering them sensitive to H_2O_2 and resistant to ASN and MV (Fig. 4 and data not shown).

H_2O_2 resistance correlates with elevated RpoS expression and catalase activity in the absence of cAMP-CRP. cAMP-CRP represses the transcription of the alternate sigma factor RpoS, a master regulator of the general stress response in *E. coli* (45). In

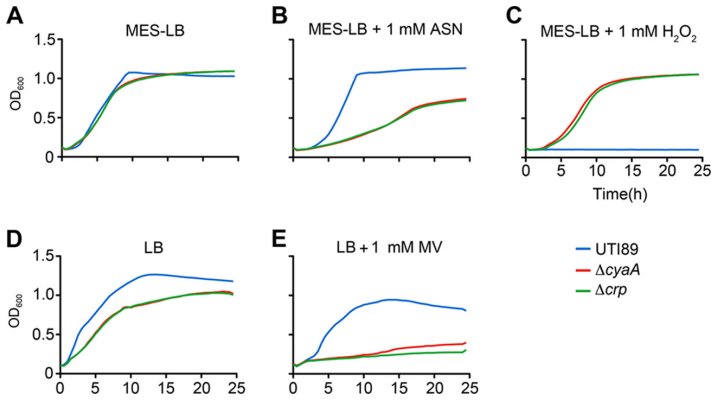

FIG 3 UTI89Δ*cyaA* and UTI89Δ*crp* are sensitive to nitrosative stress and methyl viologen but resistant to H_2O_2. Growth of UTI89, UTI89Δ*cyaA*, and UTI89Δ*crp* in MES-LB broth (A), MES-LB broth + 1 mM ASN (B), MES-LB broth + 1 mM H_2O_2 (C), LB broth (D), and LB broth containing 1 mM MV (E). Growth curves show the means of results from a single experiment and are representative of at least three independent experiments carried out in quadruplicate.

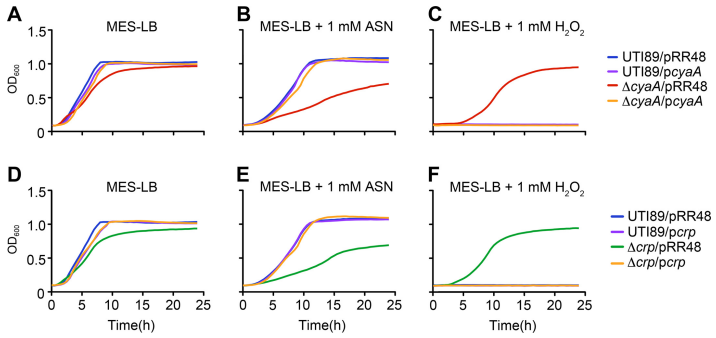

FIG 4 Complementation of UTI89Δ*cyaA* and UTI89Δ*crp* in the presence of nitrosative and oxidative stresses. Graphs show growth of UTI89 versus UTI89Δ*cyaA* (A to C) and UTI89Δ*crp* (D to F) in MES-LB (A, D), MES-LB ± 1 mM ASN (B, E), or MES-LB ± 1 mM H_2O_2 (C, F), all without added IPTG. Strains carried p*cyaA*, p*crp*, or the control plasmid pRR48, as indicated. Growth curves show the means of results from a single experiment and are representative of at least three independent experiments carried out in quadruplicate.

enterohemorrhagic *E. coli* and laboratory K-12 mutant strains that lack cAMP-CRP, RpoS levels are abnormally increased during the exponential growth phase (44, 46, 47). By Western blot analyses, we observed a similar phenomenon, with RpoS levels in UTI89Δ*cyaA* and UTI89Δ*crp* notably increased relative to those of the wild-type strain during exponential growth in broth culture (Fig. 5A). RpoS regulates the expression of various genes that enable bacteria to deal with multiple environmental stresses, including reactive oxygen species like H_2O_2 (45, 48). IPTG-induced expression of RpoS from the plasmid p*rpoS* rescued growth of wild-type UTI89 in the presence of H_2O_2, phenocopying the H_2O_2 resistance seen with the Δ*cyaA* and Δ*crp* mutants (Fig. 5B and C). The high-level resistance of UTI89/p*rpoS*, UTI89Δ*cyaA*, and UTI89Δ*crp* to H_2O_2 correlated with increased catalase activity in these strains (Fig. 5D). These results are in line with previous work showing that RpoS can stimulate expression of stress-responsive catalase genes necessary for the detoxification of H_2O_2 (48, 49).

While these data argue that enhanced expression of one or more RpoS-regulated catalases promotes high-level resistance of UTI89Δ*cyaA* and UTI89Δ*crp* toH_2O_2, it is feasible that other RpoS-regulated genes also contribute to the resistance phenotype of these mutants. To explore this possibility, we investigated two additional loci—*otsBA* and *dps*—known to be regulated by RpoS and previously linked with oxidative stress resistance. The first, *otsBA*, encodes two enzymes used to catalyze the biosynthesis of the disaccharide trehalose, a universal stress protectant produced in abundance by many prokaryotic and eukaryotic organisms (50). In yeast, trehalose protects against oxidative stress caused by H_2O_2 (51, 52). We found that UTI89 mutants lacking cAMP-CRP generate sizeable amounts of trehalose relative to an isogenic Δ*otsAB* mutant or a control mutant strain missing an unrelated gene (Δ*fimH*) (Fig. 5E). However, the addition of exogenous trehalose (up to 3,783 μg/ml) failed to rescue growth of wild-type UTI89 in broth cultures containing 1 mM H_2O_2, and the double deletion mutant UTI89Δ*cyaA*Δ*ostBA* was as resistant to H_2O_2 as UTI89Δ*cyaA* (data not shown). These results indicate that while trehalose levels are greatly elevated in bacteria lacking cAMP-CRP, this phenomenon is likely not essential to the heightened H_2O_2 resistance associated with UTI89Δ*cyaA* and UTI89Δ*crp*.

We next examined Dps, an abundant RpoS- and cAMP-CRP-regulated stationary-phase protein that can protect *E. coli* cells from multiple stresses, including oxidants (44, 46, 53–55). Dps can bind and shield DNA and also has ferritin-like properties, enabling it to sequester and oxidize ferrous ions while detoxifying H_2O_2 in the process (54). In consideration of this information, we hypothesized that forced expression of recombinant Dps would render wild-type UTI89 more resistant to H_2O_2, potentially mimicking UTI89Δ*cyaA* and UTI89Δ*crp*. However, IPTG-induced expression of Dps from plasmid p*dps* had no effect on the growth of either wild-type UTI89 or a Δ*dps* mutant in the presence or absence of H_2O_2 (Fig. 5F and G). Induced expression of Dps did promote survival of UTI89Δ*dps* in a metal ($CuSO_4$) stress resistance assay, confirming the functionality of the p*dps* plasmid (Fig. 5H). In total, these data indicate that increased Dps expression is surprisingly ineffective at promoting H_2O_2 resistance in UTI89.

Acid stress resistance of UTI89Δ*cyaA* and UTI89Δ*crp* is linked with increased RpoS and Dps expression. Within the urinary tract, UPEC will likely come across pH extremes, both within the urine and within host epithelial cells and infiltrating phagocytes (56, 57). In laboratory *E. coli* K-12 strains, cAMP-CRP, RpoS, and Dps can mediate acid stress resistance (58–60). Potential involvement of cAMP-CRP as a regulator of acid stress resistance in UTI89 was assessed using survival assays. Following a 30-min exposure of exponential-growth-phase cultures to acidic (pH 3.5) conditions, we found that the Δ*cyaA* and Δ*crp* mutants had a significant survival advantage over wild-type UTI89 (Fig. 6). In these assays, IPTG-induced expression of recombinant RpoS or Dps was sufficient to enhance survival of the wild-type strain to levels observed with UTI89Δ*cyaA* and UTI89Δ*crp*. To address whether or not RpoS or Dps is necessary for acid resistance, we constructed the mutant strains UTI89Δ*rpoS*, UTI89Δ*dps*, UTI89Δ*dps*Δ*crp*, and UTI89Δ*rpoS*Δ*crp*. In agreement with results observed with other *E. coli* strains (61–63), we found that UTI89Δ*rpoS* is highly sensitive to acid stress (Fig. 6). This sensitivity was reduced nearly 10,000-fold when *crp* was deleted along with *rpoS*. However, the Δ*rpoS* Δ*crp* mutant was still more sensitive than wild-type UTI89 and much more sensitive than UTI89 lacking only *crp*. In contrast, deletion of *dps* had only modest effects on the acid resistance of either UTI89 or UTI89Δ*crp*. Together, these data indicate that the acid stress resistance of UTI89 mutants lacking cAMP-CRP is likely attributable in part to in-

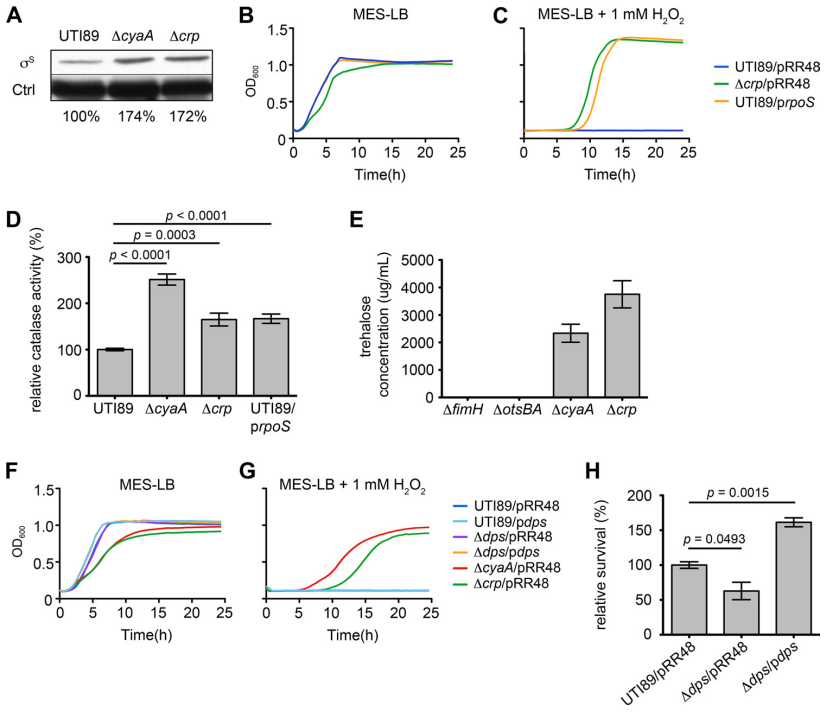

FIG 5 H_2O_2 resistance correlates with increased RpoS expression and catalase activity in UTI89Δ*cyaA* and UTI89Δ*crp*. (A) Western blot of RpoS (σ^S) in UTI89, UTI89Δ*cyaA*, and UTI89Δ*crp* after growth to mid-exponential phase in LB broth. Relative levels of RpoS normalized to loading control (Ctrl) are indicated. (B, C) Curves show growth of UTI89 and UTI89Δ*crp* carrying empty vector pRR48 or p*rpoS*, as indicated, in MES-LB ± 1 mM H_2O_2. (D) Graph of catalase activity in UTI89, UTI89Δ*cyaA*, UTI89Δ*crp*, and UTI89/p*rpoS* following growth to stationary phase in LB broth + 1 mM IPTG. Data are expressed relative to wild-type UTI89 as the means ± standard errors of three independent experiments carried out in triplicate. (E) Levels of trehalose present in UTI89Δ*fimH*, UTI89Δ*otsBA*, UTI89Δ*cyaA*, and UTI89Δ*crp* following growth to stationary phase (OD_{600} = 1.0). The Δ*fimH* mutant carries the same chloramphenicol resistance cassette as the Δ*cyaA* and Δ*crp* mutants and served as the control. (F, G) Graphs show growth of UTI89 and its mutant derivatives (Δ*cyaA*, Δ*crp*, and Δ*dps* mutants) carrying pRR48 or p*dps*, as indicated, in MES-LB ± 1 mM H_2O_2. Each growth curve (B, C, F, and G) shows the means of results from a single experiment and is representative of at least three independent experiments carried out in quadruplicate. Dps and RpoS expression in these assays was induced by addition of 0.5 mM IPTG. (H) Survival of UTI89Δ*dps* complemented with empty vector pRR48 or p*dps* following 15 min of exposure to 0.05 M $CuSO_4$. Results were obtained without addition of IPTG and are presented relative to those of wild-type UTI89/pRR48. The indicated *P* values were determined using two-tailed unpaired *t* tests.

creased cellular levels of RpoS and RpoS-regulated factors like Dps, in addition to other cAMP-CRP-repressible gene products.

DISCUSSION

The misregulation of carbon flux through metabolic pathways can restrict niche availability and alter the virulence potential of *E. coli* and other bacterial species (4, 18, 64–66). cAMP-CRP—a central regulator of carbon metabolism—has been implicated as an important facilitator of host colonization and virulence in many bacterial pathogens, including the uropathogen *Proteus mirabilis* (18, 67). This is not entirely unexpected given the known capacity of cAMP-CRP to modulate far-ranging activities in addition to metabolism (16). Among these is the ability to influence key stress response pathways such as those controlled by OxyR and RpoS (44, 45, 68). Results presented here demonstrate that cAMP-CRP is also critical to the ability of UPEC to effectively colonize the urinary tract.

Earlier work indicated that *E. coli* strains that are deficient in the production of cAMP-CRP express more type 1 pili (23). These filamentous adhesive organelles promote bacterial colonization of the bladder, suggesting that the defects observed with the Δ*cyaA* and Δ*crp* mutants in our *in vivo* assays may be attributable to misregulation of type 1 pilus expression. However, this possibility is countered by recent work showing that elevated levels of type 1 pilus expression actually enhance the ability of UPEC to colonize and persist within the bladder (69). Consequently, we conclude that the inability of the Δ*cyaA* and Δ*crp* mutants to effectively colonize the bladder is mostly due to the effects of diminished cAMP-CRP levels on factors other than type 1 pili.

In our *in vitro* assays, deletion of either *cyaA* or *crp* increased the ability of UPEC to withstand levels of H_2O_2 that prevent growth of the wild-type strain. The Δ*cyaA* and Δ*crp* mutants were also substantially more resistant to acid stress. UPEC likely comes across similar stresses during the course of a UTI, but any increase in stress resistance afforded by the deletion of *cyaA* or *crp* is apparently countered and surpassed *in vivo* by detrimental effects on other systems. For example, the Δ*cyaA* and Δ*crp* mutants are highly sensitive to nitrosative stress and the superoxide generator

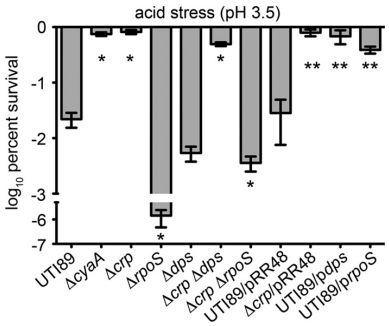

FIG 6 Expression of RpoS or Dps enables wild-type UTI89 to survive low-pH stress at levels similar to those of the Δ*cyaA* and Δ*crp* mutants. After reaching mid-logarithmic growth phase in LB broth, UTI89 and the UTI89Δ*cyaA*, UTI89Δ*crp*, UTI89Δ*dps*, UTI89Δ*rpoS*, UTI89Δ*crp*Δ*dps*, and UTI89Δ*crp*Δ*rpoS* mutants (± pRR48, p*dps*, and p*rpoS*, as indicated) were exposed to acid (pH 3.5) stress for 30 min. Following washes in PBS, numbers of surviving bacteria were determined by dilution plating. Plasmid-containing strains were grown in the presence of 0.5 mM IPTG prior to challenge with pH stress. Data are expressed as the means ± standard deviations of three independent experiments. *P* values of <0.05 are indicated by one asterisk (*) for comparison with UTI89 and by two asterisks (**) for comparison with UTI89/pRR48, as determined by two-tailed unpaired *t* tests.

MV. Both reactive nitrogen and reactive oxygen species like superoxide are abundantly produced in response to a UTI and could compromise the fitness of mutants lacking cAMP-CRP (5, 38, 39, 41, 70). An inability to utilize alternate carbon sources like amino acids may also limit successful colonization of the urinary tract by the Δ*cyaA* and Δ*crp* mutants, as peptides and amino acids are a primary energy source utilized by UPEC during a UTI (10, 12, 13). Furthermore, the massive upregulation of trehalose production by UTI89Δ*cyaA* and UTI89Δ*crp*, while potentially offering a degree of protection under some stressful conditions, may exact a high fitness cost within the nutrient-poor confines of the urinary tract.

Results obtained using C3H/HeJ mice suggest that innate host defenses, and not nutrient availability *per se*, are the primary factors that restrict UTI89Δ*cyaA* and UTI89Δ*crp* from effectively colonizing the urinary tract. C3H/HeJ mice are hyporesponsive to lipopolysaccharide and are therefore unable to mount full-on TLR4-dependent inflammatory responses (32–36, 71, 72). Specific defects associated with C3H/HeJ mice include poor expression of chemokines and greatly reduced infiltration of the bladder mucosa by neutrophils in response to UTI (35, 73, 74). In our assays, wild-type UTI89 and the Δ*cyaA* and Δ*crp* mutants colonized C3H/HeJ mice much better than immunocompetent CBA/J animals, although the bladder-associated titers of the mutant strains were more variable within C3H/HeJ mice (Fig. 2). Significantly, the clear differences in bladder titers observed between wild-type UTI89 and the Δ*cyaA* and Δ*crp* mutants in CBA/J mice were markedly diminished in the C3H/HeJ strain, probably because C3H/HeJ mice present the mutants with a less inflammatory and therefore less stressful environment.

Cumulatively, our data indicate that the effects of cAMP-CRP on multiple metabolic and stress response pathways must be balanced in order for UPEC to effectively colonize the urinary tract. This likely involves input from many cAMP-CRP-responsive regulatory factors, including the alternate sigma factor RpoS. *In vitro*, we found that UPEC mutants lacking cAMP-CRP have elevated levels of RpoS expression, in line with results obtained using other *E. coli* strains (44, 46, 47, 75, 76). The high-level resistance of UTI89Δ*cyaA* and UTI89Δ*crp* to H_2O_2 could be phenocopied by inducing the expression of RpoS in the wild-type pathogen. Other researchers have reported that a laboratory *E. coli* K-12 mutant lacking cAMP-CRP is also highly resistant to H_2O_2 (44). In this case, it was suggested that resistance of the mutant to H_2O_2 was partially attributable to increased RpoS-dependent expression of the DNA binding, ferritin-like protein Dps. We found that IPTG-induced expression of recombinant Dps is not sufficient to rescue growth of wild-type UTI89 in the presence of H_2O_2, suggesting that other, as-yet-undefined factor(s) acting downstream of RpoS mediate H_2O_2 resistance in this pathogen. Chief among the candidate gene products that may promote H_2O_2 resistance are the RpoS-inducible catalases (48, 49), which by inference appear to be upregulated in UTI89Δ*cyaA* and UTI89Δ*crp* (Fig. 5D). Interestingly, in our assays, the UTI89Δ*cyaA* mutant consistently had higher levels of catalase activity than the Δ*crp* mutant, suggesting that cAMP generated by CyaA may boost catalase activity in part via CRP-independent mechanisms.

As with the H_2O_2 sensitivity assays, induced expression of recombinant RpoS increased the acid resistance of wild-type UTI89 to levels observed with the Δ*cyaA* and Δ*crp* mutants (Fig. 6). In this case, overexpression of recombinant Dps gave similar results, suggesting that enhanced production of RpoS in the absence of cAMP-CRP promotes acid stress resistance in UPEC via transcriptional effects on *dps*. However, deletion of *dps* only slightly decreases the acid resistance of either UTI89 or the Δ*crp* mutant. In contrast, deletion of *rpoS* greatly increased the acid sensitivity of UTI89 and, to a far lesser extent, UTI89Δ*crp*. These observations indicate that acid resistance in UPEC does not require Dps, implying the possible involvement of other RpoS-regulated pH stress-responsive genes such as *asr*, *gadA*, and *gadBC* (46, 59). Furthermore, since UTI89Δ*rpoS* is much more sensitive to acid stress than the Δ*crp*Δ*rpoS* double-knockout mutant, we conclude that the absence of cAMP-CRP promotes acid resistance in UPEC via both RpoS-dependent and RpoS-independent mechanisms. The number of cAMP-CRP-repressible genes that could contribute to the observed acid resistance phenotypes independent of RpoS is potentially high (77, 78).

At first glance, the high-level resistance of UTI89Δ*cyaA* and UTI89Δ*crp* to H_2O_2 seems at odds with the increased sensitivity of these mutants to MV. While H_2O_2 and MV both generate oxidative stress, there are appreciable differences in their reactivities, duration of activity, and side effects that may differentially influence their toxicity (79). Methyl viologen is a superoxide generator that reduces diatomic oxygen to form superoxide. Oxidized MV can then be reduced by cellular electron donors, creating a redox cycle that consumes reducing equivalents like NADPH while continually producing superoxide molecules (80). In comparison, the oxidizing effects of H_2O_2 are not regenerated. Within *E. coli*, superoxide dismutase (Sod) enzymes convert superoxide into oxygen and H_2O_2. In turn, catalases convert H_2O_2 into innocuous diatomic oxygen and water. Decreased repression of RpoS within the Δ*cyaA* and Δ*crp* mutants results in increased catalase activity, as reported here (Fig. 5D), and may also stimulate the expression of cAMP-CRP- and RpoS-regulated enzymes like SodB and SodC (81, 82). Consequently, mutants lacking cAMP-CRP are likely better equipped to detoxify both superoxide and H_2O_2, which in turn may drive the redox cycle centered around MV so that reduc-

ing equivalents needed by the bacteria are consumed at a rate that disrupts essential cellular processes. The exact mechanisms by which the Δ*cyaA* and Δ*crp* mutants differentially deal with MV and H_2O_2 require further investigation. However, the opposing effects of these two oxidants on cAMP-CRP-dependent bacterial growth and fitness highlight the complex interplay that is possible between cAMP-CRP and the myriad metabolic and stress response systems that can contribute to the pathogenicity of UPEC.

ACKNOWLEDGMENTS

We are grateful to James Cox in the Metabolomics Facility of the University of Utah for help with quantifying trehalose levels, and we thank James Imlay for providing plasmid p*dps* and Sandy Parkinson for pRR48. We are also grateful to Rich Kulesus for providing UTI89Δ*rpoS*.

This work was supported by grants AI095647, AI090369, and AI088086 from the National Institute of Allergy and Infectious Diseases. J.P.N. was supported by NIH Genetics Training Grant T32-GM007464.

REFERENCES

1. **Wiles TJ, Kulesus RR, Mulvey MA.** 2008. Origins and virulence mechanisms of uropathogenic Escherichia coli. Exp. Mol. Pathol. **85**:11–19.
2. **Zasloff M.** 2007. Antimicrobial peptides, innate immunity, and the normally sterile urinary tract. J. Am. Soc. Nephrol. **18**:2810–2816.
3. **Gawel D, Seed PC.** 2011. Urinary tract infection drives genome instability in uropathogenic Escherichia coli and necessitates translesion synthesis DNA polymerase IV for virulence. Virulence **2**:222–232.
4. **Alteri CJ, Mobley HL.** 2012. Escherichia coli physiology and metabolism dictates adaptation to diverse host microenvironments. Curr. Opin. Microbiol. **15**:3–9.
5. **Li B, Smith P, Horvath DJ, Jr, Romesberg FE, Justice SS.** 2010. SOS regulatory elements are essential for UPEC pathogenesis. Microbes Infect. **12**:662–668.
6. **Foxman B.** 2010. The epidemiology of urinary tract infection. Nat. Rev. Urol. **7**:653–660.
7. **Sivick KE, Mobley HL.** 2010. Waging war against uropathogenic Escherichia coli: winning back the urinary tract. Infect. Immun. **78**:568–585.
8. **Hunstad DA, Justice SS.** 2010. Intracellular lifestyles and immune evasion strategies of uropathogenic Escherichia coli. Annu. Rev. Microbiol. **64**:203–221.
9. **Dhakal BK, Kulesus RR, Mulvey MA.** 2008. Mechanisms and consequences of bladder cell invasion by uropathogenic Escherichia coli. Eur. J. Clin. Invest. **38**(S2):2–11.
10. **Alteri CJ, Smith SN, Mobley HL.** 2009. Fitness of Escherichia coli during urinary tract infection requires gluconeogenesis and the TCA cycle. PLoS Pathog. **5**:e1000448. doi:10.1371/journal.ppat.1000448.
11. **Martinez-Jehanne V, Pichon C, du Merle L, Poupel O, Cayet N, Bouchier C, Le Bouguenec C.** 2012. Role of the Vpe carbohydrate permease in Escherichia coli urovirulence and fitness in vivo. Infect. Immun. **80**:2655–2666.
12. **Anfora AT, Haugen BJ, Roesch P, Redford P, Welch RA.** 2007. Roles of serine accumulation and catabolism in the colonization of the murine urinary tract by Escherichia coli CFT073. Infect. Immun. **75**:5298–5304.
13. **Roesch PL, Redford P, Batchelet S, Moritz RL, Pellett S, Haugen BJ, Blattner FR, Welch RA.** 2003. Uropathogenic Escherichia coli use d-serine deaminase to modulate infection of the murine urinary tract. Mol. Microbiol. **49**:55–67.
14. **Hadjifrangiskou M, Kostakioti M, Chen SL, Henderson JP, Greene SE, Hultgren SJ.** 2011. A central metabolic circuit controlled by QseC in pathogenic Escherichia coli. Mol. Microbiol. **80**:1516–1529.
15. **Kostakioti M, Hadjifrangiskou M, Pinkner JS, Hultgren SJ.** 2009. QseC-mediated dephosphorylation of QseB is required for expression of genes associated with virulence in uropathogenic Escherichia coli. Mol. Microbiol. **73**:1020–1031.
16. **Gorke B, Stulke J.** 2008. Carbon catabolite repression in bacteria: many ways to make the most out of nutrients. Nat. Rev. Microbiol. **6**:613–624.
17. **Poncet S, Milohanic E, Maze A, Nait Abdallah J, Ake F, Larribe M, Deghmane AE, Taha MK, Dozot M, De Bolle X, Letesson JJ, Deutscher J.** 2009. Correlations between carbon metabolism and virulence in bacteria. Contrib. Microbiol. **16**:88–102.
18. **McDonough KA, Rodriguez A.** 2012. The myriad roles of cyclic AMP in microbial pathogens: from signal to sword. Nat. Rev. Microbiol. **10**:27–38.
19. **Nielsen AT, Dolganov NA, Rasmussen T, Otto G, Miller MC, Felt SA, Torreilles S, Schoolnik GK.** 2010. A bistable switch and anatomical site control Vibrio cholerae virulence gene expression in the intestine. PLoS Pathog. **6**:e1001102. doi:10.1371/journal.ppat.1001102.
20. **Rickman L, Scott C, Hunt DM, Hutchinson T, Menendez MC, Whalan R, Hinds J, Colston MJ, Green J, Buxton RS.** 2005. A member of the cAMP receptor protein family of transcription regulators in Mycobacterium tuberculosis is required for virulence in mice and controls transcription of the rpfA gene coding for a resuscitation promoting factor. Mol. Microbiol. **56**:1274–1286.
21. **Curtiss R, III, Kelly SM.** 1987. Salmonella typhimurium deletion mutants lacking adenylate cyclase and cyclic AMP receptor protein are avirulent and immunogenic. Infect. Immun. **55**:3035–3043.
22. **Smith RS, Wolfgang MC, Lory S.** 2004. An adenylate cyclase-controlled signaling network regulates Pseudomonas aeruginosa virulence in a mouse model of acute pneumonia. Infect. Immun. **72**:1677–1684.
23. **Muller CM, Aberg A, Straseviciene J, Emody L, Uhlin BE, Balsalobre C.** 2009. Type 1 fimbriae, a colonization factor of uropathogenic Escherichia coli, are controlled by the metabolic sensor CRP-cAMP. PLoS Pathog. **5**:e1000303. doi:10.1371/journal.ppat.1000303.
24. **Chen SL, Hung CS, Xu J, Reigstad CS, Magrini V, Sabo A, Blasiar D, Bieri T, Meyer RR, Ozersky P, Armstrong JR, Fulton RS, Latreille JP, Spieth J, Hooton TM, Mardis ER, Hultgren SJ, Gordon JI.** 2006. Identification of genes subject to positive selection in uropathogenic strains of Escherichia coli: a comparative genomics approach. Proc. Natl. Acad. Sci. U. S. A. **103**:5977–5982.
25. **Mulvey MA, Schilling JD, Hultgren SJ.** 2001. Establishment of a persistent Escherichia coli reservoir during the acute phase of a bladder infection. Infect. Immun. **69**:4572–4579.
26. **Zhou Q, Ames P, Parkinson JS.** 2009. Mutational analyses of HAMP helices suggest a dynamic bundle model of input-output signalling in chemoreceptors. Mol. Microbiol. **73**:801–814.
27. **Murphy KC, Campellone KG.** 2003. Lambda Red-mediated recombinogenic engineering of enterohemorrhagic and enteropathogenic E. coli. BMC Mol. Biol. **4**:11. doi:10.1186/1471-2199-4-11.
28. **Datsenko KA, Wanner BL.** 2000. One-step inactivation of chromosomal genes in Escherichia coli K-12 using PCR products. Proc. Natl. Acad. Sci. U. S. A. **97**:6640–6645.
29. **Blango MG, Mulvey MA.** 2010. Persistence of uropathogenic Escherichia coli in the face of multiple antibiotics. Antimicrob. Agents Chemother. **54**:1855–1863.
30. **Eto DS, Gordon HB, Dhakal BK, Jones TA, Mulvey MA.** 2008. Clathrin, AP-2, and the NPXY-binding subset of alternate endocytic adaptors facilitate FimH-mediated bacterial invasion of host cells. Cell. Microbiol. **10**:2553–2567.
31. **Hopkins W, Gendron-Fitzpatrick A, McCarthy DO, Haine JE, Uehling DT.** 1996. Lipopolysaccharide-responder and nonresponder C3H mouse strains are equally susceptible to an induced Escherichia coli urinary tract infection. Infect. Immun. **64**:1369–1372.
32. **Hagberg L, Hull R, Hull S, McGhee JR, Michalek SM, Svanborg Eden C.** 1984. Difference in susceptibility to gram-negative urinary tract infection between C3H/HeJ and C3H/HeN mice. Infect. Immun. **46**:839–844.
33. **Suhs KA, Marthaler BR, Welch RA, Hopkins WJ.** 2011. Lack of association between the Tlr4 (Lpsd/Lpsd) genotype and increased susceptibility to Escherichia coli bladder infections in female C3H/HeJ mice. mBio **2**:e00094–11. doi:10.1128/mBio.00094-11.
34. **Hopkins WJ, Elkahwaji J, Kendziorski C, Moser AR, Briggs PM, Suhs KA.** 2009. Quantitative trait loci associated with susceptibility to bladder and kidney infections induced by Escherichia coli in female C3H/HeJ mice. J. Infect. Dis. **199**:355–361.
35. **Haraoka M, Hang L, Frendéus B, Godaly G, Burdick M, Strieter R, Svanborg C.** 1999. Neutrophil recruitment and resistance to urinary tract infection. J. Infect. Dis. **180**:1220–1229.
36. **Schilling JD, Martin SM, Hung CS, Lorenz RG, Hultgren SJ.** 2003. Toll-like receptor 4 on stromal and hematopoietic cells mediates innate resistance to uropathogenic Escherichia coli. Proc. Natl. Acad. Sci. U. S. A. **100**:4203–4208.
37. **Aubron C, Glodt J, Matar C, Huet O, Borderie D, Dobrindt U, Duranteau J, Denamur E, Conti M, Bouvet O.** 2012. Variation in endogenous oxidative stress in Escherichia coli natural isolates during growth in urine. BMC Microbiol. **12**:120. doi:10.1186/1471-2180-12-120.

38. **Bower JM, Gordon-Raagas HB, Mulvey MA.** 2009. Conditioning of uropathogenic Escherichia coli for enhanced colonization of host. Infect. Immun. **77**:2104–2112.
39. **Johnson JR, Clabots C, Rosen H.** 2006. Effect of inactivation of the global oxidative stress regulator oxyR on the colonization ability of Escherichia coli O1:K1:H7 in a mouse model of ascending urinary tract infection. Infect. Immun. **74**:461–468.
40. **Korshunov S, Imlay JA.** 2006. Detection and quantification of superoxide formed within the periplasm of Escherichia coli. J. Bacteriol. **188**:6326–6334.
41. **Lundberg JO, Ehren I, Jansson O, Adolfsson J, Lundberg JM, Weitzberg E, Alving K, Wiklund NP.** 1996. Elevated nitric oxide in the urinary bladder in infectious and noninfectious cystitis. Urology **48**:700–702.
42. **Poljakovic M, Svensson ML, Svanborg C, Johansson K, Larsson B, Persson K.** 2001. Escherichia coli-induced inducible nitric oxide synthase and cyclooxygenase expression in the mouse bladder and kidney. Kidney Int. **59**:893–904.
43. **Woolford G, Casselden RJ, Walters CL.** 1972. Gaseous products of the interaction of sodium nitrite with porcine skeletal muscle. Biochem. J. **130**:82P–83P.
44. **Barth E, Gora KV, Gebendorfer KM, Settele F, Jakob U, Winter J.** 2009. Interplay of cellular cAMP levels, {sigma}S activity and oxidative stress resistance in Escherichia coli. Microbiology **155**:1680–1689.
45. **Hengge-Aronis R.** 2002. Signal transduction and regulatory mechanisms involved in control of the sigma(S) (RpoS) subunit of RNA polymerase. Microbiol. Mol. Biol. Rev. **66**:373–395.
46. **Jeong KC, Baumler DJ, Kaspar CW.** 2006. dps expression in Escherichia coli O157:H7 requires an extended −10 region and is affected by the cAMP receptor protein. Biochim. Biophys. Acta **1759**:51–59.
47. **Lange R, Hengge-Aronis R.** 1994. The cellular concentration of the sigma S subunit of RNA polymerase in Escherichia coli is controlled at the levels of transcription, translation, and protein stability. Genes Dev. **8**:1600–1612.
48. **Eisenstark A, Calcutt MJ, Becker-Hapak M, Ivanova A.** 1996. Role of Escherichia coli rpoS and associated genes in defense against oxidative damage. Free Radic. Biol. Med. **21**:975–993.
49. **Schellhorn HE.** 1995. Regulation of hydroperoxidase (catalase) expression in Escherichia coli. FEMS Microbiol. Lett. **131**:113–119.
50. **Strom AR, Kaasen I.** 1993. Trehalose metabolism in Escherichia coli: stress protection and stress regulation of gene expression. Mol. Microbiol. **8**:205–210.
51. **Alvarez-Peral FJ, Zaragoza O, Pedreno Y, Arguelles JC.** 2002. Protective role of trehalose during severe oxidative stress caused by hydrogen peroxide and the adaptive oxidative stress response in Candida albicans. Microbiology **148**:2599–2606.
52. **Benaroudj N, Lee DH, Goldberg AL.** 2001. Trehalose accumulation during cellular stress protects cells and cellular proteins from damage by oxygen radicals. J. Biol. Chem. **276**:24261–24267.
53. **Martinez A, Kolter R.** 1997. Protection of DNA during oxidative stress by the nonspecific DNA-binding protein Dps. J. Bacteriol. **179**:5188–5194.
54. **Almiron M, Link AJ, Furlong D, Kolter R.** 1992. A novel DNA-binding protein with regulatory and protective roles in starved Escherichia coli. Genes Dev. **6**:2646–2654.
55. **Park S, You X, Imlay JA.** 2005. Substantial DNA damage from submicromolar intracellular hydrogen peroxide detected in Hpx- mutants of Escherichia coli. Proc. Natl. Acad. Sci. U. S. A. **102**:9317–9322.
56. **Eto DS, Sundsbak JL, Mulvey MA.** 2006. Actin-gated intracellular growth and resurgence of uropathogenic Escherichia coli. Cell. Microbiol. **8**:704–717.
57. **Vergne I, Constant P, Laneelle G.** 1998. Phagosomal pH determination by dual fluorescence flow cytometry. Anal. Biochem. **255**:127–132.
58. **Foster JW.** 2004. Escherichia coli acid resistance: tales of an amateur acidophile. Nat. Rev. Microbiol. **2**:898–907.
59. **Castanie-Cornet MP, Penfound TA, Smith D, Elliott JF, Foster JW.** 1999. Control of acid resistance in Escherichia coli. J. Bacteriol. **181**:3525–3535.
60. **Calhoun LN, Kwon YM.** 2011. Structure, function and regulation of the DNA-binding protein Dps and its role in acid and oxidative stress resistance in Escherichia coli: a review. J. Appl. Microbiol. **110**:375–386.
61. **Small P, Blankenhorn D, Welty D, Zinser E, Slonczewski JL.** 1994. Acid and base resistance in Escherichia coli and Shigella flexneri: role of rpoS and growth pH. J. Bacteriol. **176**:1729–1737.
62. **Cheville AM, Arnold KW, Buchrieser C, Cheng CM, Kaspar CW.** 1996. rpoS regulation of acid, heat, and salt tolerance in Escherichia coli O157:H7. Appl. Environ. Microbiol. **62**:1822–1824.
63. **Waterman SR, Small PL.** 1996. Characterization of the acid resistance phenotype and rpoS alleles of Shiga-like toxin-producing Escherichia coli. Infect. Immun. **64**:2808–2811.
64. **Le Bouguenec C, Schouler C.** 2011. Sugar metabolism, an additional virulence factor in enterobacteria. Int. J. Med. Microbiol. **301**:1–6.
65. **Loughman JA, Hunstad DA.** 2012. Induction of indoleamine 2,3-dioxygenase by uropathogenic bacteria attenuates innate responses to epithelial infection. J. Infect. Dis. **205**:1830–1839.
66. **Rouquet G, Porcheron G, Barra C, Reperant M, Chanteloup NK, Schouler C, Gilot P.** 2009. A metabolic operon in extraintestinal pathogenic Escherichia coli promotes fitness under stressful conditions and invasion of eukaryotic cells. J. Bacteriol. **191**:4427–4440.
67. **Himpsl SD, Lockatell CV, Hebel JR, Johnson DE, Mobley HL.** 2008. Identification of virulence determinants in uropathogenic Proteus mirabilis using signature-tagged mutagenesis. J. Med. Microbiol. **57**:1068–1078.
68. **Gonzalez-Flecha B, Demple B.** 1997. Transcriptional regulation of the Escherichia coli oxyR gene as a function of cell growth. J. Bacteriol. **179**:6181–6186.
69. **Kostakioti M, Hadjifrangiskou M, Cusumano CK, Hannan TJ, Janetka JW, Hultgren SJ.** 2012. Distinguishing the contribution of type 1 pili from that of other QseB-misregulated factors when QseC is absent during urinary tract infection. Infect. Immun. **80**:2826–2834.
70. **Poljakovic M, Karpman D, Svanborg C, Persson K.** 2002. Human renal epithelial cells express iNOS in response to cytokines but not bacteria. Kidney Int. **61**:444–455.
71. **Poltorak A, He X, Smirnova I, Liu MY, Huffel CV, Du X, Birdwell D, Alejos E, Silva M, Galanos C, Freudenberg M, Ricciardi-Castagnoli P, Layton B, Beutler B.** 1998. Defective LPS signaling in C3H/HeJ and C57BL/10ScCr mice: mutations in Tlr4 gene. Science **282**:2085–2088.
72. **McAdam KP, Ryan JL.** 1978. C57BL/10/CR mice: nonresponders to activation by the lipid a moiety of bacterial lipopolysaccharide. J. Immun. **120**:249–253.
73. **Justice SS, Hung C, Theriot JA, Fletcher DA, Anderson GG, Footer MJ, Hultgren SJ.** 2004. Differentiation and developmental pathways of uropathogenic Escherichia coli in urinary tract pathogenesis. Proc. Natl. Acad. Sci. U. S. A. **101**:1333–1338.
74. **Svanborg C, Frendeus B, Godaly G, Hang L, Hedlund M, Wachtler C.** 2001. Toll-like receptor signaling and chemokine receptor expression influence the severity of urinary tract infection. J. Infect. Dis. **183**(Suppl 1):S61–S65.
75. **Ma Z, Gong S, Richard H, Tucker DL, Conway T, Foster JW.** 2003. GadE (YhiE) activates glutamate decarboxylase-dependent acid resistance in Escherichia coli K-12. Mol. Microbiol. **49**:1309–1320.
76. **Ma Z, Richard H, Foster JW.** 2003. pH-dependent modulation of cyclic AMP levels and GadW-dependent repression of RpoS affect synthesis of the GadX regulator and Escherichia coli acid resistance. J. Bacteriol. **185**:6852–6859.
77. **Raghavan R, Sage A, Ochman H.** 2011. Genome-wide identification of transcription start sites yields a novel thermosensing RNA and new cyclic AMP receptor protein-regulated genes in Escherichia coli. J. Bacteriol. **193**:2871–2874.
78. **Zheng D, Constantinidou C, Hobman JL, Minchin SD.** 2004. Identification of the CRP regulon using in vitro and in vivo transcriptional profiling. Nucleic Acids Res. **32**:5874–5893.
79. **Farr SB, Kogoma T.** 1991. Oxidative stress responses in Escherichia coli and Salmonella typhimurium. Microbiol. Rev. **55**:561–585.
80. **Bus JS, Gibson JE.** 1984. Paraquat: model for oxidant-initiated toxicity. Environ. Health Perspect. **55**:37–46.
81. **Lacour S, Landini P.** 2004. SigmaS-dependent gene expression at the onset of stationary phase in Escherichia coli: function of sigmaS-dependent genes and identification of their promoter sequences. J. Bacteriol. **186**:7186–7195.
82. **Zhang Z, Gosset G, Barabote R, Gonzalez CS, Cuevas WA, Saier MH, Jr.** 2005. Functional interactions between the carbon and iron utilization regulators, Crp and Fur, in Escherichia coli. J. Bacteriol. **187**:980–990.
83. **Wiles TJ, Bower JM, Redd MJ, Mulvey MA.** 2009. Use of zebrafish to probe the divergent virulence potentials and toxin requirements of extraintestinal pathogenic Escherichia coli. PLoS Pathog. **5**:e1000697. doi: 10.1371/journal.ppat.1000697.
84. **Kulesus RR, Diaz-Perez K, Slechta ES, Eto DS, Mulvey MA.** 2008. Impact of the RNA chaperone Hfq on the fitness and virulence potential of uropathogenic Escherichia coli. Infect. Immun. **76**:3019–3026.

CHAPTER 3

TOXIN-ANTITOXIN SYSTEMS ARE IMPORTANT FOR NICHE SPECIFIC COLONIZATION AND STRESS RESISTANCE OF UROPATHOGENIC *ESCHERICHIA COLI*

Reprinted with permission from Public Library of Science

Norton, J.P., and Mulvey, M. A. Toxin-antitoxin systems are important for niche specific colonization and stress resistance of uropathogenic *Escherichia coli*. *PloS Pathog* **8**(10): e1002954, doi:10.1371/journal.ppat.1002954 (2012).

OPEN ACCESS Freely available online

PLOS | PATHOGENS

Toxin-Antitoxin Systems Are Important for Niche-Specific Colonization and Stress Resistance of Uropathogenic *Escherichia coli*

J. Paul Norton, Matthew A. Mulvey*

Division of Microbiology and Immunology, Pathology Department, University of Utah School of Medicine, Salt Lake City, Utah, United States of America

Abstract

Toxin-antitoxin (TA) systems are prevalent in many bacterial genomes and have been implicated in biofilm and persister cell formation, but the contribution of individual chromosomally encoded TA systems during bacterial pathogenesis is not well understood. Of the known TA systems encoded by *Escherichia coli*, only a subset is associated with strains of extraintestinal pathogenic *E. coli* (ExPEC). These pathogens colonize diverse niches and are a major cause of sepsis, meningitis, and urinary tract infections. Using a murine infection model, we show that two TA systems (YefM-YoeB and YbaJ-Hha) independently promote colonization of the bladder by the reference uropathogenic ExPEC isolate CFT073, while a third TA system comprised of the toxin PasT and the antitoxin PasI is critical to ExPEC survival within the kidneys. The PasTI TA system also enhances ExPEC persister cell formation in the presence of antibiotics and markedly increases pathogen resistance to nutrient limitation as well as oxidative and nitrosative stresses. On its own, low-level expression of PasT protects ExPEC from these stresses, whereas overexpression of PasT is toxic and causes bacterial stasis. PasT-induced stasis can be rescued by overexpression of PasI, indicating that PasTI is a bona fide TA system. By mutagenesis, we find that the stress resistance and toxic effects of PasT can be uncoupled and mapped to distinct domains. Toxicity was specifically linked to sequences within the N-terminus of PasT, a region that also promotes the development of persister cells. These results indicate discrete, multipurpose functions for a TA-associated toxin and demonstrate that individual TA systems can provide bacteria with pronounced fitness advantages dependent on toxin expression levels and the specific environmental niche occupied.

Citation: Norton JP, Mulvey MA (2012) Toxin-Antitoxin Systems Are Important for Niche-Specific Colonization and Stress Resistance of Uropathogenic *Escherichia coli*. PLoS Pathog 8(10): e1002954. doi:10.1371/journal.ppat.1002954

Editor: Guy Tran Van Nhieu, Institut Pasteur, France

Received April 25, 2012; **Accepted** August 16, 2012; **Published** October 4, 2012

Funding: This work was supported by grants AI095647, AI090369, and AI088086 from the National Institute of Allergy and Infectious Diseases. J.P.N. was supported by NIH Genetics Training Grant T32-GM007464. The funders had no role in study design, data collection and analysis, decision to publish, or preparation of the manuscript.

Competing Interests: The authors have declared that no competing interests exist.

* E-mail: mulvey@path.utah.edu

Introduction

Toxin-antitoxin (TA) systems consist of stable toxic proteins that are held in check by co-expression of labile antitoxin molecules, the nature of which distinguishes three classes of TA systems [1,2]. Antitoxins made by type I TA loci are small antisense RNAs that suppress translation of the toxin genes [3], while the antitoxins encoded by type II and type III TA loci are, respectively, proteins and small RNAs that complex with and inactivate their cognate protein toxins [2,4]. When freed to act, toxins encoded by TA loci can disrupt diverse bacterial cell processes, including peptidoglycan synthesis, the polymerization of cytoskeletal components, ribosome assembly, tRNA availability, and mRNA stability [5,6,7,8,9]. TA systems were initially characterized as plasmid-encoded genes that serve as addiction molecules, promoting the heritable maintenance of extra-chromosomal DNA within a bacterial population [10,11]. However, TA systems are not solely plasmid-associated, and have been found in abundance within bacterial chromosomes from diverse species. The functional relevance of individual chromosomally encoded TA systems to bacterial fitness within the environment is oftentimes ambiguous, and even less understood is the impact of these systems on bacterial pathogenesis [12,13].

Environmental stresses have been shown to stimulate the transcription of multiple chromosomal TA loci, leading to the idea that these systems may enhance bacterial survival under adverse conditions [14,15,16]. Others suggest that chromosomal TA loci represent junk DNA or selfish genetic elements, or that they primarily function akin to plasmid-encoded addiction molecules, acting to stabilize genomic parasites such as conjugative transposons and prophages [17,18]. A recent bioinformatics-based study supporting this hypothesis concluded that TA loci are selfish genetic elements that likely do not bestow any fitness advantage to the bacteria in which they reside [19]. In some cases this may be true, but there is mounting evidence that some chromosomal TA systems play larger roles in bacterial physiology and pathogenesis. Much of this evidence is circumstantial, based on expression analysis of TA systems in bacteria in the presence of various environmental stresses. For example, paralogous TA systems within the *Caulobacter crescentus* genome are differentially expressed in response to heavy metal-, heat-, and nitric oxide-induced stresses [14], while in *Mycobacterium tuberculosis* several TA systems are upregulated under hypoxic conditions or following bacterial entry into macrophages [16]. One of these, VapBC, was recently shown to regulate the balance of metabolic processes within mycobacteria [20].

Author Summary

Toxin-antitoxin (TA) systems are widespread among prokaryotes, including many important human pathogens. It has long been hypothesized that TA systems contribute to bacterial pathogenesis, but clear-cut phenotypes associated with any individual TA system have not been described. Using bioinformatics, we demonstrate that distinct subsets of TA systems are linked with a major group of bacterial pathogens known as Extraintestinal Pathogenic *E. coli* (ExPEC). These bacteria are responsible for the majority of urinary tract infections worldwide, and are major causes of sepsis and meningitis. Using murine infection models with a reference uropathogenic ExPEC isolate, we found that three of the ExPEC-associated TA systems act independently to promote bacterial survival and persistence within the host urinary tract. Furthermore, we show that the toxin protein associated with one of these TA systems increases ExPEC stress resistance and persistence in the face of antibiotics. This work demonstrates the functional importance of specific TA systems to ExPEC pathogenesis, highlighting their potential as therapeutic targets.

Among strains of *E. coli* at least 17 type II chromosomal TA systems have been identified [2]. A large subset of these was recently shown to act redundantly *in vitro* to enhance survival of a K-12 *E. coli* strain in the presence of antibiotics by driving the formation of dormant, stress resistant cells known as persisters [9]. Type II TA systems may also promote biofilm formation by some K-12 strains [21,22,23], and can be differentially expressed in response to DNA damage and nutrient deprivation [15]. Considering these observations, we were interested in understanding possible links between chromosomal type II TA systems and the fitness and virulence potential of extraintestinal pathogenic *E. coli* (ExPEC). These pathogens are able to colonize diverse niches within humans and other host animals and are a major cause of bacteremia, sepsis, peritonitis, neonatal meningitis, and urinary tract infections (UTIs) [24]. Here we report that, as a group, ExPEC isolates encode a discrete repertoire of type II TA systems, three of which can individually impact the fitness and persistence of a reference ExPEC isolate *in vivo* within the urinary tract. In addition, the toxin PasT encoded by one of these TA systems is shown to possess dual, concentration-dependent activities that either enhance bacterial stress resistance and growth or, alternatively, promote bacterial stasis and persister cell formation.

Results

ExPEC Encode a Limited Number of Known Type II TA Systems

To ascertain potential patterns in the distribution and makeup of chromosomal type II TA systems among *E. coli* strains, the allelic profiles of 35 fully sequenced *E. coli* isolates were compared and organized based on similarities among 17 type II TA loci using the eBURST algorithm (Dataset S1) [25]. This allelic-based cluster analysis, which is often used to discern patterns of descent within bacterial populations in which horizontal gene transfer is widespread [19], identified two sizable groups of *E. coli* strains that differ in the number and composition of their type II TA systems (Figure 1A). One of these groups is comprised entirely of isolates belonging to the B2 phylotype, a specific subset of phylogenetically similar *E. coli* strains that includes most ExPEC isolates [26]. Interestingly, in our analysis the enteropathogenic *E. coli* (EPEC) strain E2348/69 was also grouped with the ExPEC isolates. This is, however, in line with a previous report that classified this EPEC strain as a member of the B2 phylotype [27]. These data indicate that, at least in the case of B2 strains, the composition of type II TA systems within *E. coli* isolates can reflect their phylogenetic origin, suggesting that specific TA systems may serve an evolutionarily conserved purpose within this cohort.

Relative to K-12 *E. coli* strains, we found that ExPEC generally have a reduced repertoire of intact type II TA loci, as exemplified by comparative analysis of the lab-adapted K-12 reference strain MG1655 and the ExPEC isolate CFT073 (Figure 1B). This pathogen was isolated from the blood of a patient with pyelonephritis and is part of a large sub-category of ExPEC known as uropathogenic *E. coli* (UPEC), the primary cause of UTIs worldwide [28]. Of the 16 type II TA loci encoded by MG1655, only seven are found in CFT073. The TA loci in CFT073 are syntenic with their counterparts in MG1655, although five additional, imperfect copies of one locus (*yeeUV*) are also present at sites around the CFT073 chromosome.

TA Systems Provide Niche-Specific Benefits to ExPEC within the Host

The relative conservation of the type II TA loci subsets among ExPEC isolates indicates that select TA systems may be important fitness determinants for these pathogens. To address this possibility, each single-copy type II TA locus in CFT073 was deleted and tested in competition with the wild type strain using a well-established mouse UTI model system [29,30]. Cultures of wild type CFT073 and TA system mutant strains were mixed in a 1:1 ratio and injected via transurethral catheterization into adult female CBA/J mice, and three days later bacterial titers in the bladder and kidneys were determined. In these assays, half of the six TA system mutants (Δ*higBA*, Δ*hipBA*, and Δ*sohA(prlF)-yhaV*) tested showed no significant defects relative to the wild type strain (Figure 2A and B). In contrast, mutants lacking either the *ybaJ-hha* (*tomB-hha*) or the *yefM-yoeB* TA locus were clearly outcompeted by wild type CFT073 in the bladder, but not the kidneys (Figure 2C and D), while the Δ*pasTI* mutant (CFT073Δ*pasTI*) was outcompeted only in the kidneys (Figure 2E and F). It should be noted that *pasTI* was originally dubbed *yfjGF* and then *ratAB*, but has been renamed here for reasons described later.

The competitive defect in kidney colonization by CFT073 Δ*pasTI* was evident within 24 h post-inoculation and significantly worsened by the 3 d time point (Figure 2F). Over the same time frame, wild type CFT073 titers within the kidneys were not significantly diminished. We found that CFT073Δ*pasTI* is also significantly impaired in kidney colonization during non-competitive assays (Figure 2G and H). In contrast, defects observed with the Δ*ybaJ-hha* and Δ*yefM-yoeB* mutants in competitive assays (Figure 2C and D) were not manifest in non-competitive assays (Figure S1). The inability of CFT073Δ*pasTI* to effectively colonize the kidneys of CBA/J mice was recapitulated in experiments using two additional host strain backgrounds, C3H/HeN and C3H/HeJ (Figure 3). Of note, the Δ*pasTI* mutant was similar to wild type CFT073 in its ability to colonize and persist within the gastrointestinal tract of CBA/J mice (Fig. S2). Together, these results demonstrate that chromosomal type II TA systems like PasTI can provide significant advantages to UPEC within specific host environments.

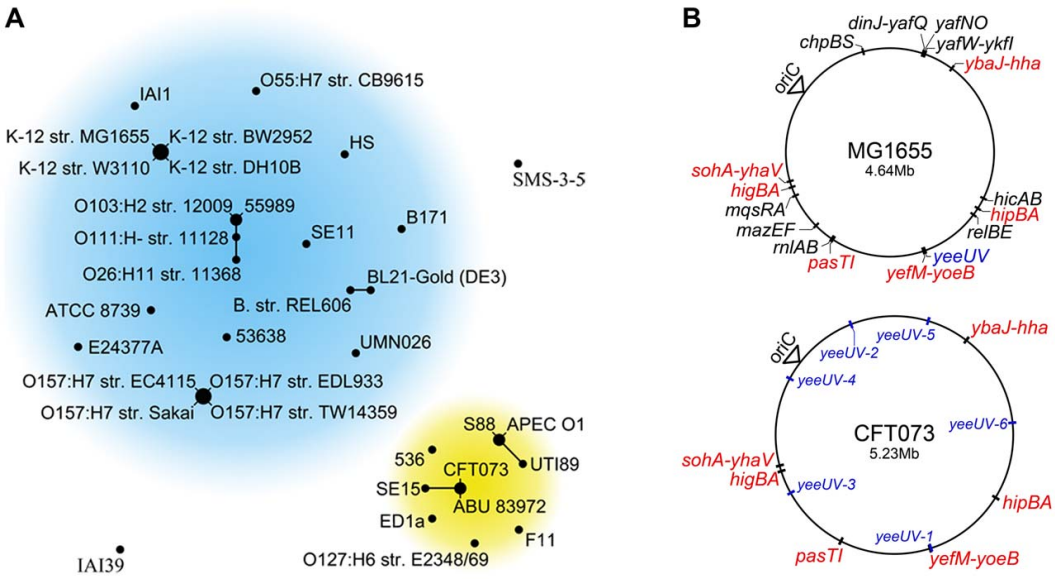

Figure 1. ExPEC encode distinct subsets of type II TA systems. (A) Based on similarities among 21 type II TA alleles, the eBURST algorithm clusters members of phylotype B2 (yellow) together, separate from other sequenced *E. coli* strains (blue). Strains connected by a line differ by a single TA allele. (B) Genomic maps denoting the relative locations of the type II TA systems encoded by MG1655 and CFT073. Red denotes TA systems that are present in both genomes; *yeeUV* and its allelic variants are shown in blue.
doi:10.1371/journal.ppat.1002954.g001

The PasTI TA System Promotes the Development of Persister Cells

In K-12 *E. coli* strains, TA systems are proposed to act redundantly in the formation of persister cells in the presence of antibiotics and other harsh environmental stresses [31,32]. For example, deletion of any one of the 10 mRNA endonuclease-encoding TA loci in the K-12 strain MG1655, individually, has no effect on bacterial persistence in the presence of either ampicillin or ciprofloxacin, whereas the successive deletion of five or more of these loci results in progressively decreased numbers of persisters [9]. In similar assays with CFT073 grown in LB broth, we found that deletion of the *pasTI* TA locus, alone, decreased bacterial persistence in the face of antibiotics by about 100-fold, while all other type II TA knockout mutants behaved like the wild type pathogen (Figure 4A). The minimal inhibitory concentrations of ampicillin and ciprofloxacin were the same for both wild type CFT073 and the Δ*pasTI* mutant (data not shown). MG1655, which has a larger pool of TA systems, was much more adept at forming persisters than CFT073, and the deletion of *pasTI* did not affect the ability of MG1655 to form persisters in our assays (Figure 4B). These data reveal that *pasTI* is dispensable for the development of persister cells by the K-12 strain, while in CFT073 the PasTI TA system acts in a more non-redundant fashion to promote persister cell formation. These results do not rule out the possibility that other gene products, including additional as-yet defined TA systems, may also contribute to the formation of persister cells by CFT073 and other UPEC isolates.

PasT Enhances the Stress Resistance of UPEC

During the course of a UTI, UPEC encounter multiple stresses, including nutrient deprivation and reactive nitrogen and oxygen species [30,33,34]. In standard LB broth and in M9 minimal medium supplemented with 0.2% casein amino acids, CFT073Δ*pasTI* grew like the wild type strain, but in M9 medium supplemented with only a single amino acid (40 μg/mL threonine), growth of the Δ*pasTI* mutant was significantly delayed (Figure 5A–C). CFT073Δ*pasTI* also displayed increased sensitivity to both oxidative and nitrosative stresses generated in broth cultures by addition of methyl viologen (MV) and acidified sodium nitrite (ASN), respectively (Figure 5D, F). Use of ASN in these assays involves the addition of sodium nitrite to MES-buffered LB broth (MES-LB, pH 5.0), leading to the generation of nitrous acid, NO, and other reactive nitrogen intermediates [35]. In control experiments, CFT073Δ*pasTI* grew normally in MES-LB without addition of ASN (Figure 5E). Corroborating these data, we observed on LB agar plates—which *E. coli* sense as a certifiable stress due in part to the presence of oxygen radicals [36]—that growth of CFT073Δ*pasTI* lags behind the wild type strain, resulting in a small colony phenotype (Figure 6A–B). Deletion of *pasTI* in other ExPEC isolates (including the neonatal meningitis isolate S88 and the UPEC strains F11 and UTI89) also resulted in small colony phenotypes as well as increased sensitivity to ASN (Figure 6E–G). None of the other type II TA system mutants in CFT073 were defective in these growth assays (Figure 5 and data not shown).

The growth defects observed with CFT073Δ*pasTI* were attributable to loss of *pasT*, as low-level, leaky expression of PasT, but not PasI, from an un-induced P*tac* promoter complemented all growth defects observed with the Δ*pasTI* mutant (Figure 7A, Figure 6C–D, and data not shown). Leaky expression of PasT did not alter bacterial growth in standard LB broth (Figure S3A). Furthermore, expression of the entire *pasTI* operon under control of its native promoter complements the Δ*pasTI* mutant similar to expression of PasT alone, restoring wild type growth on LB agar plates and providing wild type levels of ASN resistance (Figure S3B

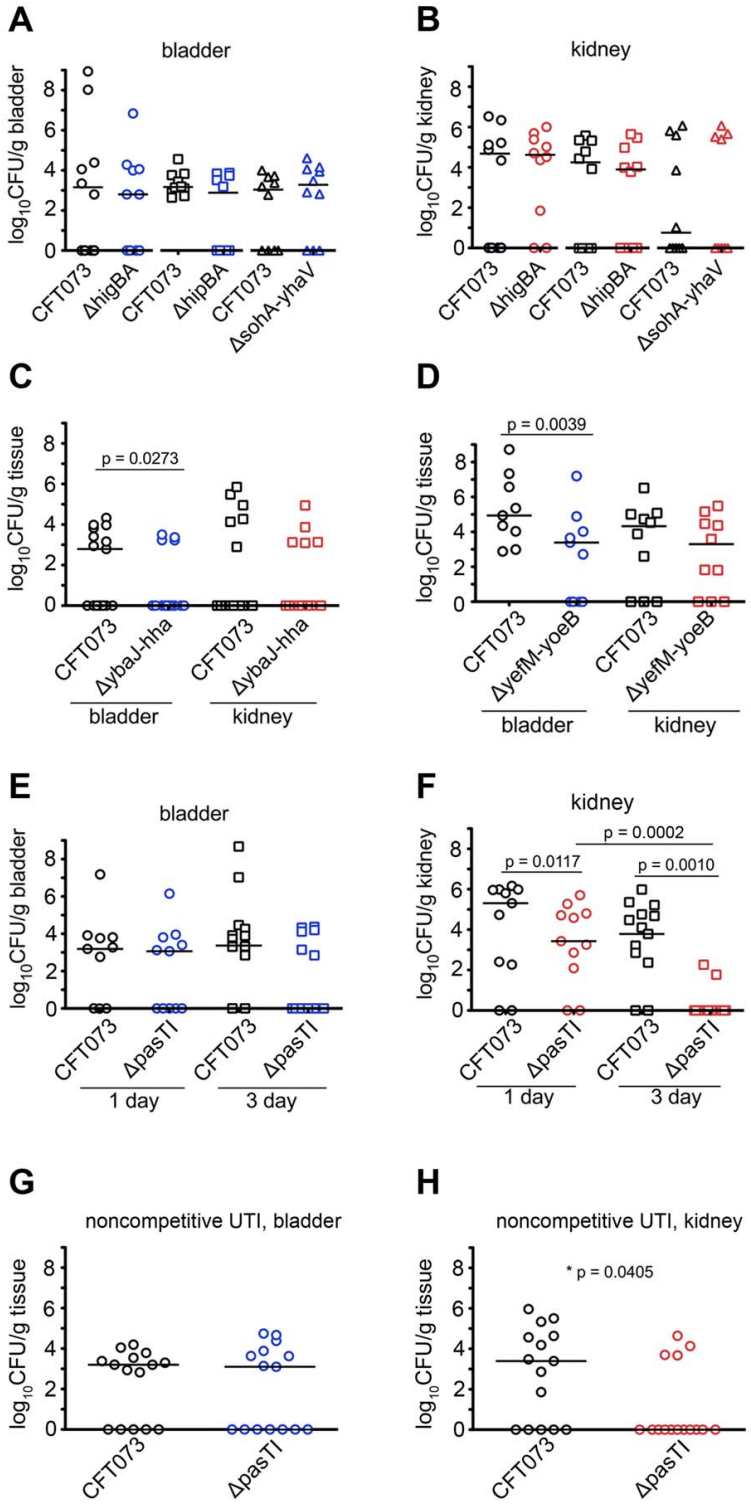
A
bladder
log10CFU/g bladder
CFT073
ΔhigBA
CFT073
ΔhipBA
CFT073
ΔsohA-yhaV
B
kidney
log10CFU/g kidney
CFT073
ΔhigBA
CFT073
ΔhipBA
CFT073
ΔsohA-yhaV
C
log10CFU/g tissue
p = 0.0273
CFT073
ΔybaJ-hha
CFT073
ΔybaJ-hha
bladder
kidney
D
p = 0.0039
log10CFU/g tissue
CFT073
ΔyefM-yoeB
CFT073
ΔyefM-yoeB
bladder
kidney
E
bladder
log10CFU/g bladder
CFT073
ΔpasTI
CFT073
ΔpasTI
1 day
3 day
F
kidney
p = 0.0002
p = 0.0117
p = 0.0010
log10CFU/g kidney
CFT073
ΔpasTI
CFT073
ΔpasTI
1 day
3 day
G
noncompetitive UTI, bladder
log10CFU/g tissue
CFT073
ΔpasTI
H
noncompetitive UTI, kidney
* p = 0.0405
log10CFU/g tissue
CFT073
ΔpasTI

Figure 2. Distinct TA systems enhance UPEC fitness within the urinary tract. (A–H) Adult female CBA/J mice were infected via catheterization with equal numbers of wild type CFT073 and isogenic mutants lacking the indicated type II TA systems as part of either (A–F) competitive or (G and H) non-competitive assays. (A–H) Graphs show bacterial titers present in the bladder or kidneys, as indicated, at 3 d post-inoculation. (E and F) For competitive assays involving wild type CFT073 and CFT073Δ*pasTI*, bacterial titers recovered from mice at 1 d post-inoculation are also indicated. Bars denote median values for each group; n≥10 mice. *P* values determined using (A–F) Wilcoxon-matched paired signed rank and (G–H) Mann-Whitney U tests.
doi:10.1371/journal.ppat.1002954.g002

and data not shown). PasT thus appears to enhance UPEC growth in the presence of diverse stresses, a phenomenon that is seemingly at odds with recent work showing that PasT (a.k.a. RatA) in K-12 *E. coli* acts as a toxin capable of binding 50S ribosomal subunits and thereby inhibiting translation and bacterial growth [7]. This discrepancy is partially reconciled by observations that high-level expression of PasT in CFT073 is toxic, resulting in growth arrest (Figure 7B). The induced expression of PasI counters the toxic effects of PasT, demonstrating that PasI can function as a *bona fide* antitoxin to PasT (Figure 7C). PasT is, therefore, conditionally toxic, depending in part on its expression levels and regulatory input from PasI.

The Toxic and Stress Resistance Effects of PasT Are Separable

The *pasTI* locus is well conserved in all sequenced *E. coli* strains, with the exception of 23 nucleotide changes within the *pasT* gene that are found primarily in ExPEC isolates (Figure 7E). These ExPEC-associated alterations are silent, except for two that result in amino acid changes (S90N and D111E) relative to the K-12 sequence. Despite these differences, both K-12 and ExPEC versions of *pasT* enhanced the resistance of CFT073Δ*pasTI* to stresses like ASN, and both were similarly toxic when expressed at high levels (Figure 7A–B). Deletion of *pasTI* did not increase the sensitivity of MG1655 to ASN (Figure 7D), possibly due to input from other TA systems acting redundantly in this K-12 strain. However, low-level expression of *pasT* alleles did increase the resistance of MG1655 to ASN, indicating that the salubrious, non-toxic effects of PasT can be discerned in K-12 strains as well as pathogens under appropriate conditions.

Using a series of genetic truncations and fusions, we next asked if the stress resistance and toxic, growth-inhibiting effects of PasT could be mapped to separable regions (Figure 8A). Removal of the N-terminal 9 to 13 amino acids of PasT completely abrogated its toxicity when overexpressed in CFT073Δ*pasTI*, as did fusion with N-terminal FLAG or His_6 epitope tags or an even smaller two-

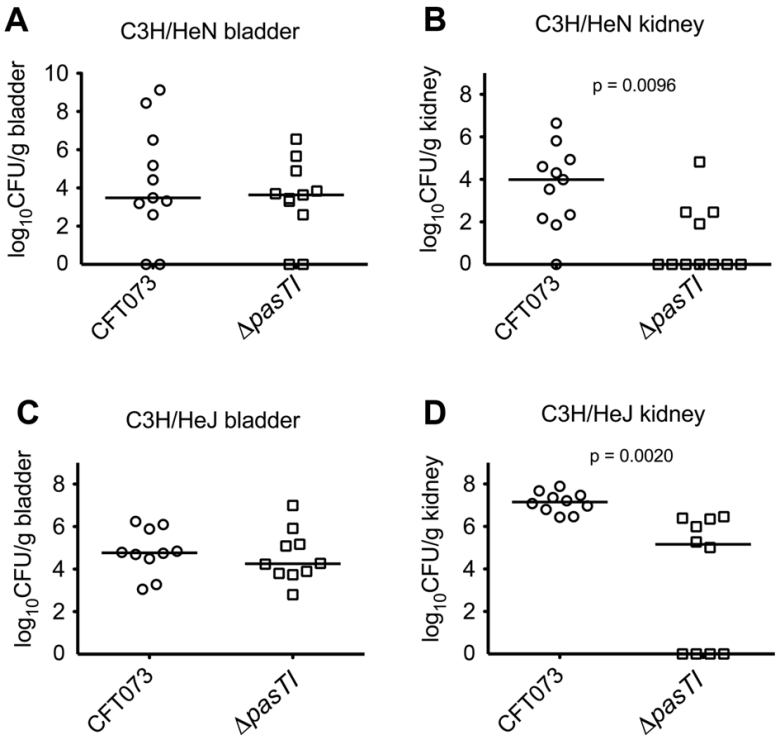

Figure 3. Defective colonization of the kidneys by CFT073Δ*pasTI* in C3H/HeN and C3H/HeJ mice. Adult female (A–B) C3H/HeN and (C–D) C3H/HeJ mice were infected via catheterization with equal numbers of wild type CFT073 and CFT073Δ*pasTI*. Graphs show bacterial titers present in the (A, C) bladders and (B, D) kidneys at 3 d post-inoculation. Bars indicate median values for each group; n≥10 mice per competitive assay. *P* values were determined using the Wilcoxon-matched paired signed rank test.
doi:10.1371/journal.ppat.1002954.g003

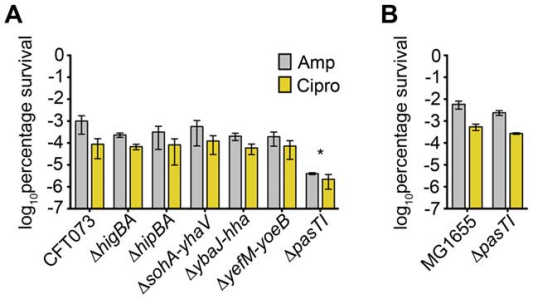

Figure 4. Persister cell formation by CFT073, but not MG1655, requires PasTI. Development of persister cells by (A) wild type CFT073 and associated type II TA system knockout mutants or (B) MG1655 and associated Δ*pasTI* mutant 5 h after the addition of 100 μg/mL ampicillin or 10 μg/mL ciprofloxacin to cultures in exponential growth phase. Data represent mean results ± SD from three independent experiments. *P* values were determined by Student's *t* test.
doi:10.1371/journal.ppat.1002954.g004

amino acid (DP) addition. Although no longer toxic, these PasT variants were still able to restore wild type growth of CFT073Δ*pasTI* on agar plates and in the presence of ASN (Figure 8A). Overexpression of a non-toxic version of PasT (DP-PasT) also enhanced the resistance of MG1655 to nitrosative stress (Figure 7D). The addition of C-terminal epitope tags had no effect on PasT functionality (Figure 8A). Overexpression of just the N-terminal 69 residues of PasT was sufficient to induce growth arrest, but low-level expression of this PasT fragment provided no benefits on agar plates or upon exposure to ASN. As assessed by Western blot analysis, loss of PasT toxicity by modification of its N-terminus was not due to reduced expression of the non-toxic PasT variants relative to the full-length protein (Figure 8B). However, removal of the N-terminal 29 residues of PasT did render it barely detectable by western blot (Figure 8B), coordinate with loss of both the toxic and stress-resistance activities of this PasT mutant (Figure 8A). In total, these results demonstrate that the toxic and stress resistance effects of PasT can be uncoupled.

In light of these results, we next assessed the role of PasT in the development of persister cells by CFT073. The attenuated ability of CFT073Δ*pasTI* to form persisters in the presence of ciprofloxacin (Figure 4A), was rescued by low-level expression of either full-length PasT or the N-terminal 69 amino acid toxic domain (Figure 8A and Figure S4). In contrast, expression of non-toxic variants of PasT did not complement the Δ*pasTI* mutant in persister assays. We conclude that the same N-terminal toxic domain of PasT that halts bacterial growth when overexpressed also promotes the development of persister cells in the presence of antibiotic stress.

Discussion

Chromosomal TA systems are widespread and functionally diverse, having the capacity to modulate an array of bacterial activities including phage resistance, biofilm formation, and persister cell development [17,23,37]. Results presented here extend these findings, demonstrating that type II TA systems can act independently within ExPEC to increase stress and antibiotic resistance as well as pathogen colonization and persistence within host tissues. Using a mouse UTI model we found that the YefM-YoeB and YbaJ-Hha TA systems each enhanced bladder colonization by the ExPEC isolate CFT073, but had no significant effect on bacterial colonization of the kidneys in competitive assays (Figure 2C–D). On the other hand, the PasTI TA system was not required for CFT073 survival within the bladder or intestinal tract but did promote pathogen colonization and persistence within the kidneys in both competitive and non-competitive assays (Figs. 2E–H, 3, and S2). These results indicate that individual TA systems can have profound effects on bacterial fitness within distinct host environments. It is feasible that phenotypes associated with some of the TA system mutants, but not discernable in the assays used in this study, may become evident by analysis of additional time points and possibly other hosts and environmental challenges.

The specific mechanisms by which these TA systems stimulate UPEC colonization of the host are likely complex. YoeB is an endoribonuclease that cleaves mRNA situated within the ribosomal A site [38], and the *yefM-yoeB* locus is one of 10 type II TA loci that can work cooperatively to facilitate persister cell formation by the K-12 *E. coli* strain MG1655 [9]. The toxin Hha acts differently, repressing the transcription of rare codon tRNAs and consequently inhibiting the expression of type 1 pili and the pore-forming toxin HlyA, among other genes [8,39]. In K-12 *E. coli*, Hha activity can also stimulate bacterial cell lysis and biofilm dispersal [8]. In our assays, none of the type II TA system mutants, including Δ*yefM-yoeB* and Δ*ybaJ-hha*, were negatively affected in their ability to express type 1 pili or HlyA, and none were impaired in biofilm production in microtiter plate assays (data not shown). Furthermore, deletion of either *yefM-yoeB* or *ybaJ-hha* individually did not affect the development of persister cells in the face of ciprofloxacin or ampicillin (Figure 4A), leaving open the question of how these two TA systems contribute to UPEC survival within the bladder.

In contrast to the Δ*yefM-yoeB* and Δ*ybaJ-hha* strains, CFT073 lacking *pasTI* was significantly compromised in its capacity to form persister cells (Figure 4A). Our ability to detect clear phenotypic defects in these assays with CFT073Δ*pasTI*, but not with MG1655Δ*pasTI*, is likely attributable to decreased functional redundancy among the fewer TA systems carried by CFT073 relative to the K-12 strain [9]. The generation of persisters mediated by TA systems like PasTI may enhance the long-term survival of UPEC under hostile conditions within the host, including the administration of antibiotics used to treat UTIs [29]. However, persister cell formation does not appear to be the only way by which PasTI may promote UPEC survival *in vivo*. Specifically, low-level expression of PasT substantially increased the resistance of CFT073 to nitrosative and oxidative stresses, and enhanced growth of the pathogen under nutrient-limiting conditions. These environmental stresses are commonly encountered by UPEC during the course of a UTI [30,40,41,42,43]. Inherent differences between the bladder and kidney environments, such as the distribution of pathogen recognition receptors and dissimilar concentrations of various antimicrobial factors [44,45], may account for the differential effects of *pasTI* deletion on bacterial fitness in the bladder versus the kidneys.

In this study, host defenses that may limit colonization of the kidneys by the Δ*pasTI* mutant were further assessed using C3H/HeJ mice (Figure 3). These animals have an impaired ability to respond to lipopolysaccharide (LPS) and increased susceptibility to both bladder and kidney infections [46,47]. The increased sensitivity of C3H/HeJ mice to kidney infections has been linked by quantitative trait loci analysis to a site on chromosome 6, with possible input from loci on chromosomes 1, 4, and 9 [46]. Specific genes suggested to mediate host resistance to kidney infections include those encoding Toll-like receptor 5 (Tlr5) and the antimicrobial peptide cathelicidin. In our assays, we observed elevated levels of both wild type CFT073 and the Δ*pasTI* mutant

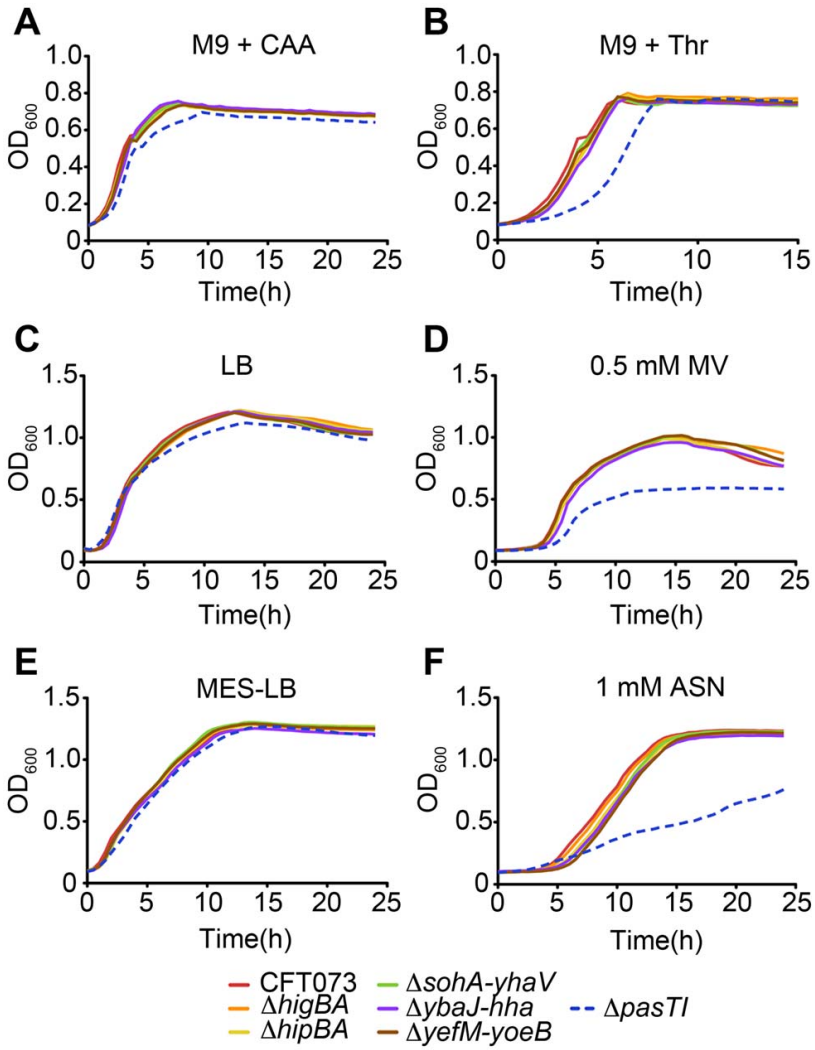

Figure 5. PasTI promotes the stress resistance of CFT073. Growth of wild type CFT073 and type II TA system knockouts in (A) M9 medium+0.2% casein amino acids, (B) a modified, lower-nutrient M9 medium+Thr, (C) LB broth, (D) LB broth containing 0.5 mM MV, (E) LB buffered to pH 5.0 with MES (MES-LB), and (F) MES-LB with 1 mM ASN. Graphs are representative of at least three independent experiments performed in quadruplicate.
doi:10.1371/journal.ppat.1002954.g005

in the bladders and kidneys of infected C3H/HeJ mice, relative to control immunocompetent C3H/HeN animals. However, kidney colonization by CFT073Δ*pasTI* was significantly attenuated in both types of mice, despite the overall increased sensitivity of the C3H/HeJ animals to UTI. These results indicate that the PasTI system promotes UPEC resistance to factors present in the kidneys of both the C3H/HeJ and C3H/HeN strains. Our *in vitro* assays (Figure 5) suggest that these defensive host factors may include amino acid limitation, superoxide radicals, and reactive nitrogen species.

The *pasT* locus is predicted to encode an oligoketide cyclase, while the *pasI* gene product is predicted to assume a ubiquitin-like β-grasp fold, a structural motif that is present in a wide variety of functionally distinct proteins [48,49]. Previous work demonstrated that PasT could bind 50S ribosomal subunits and thereby inhibit protein translation [7]. In that study, PasT was referred to as RatA, for **R**ibosomal **a**ssociated **t**oxin A. We opted to avoid use of this name in the current study to reduce confusion with i) the *ratA* antitoxin encoded by *Bacillus subtilis* [50] and ii) the unrelated RatA and RatA-like proteins that are expressed by *Salmonella* species as well as many ExPEC isolates (e.g. NP_754911). Consequently, we refer to RatAB here as PasTI, for **P**ersistence **a**nd **s**tress-resistance **T**oxin and **I**mmunity proteins.

PasT functioned like a toxin and inhibited bacterial growth in our assays only when expressed at high levels, similar to toxins within other TA systems. The toxic effects of PasT were completely reversible by induced expression of PasI, confirming that these two proteins can function as a TA pair (Figure 7). The

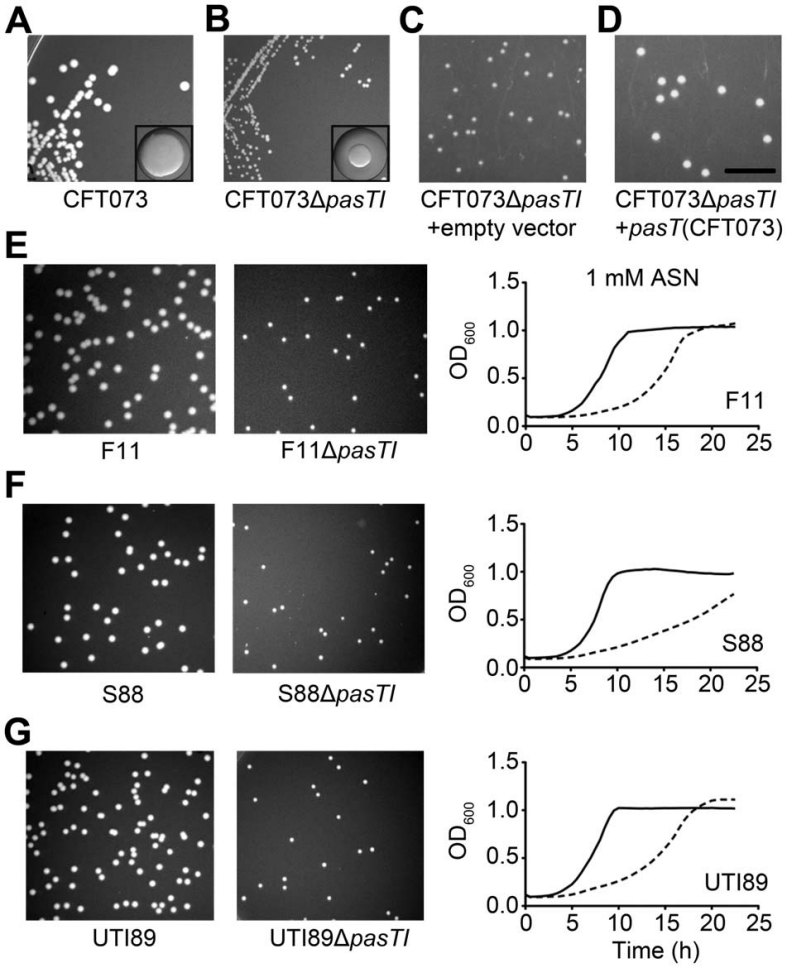

Figure 6. Deletion of *pasTI* reduces the stress resistance of multiple ExPEC isolates. (A–B) Images show wild type and CFT073Δ*pasTI* colonies on LB agar after overnight growth at 37°C; inset images show images of individual wild type and CFT073Δ*pasTI* colonies at identical magnification. (C–D) Colony sizes of CFT073Δ*pasTI* complemented with empty vector (pRR48) or pPN007, which allows for leaky expression of PasT from a P*tac* promoter. (E–G, left) Images show colonies of ExPEC strains and associated Δ*pasTI* mutants on LB agar after overnight growth at 37°C. (E–G, right) Growth of the ExPEC Δ*pasTI* mutants in 1 mM ASN is delayed compared to wild type. In each graph, solid lines represent the wild type strains and dashed lines indicate the Δ*pasTI* mutants. Images in A–G were taken at the same magnification (scale bar, 1 cm). All Δ*pasTI* colonies eventually reach wild type size.
doi:10.1371/journal.ppat.1002954.g006

toxic effects of PasT were also ameliorated by modification of its N-terminus, either by the removal or addition of amino acids. Although no longer toxic when overexpressed, many of these PasT variants still maintained their salubrious functions, enhancing bacterial resistance to oxidative and nitrosative stresses. Loss of toxicity associated with these mutant proteins was not due to diminished PasT levels within the bacteria, but instead likely results from altered substrate recognition and/or activity. Regardless of the mode of action, these data show that the toxic and salubrious effects of PasT are separable. Consequently, it is feasible that the disparate functions of PasT may be differentially regulated in order to optimize bacterial stress resistance and persister cell phenotypes in response to changing environmental pressures. This may be especially important to the PasTI-dependent development of persister cells in the presence of antibiotics, a process that requires the N-terminal toxic domain of PasT.

Relative to other *E. coli* isolates, ExPEC and other members of the B2 phylotype encode a condensed set of the known type II TA systems. *E. coli* strains are traditionally grouped within the B2 phylotype based in part on the presence of distinct virulence factors, such as fimbrial and toxin genes like *papA*, *sfa/foc*, *hly*, and *cnf1* [51,52]. It is remarkable that members of the B2 phylotype can also be distinguished from other *E. coli* isolates based solely on the makeup of their type II TA systems (see Figure 1A and Dataset S1). This suggests a common lineage among B2 strains in which a core set of TA systems has been selected. The ability to discern clear-cut phenotypes associated with the deletion of individual TA

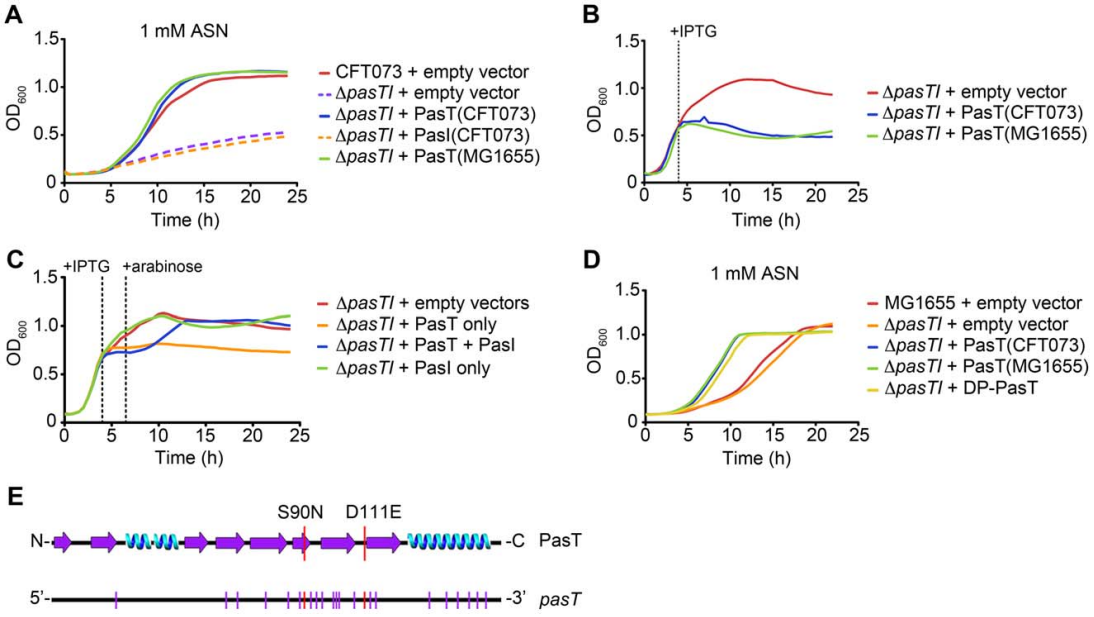

Figure 7. PasT has stress resistance and toxic effects, the latter of which can be countered by PasI. (A–C) Graphs show growth of recombinant CFT073 strains in (A) 1 mM ASN or (B, C) standard LB broth. (D) Curves show growth of recombinant MG1655 strains in 1 mM ASN. In B and C, IPTG and arabinose were added as indicated to induce high-level expression of PasT and PasI, respectively. (A, D) Alternatively, recombinant PasT and PasI were expressed at lower levels from a leaky P*tac* promoter. The *pasT* gene cloned from MG1655 was used as indicated. Otherwise, recombinant genes were derived from CFT073. Graphs are representative of at least 3 independent experiments performed in quadruplicate. (E) Bottom, the *pasT* gene carried by CFT073 and other ExPEC has a conserved set of synonymous (purple hashes) and two non-synonymous (red hashes) base pair changes relative to *pasT* encoded by MG1655 and many other *E. coli* strains. Top, the predicted secondary structure of PasT, with two conserved amino acid differences between the MG1655 and ExPEC-associated protein sequences highlighted.
doi:10.1371/journal.ppat.1002954.g007

loci in ExPEC indicates that the fitness of these pathogens is likely more dependent on specific TA systems than K-12 strains like MG1655. These findings reveal the potential utility of ExPEC for defining the functional relevance of discrete TA systems, while also highlighting TA systems as compelling targets for therapeutic intervention. For example, compounds that selectively disrupt TA systems like PasTI may effectively attenuate the survival and growth of ExPEC within the host while having nominal effects on commensal *E. coli* strains that encode a larger, seemingly more redundant repertoire of TA systems.

Materials and Methods

Ethics Statement

Mice used in this study were handled in accordance with protocols approved by the Institutional Animal Care and Use Committee at the University of Utah (Protocol number 10-02014), following US federal guidelines indicated by the Office of Laboratory Animal Welfare (OLAW) and described in the Guide for the Care and Use of Laboratory Animals, 8th Edition.

Cluster Analysis of Type II TA Loci in Sequenced *E. coli* Strains

Specific allelic values were assigned to indicate the presence, absence, or truncation of the known type II TA loci encoded by *E. coli* strains. These values were used to create an allelic profile for each fully sequenced *E. coli* isolate. The compiled allelic profiles were analyzed using the eBURST algorithm (http://eburst.mlst.net/) with 1,000 bootstrap iterations to organize strains into clusters within groups that share 17 out of 21 alleles [25]. See Dataset S1 (Excel) for further details on the assembly, grouping, and analysis of type II TA alleles by the eBURST algorithm.

Genomic Localization of Type II TA Systems

Genomic locations of known type II TA systems encoded by MG1655 and CFT073 were obtained from NCBI and mapped onto circles that are proportional to the genome size of each strain. Origins of replication (OriC) were determined based on homology to "oriC" sequence: ATCTATTTATTTAGAGATCTGTTC-TATTGTGATCTCTTATTAGGATCGCACTGCCCTGTGG ATAACAAGGATCCGGCTTTTAAGATCAACAACCTGGA AAGGATCATTAACTGTGAATGATCGGTGATCCTGGAC CGTATAAGCTGGGATCAGAATGAGGGGTTATACACAA CTCAAAAACTGAACAACAGTTGTTCTTTGGATAACTA CCGGTTGATCCAAGCTTCCTGA.

Bacterial Strains and Plasmids

All bacterial strains and plasmids used in this study are listed in Tables S1 and S2. *E. coli* strains MG1655, CFT073, UTI89, F11, and S88 have been described previously [28,53,54,55]. PasT and PasI expression constructs were made using standard molecular biology techniques employing the plasmids pRR48 and pBAD33 [56,57]. Gene expression from the P*tac* promoter in the pRR48 backbone was induced by addition of 500 μM isopropyl-β-D-thiogalactopyranoside (IPTG), while gene expression from the pBAD33 promoter was induced using 0.2% L-arabinose. Primers

A

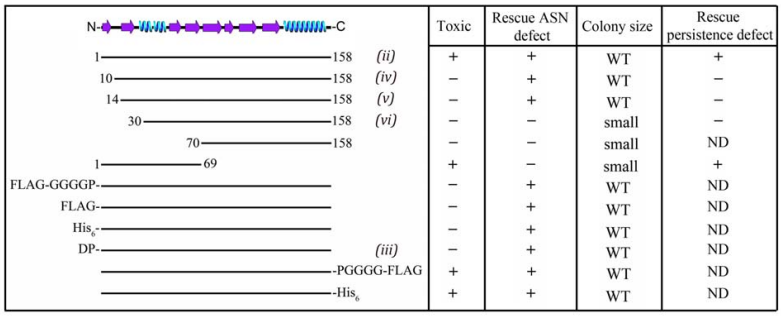

Toxic	Rescue ASN defect	Colony size	Rescue persistence defect
+	+	WT	+
−	+	WT	−
−	+	WT	−
−	−	small	−
−	−	small	ND
+	−	small	+
−	+	WT	ND
−	+	WT	ND
−	+	WT	ND
−	+	WT	ND
+	+	WT	ND
+	+	WT	ND

B

Figure 8. The toxic and salubrious effects of PasT can be genetically uncoupled. (A) Table indicates if the specified PasT truncation mutants and fusions display toxic, growth inhibitory effects when overexpressed in CFT073Δ*pasTI*, if their leaky expression rescues wild type (WT) growth of the Δ*pasTI* mutant in 1 mM ASN and on LB agar plates, and if their leaky expression rescues the ability of CFT073Δ*pasTI* to form persisters in the presence of ciprofloxacin (10 μg/mL). ND, not determined. (B) Western blot shows expression levels of C-terminal FLAG-tagged PasT constructs—denoted (ii)–(vi), as in (A)—following induction with IPTG. Lane (i) represents an empty vector control. A nonspecific band recognized by the anti-FLAG antibody was used as loading control. Equal loading was also verified by Coomassie staining (data not shown).
doi:10.1371/journal.ppat.1002954.g008

and restriction sites used to construct all plasmids are indicated in Table S3, along with primers used to verify each clone by sequencing. Antibiotics (50 μg/mL kanamycin, 20 μg/mL chloramphenicol, or 100 g/mL ampicillin) were added to plates and growth medium to select for and maintain plasmids when necessary.

Targeted gene knockouts were generated in CFT073, MG1655, UTI89, F11, and S88 using the lambda Red-mediated linear transformation system [58,59]. Briefly, a kanamycin resistance cassette was amplified from pKD4 with 40-base pair overhangs specific to the 5′ and 3′ ends of each target TA system locus (*higBA, hipBA, sohA-yhaV, ybaJ-hha, yefM-yoeB,* or *pasTI*). PCR products were introduced via electroporation into the strains carrying pKM208, which encodes for an IPTG-inducible lambda red recombinase. Knockouts were confirmed by PCR using the primers listed in Table S3. The chloramphenicol resistant cassette amplified from pKD3 was similarly added to the chromosome of CFT073, inserted within the intergenic region between genes *c3028* and *c3029* to create CFT073-Clm^R. This strain serves as a tagged wild type control in the gastrointestinal tract colonization assays.

Mouse UTI Model

Seven- to nine-week old female CBA/J mice (Jackson Labs), C3H/HeN mice (Harlan Laboratories), or C3H/HeJ mice (Jackson Labs) were used in accordance with IACUC-approved protocols as previously described [29,60,61]. Mice were anesthetized using isoflurane inhalation and inoculated via transurethral catheterization with 50 μL of a bacterial suspension containing approximately 1×10^7 bacteria. CFT073 and isogenic knockout mutants were grown statically for 24 h in M9 medium, pelleted by spinning at 10,000 r.c.f. for 8 min, and resuspended in phosphate buffered saline (PBS) prior to inoculation. For competition assays, wild type and mutant strains were mixed 1:1 prior to inoculation. The 1:1 inoculation dosage was confirmed by plating serial dilutions on LB plates and LB plates containing 50 μg/mL kanamycin. Bladders and kidneys were recovered 1 or 3 d later, as indicated, and each was weighed and homogenized in 1 mL containing 0.025% Triton X-100. Homogenates were serially diluted and plated on LB agar plates to determine the number of bacteria per gram of tissue. For competition assays, plates containing kanamycin (50 μg/mL) were used to identify and enumerate the TA system knockout mutants, which carried Kan^R cassettes. Mouse experiments were repeated at least twice, and the total combined data from 10 or more animals is presented.

UPEC Colonization of the Murine Gastrointestinal Tract

Cultures of CFT073-Clm^R (containing a chromosomal chloramphenicol-resistance cassette, *clm^R*) and CFT073Δ*pasTI* (*kan^R*) grown 20 mL static in M9 broth were pelleted and resuspended in PBS. Adult female CBA/J mice were each gavaged with 50 μL of the bacterial suspension containing 1×10^9 CFU. Feces (~100 mg) were collected at the indicated time points, weighed, and resuspended in 1 mL 0.7% NaCl. Serial dilutions were plated on LB agar containing either chloramphenicol (10 μg/mL) or kanamycin (50 μg/mL) in order to distinguish the Δ*pasTI* mutant and the Clm^R-tagged strains. Mice receiving the CFT073 strains showed no overt signs of sickness. No chloramphenicol- or kanamycin-resistant bacteria were recovered in the feces of untreated mice.

Statistics

Results from *in vivo* competition assays were analyzed by Wilcoxon matched-pairs signed rank test. Results from non-competitive assays in mice, including comparisons between 1- and 3-day titers of wild type CFT073 and CFT073Δ*pasTI* in the kidneys, were analyzed by Mann-Whitney two-tailed *t* tests. All statistical tests were performed using Prism 5.0c (GraphPad Software, Inc.). *P* values less than 0.05 are considered significant.

Persister Assays

Persister assays were carried out with CFT073, MG1655, and their derivatives as previously described [9]. Briefly, 1 μg/mL

ciprofloxacin or 100 μg/mL ampicillin was added to logarithmically growing bacterial cultures in LB broth and 5 h later the cultures were pelleted, washed once with PBS, and surviving bacteria were serially diluted and plated on LB agar. Total numbers of persister cells were calculated by dividing the number of viable bacteria present after antibiotic treatment by the number present prior to antibiotic addition.

Growth Assays

Cultures of CFT073, MG1655 and their derivatives were grown shaking overnight at 37°C in 5 mL of LB broth, 100 mM morpholineethanesulfonic acid (MES)-buffered LB (MES-LB; pH 5.0), or modified M9 minimal medium+casein amino acids (6 g/L Na_2HPO_4, 3 g/L KH_2PO_4, 1 g/L NH_4Cl, 0.5 g/L NaCl, 1 mM $MgSO_4$, 0.1 mM $CaCl_2$, 0.1% glucose, 0.0025% nicotinic acid, 16.5 μg/mL thiamine, and 0.2% casein amino acids). Overnight cultures were diluted 1:100 and growth of quadruplicate 200-μl samples in 100-well honeycomb plates was assessed at 37°C using a Bioscreen C instrument (Growth Curves USA). Bacteria assayed for growth in 1 mM acidified sodium nitrite (ASN) were first grown from frozen stocks overnight in MES-LB. Strains assayed for growth in more nutrient-limited, M9 medium supplemented with threonine (6 g/L Na_2HPO_4, 3 g/L KH_2PO_4, 1 g/L NH_4Cl, 0.5 g/L NaCl, 1 mM $MgSO_4$, 0.1 mM $CaCl_2$, 0.2% glucose, 0.0025% nicotinic acid, 40 μg/mL threonine, and 16.5 μg/mL thiamine) were initiated from cultures grown overnight in standard M9 medium. IPTG (500 μM) and 0.2% L-arabinose were added to cultures to induce high-level expression of PasT or PasI, as indicated. Methyl viologen (MV; a.k.a. paraquat) and ASN were prepared fresh prior to addition to LB or MES-LB broth cultures, respectively. All reagents were obtained from Sigma-Aldrich.

Allelic Variants of *pasT* and Predicted Domain Structure of the Protein

The *pasT* nucleotide sequences of from ExPEC and K-12 strains were aligned and compared using ClustalX (downloaded at http://www.clustal.org/clustal2/) [62]. The secondary structure of PasT was predicted using Protein Homology/analogY Recognition Engine V 2.0 (Phyre[2]; http://www.sbg.bio.ic.ac.uk/phyre2/html/page.cgi?id = index) [49].

Protein Analysis

Cultures of each strain indicated were grown overnight shaking in LB broth plus 100 μg/mL ampicillin (added for plasmid retention). Cultures were diluted 1:50 into fresh LB broth and grown shaking at 37°C for 5 h, at which point IPTG was added to each culture to a final concentration of 500 μM. After an additional 1 h incubation, 1 mL of each culture was pelleted and resuspended in 200 μL SDS-TE (0.5% SDS in Tris-EDTA, pH 8.0). Proteins were resolved by SDS-PAGE and transferred to Immobilon PVDF-FL membrane (Millipore). Western blots were probed using ANTI-FLAG M2 antibody (Sigma-Aldrich) and visualized by enhanced chemiluminescence as previously described [63].

Supporting Information

Dataset S1 Tables used to define the Type II TA system allelic profiles of *E. coli* by eBURST analysis. (Tab 1) Table showing TA system content among sequenced *E. coli*. (Tab 2) Table showing TA system content among phylotype B2 ExPEC strains. (Tab 3) Graph of the relative abundance of TA systems among all sequenced *E. coli* strains versus phylotype B2 isoaltes. (Tab 4) Table shows the individual allelic profiles of type II TA systems generated from Tab 1. (Tab 5) Table of allelic profiles that were used for input into the eBURST algorithm. (Tab 6) Separate tables with representative output from the eBURST algorithm, showing how the strains that are clustered together shift dependent upon based on the number of shared type II TA alleles considered.
(XLS)

Figure S1 The CFT073Δ*yefM-yoeB* and CFT073Δ*ybaJ-hha* mutants colonize the murine urinary tract at similar levels to wild type CFT073 in noncompetitive assays. (A–D) Adult female C3H/HeN and C3H/HeJ mice were infected via catheterization with 10^7 CFU of wild type CFT073, CFT073Δ*yefM-yoeB* or CFT073Δ*ybaJ-hha*. Graphs show bacterial titers present in the (A) bladders and (B) kidneys at 3 d post-inoculation. Bars indicate median values for each group; n≥10 mice. *P* values were determined using Mann-Whitney U tests.
(TIF)

Figure S2 CFT073 does not require *pasTI* for colonization of the murine gastrointestinal tract. Adult female CBA/J mice were each gavaged with 50 μL of a bacterial suspension containing 1×10^9 CFU CFT073-Clm^R or CFT073Δ*pasTI* (*kan*^{R}). CFT073-Clm^R served as the wild type control in these assays. Gastrointestinal tract colonization was assessed by enumerating total CFU of the mutant and wild type strains per gram of feces collected at the indicated time points. Data represent mean CFU/g feces ± SEM. n = 3 to 5 mice.
(TIF)

Figure S3 Low-level expression of PasT does not alter growth of the Δ*pasTI* mutant, while transcription of PasTI from its native promoter provides resistance to ASN. Curves show growth of CFT073 and its derivatives in (A) LB broth and (B) MES-LB broth+1 mM ASN. (A) Leaky expression of *pasT* from a P*tac* promoter or expression of *pasTI* from its native promoter does not affect the growth of CFT073Δ*pasTI* in standard LB broth. In these assays, pRR48 served as an empty vector control. (B) Complementation of the Δ*pasTI* mutant growth defect in 1 mM ASN by the *pasTI* operon from its native promoter. Graphs are representative of at least two independent experiments performed in quadruplicate.
(TIF)

Figure S4 Persister cell formation by CFT073 requires the toxic domain of PasT. Graph shows numbers of viable bacteria (persisters) recovered 5 h after the addition of ciprofloxacin (10 μg/L) to broth cultures in exponential growth phase. The plasmid pRR48 serves as an empty vector control. Plasmid pPN007 encodes full-length PasT, pPN055 encodes the N-terminal 69 amino acids of PasT, and pPN068–069 encode non-toxic PasT variants lacking portions of the PasT N-terminus (see Figure 8). Data represent mean results ± SD from three independent experiments. *P* values were determined by Student's *t* test; ns indicates non-significant differences between the complemented strain and CFT073Δ*pasTI*/pRR48.
(TIF)

Table S1 Strains used in this study.
(PDF)

Table S2 Plasmids used in this study.
(PDF)

Table S3 Primers used in this study.
(PDF)

Acknowledgments

We thank Erick Denamur for providing S88 and Travis Wiles for CFT073-Clm^R.

Author Contributions

Conceived and designed the experiments: MAM JPN. Performed the experiments: JPN. Analyzed the data: MAM JPN. Contributed reagents/materials/analysis tools: MAM JPN. Wrote the paper: MAM JPN.

References

1. Blower TR, Salmond GP, Luisi BF (2011) Balancing at survival's edge: the structure and adaptive benefits of prokaryotic toxin-antitoxin partners. Curr Opin Struct Biol 21: 109–118.
2. Yamaguchi Y, Inouye M (2011) Regulation of growth and death in *Escherichia coli* by toxin-antitoxin systems. Nat Rev Microbiol 9: 779–790.
3. Fozo EM, Makarova KS, Shabalina SA, Yutin N, Koonin EV, et al. (2010) Abundance of type I toxin-antitoxin systems in bacteria: searches for new candidates and discovery of novel families. Nucleic Acids Res 38: 3743–3759.
4. Blower TR, Pei XY, Short FL, Fineran PC, Humphreys DP, et al. (2011) A processed noncoding RNA regulates an altruistic bacterial antiviral system. Nat Struct Mol Biol 18: 185–190.
5. Mutschler H, Gebhardt M, Shoeman RL, Meinhart A (2011) A novel mechanism of programmed cell death in bacteria by toxin-antitoxin systems corrupts peptidoglycan synthesis. PLoS Biol 9: e1001033.
6. Tan Q, Awano N, Inouye M (2011) YeeV is an *Escherichia coli* toxin that inhibits cell division by targeting the cytoskeleton proteins, FtsZ and MreB. Mol Microbiol 79: 109–118.
7. Zhang Y, Inouye M (2011) RatA (YfjG), an *Escherichia coli* toxin, inhibits 70S ribosome association to block translation initiation. Mol Microbiol 79: 1418–1429.
8. Garcia-Contreras R, Zhang XS, Kim Y, Wood TK (2008) Protein translation and cell death: the role of rare tRNAs in biofilm formation and in activating dormant phage killer genes. PLoS ONE 3: e2394.
9. Maisonneuve E, Shakespeare LJ, Jorgensen MG, Gerdes K (2011) Bacterial persistence by RNA endonucleases. Proc Natl Acad Sci U S A 108: 13206–13211.
10. Lehnherr H, Maguin E, Jafri S, Yarmolinsky MB (1993) Plasmid addiction genes of bacteriophage P1: doc, which causes cell death on curing of prophage, and phd, which prevents host death when prophage is retained. J Mol Biol 233: 414–428.
11. Van Melderen L, Saavedra De Bast M (2009) Bacterial toxin-antitoxin systems: more than selfish entities? PLoS Genet 5: e1000437.
12. Tsilibaris V, Maenhaut-Michel G, Mine N, Van Melderen L (2007) What is the benefit to *Escherichia coli* of having multiple toxin-antitoxin systems in its genome? J Bacteriol 189: 6101–6108.
13. Van Melderen L (2010) Toxin-antitoxin systems: why so many, what for? Curr Opin Microbiol 13: 781–785.
14. Fiebig A, Castro Rojas CM, Siegal-Gaskins D, Crosson S (2010) Interaction specificity, toxicity and regulation of a paralogous set of ParE/RelE-family toxin-antitoxin systems. Mol Microbiol 77: 236–251.
15. Christensen-Dalsgaard M, Jorgensen MG, Gerdes K (2010) Three new RelE-homologous mRNA interferases of *Escherichia coli* differentially induced by environmental stresses. Mol Microbiol 75: 333–348.
16. Ramage HR, Connolly LE, Cox JS (2009) Comprehensive functional analysis of *Mycobacterium tuberculosis* toxin-antitoxin systems: implications for pathogenesis, stress responses, and evolution. PLoS Genet 5: e1000767.
17. Magnuson RD (2007) Hypothetical functions of toxin-antitoxin systems. J Bacteriol 189: 6089–6092.
18. Gerdes K, Christensen SK, Lobner-Olesen A (2005) Prokaryotic toxin-antitoxin stress response loci. Nat Rev Microbiol 3: 371–382.
19. Leplae R, Geeraerts D, Hallez R, Guglielmini J, Dreze P, et al. (2011) Diversity of bacterial type II toxin-antitoxin systems: a comprehensive search and functional analysis of novel families. Nucleic Acids Res 39: 5513–5525.
20. McKenzie JL, Robson J, Berney M, Smith TC, Ruthe A, et al. (2012) A VapBC Toxin-Antitoxin Module is a Post-Transcriptional Regulator of Metabolic Flux in Mycobacteria. J Bacteriol 194: 2189–2204.
21. Kasari V, Kurg K, Margus T, Tenson T, Kaldalu N (2010) The *Escherichia coli* mqsR and ygiT genes encode a new toxin-antitoxin pair. J Bacteriol 192: 2908–2919.
22. Zhang XS, Garcia-Contreras R, Wood TK (2008) *Escherichia coli* transcription factor YncC (McbR) regulates colanic acid and biofilm formation by repressing expression of periplasmic protein YbiM (McbA). ISME J 2: 615–631.
23. Wang X, Wood TK (2011) Toxin-antitoxin systems influence biofilm and persister cell formation and the general stress response. Appl Environ Microbiol 77: 5577–5583.
24. Kaper JB, Nataro JP, Mobley HL (2004) Pathogenic *Escherichia coli*. Nat Rev Microbiol 2: 123–140.
25. Feil EJ, Li BC, Aanensen DM, Hanage WP, Spratt BG (2004) eBURST: inferring patterns of evolutionary descent among clusters of related bacterial genotypes from multilocus sequence typing data. J Bacteriol 186: 1518–1530.
26. Johnson JR, Clermont O, Menard M, Kuskowski MA, Picard B, et al. (2006) Experimental mouse lethality of *Escherichia coli* isolates, in relation to accessory traits, phylogenetic group, and ecological source. J Infect Dis 194: 1141–1150.
27. Le Gall T, Clermont O, Gouriou S, Picard B, Nassif X, et al. (2007) Extraintestinal virulence is a coincidental by-product of commensalism in B2 phylogenetic group *Escherichia coli* strains. Mol Biol Evol 24: 2373–2384.
28. Welch RA, Burland V, Plunkett G, 3rd, Redford P, Roesch P, et al. (2002) Extensive mosaic structure revealed by the complete genome sequence of uropathogenic *Escherichia coli*. Proc Natl Acad Sci U S A 99: 17020–17024.
29. Blango MG, Mulvey MA (2010) Persistence of uropathogenic *Escherichia coli* in the face of multiple antibiotics. Antimicrob Agents Chemother 54: 1855–1863.
30. Alteri CJ, Smith SN, Mobley HL (2009) Fitness of *Escherichia coli* during urinary tract infection requires gluconeogenesis and the TCA cycle. PLoS Pathog 5: e1000448.
31. Lennon JT, Jones SE (2011) Microbial seed banks: the ecological and evolutionary implications of dormancy. Nat Rev Microbiol 9: 119–130.
32. Shah D, Zhang Z, Khodursky A, Kaldalu N, Kurg K, et al. (2006) Persisters: a distinct physiological state of *E. coli*. BMC Microbiol 6: 53.
33. Anfora AT, Haugen BJ, Roesch P, Redford P, Welch RA (2007) Roles of serine accumulation and catabolism in the colonization of the murine urinary tract by *Escherichia coli* CFT073. Infect Immun 75: 5298–5304.
34. Bower JM, Mulvey MA (2006) Polyamine-mediated resistance of uropathogenic *Escherichia coli* to nitrosative stress. J Bacteriol 188: 928–933.
35. Woolford G, Casselden RJ, Walters CL (1972) Gaseous products of the interaction of sodium nitrite with procine skeletal muscle. Biochem J 130: 82P–83P.
36. Cuny C, Lesbats M, Dukan S (2007) Induction of a global stress response during the first step of *Escherichia coli* plate growth. Appl Environ Microbiol 73: 885–889.
37. Lewis K (2010) Persister cells. Annu Rev Microbiol 64: 357–372.
38. Christensen-Dalsgaard M, Gerdes K (2008) Translation affects YoeB and MazF messenger RNA interferase activities by different mechanisms. Nucleic Acids Res 36: 6472–6481.
39. Nieto JM, Madrid C, Prenafeta A, Miquelay E, Balsalobre C, et al. (2000) Expression of the hemolysin operon in *Escherichia coli* is modulated by a nucleoid-protein complex that includes the proteins Hha and H-NS. Mol Gen Genetics 263: 349–358.
40. Bower JM, Gordon-Raagas HB, Mulvey MA (2009) Conditioning of uropathogenic *Escherichia coli* for enhanced colonization of host. Infect Immun 77: 2104–2112.
41. Johnson JR, Clabots C, Rosen H (2006) Effect of inactivation of the global oxidative stress regulator oxyR on the colonization ability of *Escherichia coli* O1:K1:H7 in a mouse model of ascending urinary tract infection. Infect Immun 74: 461–468.
42. Gawel D, Seed PC (2011) Urinary tract infection drives genome instability in uropathogenic *Escherichia coli* and necessitates translesion synthesis DNA polymerase IV for virulence. Virulence 2: 222–232.
43. Li B, Smith P, Horvath DJ, Jr., Romesberg FE, Justice SS (2010) SOS regulatory elements are essential for UPEC pathogenesis. Microbes Infect 12: 662–668.
44. Zasloff M (2007) Antimicrobial peptides, innate immunity, and the normally sterile urinary tract. J Am Soc Nephrol 18: 2810–2816.
45. Ragnarsdottir B, Lutay N, Gronberg-Hernandez J, Koves B, Svanborg C (2011) Genetics of innate immunity and UTI susceptibility. Nature Rev Urology 8: 449–468.
46. Hopkins W, Gendron-Fitzpatrick A, McCarthy DO, Haine JE, Uehling DT (1996) Lipopolysaccharide-responder and nonresponder C3H mouse strains are equally susceptible to an induced *Escherichia coli* urinary tract infection. Infect Immun 64: 1369–1372.
47. Hagberg L, Hull R, Hull S, McGhee JR, Michalek SM, et al. (1984) Difference in susceptibility to gram-negative urinary tract infection between C3H/HeJ and C3H/HeN mice. Infect Immun 46: 839–844.
48. Burroughs AM, Balaji S, Iyer LM, Aravind L (2007) Small but versatile: the extraordinary functional and structural diversity of the beta-grasp fold. Biol Direct 2: 18.
49. Kelley LA, Sternberg MJ (2009) Protein structure prediction on the Web: a case study using the Phyre server. Nat Protoc 4: 363–371.
50. Silvaggi JM, Perkins JB, Losick R (2005) Small untranslated RNA antitoxin in *Bacillus subtilis*. J Bacteriol 187: 6641–6650.
51. Picard B, Garcia JS, Gouriou S, Duriez P, Brahimi N, et al. (1999) The link between phylogeny and virulence in *Escherichia coli* extraintestinal infection. Infect Immun 67: 546–553.
52. Johnson JR, Delavari P, Kuskowski M, Stell AL (2001) Phylogenetic distribution of extraintestinal virulence-associated traits in *Escherichia coli*. J Infect Dis 183: 78–88.
53. Blattner FR, Plunkett G, 3rd, Bloch CA, Perna NT, Burland V, et al. (1997) The complete genome sequence of *Escherichia coli* K-12. Science 277: 1453–1474.
54. Chen SL, Hung CS, Xu J, Reigstad CS, Magrini V, et al. (2006) Identification of genes subject to positive selection in uropathogenic strains of *Escherichia coli*: a comparative genomics approach. Proc Natl Acad Sci U S A 103: 5977–5982.

55. Bonacorsi S, Clermont O, Houdouin V, Cordevant C, Brahimi N, et al. (2003) Molecular analysis and experimental virulence of French and North American *Escherichia coli* neonatal meningitis isolates: identification of a new virulent clone. J Infect Dis 187: 1895–1906.
56. Zhou Q, Ames P, Parkinson JS (2009) Mutational analyses of HAMP helices suggest a dynamic bundle model of input-output signalling in chemoreceptors. Mol Microbiol 73: 801–814.
57. Guzman LM, Belin D, Carson MJ, Beckwith J (1995) Tight regulation, modulation, and high-level expression by vectors containing the arabinose PBAD promoter. J Bacteriol 177: 4121–4130.
58. Murphy KC, Campellone KG (2003) Lambda Red-mediated recombinogenic engineering of enterohemorrhagic and enteropathogenic *E. coli*. BMC Mol Biol 4: 11.
59. Datsenko KA, Wanner BL (2000) One-step inactivation of chromosomal genes in *Escherichia coli* K-12 using PCR products. Proc Natl Acad Sci U S A 97: 6640–6645.
60. Mulvey MA, Lopez-Boado YS, Wilson CL, Roth R, Parks WC, et al. (1998) Induction and evasion of host defenses by type 1-piliated uropathogenic *Escherichia coli*. Science 282: 1494–1497.
61. Vigil PD, Alteri CJ, Mobley HL (2011) Identification of in vivo-induced antigens including an RTX family exoprotein required for uropathogenic *Escherichia coli* virulence. Infect Immun 79: 2335–2344.
62. Larkin MA, Blackshields G, Brown NP, Chenna R, McGettigan PA, et al. (2007) Clustal W and Clustal X version 2.0. Bioinformatics 23: 2947–2948.
63. Eto DS, Gordon HB, Dhakal BK, Jones TA, Mulvey MA (2008) Clathrin, AP-2, and the NPXY-binding subset of alternate endocytic adaptors facilitate FimH-mediated bacterial invasion of host cells. Cell Microbiol 12:2553–2567.

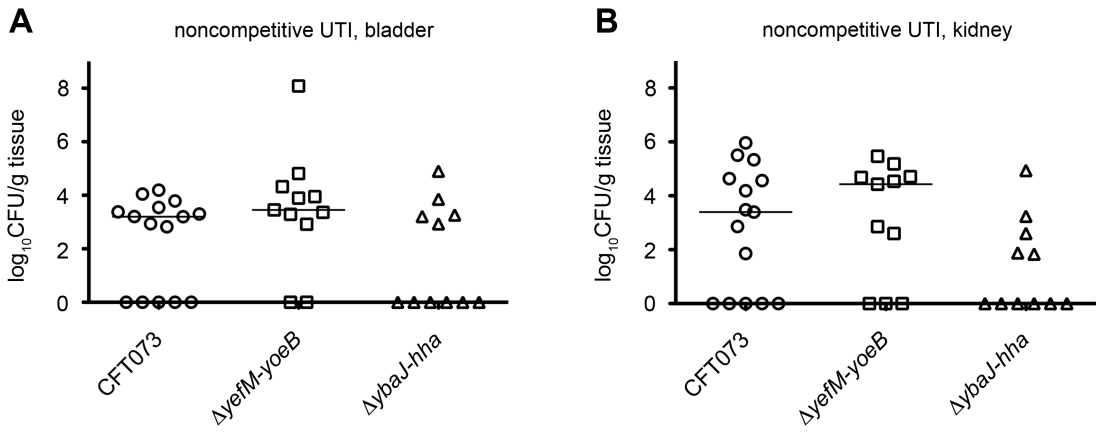

Figure 3.S1. The CFT073Δ*yefM-yoeB* and CFT073Δ*ybaJ-hha* mutants colonize the murine urinary tract at similar levels to wild type CFT073 in noncompetitive assays. (A–D) Adult female C3H/HeN and C3H/HeJ mice were infected via catheterization with 10^7 CFU of wild type CFT073, CFT073Δ*yefM-yoeB* or CFT073Δ*ybaJ-hha*. Graphs show bacterial titers present in the (A) bladders and (B) kidneys at 3 days postinoculation. Bars indicate median values for each group; n≥10 mice. *P* values were determined using Mann-Whitney U tests.

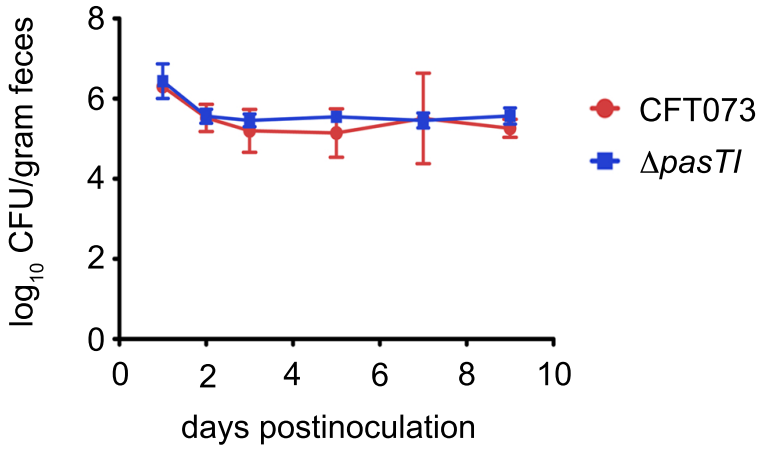

Figure 3.S2. CFT073 does not require *pasTI* for colonization of the murine gastrointestinal tract. Adult female CBA/J mice were each gavaged with 50 µL of a bacterial suspension containing 1×10^{9}CFU CFT073-Clm^{R} or CFT073Δ*pasTI* (*kan*^{R}). CFT073-Clm^{R} served as the wild type control in these assays. Gastrointestinal tract colonization was assessed by enumerating total CFU of the mutant and wild type strains per gram of feces collected at the indicated time points. Data represent mean CFU/g feces ± SEM. N = 3 to 5 mice.

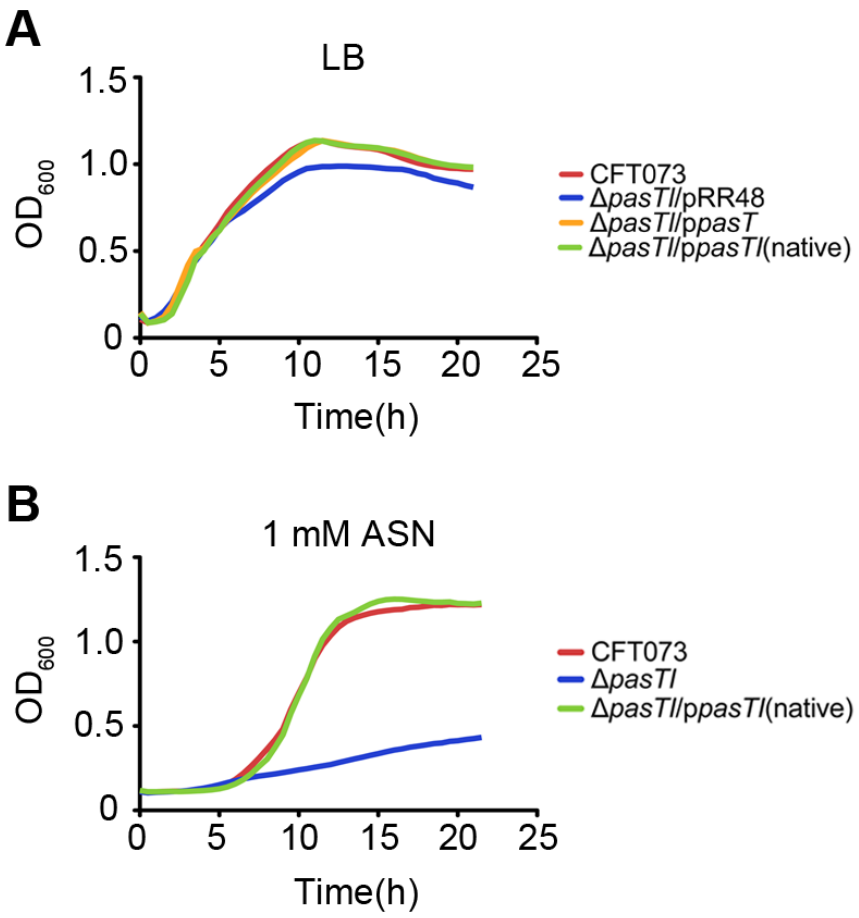

Figure 3.S3. Low-level expression of PasT does not alter growth of the Δ*pasTI* mutant, while transcription of PasTI from its native promoter provides resistance to ASN. Curves show growth of CFT073 and its derivatives in (A) LB broth and (B) MES-LB broth+1 mM ASN. (A) Leaky expression of *55ast* from a P*tac* promoter or expression of *pasTI* from its native promoter does not affect the growth of CFT073Δ*pasTI* in standard LB broth. In these assays, pRR48 served as an empty vector control. (B) Complementation of the Δ*pasTI* mutant growth defect in 1 mM ASN by the *pasTI* operon from its native promoter. Graphs are representative of at least two independent experiments performed in quadruplicate.

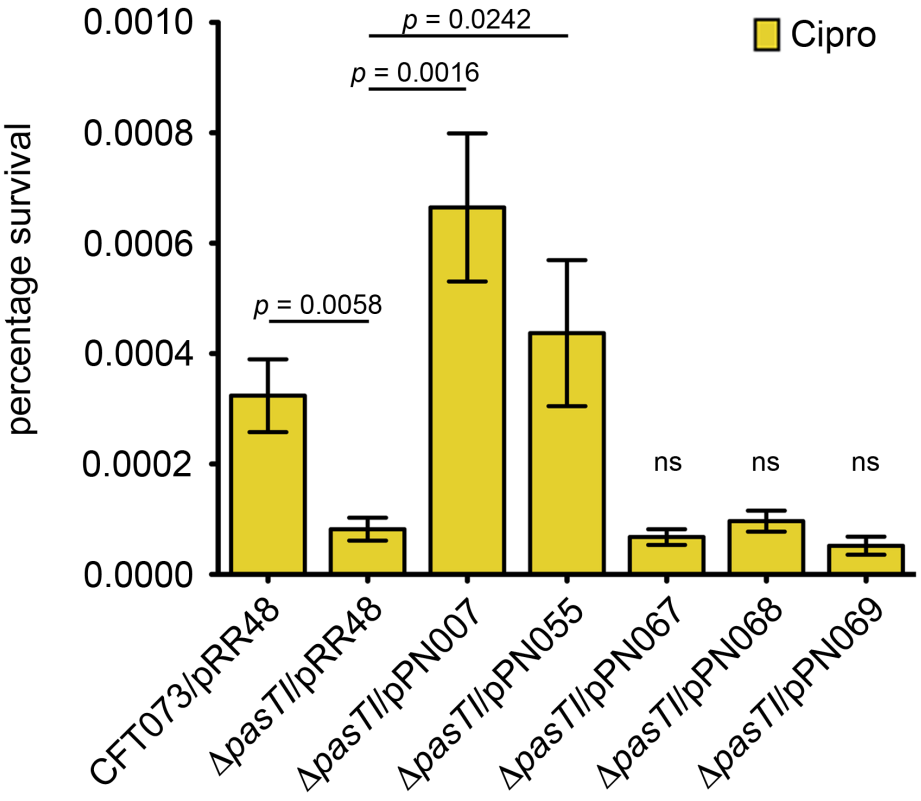

Figure 3.S4. Persister cell formation by CFT073 requires the toxic domain of PasT. Graph shows numbers of viable bacteria (persisters) recovered 5 h after the addition of ciprofloxacin (10 μg/L) to broth cultures in exponential growth phase. The plasmid pRR48 serves as an empty vector control. Plasmid pPN007 encodes full-length PasT, pPN055 encodes the N-terminal 69 amino acids of PasT, and pPN068–069 encode nontoxic PasT variants lacking portions of the PasT N-terminus (see Figure 3.8). Data represent mean results ± SD from three independent experiments. *P* values were determined by Student's *t* test; ns indicates nonsignificant differences between the complemented strain and CFT073Δ*pasTI*/pRR48.

CHAPTER 4

HICE OR NOT *HICE*, THAT IS THE QUESTION: USE OF A TRUNCATED TOXIN-ANTITOXIN SYSTEM TO DEFINE PHYLOGROUP B2 *ESCHERICHIA COLI*

J. Paul Norton, Travis, J. Wiles, and Matthew A. Mulvey

Division of Microbiolgoy and Immunology, Pathology Department, University of Utah School of Medicine, Salt Lake City, USA 84112

Submitted to Journal of Bacteriology

Introduction

Escherichia coli represent a diverse group of Gram-negative bacteria that are typically associated with the intestinal tract of warm-blooded vertebrates. Most strains of *E. coli* are nonpathogenic in nature and exist with their host in a commensal relationship. However, pathogenic subsets of *E. coli* can cause infections both within and outside the gastrointestinal tract. The number of experimentally characterized phenotypic differences (i.e., nonpathogenic versus pathogenic) that distinguish *E. coli* strains is somewhat limiting compared to the genetic diversity of this species. Isolates of *E. coli* can differ from one another by up to 30% in their coding sequence [1]. Despite this extensive variation, comparative genetic analysis (e.g., MLST) of this species resolves at least four distinct phylogroups (i.e., A, B1, B2, and D). Members of the B2 phylogroup—and to a lesser extent the D phylogroup—are associated with extraintestinal disease [2-4]. This is mostly attributed to the prevalence of extraintestinal pathogenic *E. coli* (ExPEC) strains. ExPEC cause diseases such as neonatal meningitis and sepsis and are the most common etiologic agent of community-acquired urinary tract infections. These strains are of increasing importance to the global health community due to recent increases in the worldwide incidence of antibiotic resistant ExPEC isolates [5,6].

A significant amount of work has been done characterizing ExPEC virulence. It is now appreciated that members of this lineage are capable of colonizing and infecting an overlapping set of host-associated extraintestinal niches but do so through different genetically encoded mechanisms [7]. This

complicates the diagnostic identification and categorization of ExPEC strains. The increasing incidence of antibiotic resistant ExPEC strains will likely change treatment procedures for ExPEC associated infections, and having the capacity to reliably differentiate ExPEC from other lineages in a rapid, high-throughput fashion would allow physicians to make better informed treatment decisions. A singular genetic marker to identify ExPEC would, therefore, be of great use, but to the author's knowledge, such a marker has not been described.

In previous work, we determined that the B2 phylogroup—and by extension, most ExPEC strains—could be differentiated from all other *E. coli* based solely on the composition of chromosomally encoded type-II toxin-antitoxin (TA) systems [8]. In this way, the composition of an isolate's TA systems could potentially be leveraged for identification much like a fingerprint. Here, we report the discovery of a phylogroup B2-specific truncation of the toxin-antitoxin system *hicAB* and term it *hicE*. We verified the conservation of the *hicE* truncation within phylogroup B2 *E. coli* using a combination of publically available sequenced *E. coli* strains and an array of clinical *E. coli* isolates. In all cases, we found *hicE* is 100% indicative of phylogroup B2 *E. coli*. Furthermore, a different, distinct truncation of the *hicAB* locus—*hicE.2*—was observed in a subset of phylogroup D *E. coli*, suggesting an evolutionarily redundant truncation of this TA system in ExPEC lineages.

The conservation of *hicE* within phylogroup B2 *E. coli*—but not other lineages—led us to hypothesize that *hicE* may represent an evolutionary vestige that tracked with the emergence of ExPEC, possibly providing an immediate

benefit that relieved certain evolutionary constraints. We tested this by engineering the phylogroup B2-specific *hicE* truncation on the chromosome of the inferred ancestral strain MG1655 and monitoring the capacity of this strain to resist stresses and survive in ExPEC-associated environments. We found that MG1655 containing the *hicE* truncation showed a modest increase in resistance to various envelope stresses, including an increased resistance to ampicillin and polymyxin B exposure, and increased resistance to these stresses in is concomitant with heightened expression of the Cpx pathway. Forced expression of *hicE* in MG1655 allowed resistance to human serum similar to that observed in the serum resistant ExPEC strains CFT073 and UTI89. However, we find ExPEC strains are differentially reliant upon the *hicE* locus for resistance to similar envelope stresses. Most importantly, our data indicate the *hicE* truncation is specific to phylogroup B2 and can, therefore, be used as a singular genetic marker for identifying this subgroup of *E. coli*.

Materials and methods

Bacterial strains and plasmids

All bacterial strains, plasmids, and primers used in this study are listed in Tables 4.1-4.4. Expression constructs were made using standard molecular biology techniques employing the plasmid pRR48 or pGEN-MCS. Expression of genes cloned into pRR48 is driven by the P*tac* promoter which was induced by addition of 500 μM isopropyl-β-D-thiogalactopyranoside (IPTG) where indicated. Primers used to construct plasmids used in this study are indicated in Table 4.2

Table 4.1. Bacterial strains and plasmids

Strain	Description	Source
MG1655	K-12 lab strain	[18]
MG1655Δ*hicAB::clmR*	MG1655 containing a chromosomal replacement of the *hicAB* locus with the chloramphenicol resistance cassette from pKD3	This study
MG1655^{hicE}	MG1655 with the B2 specific *hicE* truncation generated on the chromosome by replacing nucleotides with a chloramphenicol resistance cassette from pKD3	This study
CFT073	UPEC strain (urosepsis isolate, O6:K2:H1)	[19]
CFT073Δ*hicE*::clmR	CFT073 containing a chromosomal replacement of the *hicE* locus with the chloramphenicol resistance cassette from pKD3	This study
UTI89	UPEC cystitis isolate (O18:K1:H7)	[20]
UTI89Δ*hicE*::clmR	UTI89 containing a chromosomal replacement of the *hicE* locus with the chloramphenicol resistance cassette from pKD3	This study
Plasmid	**Description**	**Source**
pGEN-MCS	Amp^R high retention cloning plasmid for native expression	[21]
pRR48	Amp^R; contains MCS under the control of *tac* promoter	[22]
p*hicE*^{Pnative}	Amp^R; native expression of *hicE*; contains *hicE* locus and 100bp upstream cloned from UTI89 sequence into EcoRI, BamHI sites of pGEN-MCS	This study
p*hicAB*	Amp^R; *hicAB* sequence from MG1655 cloned into PstI, HindIII sites of pRR48	This study
pNLP10	Kan^R; low-copy-number cloning vector with promoterless *luxCDABE* operon	[23]
pNLP19	Kan^R; pNLP10 with *rpoErseABC* promoter driving *luxCDABE*	[23]
pJW1	Kan^R; pNLP10 with *cpxP* promoter driving *luxCDABE*	[23]
pKM208	Amp^R; IPTG inducible Red recombinase expression plasmid	[24]
pKD3	Amp^R/Clm^R; template plasmid containing clm^R cassette for use in generating knockout strains	[25]

Table 4.2. Primer sequences

Primer	Sequence
hicAB KO	
Forward	GTTTACTTTGTTGATATACTCAGCGGCAGGGAGGCGATTGTGTAGGCTGGAGCTGCTTCG
Reverse	ATATCAGTTGTTAAAAATGACAACTTTTCGTTAACTGTAACATATGAATATCCTCCTTAG
hicAB KO confirmation	
Forward	TGCCATGAGTTGTCCTG
Reverse	TGTTCTGCAAGCTGCTG
hicE truncation	
Forward	TAGTGCTATTTTCGAGCAAATTACACACGGAGGTAAACTGTGTAGGCTGGAGCTGCTTCG
Reverse	AGGTACTTCAATAAAGTGATCGTGACTATTTAATGGCGAACATATGAATATCCTCCTTAG
hicE KO	
Forward	GTGCCTTTGAGCGTCGCCTCTAAGGTATTGCTGTTAAATGTGTAGGCTGGAGCTGCTTCG
Reverse	TCAAACCATCACCAGCGATAACTCTTTGCCAAGCGCATTACATATGAATATCCTCCTTAG
hicE truncation/KO confirmation	
Forward	TGCCATGAGTTGTCCTG
Reverse	TGTTCTGCAAGCTGCTG
p*hicE*$^{\text{Pnative}}$ (pPN001)	
Forward	TCCTC GAATTC TGCATTGCATTCTGCCGTTGCGGCGATTTAG
Reverse	CACT GGATCC CTGTAATCAAACCATCACCAGCGATAACTC
p*hicAB* (pPN008)	
Forward	AATCG CTGCAG GTGAAACAAAGCGAGTTCAG
Reverse	GGGCG AAGCTT TTAAACCATCACCAGCGATAAC
hicE diagnostic	
Forward	TGCCATGAGTTGTCCTG
Reverse	TGTTCTGCAAGCTGCTG
chuA diagnostic	
chuA.1	GACGAACCAACGGTCAGGAT
chuA.2	TGCCGCCAGTACCAAAGACA
yjaA diagnostic	
yjaA.1	TGAAGTGTCAGGAGACGCTG
yjaA.2	ATGGAGAATGCGTTCCTCAAC
TspE4.C2 diagnostic	
TspE4C2.1	GAGTAATGTCGGGGCATTCA
TspE4C2.2	CGCGCCAACAAAGTATTACG

Table 4.3. In silico phylotyping and *hicE* analysis of reference *E. coli* strains

Strain	Origin	*chuA*	*yjaA*	TSPE4.C2	Phylogroup	*hicE*
P12b	Commensal	−	−	−	A	−
MG1655	Commensal (K-12)	−	+	−	A	−
UMNK88	Porcine ETEC	−	−	−	A	−
ETEC H10407	ETEC	−	+	−	A	−
ATCC 8739	Commensal	−	−	−	A	−
W3110	Commensal (K-12)	−	+	−	A	−
BL21(DE3)	Commensal (K-12)	−	−	−	A	−
BW2952	Commensal	−	+	−	A	−
B str. REL606	Commensal	−	−	−	A	−
HS	Commensal	−	−	−	A	−
IAI1	Commensal	−	−	+	B1	−
55989	Diarrhea (EAEC)	−	−	+	B1	−
W	Nonpathogenic	−	−	+	B1	−
SE11	Commensal	−	−	+	B1	−
E24377A	Diarrhea (ETEC)	−	−	+	B1	−
O103:H2 str. 12009	EHEC	−	−	+	B1	−
O26:H11 str. 11368	EHEC	−	−	+	B1	−
O111:H- str. 11128	EHEC	−	−	+	B1	−
KO11FL	Nonpathogenic	−	−	+	B1	−
UTI89	Cystitis (ExPEC)	+	+	+	B2	+
APEC O1	Septitcemia (ExPEC)	+	+	+	B2	+
S88	NMEC (ExPEC)	+	+	+	B2	+
CFT073	Pyelonephritis (ExPEC)	+	+	+	B2	+
ED1a	Commensal	+	+	+	B2	+
536	Pyelonephritis (ExPEC)	+	+	+	B2	+
ABU 83972	Commensal	+	+	+	B2	+
O127:H6 str E2348/69	Diarrhea (EPEC)	+	+	+	B2	+
IHE3034	NMEC (ExPEC)	+	+	+	B2	+
UM146	Crohn's Disease (AIEC)	+	+	+	B2	+
O83:H1 NRG 857C	Crohn's Disease (AIEC)	+	+	+	B2	+
LF82	Crohn's Disease (AIEC)	+	+	+	B2	+
SE15	Commensal	+	+	+	B2	+
NA114	UPEC (ST131)	+	+	+	B2	+
SMS-3-5	Environmental (SESEC)	+	−	−	D	−
UMN026	Cystitis (ExPEC)	+	−	−	D	−
042	Diarrhea (EAEC)	+	−	−	D	−
IAI39	Pyelonephritis (ExPEC)	+	−	−	D	N/A

Table 4.3. Continued

Strain	Origin	*chuA*	*yjaA*	TSPE4.C2	Phylogroup	*hicE*
O7:K1 str. CE10	NMEC (ExPEC)	+	−	−	D	−*
O55:H7 str. RM12579	EPEC	+	−	−	D	−
O55:H7 str. CB9615	Infantile diarrhea (EPEC)	+	−	−	D	−
O157:H7 str. EDL933	Diarrhea (EHEC)	+	−	−	D	−
O157:H7 str. Sakai	Diarrhea (EHEC)	+	−	−	D	−
O157:H7 XuZhou21	EHEC	+	−	−	D	−
O157:H7 str. TW14359	EHEC	+	−	−	D	−
O157:H7 str. EC4115	EHEC	+	−	−	D	−

−* *hicE.2* allele

Table 4.4. Phylotyping and *hicE* analysis of clinical *E. coli* isolates

Strain	Origin	*chuA*	*yjaA*	TSPE4.C2	Phylogroup	*hicE*
AB1	Septicemia	+	+	+	B2	+
AB2	Septicemia	+	+	+	B2	+
AB3	Septicemia	+	+	+	B2	+
AB4	Septicemia	+	+	+	B2	+
AB5	Septicemia	+	+	−	B2	+
WB1	Septicemia	+	−	−	D	−*
WB2	Septicemia	+	+	+	B2	+
WB3	Septicemia	+	+	+	B2	+
WB8	Septicemia	+	+	+	B2	+
WB11	Septicemia	+	−	−	D	−
AU1	Cystitis	+	+	+	B2	+
AU2	Cystitis	+	+	−	B2	+
AU3	Cystitis	+	+	+	B2	+
AU4	Cystitis	+	+	+	B2	+
AU5	Cystitis	+	+	+	B2	+
AU6	Cystitis	+	+	+	B2	+
AU7	Cystitis	+	+	+	B2	+
AU8	Cystitis	−	−	+	B1	−
ABF	Body Fluid	+	−	+	D	−
A70	Stool	+	−	+	D	−
A71	Stool	−	+	−	A	−
A81	Stool	+	−	−	D	−
A84	Stool	−	+	−	A	−
A15	Asymptomatic bacteriuria	−	+	−	A	−
A18	Asymptomatic bacteriuria	−	−	+	B1	−
A34	Asymptomatic bacteriuria	−	−	−	A	−
A37	Asymptomatic bacteriuria	−	+	−	A	−
A58	Asymptomatic bacteriuria	−	+	−	A	−
AS1	Stool	+	+	+	B2	+
AS2	Stool	+	−	−	D	−*
AS3	Stool	−	−	+	B1	−
AS4	Stool	−	+	−	A	−
AS5	Stool	−	+	−	A	−
AS6	Stool	+	−	−	D	−*
AS7	Stool	−	+	−	A	−
AS8	Stool	+	+	+	B2	+

−* *hicE.2* allele

along with primers used to verify each clone by sequencing. Antibiotics (50 µg/ml kanamycin or 100 µg/ml ampicillin) were added to plates and growth medium to select for and maintain strains and plasmids when necessary.

Phylotyping PCR

Each PCR sample contained crude genomic DNA extracted from isolates by heat lysis, 200 µM dNTPs, 500 nM specfic primers (found in Table 4.2), 2% dimethyl sulfoxide, Roche PCR buffer containing $MgCl_2$ (10X buffer composition: 100 mM Tris-HCl, 15 mM $MgCl_2$, 500 mM KCl, pH 8.3), and 2.5 U Taq DNA polymerase (Roche). The PCR was run with a 55ºC annealing temperature for 32 cycles on a Veriti Thermal Cycler (Applied Biosciences). Equal amounts of each PCR sample were resolved on a 1% agarose gel.

Growth assays

Cultures of UTI89, CFT073, MG1655, and their derivatives were grown shaking overnight at 37ºC in 5 ml of LB broth or modified M9 minimal medium containing casein amino acids (6 g/L NA_2HPO_4, 3 g/L KH_2PO_4, 1 g/L NH_4Cl, 0.5 g/L NaCl, 1 mM $MgSO_4$, 0.1 mM $CaCl_2$, 0.1% glucose, 0.0025% nicotinic acid, 16.5 µg/ml thiamine, and 0.2% casein amino acids). Bacteria assayed for growth in 100 mM morpholineethanesulfonic acid (MES)-buffered LB (MES-LB) or methyl viologen (MV; aka paraquat) were first grown from frozen stocks overnight in LB. For growth in human serum, frozen aliquots of pooled human sera—taken from 7 healthy volunteers using standard protocols approved by the University of

Utah Institutional Review Board and provided by Dr. Andrew Weyrich—were thawed and diluted to the appropriate concentration using modified M9 medium. Heat inactivated serum (treated at 55ºC for 30 minutes) was diluted to 10% final concentration in modified M9 and used as a control. Overnight cultures were OD matched to OD_{600} = 0.6 and diluted 1:100 into appropriate growth media where growth of quadruplicate 200 µl samples in 100-well honeycomb plates was assessed at 37ºC using a Bioscreen C instrument (Growth Curves USA). MV was prepared fresh prior to addition to LB cultures. All reagents were obtained from Sigma-Aldrich unless specified otherwise.

Reporter assays

Bacteria carrying plasmids pNLP19 (*rpoErseABC*-lux) or pJW1 (*cpxP*-lux) were grown from frozen stocks at 37ºC with shaking overnight in 5 ml LB medium containing 50 µg/ml kanamycin. Overnight cultures were diluted 1:100 into 5 ml LB medium containing 50 µg/ml kanamycin and incubated with shaking at 37ºC for 2.5 h to reach exponential phase. Triplicate 200-µl aliquots of each sample were then transferred into a 96-well white, opaque-walled polystyrene microplate (Dynex Technologies), and luminescence was measured immediately with a Synergy HT multidetection microplate reader (BioTek Instruments, Inc.).

Polymyxin B survival assays

Bacterial cultures were grown from frozen stocks in 5 ml LB broth overnight (18 h) with shaking at 37ºC. Cultures were back-diluted 1:100 into fresh

LB medium and incubated with shaking at 37ºC for 2.5 h to reach exponential phase. Polymyxin B was added to each culture to a final concentration of 1 μg/ml and the cultures were incubated with shaking at 37ºC for 90 minutes. One milliliter of each culture was pelleted by centrifugation and rinsed twice with sterile PBS followed by serial dilution and plating on LB agar medium. Surviving bacteria were enumerated after incubation at 37ºC for 20 h. Data represent three independent experiments, and graphed values were calculated using the following equation:

$\log_{10}$(percent survival normalized to WT) = $\log_{10}${[(CFU/ml output)/(CFU/ml input)]/(average survival WT)}.

Ampicillin persistence assays

Bacterial cultures were grown from frozen stocks in 5 ml LB broth overnight (18 h) with shaking at 37ºC. Cultures were then back-diluted 1:10 into 5 ml fresh LB broth containing 100 μg/ml ampicillin and incubated shaking at 37ºC for 6 h. Surviving bacteria were determined by enumerating CFUs of serial dilutions plated on LB agar plates incubated overnight at 37ºC. Data represent three independent experiments, and graphed values were calculated using the following equation:

$\log_{10}$(percent survival normalized to WT) = $\log_{10}${[(CFU/ml output)/(CFU/ml input)]/(average survival WT)}.

Statistics

Unless otherwise stated, P-values were determined using a two-tailed unpaired *t*-test, calculated using GraphPad Prism 5 software.

Results

Phylogrouping of reference strains and clinical isolates of *E. coli* using the Clermont method

Our findings are predicated upon the differentiation of *E. coli* strains into distinct phylogenetic groups or phylogroups. One PCR-based method for separating *E. coli* into four distinct phylogroups (i.e., A, B1, B2, or D) is the Clermont method. This approach relies on distinguishing these four phylgroups based on the presence or absence of the three genetic markers *chuA, yjaA,* and TspE4.C2 (Fig. 4.1A). The accuracy of the Clermont method has been shown to be comparable to multilocus sequence typing, especially in identifying phylogroup B2 *E. coli* [9]. In this study, we utilize the Clermont method to phylogroup strains. Each of 45 different reference *E. coli* strains available in NCBI was parsed into its corresponding phylogroup based on the Clermont loci using the basic local alignment search tool (BLAST), and our results corroborate previous phylogenetic characterization of these strains (Table 4.3). Similarly, 36 clinical *E. coli* isolates were categorized and typed through a PCR approach (Table 4.4).

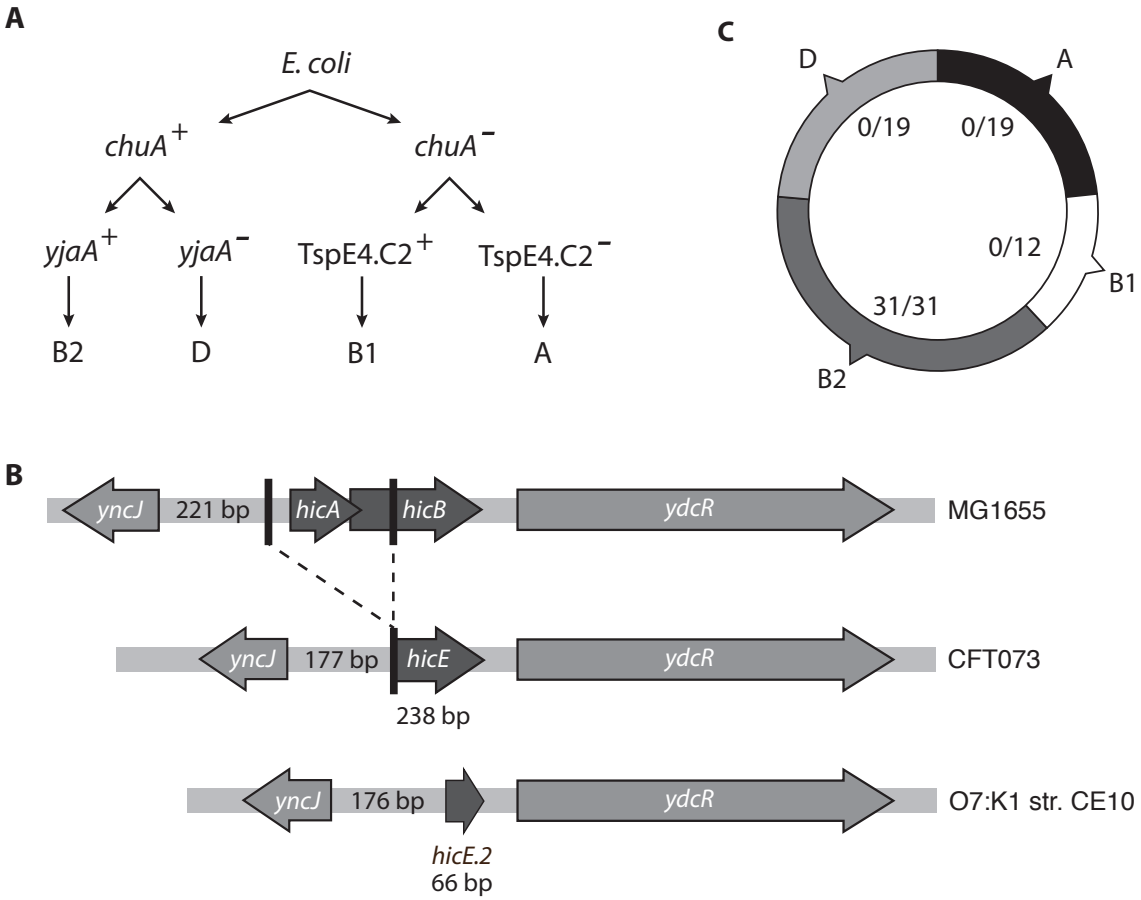

Figure 4.1. Phylogroup analysis of publically available sequenced *E. coli* strains and clinical *E. coli* isolates reveals a conserved truncation of *hicAB* within phylogroup B2 strains. (A) Flowchart depicting the Clermont method of organizing *E. coli* into four phylogroups (A, B1, B2, and D) determined by the presence or absence of three DNA markers—*chuA*, *yjaA*, and TspE4.C2. (B) Diagram representing the *hicAB* genomic region of MG1655, CFT073, and O7:K1 str. CE10. Urosepsis isolate CFT073 is representative of phylogroup B2 *E. coli* harboring the *hicE* truncation, and O7:K1 str. CE10 represents a phylogroup D strain containing the *hicE.2* allele. (C) Pie chart showing the relative abundance of strains represented in the phylogroup analysis of sequenced and clinical *E. coli* isolates. The inner fractions correlate with the total number of strains containing the *hicE* locus within each phylogroup.

Phylogroup B2 *E. coli* harbor a conserved truncation of toxin-antitoxin system hicAB

In previous work, we determined that phylogroup B2 *E. coli* could be differentiated from other sequenced *E. coli* based solely on the chromosomal composition of type-II TA systems [8]. Upon further investigation into the qualitative characteristics of TA systems harbored by the B2 phylogroup, we observed a consistent 445bp truncation of the *hicAB* locus. This truncation event begins 44 base pairs upstream of the *hicA* translational start site and ends 200 bp into the 5' portion of *hicB*, leaving behind a 238 bp fragment of *hicB* (Fig. 4.1B). The resulting truncated *hicB* allele was termed *hicE* (named so because after truncation of the letter "B", the letter "E" remains). We developed a PCR-typing method to differentiate strains carrying full-length *hicAB* the *hicE* locus; *hicAB*-positive strains yield a 1,033 bp product compared to a 588 bp product yielded by *hicE*-positive strains. Using this strategy, we determined the presence or absence of the *hicE* truncation within the 81 reference and clinical *E. coli* strains. In 100% (31/31) of instances, the *hicE* locus correlated with phylogroup B2 *E. coli* (Fig. 4.1C and Tables 4.3 and 4.4). While surveying isolates for the *hicE* locus, we observed a 416 bp product in 21% (4/19) of phylogroup D strains (Tables 4.3 and 4.4). Sequencing the genomic region where the ancestral *hicAB* locus is expected to be located revealed a truncation of the *hicAB* locus, distinct from *hicE*, but consistent between the four phylogroup D isolates. This truncation—deemed *hicE.2*—begins 45 bp upstream of the *hicAB* operon and continues through *hicA* and *hicB* coding sequences, leaving only 66 bp of the 3'

end of *hicB* intact. We did not observe any correlation between the *hicE.2* containing strains and other phylogroup D strains containing the full-length *hicAB* locus.

Introduction of the phylogroup B2-specific hicE locus into an ancestral hicAB-positive *E. coli* strain augments polymyxin B and ampicillin resistance

To better understand the physiological effects of the *hicE* locus within *E. coli,* we engineered the *hicE* truncation within the chromosome of the inferred ancestral strain MG1655 (referred to herein as MG1655^{hicE}) and compared the average survival of this recombinant strain to the wild type parent strain and a MG1655Δ*hicAB* mutant under different conditions. We found that relative to both wild type MG1655 and MG1655Δ*hicAB*, the MG1655^{hicE} mutant exhibited a significantly elevated resistance to killing by either polymyxin B (a membrane permeabilizing antibiotic) or ampicillin (a cell wall synthesis inhibiting antibiotic) (Fig. 4.2). Phylogroup B2 *E. coli* strains CFT073 and UTI89 showed marked differences in their reliance upon the *hicE* locus for survival under the same conditions. CFT073Δ*hicE* survived significantly better than wild type CFT073, whereas UTI89Δ*hicE* showed a significant decrease in survival compared to wild type UTI89 (Fig 4.2).

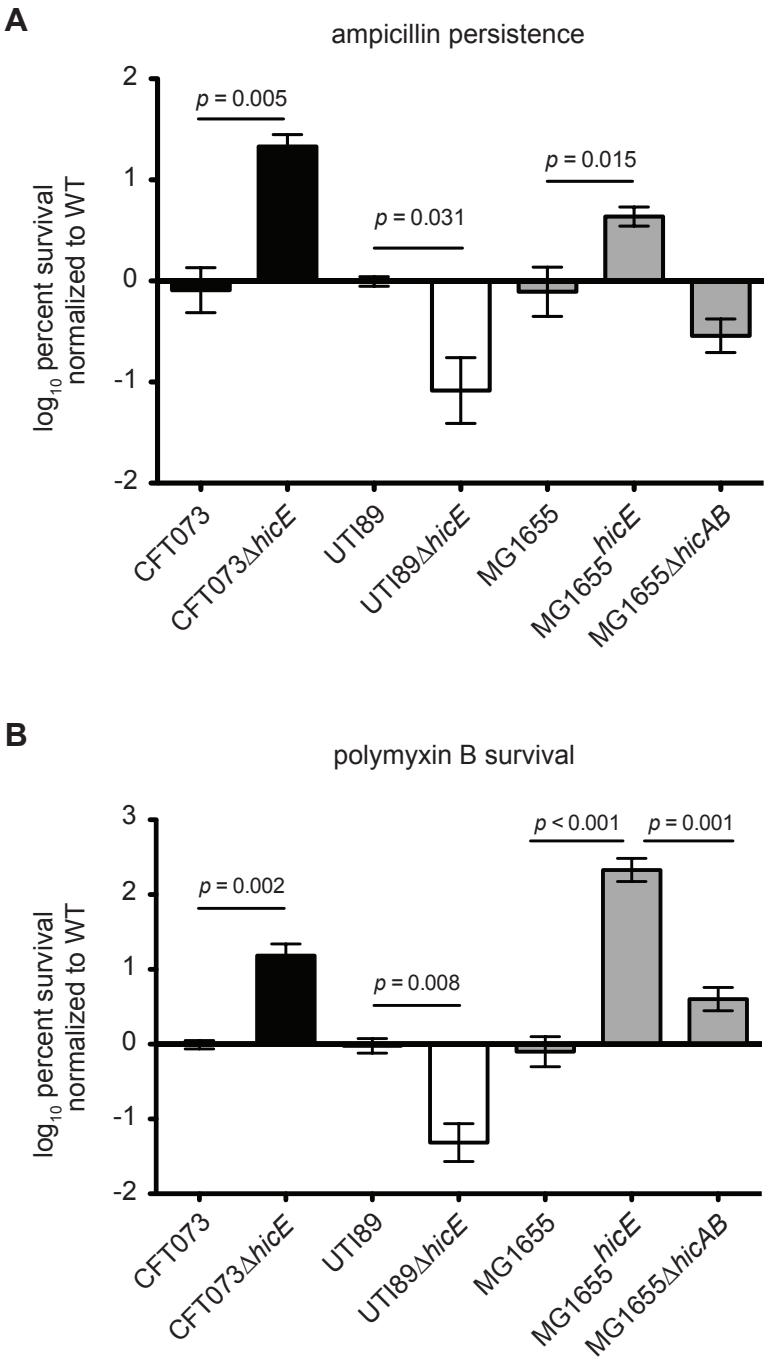

Figure 4.2. The *hicE* locus effects survival in polymyxin B and ampicillin. Each strain was subjected to (A) 100 µg/ml ampicillin for 6 h or (B) 1 µg/ml polymyxin B for 90 minutes. The survival of mutant strains was normalized to the survival of the accompanying wild type strain in each stress. Data represent the average of $\log_{10}$ transformed values from three independent experiments.

hicE influences the growth of the ancestral *E. coli* strain MG1655 in various stressing conditions

The strain MG1655^{hicE} demonstrated a significant survival advantage when challenged with membrane stresses. Therefore, we wanted to determine the extent to which the *hicE* locus confers a survival advantage in other stressful environments. The bloodstream, which is encountered by ExPEC during bacteremic infections, contains several antibacterial factors such as complement. When activated, complement components in human serum attach to the outer membrane of serum sensitive bacteria and form a pore structure known as the membrane attack complex (MAC). MAC formation disrupts the integrity of the bacterial membrane leading to cell death. When challenged with active serum, we found that serum resistant strains CFT073 and UTI89 grew as expected, and MG1655^{hicE}, although delayed, was able to grow while wild type MG1655 was not (Fig. 4.3B). The serum resistance observed in MG1655^{hicE} was not simply due to the loss of function in *hicAB,* as MG1655Δ*hicAB* was also unable to grow in the presence of active serum (Fig. 4.3B). To confirm if complement proteins were inhibiting the growth of wild type MG1655, we tested the ability of all strains to grow in serum that had been heat-treated, which renders complement proteins inactive. Indeed, all strains grew to similar densities in heat-killed serum (Fig. 4.3A). Complementation of MG1655 with a plasmid encoding the *hicE* locus from UTI89 driven by its native promoter was sufficient for serum resistance, indicating that both *cis* and *trans* complementation of *hicE* within the ancestral strain

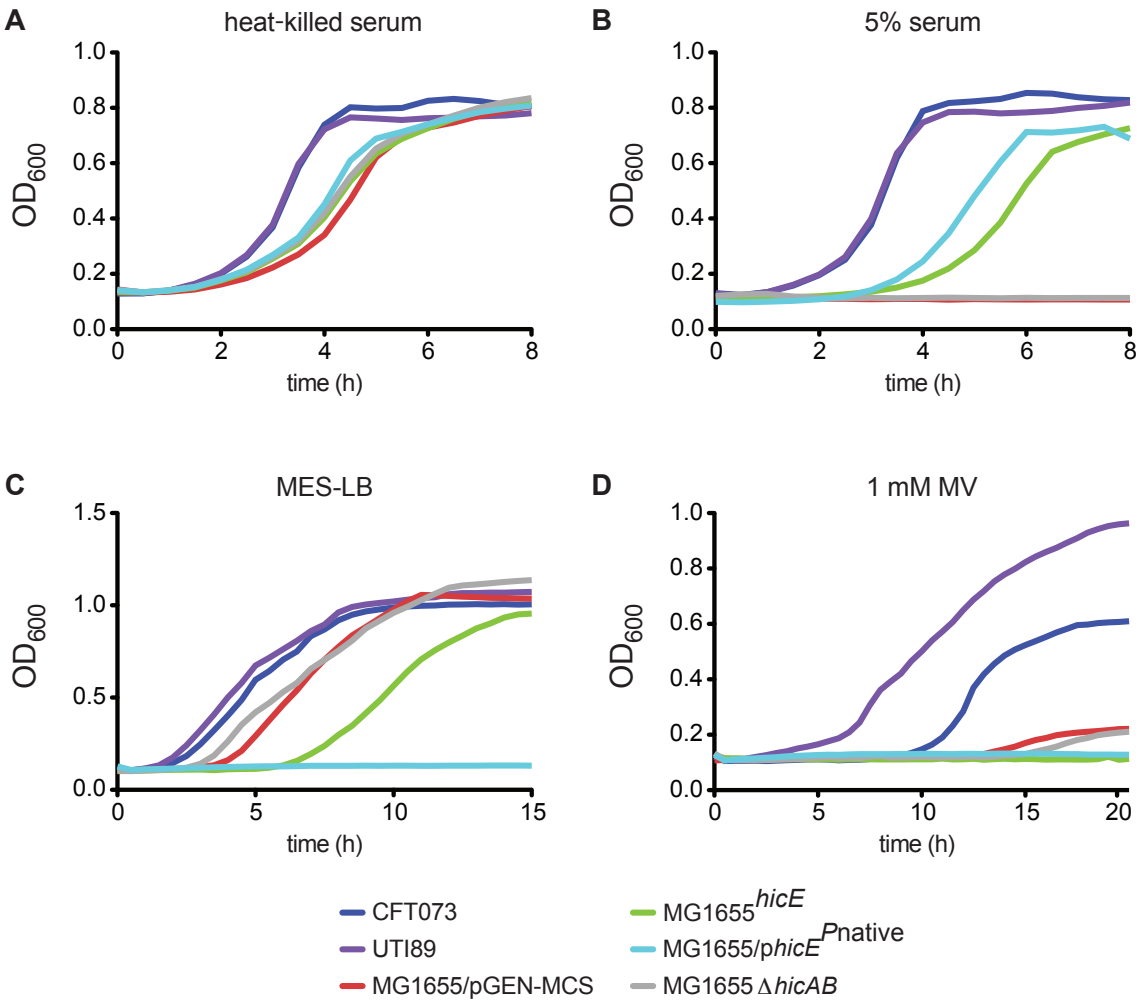

Figure 4.3. Expression of *hicE* has context dependent effects on growth of MG1655. Growth of ExPEC strains CFT073 and UTI89 together with inferred ancestral strain MG1655 and its associated mutants in (A) 10% heat killed serum, (B) 5% human serum, (C) LB buffered to pH 5.0 with MES (MES-LB), and (D) 1 mM methyl viologen (MV). Graphs are representative of at least two independent experiments performed in quadruplicate.

MG1655 promotes serum resistance (Fig. 4.3B). Although demonstrating the novel capacity to grow in human serum, we found that MG1655^{hicE} and MG1655/p*hicE*^{Pnative} strains were more sensitive to growth in the low-pH media MES-LB and in media containing the superoxide generator methyl viologen (MV) compared to MG1655 and MG1655Δ*hicAB* (Fig. 4.3C-D).

Presence of the *hicE* locus results in increased activity of the Cpx envelope stress response in MG1655

We hypothesized that increased resistance to membrane stresses within MG1655^{hicE} could be due to increased activity in the envelope stress response. To test this, we measured the activity of two major envelope stress response pathways—the *rpoE* and Cpx pathways. Activation of these pathways can be monitored by expression of the *rpoE* and *cpxP* genes, respectively. Plasmids carrying the *luxCDABE* operon driven by either the *rpoE* promoter or the *cpxP* promoter were transformed into MG1655, MG1655^{hicE}, and MG1655Δ*hicAB*, and luciferase expression was determined during exponential growth in LB media. There was no significant difference in expression levels of *rpoE* (DNS), but MG1655^{hicE} showed a significant, three-fold increase in *cpxP* expression compared to both MG1655 and MG1655Δ*hicAB* (Fig. 4.4).

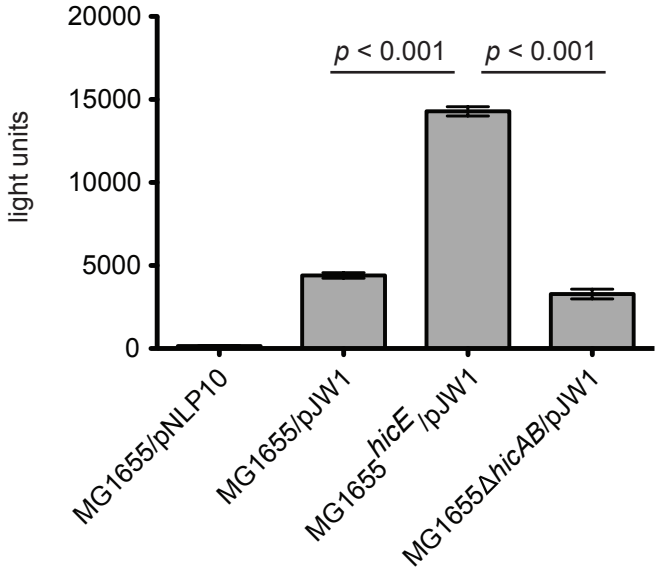

Figure 4.4. The *hicE* truncation increases *cpxP* activity in MG1655. The graph indicates expression levels of the *luxCDABE* operon driven by the *cpxP* promoter (pJW1) or a promoterless construct (pNLP10) following growth to exponential phase in LB broth. Data are shown as means ± standard errors of the means from three independent experiments performed in triplicate.

Discussion

Our analysis of 81 *E. coli* strains shows a direct correlation between a truncation in the *hicAB* toxin-antitoxin system—named here *hicE*—and the B2 phylogroup. This event may provide evidence of some selective pressures involved in the generation of the B2 lineage. When considering different genetic mechanisms of selection-driven fitness, the gross loss of genetic material has been shown to provide a better platform for adaptation to environmental challenge than a series of single nucleotide alterations [10,11]. Once a foothold is obtained within a newly acquired niche, fine-tuning of fitness can continue, usually through gene gain or gene repurposing events [12,13]. We can apply this rationale to what we observe with the *hicE* locus. Generation of the *hicE* locus involves the loss of genetic material (i.e., *hicA* and part of *hicB*), and when this truncation is engineered within MG1655, it confers resistance to various envelope stresses, including human serum (Fig. 4.1B, 4.2, 4.3A-B). However, this advantageous adaptation to a new environment comes with certain fitness trade-offs; MG1655^{hicE} showed a decreased capacity to grow in low pH and in the presence of reactive oxygen species (Fig. 4.3C-D). Coupling our phylogrouping data showing 100% of B2 *E. coli* contain the *hicE* locus together with the notion that the *hicE* locus offers a fitness advantage to an inferred ancestral strain within an ExPEC-associated niche, it is plausible that generation of the *hicE* locus was a defining event in the formation of the B2 lineage by allowing for niche expansion. It has been established that while modern-day

phylogroup B2 *E. coli* may be phenotypically similar (i.e., they cause similar pathologies within the human host), these bacteria

have arrived at this virulence potential through different evolutionary trajectories [1,14,15]. For example, our lab has previously characterized phylogroup B2 strains CFT073 and UTI89 to be differentially reliant upon the pore-forming toxin α-hemolysin for virulence within a zebrafish infection model [15]. In our current study, this trend continues, as these strains exhibit divergent reliance upon endogenous *hicE* for survival in polymyxin B and ampicillin (Fig. 2). Deletion of the *hicE* locus from CFT073 and UTI89 had no effect on survival in human serum (DNS). These data are not entirely surprising as both strains are known to express capsular polysaccharide, which itself contributes to serum resistance [16]. Of note, both CFT073 and UTI89 have ameliorated the fitness cost of maintaining *hicE*, as each strain grew to higher densities in low pH media and in the presence of reactive oxygen species than MG1655^{hicE} (Fig. 4.3C-D).

The Cpx pathway is a key envelope stress response pathway in *E. coli*, and activation of *cpxP*—the small periplasmic component of the Cpx system—is indicative of an active response to envelope stress [17]. Using a luciferase reporter driven by the *cpxP* promoter, we were able to show that MG1655^{hicE} had heightened activation of the Cpx pathway (Fig. 4.4). This could potentially precondition bacterial cells to respond more quickly to envelope stresses, thereby promoting resistance and survival. The HicE protein encodes a putative DNA binding protein, and given the multifaceted phenotypes associated with this truncation, it could potentially act as a novel transcription factor to regulate expression of genes, including genes involved in the Cpx pathway.

Characterization of the putative molecular effects of *hicE* requires further investigation. This study's primary focus was identifying a single genetic marker for differentiating phylogroup B2 *E. coli*, and we believe the *hicE* locus provides clinicians with a high fidelity diagnostic marker for identifying B2 pathogens.

References

1 Touchon, M. *et al.* Organised genome dynamics in the *Escherichia coli* species results in highly diverse adaptive paths. *PLoS Genet* **5**, e1000344, (2009).

2 Boyd, E. F. & Hartl, D. L. Chromosomal regions specific to pathogenic isolates of *Escherichia coli* have a phylogenetically clustered distribution. *J Bacteriol* **180**, 1159-1165 (1998).

3 Clermont, O., Bonacorsi, S. & Bingen, E. Rapid and simple determination of the *Escherichia coli* phylogenetic group. *Appl Environ Microbiol* **66**, 4555-4558 (2000).

4 Picard, B. *et al.* The link between phylogeny and virulence in *Escherichia coli* extraintestinal infection. *Infect Immun* **67**, 546-553 (1999).

5 Novais, A. *et al.* Characterization of globally spread *Escherichia coli* ST131 isolates (1991 to 2010). *Antimicrob Agents Chemother* **56**, 3973-3976, (2012).

6 Johnson, J. R. *et al.* Comparison of *Escherichia coli* ST131 pulsotypes, by epidemiologic traits, 1967-2009. *Emerg Infect Dis* **18**, 598-607, (2012).

7 Reid, S. D., Herbelin, C. J., Bumbaugh, A. C., Selander, R. K. & Whittam, T. S. Parallel evolution of virulence in pathogenic *Escherichia coli*. *Nature* **406**, 64-67, (2000).

8 Norton, J. P. & Mulvey, M. A. Toxin-antitoxin systems are important for niche-specific colonization and stress resistance of uropathogenic *Escherichia coli*. *PLoS Pathog* **8**, e1002954, (2012).

9 Gordon, D. M., Clermont, O., Tolley, H. & Denamur, E. Assigning *Escherichia coli* strains to phylogenetic groups: multi-locus sequence typing versus the PCR triplex method. *Environ Microbiol* **10**, 2484-2496, (2008).

10 Hottes, A. K. *et al.* Bacterial adaptation through loss of function. *PLoS Genet* **9**, e1003617, (2013).

11 Nichols, R. J. *et al.* Phenotypic landscape of a bacterial cell. *Cell* **144**, 143-156, (2011).

12 Wiedenbeck, J. & Cohan, F. M. Origins of bacterial diversity through horizontal genetic transfer and adaptation to new ecological niches. *FEMS Microbiol Rev* **35**, 957-976, (2011).

13 Andersson, D. I. & Hughes, D. Gene amplification and adaptive evolution in bacteria. *Annu Rev Genet* **43**, 167-195, (2009).

14 Wiles, T. J. *et al.* A phyletically rare gene promotes the niche-specific fitness of an *E. coli* pathogen during bacteremia. *PLoS Pathog* **9**, e1003175, (2013).

15 Wiles, T. J., Bower, J. M., Redd, M. J. & Mulvey, M. A. Use of zebrafish to probe the divergent virulence potentials and toxin requirements of extraintestinal pathogenic *Escherichia coli*. *PLoS Pathog* **5**, e1000697, (2009).

16 Buckles, E. L. *et al.* Role of the K2 capsule in *Escherichia coli* urinary tract infection and serum resistance. *J Infect Dis* **199**, 1689-1697, (2009).

17 Raivio, T. L., Popkin, D. L. & Silhavy, T. J. The Cpx envelope stress response is controlled by amplification and feedback inhibition. *J Bacteriol* **181**, 5263-5272 (1999).

18 Blattner, F. R. *et al.* The complete genome sequence of *Escherichia coli* K-12. *Science* **277**, 1453-1474 (1997).

19 Welch, R. A. *et al.* Extensive mosaic structure revealed by the complete genome sequence of uropathogenic *Escherichia coli*. *Proc Natl Acad Sci U S A* **99**, 17020-17024 (2002).

20 Mulvey, M. A., Schilling, J. D. & Hultgren, S. J. Establishment of a persistent *Escherichia coli* reservoir during the acute phase of a bladder infection. *Infect Immun* **69**, 4572-4579 (2001).

21 Lane, M. C., Alteri, C. J., Smith, S. N. & Mobley, H. L. Expression of flagella is coincident with uropathogenic *Escherichia coli* ascension to the upper urinary tract. *Proc Natl Acad Sci U S A* **104**, 16669-16674, (2007).

22 Zhou, Q., Ames, P. & Parkinson, J. S. Mutational analyses of HAMP helices suggest a dynamic bundle model of input-output signalling in chemoreceptors. *Molecular microbiology* **73**, 801-814, (2009).

23 Price, N. L. & Raivio, T. L. Characterization of the Cpx regulon in *Escherichia coli* strain MC4100. *J Bacteriol* **191**, 1798-1815, (2009).

24 Murphy, K. C. & Campellone, K. G. Lambda Red-mediated recombinogenic engineering of enterohemorrhagic and enteropathogenic *E. coli*. *BMC Mol Biol* **4**, 11 (2003).

25 Datsenko, K. A. & Wanner, B. L. One-step inactivation of chromosomal genes in *Escherichia coli* K-12 using PCR products. *Proc Natl Acad Sci U S A* **97**, 6640-6645 (2000).

CHAPTER 5

DISCUSSION

UPEC encode an array of genes required for the colonization and survival of host-associated niches such as the urinary tract. In the introduction to this dissertation, I outlined some previously characterized virulence factors that contribute to UPEC fitness and discussed various aspects of the host defense that would discourage these bacteria from effectively colonizing the urinary tract. From epidemiological data, we know that despite precautions taken by the host to maintain a sterile genitourinary system, invading bacteria can frequently cause infection therein. In addition to the discouraging frequency of UTI, UPEC are also competent to persist within the host and cause recurrent infections. A better understanding of persistence and subsequent recurrence is much needed. This dissertation was focused on gaining a better understanding of the genetic elements involved in UPEC stress resistance and persistence, focusing specifically on how the genetic makeup of these pathogens affects their physiology within the host.

Our findings in Chapters 2 and 3 highlight specific genes that are required by UPEC for efficient stress resistance and are, ultimately, necessary for robust colonization of the urinary tract. In particular, the *pasTI* TA system is an attractive chemotherapeutic target due to the seemingly pathogen-specific effects on bacterial stress resistance and kidney colonization that we observed. Current antibiotic therapies do not discriminate pathogen from nonpathogen, and when given a regimen of broad-spectrum antibiotics to treat an infection, patients' endogenous microbiota are targeted nondiscriminately. Recent evidence suggests that antibiotic therapy can significantly alter the bacterial diversity,

affecting changes on the microbial diversity and associated metagenome [1]. How these perturbations in the microbial community are related to complex illnesses such as Crohn's disease and irritable bowel disease have not been definitively characterized, but there is mounting evidence that frequent antibiotic use can have long-term detrimental effects on the immune system and general physiology of the patient [2,3]. For these reasons, among others, it is important that we find pathogen specific targets for common bacterial infections. We offer compelling evidence that TA systems—as opposed to global regulators of bacterial physiology such as the cAMP-CRP complex—may be good candidates for the generation of novel chemotherapeutic agents.

In order to find targets for pathogen-specific therapies, we felt it was best to understand the fundamental aspects of pathogenesis. That is, what differentiates a pathogen from a commensal bacterium? We know that the accumulation of virulence factors such as iron acquisition systems, secreted toxins, and adhesive organelles correlates with pathogenic variants of *E. coli*, but we have little understanding of how these strains evolved to their current states [4]. In Chapter 4, we provide evidence that a degraded chromosomal TA system—what we named the *hicE* locus—could have contributed to the evolution and pathogenicity of UPEC. While this locus seems clearly useful as a diagnostic marker for phylogroup B2 *E. coli,* it does not seem to be a realistic candidate for chemotherapeutic targeting. A chromosomal deletion of this locus within UPEC strains does not affect colonization of either the urinary tract or the gastrointestinal tract. These data highlight the redundancies of stress resistance

found in these pathogenic strains and provide us with a better understanding of possible evolutionary pathways that led to the formation of modern day UPEC. Future studies may unearth other evolutionarily conserved traits that affect pathogenesis and are, therefore, realistic candidates for pathogen-specific chemotherapeutic agents. Our hope is that the work of this dissertation will contribute to the knowledge necessary for discovering novel clinical therapies for the treatment of UTI and recurrent UTI.

References

1 Antunes, L. C. *et al.* Effect of antibiotic treatment on the intestinal metabolome. *Antimicrob Agents Chemother* **55**, 1494-1503, (2011).

2 Hviid, A., Svanstrom, H. & Frisch, M. Antibiotic use and inflammatory bowel diseases in childhood. *Gut* **60**, 49-54, (2011).

3 Cho, I. & Blaser, M. J. The human microbiome: at the interface of health and disease. *Nat Rev Genet* **13**, 260-270, (2012).

4 Wiles, T. J. *et al.* A phyletically rare gene promotes the niche-specific fitness of an *E. coli* pathogen during bacteremia. *PLoS Pathog* **9**, e1003175, (2013).

APPENDIX A

A PHYLETICALLY RARE GENE PROMOTES THE NICHE-SPECIFIC FITNESS OF AN *E. COLI* PATHOGEN DURING BACTEREMIA

Reprinted with permission from Public Library of Science

Wiles, T.J., Norton, J.P., Smith, S.N., Lewis, A.J., Mobley, H.L.T., Casjens, S.R., and Mulvey, M. A. A phyletically rare gene promotes the niche-specific fitness of an *E. coli* pathogen during bacteremia. *PLoS Pathog*. **9**(2): e1003175, doi:10.1371/journal.ppat.1003175 (2013).

OPEN ACCESS Freely available online

PLOS | PATHOGENS

A Phyletically Rare Gene Promotes the Niche-specific Fitness of an *E. coli* Pathogen during Bacteremia

Travis J. Wiles[1], J. Paul Norton[1☯], Sara N. Smith[2☯], Adam J. Lewis[1], Harry L. T. Mobley[2], Sherwood R. Casjens[1], Matthew A. Mulvey[1]*

1 Division of Microbiology and Immunology, Pathology Department, University of Utah School of Medicine, Salt Lake City, Utah, United States of America, **2** Department of Microbiology and Immunology, University of Michigan Medical School, Ann Arbor, Michigan, United States of America

Abstract

In bacteria, laterally acquired genes are often concentrated within chromosomal regions known as genomic islands. Using a recently developed zebrafish infection model, we set out to identify unique factors encoded within genomic islands that contribute to the fitness and virulence of a reference urosepsis isolate—extraintestinal pathogenic *Escherichia coli* strain CFT073. By screening a series of deletion mutants, we discovered a previously uncharacterized gene, *neaT*, that is conditionally required by the pathogen during systemic infections. *In vitro* assays indicate that *neaT* can limit bacterial interactions with host phagocytes and alter the aggregative properties of CFT073. The *neaT* gene is localized within an integrated P2-like bacteriophage in CFT073, but was rarely found within other proteobacterial genomes. Sequence-based analyses revealed that *neaT* homologues are present, but discordantly conserved, within a phyletically diverse set of bacterial species. In CFT073, *neaT* appears to be unameliorated, having an exceptionally A+T-rich composition along with a notably altered codon bias. These data suggest that *neaT* was recently brought into the proteobacterial pan-genome from an extra-phyletic source. Interestingly, even in G+C-poor genomes, as found within the Firmicutes lineage, *neaT*-like genes are often unameliorated. Sequence-level features of *neaT* homologues challenge the common supposition that the A+T-rich nature of many recently acquired genes reflects the nucleotide composition of their genomes of origin. In total, these findings highlight the complexity of the evolutionary forces that can affect the acquisition, utilization, and assimilation of rare genes that promote the niche-dependent fitness and virulence of a bacterial pathogen.

Citation: Wiles TJ, Norton JP, Smith SN, Lewis AJ, Mobley HLT, et al. (2013) A Phyletically Rare Gene Promotes the Niche-specific Fitness of an *E. coli* Pathogen during Bacteremia. PLoS Pathog 9(2): e1003175. doi:10.1371/journal.ppat.1003175

Editor: Frank R. DeLeo, National Institute of Allergy and Infectious Diseases, National Institutes of Health, United States of America

Received June 15, 2012; **Accepted** December 19, 2012; **Published** February 14, 2013

Funding: This work was supported by NIH grants AI095647, AI090369, and AI088086 (to M.A.M); AI074825 (to S.R.C.); and AI043363 and DK094777 (to H.L.T.M.). T.J.W. was funded by NIH Genetics Training Grant T32-GM007464. The funders had no role in study design, data collection and analysis, decision to publish, or preparation of the manuscript.

Competing Interests: The authors have declared that no competing interests exist.

* E-mail: mulvey@path.utah.edu

☯ These authors contributed equally to this work.

Introduction

As a species, *Escherichia coli* is best known for colonizing the lower intestine of humans and other warm-blooded vertebrates [1,2]. The contingent exit from the intestinal tract presents strains of *E. coli* with a multitude of secondary habitats, including host-associated and free-living niches [2,3,4,5,6]. A subset of *E. coli* designated **ex**traintestinal **p**athogenic ***E. c**oli* (ExPEC) excels at colonizing host-associated extraintestinal environments, resulting in an array of human diseases including urinary tract infections, bacteremia, and meningitis [7]. ExPEC strains also exhibit an impressive zoonotic capacity, being able to persist and cause disease in a variety of domesticated animals [8,9,10,11]. Collectively, ExPEC-related diseases represent daunting medical, agricultural, and economic burdens that threaten to worsen as antibiotic-resistant strains become more prevalent [8,12,13]. The evolutionary forces that underlie the emergence and niche tropisms of ExPEC have yet to be completely defined. Considering gene content, substantial intra-specific variation often exists between bacterial isolates, particularly among strains of pathogenic *E. coli*. Key questions regarding the origin of this heterogeneity and its impact on the fitness of virulent strains remain unanswered.

Bacteria are proficient at rapidly developing innovative, selectable traits to maintain fitness within complex environments—a property known as 'evolvability' [14,15,16,17,18]. Despite being largely asexual organisms that multiply by binary fission, bacteria engage in a genetically promiscuous behavior known as 'lateral gene transfer' (LGT). Laterally acquired genes can provide context-specific functions, such as the ability to metabolize atypical substrates [19], adhere to a variety of surfaces [7], neutralize antibiotics and other toxic compounds [5], or participate in niche construction [20]. Bacteria have several means of obtaining potentially beneficial elements through LGT: direct acquisition from the environment (transformation), transfer through cell-to-cell mating (conjugation), and acquisition from bacterial viruses known as bacteriophages (transduction) [14,21,22,23,24]. It has been estimated that ~81% of all genes within a bacterial chromosome have been involved in LGT at some point, suggesting that this behavior is not just an anomalous event, but that over time it is a foundational component of bacterial evolution [25].

Author Summary

Bacterial pathogens, even those belonging to the same species, can be incredibly diverse with regard to the genes they carry. However, the design of vaccines and antibiotics typically relies upon identification of general molecular features shared by the targeted organisms. Thus, we have traditionally focused on broadly conserved characteristics of pathogenic bacteria, often ignoring the genes that account for their individuality. In this article we report the discovery of a unique gene, *neaT*, that promotes the fitness of a pathogenic *Escherichia coli* isolate in zebrafish and mouse models of systemic blood infections. Surprisingly, *neaT* is rarely found in other related strains of *E. coli* and appears to have been recently acquired from distant lineages of bacteria via a process known as 'lateral gene transfer' that is used by microbes to swap genetic material. Expression of the *neaT* gene appears to help *pathogens* avoid interactions with host immune cells, possibly by altering bacterial surface structures. This work provides an interesting example of how the lateral acquisition of a rare gene can impact the niche-specific virulence properties of a pathogen, shedding light on the mechanisms that drive pathogen evolution and diversity.

The genomes of *E. coli* are laden with the signatures of past LGT events. Since the first genome sequencing projects it has been apparent that *E. coli* chromosomes are highly mosaic [26,27,28]. In part, this chromosomal architecture results from the presence of 'genomic islands' (GI) that intermittently disrupt synteny [29,30,31,32,33,34]. Many GIs exhibit clear signs of having been involved in past LGT events as they are often in proximity to mobile elements, such as transposons, or are themselves integrated phages or plasmids [35]. Accompanying this interchangeable chromosomal arrangement is a vast superset of genes defined as the pan-genome [32,36,37]. Whereas an average *E. coli* genome contains about 4,700 genes, the pan-genome of this species is estimated to be over 17,000 genes. Most *E. coli* strains share a subset of the pan-genome, which encodes vertically inherited genes that dictate the fundamental cellular properties of the lineage. This core genome surprisingly accounts for only 40–50% of the genetic makeup of any particular isolate. The rest of the chromosome contains strain-specific combinations of genes that are infused throughout the core genome and encode a variety of accessory functions that can provide unique selective advantages [32,37,38].

With this information in mind, we systematically screened GIs of a urosepsis ExPEC isolate for laterally acquired genes that affect virulence in a surrogate zebrafish host model. We identified a novel gene—designated *neaT* (**n**omadically **e**volved **a**cyl**t**ransferase)—that is required during blood-borne, but not localized, infections in both zebrafish and mice. The *neaT* locus was unexpectedly rare in the genomes of closely related *E. coli* strains and other Proteobacteria, suggesting that it was obtained from outside the contemporary *E. coli* pan-genome. Proteobacterial *neaT* homologues, in general, exhibit a high degree of allelic variance, have reduced guanine and cytosine (G+C) content, and are often localized within the integrated genomes of unrelated bacteriophages. These observations indicate that *neaT*-like alleles may have been recently acquired on multiple occasions by the proteobacterial supraspecies pan-genome. Together, our results provide molecular and bioinformatic evidence that the acquisition of unique genes like *neaT* during the evolution of particular ExPEC isolates can significantly impact bacterial fitness and virulence within specific host environments. Possible evolutionary forces that generate the observed sequence-level features of *neaT* and the role that bacterial individuality plays in pathogenesis are considered.

Results

The P2-like prophage b0847 promotes the fitness and virulence of ExPEC strain CFT073 during systemic infection of zebrafish embryos

The ExPEC strain CFT073 was isolated from the blood of a human patient with acute pyelonephritis (kidney infection) [26,39]. This urosepsis isolate is versatile, with the apparent ability to traverse several host microenvironments to reach the bloodstream, and has a relatively large genome of 5,369 protein-coding genes and several GIs. In previous work, we found that CFT073 is exceptionally lethal in an infection model that uses zebrafish embryos as surrogate hosts for the high-throughput analysis of ExPEC virulence [40]. At 48 h post-fertilization (hpf), zebrafish possess an innate immune system composed primarily of phagocytic cells and antimicrobial peptides [41,42,43,44]. These defenses mirror those employed by mammalian hosts to combat ExPEC.

To identify GI-associated virulence factors carried by CFT073, we screened 11 previously described deletion mutants that each lack a specific GI (Table 1 and Figure 1A) [45]. In blinded assays, 48 hpf zebrafish embryos were infected with 1,000 to 2,000 colony-forming units (CFU) of either wild type CFT073 or one of the 11 GI mutants. Bacteria were delivered into one of two injection sites: the fluid-filled sac surrounding the heart referred to as the pericardial cavity (PC), which mimics a localized tissue infection, and the circulation valley (CV), which facilitates rapid dispersal of bacteria into the bloodstream [40]. Each of these sites likely challenges the pathogen with different nutrient limitations, receptor availability, and host defenses.

In this infection model, increased growth of ExPEC is associated with decreased survival of the host [40]. All 11 GI mutants, with the exception of ΔGI-*aspV*, grew equally well in broth culture at 28.5°C and 37°C (data not shown). Following inoculation into the PC, only deletion of the 123 kb GI PAI-*pheV* [I] resulted in a significant decrease in virulence relative to wild type CFT073 (Figure 1B, top). This was not surprising as PAI-*pheV* [I] encodes

Table 1. Summary of GI screen in zebrafish infection sites.

GI deletion variant	Size (Kbp)	PC		Blood	
		n	*p* value	*n*	*p* value
Φ*potB*	44	9	0.2272	10	0.3581
GI-*selC*	68	9	0.6862	9	**0.0307**
GI-*cobU*	44	10	0.6689	10	0.0702
ϕb0847	33	9	0.2831	9	**0.0056**
GI-*asnW*	54	10	0.1338	10	0.9703
PAI-*asnT* [HPI]	32	10	0.7036	10	0.6317
PAI-*pheV* [I]	123	30	**<0.0001**	30	**<0.0001**
PAI-*metV*	32	10	0.7586	9	0.179
PAI-*pheU* [II]	52	10	0.2322	10	0.6321
PAI-*aspV*	100	10	0.2322	10	0.7972
PAI-*serX*	113	9	0.4113	10	0.6163

n denotes number of individual embryos used.
p values reflect the statistical significance of differences between wild type and mutant killing kinetics.
doi:10.1371/journal.ppat.1003175.t001

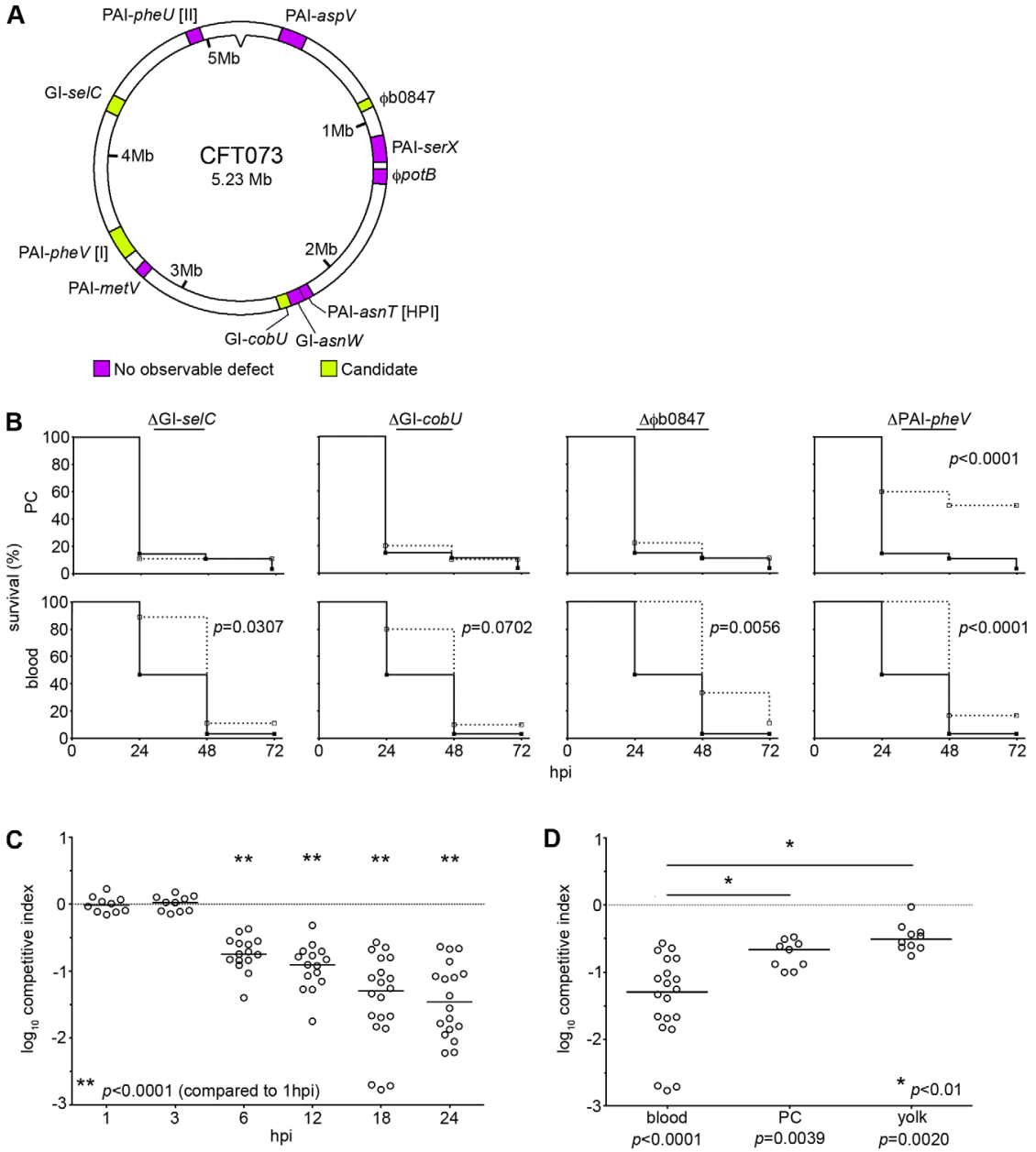

Figure 1. The ϕb0847 island is important for CFT073 pathogenicity during systemic infection in zebrafish embryos. (A) Diagram of GIs and their location within the CFT073 chromosome that were screened in the zebrafish host. Magenta indicates island mutants that had no observable defects, while green denotes island mutants that displayed significant attenuation. (B) The pericardial cavity (PC, top row) and blood (bottom row) of 48 hpf embryos were inoculated with 1,000–2,000 CFU. Fish were scored for death at 0, 24, 48, and 72 h post-inoculation (hpi). Data are presented as Kaplan-Meier survival plots and *p* values were calculated using a log-rank (Mantel-Cox) test (sample sizes for each curve are listed in Table 1). (C) Equal numbers (1,000–2,000 CFU total) of wild type and CFT073Δϕb0847 were inoculated into the bloodstream of embryos. Fish were sacrificed and bacterial loads enumerated at the indicated times by differential plating ($n = 10$ to 20 embryos). Data are represented as competitive indices, where negative values indicate a reduction in fitness of the mutant strain. (D) Bacteria were prepared as in (C) and inoculated into the PC or yolk. Fish were sacrificed at 18 hpi and bacterial numbers determined ($n = 9$–10 embryos). Data from blood infections is the same as in (C), provided as a reference. *P* values were determined using two-tailed Mann-Whitney *t* tests. Median values are indicated by bars in (C) and (D).
doi:10.1371/journal.ppat.1003175.g001

the notable ExPEC-associated virulence factors α-hemolysin (pore-forming toxin), SAT (vacuolating toxin), P pili (adhesive organelles), aerobactin (iron acquisition system), and K2 capsule (immune evasion). The ability of the ΔPAI-*pheV* mutant to still kill approximately half of the embryos suggests that additional factors with overlapping roles in virulence within the PC are encoded outside of PAI-*pheV* and the 10 other GIs tested.

The ΔPAI-*pheV* mutant was also attenuated following inoculation of the CV to initiate systemic infection, as were the GI mutants ΔGI-*selC*, ΔGI-*cobU*, and Δϕb0847 (Figure 1B, bottom). In addition to several hypothetical genes, the *selC* and *cobU* islands harbor genes that appear to be components of polyamine and iron transport systems, respectively. Both polyamines and iron acquisition systems are known to be important mediators of ExPEC fitness in mouse models of infection [46,47,48]. Although the ΔGI-*cobU* mutant exhibited only a modest reduction in virulence in these assays using inoculation doses of 1,000–2,000 CFU/embryo, with slightly higher doses between 2,000 to 3,000 CFU/embryo this mutant displayed more dramatic and significant ($p<0.05$) attenuation (Table S1). This observation supports previous findings indicating that the inoculation dose can markedly influence the discernibility of some mutant phenotypes in the zebrafish host [40].

The remaining GI showing a phenotype in our screen is composed of an intact integrated phage genome (prophage) named 'ϕb0847' (Figure 1B) [45]. This prophage is 33 kb in length and contains 48 predicted open reading frames, most of which encode recognizable phage proteins that share homology with genes of tailed phages belonging to the order *Caudovirales*. More specifically, ϕb0847 carries genes involved in regulation, replication, and virion assembly that are related to and syntenic with the genes of phage P2 and its relatives (Figure 2). From this analysis, it is clear that the ϕb0847 prophage is a member of the P2-like phage group and likely represents a fully functional phage genome complete with all the essential genes associated with P2-like phages [49]. Aside from the Δ*pheV* mutant, with its fairly well characterized assortment of virulence genes, Δϕb0847 displayed the most pronounced defect of the island mutants examined. Therefore, the ϕb0847 GI became the primary focus of our investigation.

To further define the contribution of ϕb0847 to the virulence and fitness of CFT073, we carried out competitive assays in which a one-to-one mixture of wild type and mutant bacteria were injected into the CV of zebrafish embryos (Figure 1C). At the indicated time points, the infected embryos were homogenized and bacteria present were enumerated by dilution plating on selective agar. Δϕb0847 carries a kanamycin resistance cassette that was used to distinguish wild type and mutant strains. No differences between wild type CFT073 and the Δϕb0847 mutant were observed until 6 h post-inoculation (hpi), when Δϕb0847 titers began to decline (Figure 1C). These results indicate that the ϕb0847 island is dispensable during initial stages of a systemic infection, but enhances bacterial fitness at later time points, coordinate with the upregulation of host inflammatory responses engage. The Δϕb0847 mutant displayed more modest, though still significant, decreases in fitness during competitive assays against wild type CFT073 within the PC and yolk sac at 18 hpi (Figure 1D). Phagocytes are recruited into the PC *en masse* in response to infection with ExPEC [40], possibly contributing to the competitive disadvantage of the Δϕb0847 mutant within this niche. On the other hand, the yolk is a rich source of nutrients for bacteria and is mostly free of phagocytes and other immunosurveillance mechanisms. However, the yolk does contain maternally inherited antimicrobial compounds that could account for the slight reduction in fitness of Δϕb0847 within this host environment

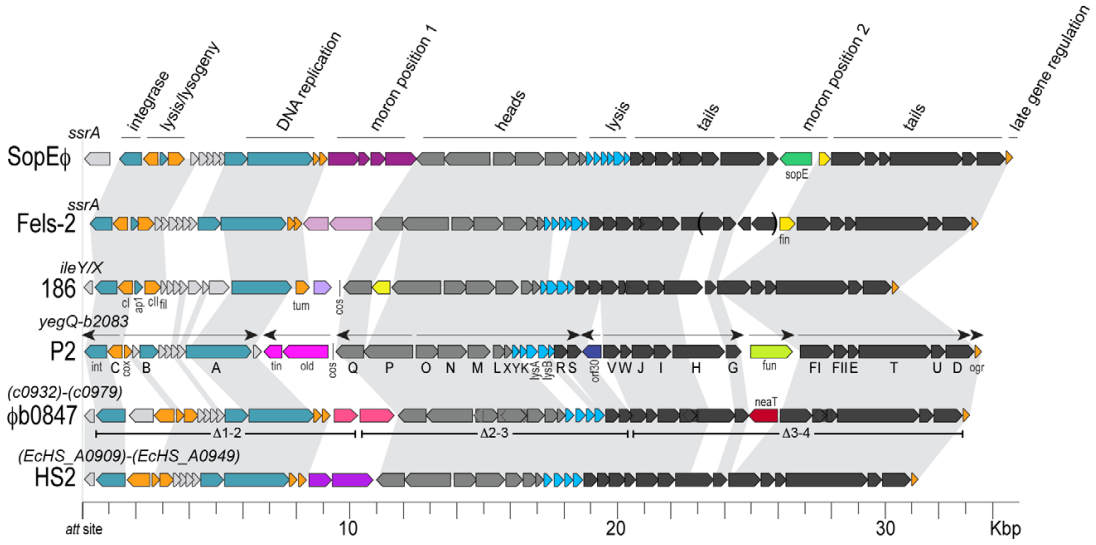

Figure 2. Alignment of ϕb0847 genome to other P2-like bacteriophage. Related P2-like prophages are aligned relative to their respective integration sites (att). Size is measured in kilobase pairs (Kbp). E. coli phages P2 and 186 and Salmonella phages Fels-2 and SopE5 were previously characterized. HS2 is an uncharacterized prophage contained within the genome of the commensal E. coli strain HS. Our unpublished analysis indicates that P2, 186, and Fels-2 represent three different "sequence types" based on virion proteins, which are typically >85% identical within each of these three groups and 50–70% identical between the groups. Bracketed numbers below ϕb0847 indicate positions of the deletion mutants generated to assess the functionality of genes within broad regions of ϕb0847. The neaT gene is distinguished by a red open reading frame in moron position 2.
doi:10.1371/journal.ppat.1003175.g002

[50]. Competitive experiments in broth culture did not reveal appreciable differences between the wild type and mutant strains (data not shown).

ϕb0847 harbors a multigenic region that contributes to fitness

To identify genes within ϕb0847 that, when deleted, recapitulate the attenuated phenotypes of Δϕb0847, we constructed partial deletion mutants lacking one of three nearly equal-sized regions of the prophage island (designated Δ1–2, Δ2–3, and Δ3–4, as indicated along the ϕb0847 genome in Figure 2). In competitive assays, the Δ1–2 and Δ2–3 mutants were significantly more fit than the full Δϕb0847 mutant at 12 hpi (Figure 3A). Analysis at 12 hpi allowed time for selection to take place, while limiting artifacts due to bacterial replication at later time points in dead and dying hosts where selective pressures are presumably weaker. In these assays, only the Δ3–4 mutant phenocopied the complete ϕb0847 island deletion mutant (Figure 3A). Lethality of this mutant variant was also significantly reduced in comparison to wild type CFT073 and the Δ1–2 and Δ2–3 mutants in independent challenges (Figure 3B). These results indicate that one or more genes within the terminal 3–4 region of the ϕb0847 prophage enhances both the fitness and virulence of CFT073 during systemic infections within the zebrafish host.

Temperate prophage genomes like ϕb0847 can carry 'lysogenic conversion' genes that affect the bacterial host but are not essential for lytic phage growth. To avoid disruption of critical phage processes, the integration of this genetic material is generally tolerated only in certain regions of the prophage genome. These added sequences are known as 'morons', because bacteriophages with such insertions have *more* DNA [51,52]. Moron genes typically contain their own regulatory elements and vary among individual phage genomes. They often alter the surface structure or physiology of the bacterial host and can benefit the phage by making its host refractory to competing parasites or otherwise promoting bacterial survival and growth [52,53].

The P2-like phages appear to have at least two variable moron positions (Figure 2). Using phage P2 as a reference, the location of moron position 1 is between the DNA replication gene *A* and head assembly gene *Q*, and moron position 2 is between the tail fiber gene *G* and tail sheath gene *FI* (Figure 2) [49]. In ϕb0847 within CFT073, the second moron site, which is absent from the Δ3–4 mutant, contains one open reading frame that is oriented in the opposite transcriptional direction to the flanking tail genes. This gene, which we named *neaT* for reasons described later, encodes a putative acyltransferase (Pfam:PF01757). This gene is not conserved among P2-like phages and is likely not critical for lytic replication of ϕb0847.

In light of this information, *neaT*, the immediately proximal gene *yfdK* (homologous to P2 phage tail gene *G*), and the collection of distal tail genes (*FI* through *D*) were individually deleted from the ϕb0847 prophage in CFT073. All three mutant derivatives—Δ*yfdK*, Δ*neaT*, and Δ*FI-D*—were attenuated in their ability to kill zebrafish embryos after injection into the blood via the CV (Figure 3C). Despite the significantly reduced virulence of these mutants, no defects in fitness were observed in competitive assays with wild type CFT073 (data not shown). The lack of any discernable fitness defects in competition assays may 1) reflect the ability of wild type CFT073 to trans-complement the mutant strains *in vivo* and/or 2) indicate that there is cooperative interplay among the *yfdK*, *neaT*, and *FI-D* loci. Of note, disruption of loci flanking *neaT* did not appreciably alter its expression in broth culture (Figure S1). Furthermore, we found no evidence that the *neaT* mutant could be complemented *in vivo* during competition assays by acquiring ϕb0847 sequences from the wild type strain (Figure S2). Interestingly, a *yfdK* homologue was recently shown to aid the survival of a K-12 laboratory strain of *E. coli* in acidic environments [54], but no mechanism for this effect is known, and to the authors' knowledge, *yfdK* homologues have not been implicated in pathogenesis.

The *neaT* gene restores virulence to the ϕb0847 island deletion mutant

The *in vivo* assays presented in Figure 3C and bioinformatic analyses described below highlight *neaT* as a gene of potential importance to the fitness and virulence of CFT073. To test this possibility, the *neaT* locus, including an upstream promoter region of 211 bp, was amplified from the CFT073 chromosome and cloned into the high-retention plasmid pGEN-mcs, yielding pGEN-*neaT*^{Pnative}. Semi-quantitative reverse transcription polymerase chain reaction (RT-PCR) indicated that *neaT* transcript levels made from the pGEN-*neaT*^{Pnative} vector in broth culture were about 1.7-fold higher than those observed in wild type CFT073 (Figure S3). Complementation experiments were performed comparing the lethality of wild type CFT073/pGEN-mcs, Δϕb0847/pGEN-mcs, and Δϕb0847/pGEN-*neaT*^{Pnative} in zebrafish embryos after inoculation of the CV (Figure 3D). The complete prophage deletion mutant Δϕb0847 carrying the empty vector pGEN-mcs exhibited a significant delay in killing relative to either the wild type strain CFT073/pGEN-mcs or the complemented mutant Δϕb0847/pGEN-*neaT*^{Pnative}. In total, these experiments identify *neaT* as a virulence determinant contained within the ϕb0847 island of CFT073; therefore, the uncharacterized *neaT* gene became the focal point for the remainder of our investigation.

neaT is required for fitness during systemic, but not localized infections in a mammalian host

To extend our observations made using zebrafish, we employed a murine model to further define the requirement for *neaT* during localized and systemic infections. For localized challenges, we took advantage of a well-characterized mouse model of urinary tract infection. Wild type CFT073 and the Δ*neaT* mutant were mixed at a one-to-one ratio and inoculated via transurethral catheterization into adult female CBA/J mice. After 3 days, animals were sacrificed and bacterial titers within the bladders and kidneys were enumerated, revealing no outright competitive advantage for wild type CFT073 over the Δ*neaT* mutant in either organ (Figure 4A). To appraise the requirement for *neaT* during systemic infections, we utilized a recently described sub-lethal bacteremia model in which CBA/J mice were injected with a one-to-one mixture of wild type and mutant bacteria via the tail vein [55]. At 24 hpi the Δ*neaT* mutant was recovered at significantly reduced levels from the spleen and liver compared to wild type CFT073 (Figure 4B). These results confirm and extend our findings in the zebrafish host, demonstrating that *neaT* provides niche-specific advantages to CFT073 during systemic infections.

Diversity and phage association of NeaT homologues

There are no closely related homologues of NeaT in *E. coli*. Only four matches were found in the current NCBI collection of 170 RefSeq *E. coli* genomes (as of June 2012) that produce an alignment E value$<10^{-6}$ with similarity over >50% of the NeaT protein length. A PCR-based survey for the presence of *neaT* within various clinical *E. coli* isolates corroborated our *in silico* observation that *neaT* is rare among this taxon (Figure S4). Out of 21 randomly chosen isolates, none carried the CFT073 *neaT* allele.

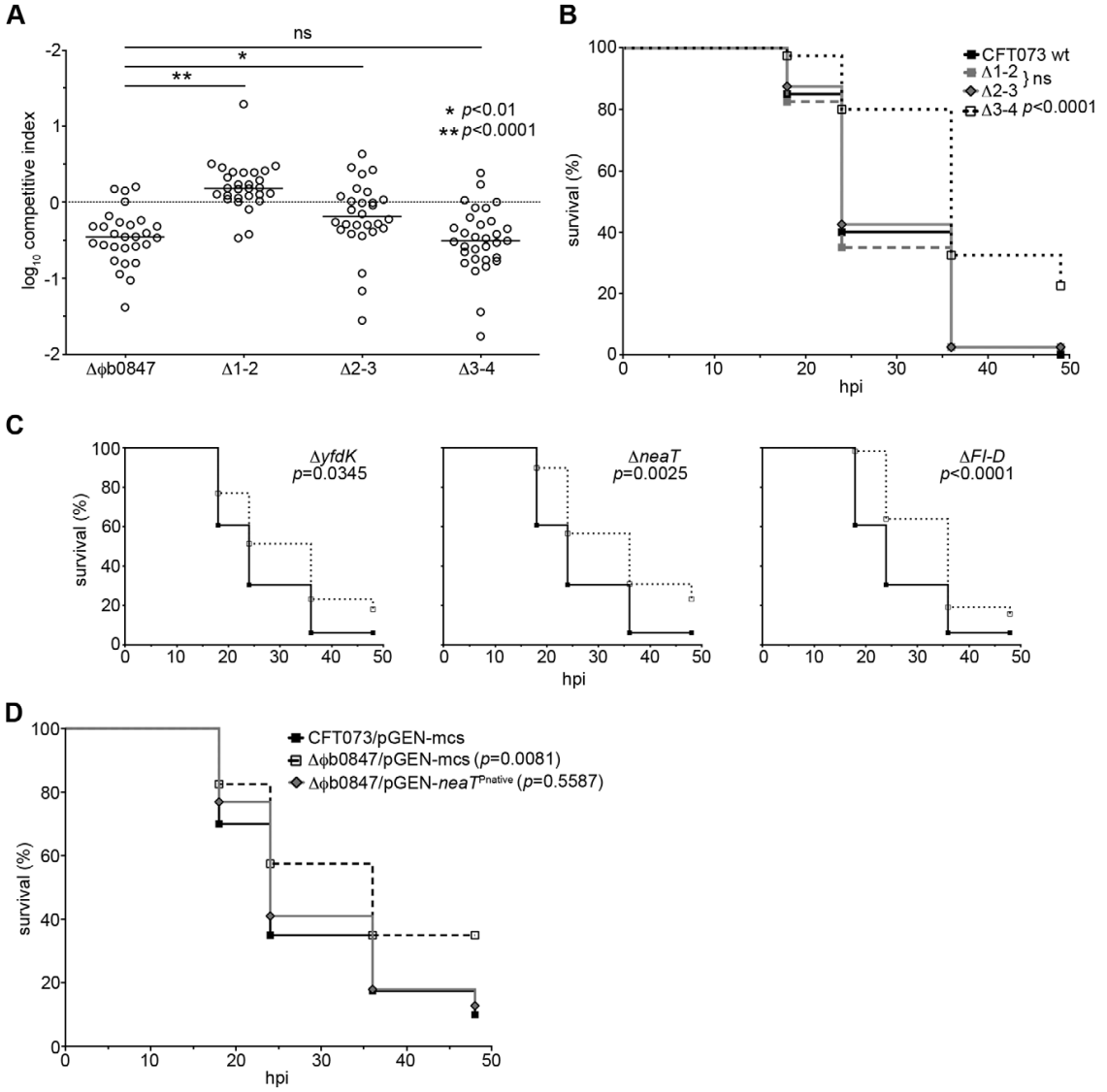

Figure 3. ϕb0847 harbors multiple loci that contribute to the fitness of CFT073 during systemic challenge. (A) Equal numbers (1,000–2,000 CFU total) of wild type CFT073 and each mutant derivative indicated were inoculated into the bloodstream of embryos. Fish were sacrificed and bacterial loads enumerated at 12 hours post inoculation (hpi) by differential plating ($n>28$). Data are presented as competitive indices with negative values indicating a reduction in fitness of the mutant. *P* values were determined using two-tailed Mann-Whitney *t* tests; bars indicate median values. (B), (C), and (D) 1,000–2,000 CFU of wild type CFT073, the indicated mutant, or recombinant derivative were each inoculated into the blood of 48 hpf embryos. Fish were scored for death every 6 h starting at 18 hpi until 48 hpi ($n=40$ or more embryos for each curve). pGEN-mcs in (D) serves as an empty vector control for pGEN-*neaT*^{Pnative}. Data in (B), (C), and (D) are presented as Kaplan-Meier survival plots. A log-rank (Mantel-Cox) test was used to determine *p* values; ns = not significant.
doi:10.1371/journal.ppat.1003175.g003

Homologues of *neaT* are also rarely detected in P2-like phage genomes; among 45 randomly chosen P2-like phages and prophages in *E. coli*, *Salmonella*, *Shigella*, and *Enterobacter* that we examined, only ϕb0847 carries a *neaT*-like gene. The closest match to NeaT in the NCBI database is encoded by locus *Ent638_2581* of *Enterobacter sp.* 638, whose protein product is only about 33% identical to NeaT. We note that several more distantly related *neaT* homologues are present in the genomes of other temperate phages and prophages of the bacterial family *Enterobacteriaceae* (Table 2). They are found, for example, in the *Shigella flexneri* phage Sf6 genome and several uncharacterized prophages of *S. flexneri*, in *E. coli* phage ϕV10 and a nearly identical prophage in the Shiga toxin-producing *E. coli* isolate DEC4D, and in a putative prophage within *Citrobacter rodentium* strain ICC168. The above *Enterobacter*

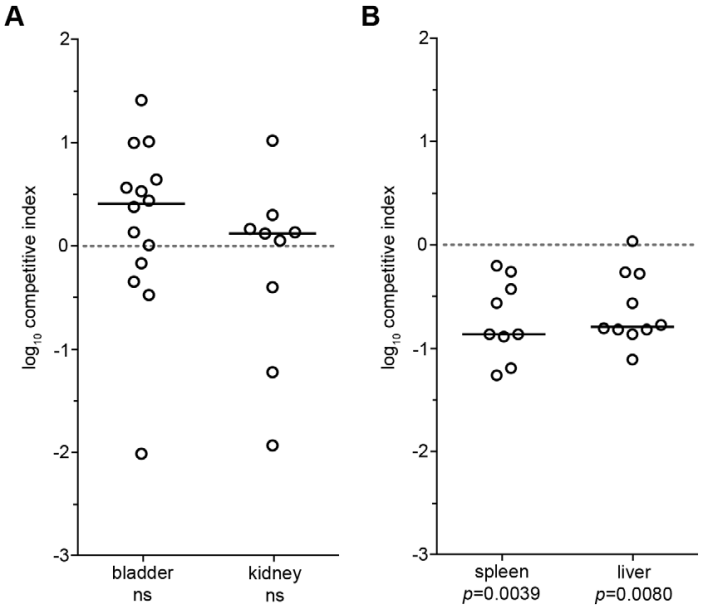

Figure 4. *neaT* enhances the fitness of CFT073 in a murine model of bacteremia. (A) Equal numbers (10^7 CFU total) of wild type CFT073 and CFT073Δ*neaT* were transurethrally inoculated into the bladder of CBA/J female mice. Mice were sacrificed, organs harvested, and bacterial loads enumerated at 3 d post inoculation. (B) Equal numbers (10^6 CFU total) of wild type and CFT073Δ*neaT* were inoculated into the bloodstream of CBA/J female mice via tail vein injection and bacterial titers present in the spleen and liver were enumerated 24 h later. Data are shown as competitive indices, where negative values indicate a reduction in the fitness of CFT073Δ*neaT*. Bars indicate median values for each group; $n \geq 9$ mice. *P* values determined using Wilcoxon-matched paired signed rank; ns = not significant.
doi:10.1371/journal.ppat.1003175.g004

homologue *Ent638_2581* is also carried within a putative prophage that is similar to *Shigella* phage SfV. Each of these phage-associated *neaT* homologues is un-ameliorated with respect to its bacterial host genome (see below), and each lies within a known moron position in its phage genome. Because *neaT* homologues differ substantially in sequence conservation and are found in a variety of tailed-phages, *neaT*-like genes may have been laterally acquired by *Enterobacteriaceae* lineages on several occasions, possibly via phage. Multiple *neaT* acquisition events would indicate that this gene has an underlying evolutionary importance to either the phages themselves or their hosts. In considering its putative function (see Figures S5, S6, and Text S1), its apparent lateral acquisition, and its allelic variance within the proteobacterial lineage, this gene was named '*neaT*'—**n**omadically **e**volved **a**cyl**t**ransferase. In the following sections we explore the evolutionary history of this gene by analyzing the diversity and distribution of *neaT*-like genes in more detail.

Table 2. *neaT* homologues associated with bacteriophages.

			%GC		
Bacterial host strain	**Associated phage genome**	**Gene ID**	***neaT* homologue**	**bacterial genome**	**% identity to *neaT*^{CFT073} (% query coverage)**
E. coli CFT073	P2-like ϕb0847 prophage	26107260	30	51	100 (100)
E. coli DEC4D	ε15-like prophage	377941589	31	50	22 (96)
E. coli O157:H7	ε15-like phage ϕV10	89152472	31	49	22 (94)
Enterobacter sp. 638	unnamed lambdoid prophage	146312226	38	53	34 (98)
C. rodentium ICC168	unknown prophage fragment	283784796	37	55	32 (41)
S. flexneri serotype X	Sf6	33334172	42	51	29 (35)
S. flexneri VA-6	Sf6-like defective prophage	333006890	42	51	29 (35)
S. flexneri K-218	unknown prophage	333006144	39	51	34 (86)
S. flexneri 4343-70	unknown prophage	332759112	39	51	34 (86)

doi:10.1371/journal.ppat.1003175.t002

Phyletic distribution of *neaT*

To investigate the evolutionary source of *E. coli neaT* genes, we assessed the phyletic distribution of its homologues. BLASTp alignments were performed on the publically available NCBI database using NeaT from CFT073 as a probe for the search sets of Proteobacteria, Firmicutes, Bacteroidetes, Actinobacteria, Spirochaetes, and Fusobacteria [56]. Sequences were declared to be homologous if they had an alignment significance (E value) of $<10^{-6}$ over >50% of their lengths [57]. These searches retrieved a total of 317 non-paralogous NeaT-like sequences. The distribution of phyla containing these sequences is depicted in Figure 5A (left), revealing that the majority of *neaT* homologues are from the Firmicutes and Bacteroidetes rather than Proteobacteria. In an attempt to control for the inherent bias of NCBI databases, we plotted the number of available gene sequences for each phylum represented in Figure 5A (right). This plot demonstrates that the high number of *neaT* homologues identified among non-proteobacterial phyla is not due to a skew in sequence abundances. To the contrary, total proteobacterial gene sequences overshadow those from other phyla and therefore underscore the relative rarity of *neaT* alleles in this taxon.

To quantify the phyletic distribution of NeaT homologues with greater statistical confidence, we performed bi-directional alignments of NeaT using BLASTp with a manually assembled database of open reading frames from a representative, yet broad, assortment of 165 phylogenetically classified bacterial genomes and associated plasmids obtained from NCBI (Table S3). This analysis confirmed that, compared to random chance, *neaT* homologues are significantly enriched among species belonging to the phyla Firmicutes and Bacteroidetes (Figure 5B). Moreover, many of the *neaT* homologues were detected in notable plant and animal pathogens, including *Erwinia spp.*, *Bacillus spp.*, *Staphylococcus aureus*, *Streptococcus oralis*, *Clostridium botulinum*, and *Porphyromonas spp.*

Results from similar alignments of *neaT* and all other ϕb0847-encoded genes are presented graphically in Figure 5C. For each prophage gene, the number of non-paralogous matches found in the custom database are represented as bars (upper axis) and the percent of those hits that are harbored within proteobacterial genomes (lower axis) are plotted against the position of the gene within ϕb0847 (x-axis). Given the host range of known P2-like phages, it is not unexpected that the majority of genes within ϕb0847 were exclusive to the proteobacterial phylum. Exceptions, in addition to *neaT*, include homologues of ϕb0847 genes encoding the phage integrase and a Dam methylase. However, *neaT* is unique among the ϕb0847 prophage genes in that over 75% of its matches (16 of 21) were from outside the Proteobacteria (Figure 5C and Table S4). The discordant conservation of *neaT* highlights its likely extra-phyletic origin.

neaT displays signatures of recent lateral transfer

If a gene has origins outside its immediate genome, it would carry sequence-level vestiges of its previous host until it adopts the characteristics of the current host—a process known as 'amelioration' [27,58]. Commonly used parameters that distinguish laterally transferred and unameliorated genes are atypical codon usage and guanine-cytosine (G+C) content [57,59,60]. We

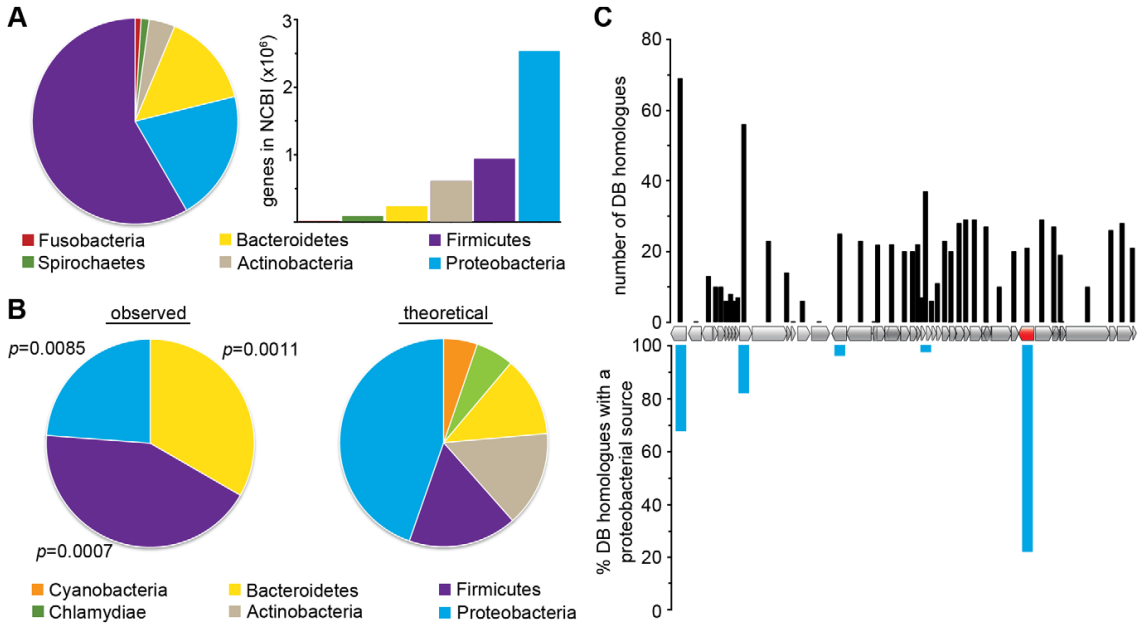

Figure 5. *neaT* is discordantly conserved. (A) Left: Phyletic distribution of neaT homologues among genomes retrieved from NCBI (n = 317). Right: Number of gene sequences deposited in NCBI for each phylum as of November 2011. (B) Left: Pie graph showing distribution of neaT homologues among each phylum represented in the custom database (n = 21 non-paralogous neaT genes). Right: Theoretical distribution of neaT homologues within phyla present in the custom database based on random chance. P values for the observed versus theoretical phyletic abundance of neaT homologues were calculated by .score analysis. (C) Upper y-axis: bar graph depicts total number of non-paralogous homologues retrieved from the custom database (DB) for each gene encoded within ϕb0847 (plotted along the x-axis with respect to its position within the prophage genome). The neaT open reading frame is indicated in red. Lower y-axis: bar graph showing the percent of proteobacterial homologuesfound in the homologue set for each ϕb0847 gene. Sequences unique to CFT073 were assigned 100% proteobacterial conservation.
doi:10.1371/journal.ppat.1003175.g005

analyzed these features of *neaT* in the context of the CFT073 genome and ϕb0847 prophage. Using all 5,369 protein-coding genes of CFT073, the frequency with which specific codons are used for each amino acid was calculated (Table S5). Each gene was then assigned a 'codon deviation score' representing how often it uses atypical codons (Methods and Table S6). Scoring correlates with conformity; genes scoring low have a more typical codon usage, whereas poorly conformed genes score high. This analysis shows that *neaT* possesses a significantly abnormal codon usage compared to the rest of the CFT073 genome ($p = 0.0260$) (Figure 6A, left panel). The *neaT* gene was also observed to be G+C-poor (29.84%), making it a significant outlier from the CFT073 genome-wide median of 51.5% ($p = 0.0001$) (Figure 6A, right panel). We also analyzed the codon deviation score (Figure 6B, upper axis) and nucleotide composition (Figure 6B, lower axis) of *neaT* with respect to the genome of ϕb0847. Most genes withinϕb0847 conform to the codon usage and G+C content of CFT073. This is expected for a parasite that has been co-evolving with proteobacterial hosts over an extensive period of evolutionary time [59]. Thus, the aberrant codon usage and nucleotide composition of *neaT* is not simply an inherited trait of ϕb0847. Because of its relatively low G+C content and poorly conformed codon usage, we conclude that *neaT* is a relatively recent acquisition by both ϕb0847 and the genome of CFT073.

To determine if the apparently unameliorated state of *neaT* in CFT073 is unique or if it is hinting at a more widespread phenomenon, we plotted the G+C content of a representative subset of *neaT* homologues identified in Figure 5 against the G+C content of their respective genomes (Figure 6C). As a control, we also plotted the G+C content of *poxB*, which encodes the metabolic enzyme pyruvate oxidase and exists in an ameliorated state within several phyla (Figure 6C, inset). Most proteobacterial *neaT* genes

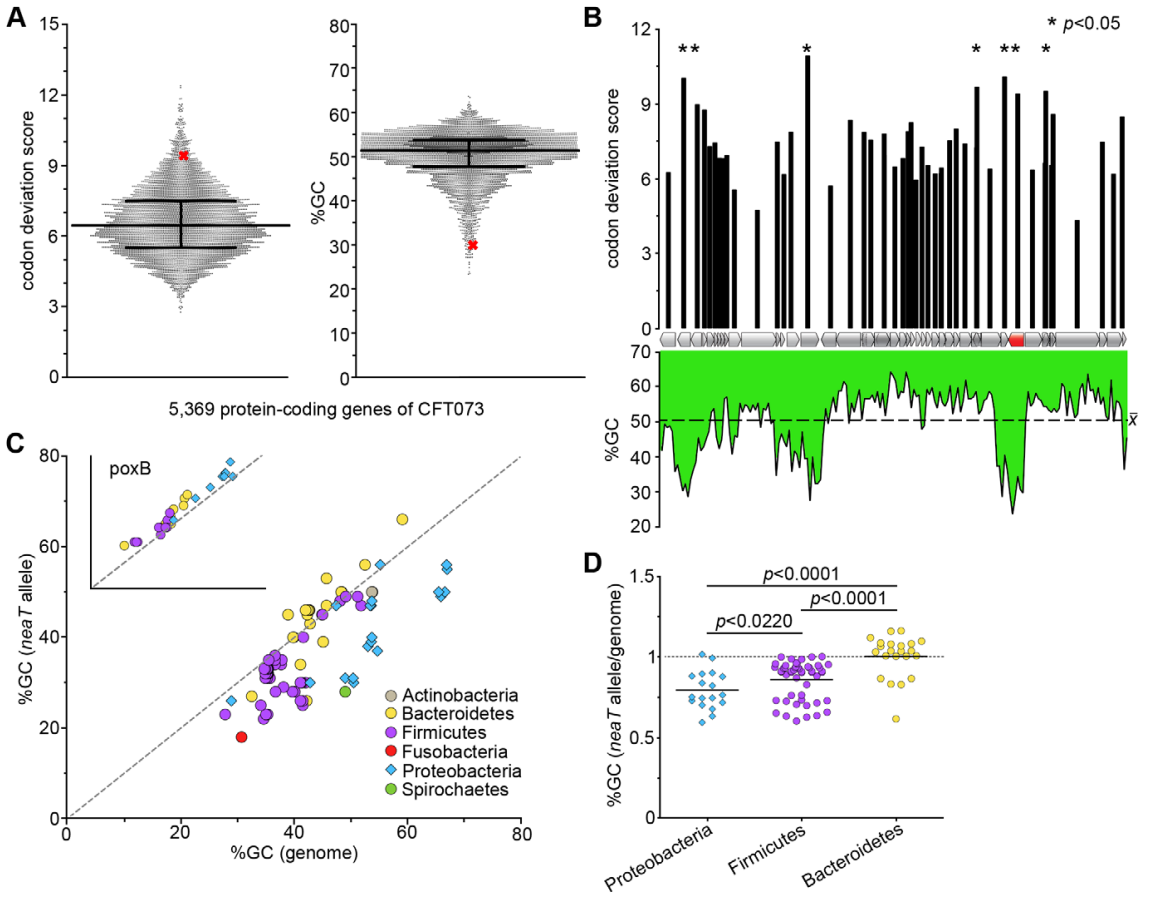

Figure 6. *neaT* is maintained in an un-ameliorated state. (A) Left: distribution of codon deviation scores assigned to the 5,369 protein-coding genes of CFT073. Right: distribution of %GC content of each protein-coding gene of CFT073. Bar and whiskers indicate median and interquartile ranges. Red 'X' marks position of *neaT* within each distribution. (B) Upper y-axis: bar graph depicting codon deviation score for each ϕb0847 gene plotted with respect to position within the prophage (x-axis cartoon, with the *neaT* gene highlighted in red.). Lower y-axis: line graph representing fluctuations in %GC content across ϕb0847 (window = 182 bp, step = 182 bp). (C) %GC content of *neaT* alleles found across phyla (color-coded) plotted against the %GC content of each respective genome (x-axis). Inset shows the same sort of analysis for the *poxB* allele as a comparison. Points falling on the dashed lines represent alleles that are completely ameliorated with respect to their host genomes. (D) Graph shows the ratio of %GC content of *neaT* alleles and total genomic %GC content for individual isolates within the indicated phyla. Bars indicate medians, and *p* values were determined using two-tailed Mann-Whitney *t* tests ($n = 18$ (Proteobacteria), 51 (Firmicutes), 22 (Bacteroidetes)).
doi:10.1371/journal.ppat.1003175.g006

were significantly less ameliorated than those found in the genomes of Bacteroidetes and many Firmicutes (Figure 6C and D). Interestingly, even though Firmicutes genomes generally have a low G+C content, *neaT*-like genes within this lineage are still relatively G+C-poor, at least in a major fraction of Firmicute species (Figure 6C). Cumulatively, these results indicate that, at least among the three phyla compared here, *neaT*-like genes have likely been associated with Bacteroidetes the longest, whereas acquisition by the Proteobacteria was a more recent event.

Discussion

Summary and impact of findings

Presented here are the results from a screen conducted using the ExPEC isolate CFT073 and a high-throughput zebrafish surrogate host model of infection. We screened GIs for novel virulence genes, which were expected to have a history of lateral gene transfer. Three loci within the P2-like prophage ϕb0847 were found to contribute to the virulence of CFT073 during systemic infection. A previously uncharacterized gene—designated here as *neaT*—was discovered to augment the virulence capacity of CFT073, independent of other prophage components (Figure 3D). We demonstrated that *neaT* is conditionally required for maximal fitness during bacteremic infections of both zebrafish and mice, suggesting that CFT073 has potentially co-opted this phage-borne gene for specific virulence behaviors. By tracing the evolutionary history of the *neaT* gene, we found that it is relatively rare and has sequence-based features suggesting that it was recently absorbed into the proteobacterial supraspecies pan-genome. Signs of its novelty are typified by high allelic variance—possibly a result of multiple entries into the Proteobacteria lineage via phage—and its mostly unameliorated state within proteobacterial genomes.

We also investigated the putative function(s) of NeaT *in vitro*. The NeaT protein shares homology with several characterized acyltransferases encoded within a variety of non-*E. coli* genomes. These putative membrane-localized enzymes can modify components of the bacterial cell wall, particularly peptidoglycan [61,62,63,64]. Alteration of this macromolecule can often provide bacterial pathogens with protection from host antimicrobial peptides and enzymes such as lysozyme. However, deletion of *neaT* had no effect on the sensitivity of CFT073 to lysozyme, the antimicrobial cationic peptide polymyxin B, or antibacterial factors present in human serum (see accompanying supplemental Text S1). Interestingly, expression of *neaT* did alter the behavior of CFT073 in swarming assays and induced bacterial aggregation on swim plates (Figure S5A–C, Text S1)—phenotypes that may be attributable to NeaT-mediated modification of components within the bacterial envelope. We also found that expression of recombinant NeaT can inhibit production of surface structures like curli and cellulose in some strain backgrounds (Fig. S5D–E, Text S1), supporting the notion that NeaT can affect salient properties of the bacterial surface and thereby alter bacterial group behavior.

The apparent capacity of NeaT to modulate bacterial aggregation (Fig. S5C) is especially intriguing in light of a recent work demonstrating that aggregate formation can promote bacterial survival within the bloodstream of infected mice [65]. Building on these observations, we found that expression of the *neaT* gene from a low copy number plasmid significantly decreased the capacity of CFT073 to associate with murine macrophages, suggesting that NeaT serves as an immune evasion factor (Fig. S6). The specific mechanism(s) by which NeaT promotes bacterial fitness during systemic infections, as well as the environmental cues that control *neaT* expression, require further investigation. As it stands, this work contributes to the idea that ExPEC isolates do not all share the same set of virulence factors, which are likely dictated by the distinct evolutionary trajectory and particular niche tropism of each strain.

neaT-based models for evolution of laterally acquired genes

Our analysis defines *neaT* as a recently acquired locus of the Proteobacteria. Evidence for this is drawn from its discordant conservation, abnormal codon usage, and low G+C content. In large part, the unameliorated state of *neaT*-like genes in Proteobacteria and Firmicutes genomes suggests that there is a general phenomenon accounting for its relative A+T-rich composition beyond having originated in an A+T-rich genome, as previously suggested [59]. We posit that the observed A+T-richness of laterally transferred genes can be, to some extent, accounted for by an 'exploratory mechanism' [16]. Upon introgression of a foreign gene, its retention depends on its adaption to the host's genetic and cellular machinery, a process that can take several millions of years [66]. During this time the gene may fall under relaxed selection whereby mutations accrue until a beneficial allele is 'discovered' and acted upon by selection. Connecting relaxed selection to reduced G+C content is the observation that there is a universal mutation bias for G/C to A/T transitions in bacterial genomes [67,68,69]. It then follows that immediately after a gene is acquired, it will initially accumulate A+T-rich character until a selectable version is ameliorated. From the findings presented here, we speculate that the *neaT* variant in CFT073 is an example of a newfound allele that is being used to promote bacterial fitness in pathogenic contexts.

Arguably, *neaT* may represent an ancient gene that has simply failed to fix within the proteobacterial lineage. Therefore, an alternative hypothesis is that the conditional requirement for *neaT* by CFT073 within different environments may have driven its current evolved state. We observed in two vertebrate model systems that *neaT* contributes significantly to pathogen fitness primarily during systemic infections. Considering the ecology of many bacterial pathogens, a question often left unaddressed is: what are the evolutionary forces that act on niche-specific genes in the absence of selective pressure? Particularly for *E. coli*, which has a complex multi-niche life cycle, the evolutionary consequences resulting from time outside selective environments on genes like *neaT* are not clear.

Work directly addressing this question is scarce. However, insight into this issue is provided by findings that genes under relaxed constraint have increased variance at the sequence level [17,70,71,72,73]. In contrast to relaxed selection, which occurs when purifying selection is alleviated, as discussed above, 'relaxed constraint' refers to a limitation in the exposure of a particular gene to selection. For example, eukaryotic genes with expression patterns that are sex-restricted are effectively 'hidden' from selection in half of the population. This is the case for the *Drosophila spp.* maternal-effect gene *bicoid*, which is maternally-restricted and critical for the embryonic development of fruit flies [70]. The *bicoid* gene was found to have a 2-fold higher heterozygosity compared to zygotically-expressed genes. Similarly, genes with caste-biased expression (*i.e.*, queen versus worker) in the social insects *Solenopsis invicta* (fire ant) and *Apis mellifera* (honey bee) were shown to be evolving more rapidly than genes expressed among all castes [71]. For both of these situations, the higher mutation rate observed for contextually expressed genes was concluded to be due to relaxed constraint. Further investigation into the exploratory mechanism and relaxed constraint hypotheses

of *neaT* evolution is required and must be considered in parallel with other processes and factors, including, for example, the susceptibility of laterally transferred genes to endogenous restriction enzymes [59].

ExPEC individuality and virulence

There exists an enormous amount of genetic heterogeneity among Eubacteria lineages. Genome sequencing and bioinformatic analyses have underscored this extensively. Perhaps the most intriguing aspect of this diversity is that even closely related members of the same species can differ greatly with respect to their gene contents. Strikingly, any two *E. coli* genomes can differ by up to 20–30% of their respective gene contents—in sharp contrast to the relatively minor difference of 1% that exists between, for example, the mouse and human species [32,74]. Decades worth of epidemiological and experimental studies have focused on the identification of genes that define the pathogenic behavior of ExPEC [7,32]. However, it appears that a single, ubiquitous genetic identifier of ExPEC, such as a gene encoding a particular toxin or adhesin, does not exist and, rather, what actually binds these pathogens is more qualitative and multigenic in nature [32,75].

In support of this view, we recently demonstrated that the toxin α-hemolysin, shared among many ExPEC isolates, is differentially required for virulence depending on strain background [40]. Similarly, we found that the pathogenicity of particular ExPEC isolates depends on another toxin, cytotoxic necrotizing factor, while other equally virulent strains naturally lack this gene. Coupled with the work presented here, these observations suggest that there exists a spectrum of only partially overlapping virulence gene requirements among ExPEC, reflecting the idea that these pathogens have emerged from distinct evolutionary trajectories driven by LGT [76,77]. Accordingly, we found that the expression of NeaT from plasmid pGEN-*neaT*$^{\text{Pnative}}$ in other *E. coli* strains, including Nissle 1917 (gut isolate), F11 (cystitis isolate), and S88 (meningitis isolate), did not augment virulence in the zebrafish infection model (data not shown). These findings suggest that the ability of a rare gene like *neaT* to affect fitness and virulence is dependent upon the genetic background of individual bacterial strains. The beneficial effects of *neaT*, and its potential to sweep through bacterial populations, is therefore likely linked to the presence, or coordinate acquisition, of other as-yet undefined bacterial factor(s). The identification, characterization, and continued monitoring of rare genes like *neaT* will be important to our understanding of ExPEC evolution. As a case in point, we note that the *sasX* gene, originally defined as *rare* among strains of methicillin resistant *Staphylococcus aureus* (MRSA), increased in prevalence among MRSA isolates between 2003 and 2011 and is now considered an emerging virulence determinant [78]. Interestingly, like *neaT*, *sasX* is also maintained within a prophage and can affect bacterial interactions with phagocytes. At this point, it is difficult to predict if *neaT* will sweep ExPEC populations in the future, but work presented here along with recent findings concerning *sasX* underscore how laterally acquired genes can alter the virulence potential of bacterial pathogens, continually challenging the development of broad spectrum therapeutics.

Going forward, as we continue to characterize the composition of pan-genomic elements of ExPEC and other pathogens, it will be important to consider the evolutionary context of their virulence genes. Identifying the spatial and temporal parameters that govern the lateral acquisition of virulence genes from distant lineages will need to be reconciled. Genome compatibility (codon and tRNA usage) and ecology are thought to be influential in the success of LGT events between bacteria [79,80,81]. In light of this, several interesting questions arise. How did *neaT* come to be in the proteobacterial gene pool? How does residence of *neaT* within a prophage impact its evolution? What conditions fostered the assimilation of *neaT* into the virulence regulon of its host? Using *neaT* as a stepping-stone, it will be informative to resolve the amount of strain-specific innovation that goes into producing and fine-tuning pathogen genomes. By understanding the mechanisms of chromosome assembly and the sources of individual genetic components, unrealized patterns may emerge that could prove useful for future diagnostics and disease mitigation.

Methods

Ethics statement

Animals used in this study were handled in accordance with IACUC protocols approved at either the University of Utah or the University of Michigan Medical School following standard guidelines as described at www.zfin.org and in the Guide for the Care and Use of Laboratory Animals, 8th Edition [55,82].

Bacterial strains and plasmids

All bacterial strains and plasmids used in this study are listed in Table 3. Unless specified otherwise, bacteria were cultured statically at 37°C for 24 h in 20 ml of a defined M9 minimal medium (6 g/l Na_2HPO_4, 3 g/l KH_2PO_4, 1 g/l NH_4Cl, 0.5 g/l NaCl, 1 mM $MgSO_4$, 0.1 mM $CaCl_2$, 0.1% glucose, 0.0025% nicotinic acid, 0.2% casein amino acids, and 16.5 mg/ml thiamine in H_2O). Antibiotics (kanamycin or ampicillin) were added to the growth medium when necessary to maintain recombinant plasmids or select for mutants.

Targeted gene knockouts were generated in the ExPEC isolate CFT073 using the lambda Red-mediated linear transformation system [83,84]. Briefly, a kanamycin resistance cassette was amplified using polymerase chain reaction (PCR) from pKD4 with 40-base pair overhangs specific to the 5′ and 3′ ends of each targeted locus. PCR products were introduced via electroporation into CFT073 carrying pKM208, which encodes an IPTG (isopropyl-β-D-thiogalactopyranoside)-inducible lambda red recombinase. Knockouts were confirmed by PCR. Primer sets used are listed in Table S8.

Cloning and construction of *neaT* expression constructs were done using standard molecular techniques employing the high-retention plasmid pGEN-mcs [85]. For native regulation, *neaT* (locus tag: c0970), plus 211 bp of upstream sequences, were amplified from the chromosome of CFT073 and TA-cloned into pCR2.1-TOPO vector per manufacture's protocol (Invitrogen). Subsequently, the cloned fragment was isolated using BamHI and NotI restriction enzymes (New England Biosciences) and ligated into pGEN-mcs using the same sites, yielding pGEN-*neaT*$^{\text{Pnative}}$. For construction of pGEN-*neaT*$^{\text{Plac}}$, a synthetic ribosome binding sequence was introduced upstream of *neaT* within the 5′ PCR primer, and the resulting PCR product was ligated via an engineered NdeI restriction site with the *lac* promoter amplified from pGFPmut3.1 (Clonetech). The ligated P*lac*-*neaT* product was amplified and TA-cloned into the pCR2.1-TOPO vector. Using BamHI and NcoI restrictions sites, the P*lac* controlled *neaT* variant was then sub-cloned into pGEN-mcs. All experiments involving pGEN-*neaT*$^{\text{Plac}}$ were performed without IPTG induction. Primer sequences used to generate these plasmids are listed in Table S8.

Zebrafish embryos

*AB wild-type zebrafish embryos were collected from a laboratory-breeding colony that was maintained on a 14-h/10-h light/dark cycle. Embryos were grown at 28.5°C in E3 medium

Table 3. Bacterial strains and plasmids.

Strain or Plasmid	Description	Reference
E. coli		
CFT073	ExPEC (urosepsis isolate, O6:K2:H1)	[26]
Nissle 1917	Probiotic (gut isolate, O6:K5:H1)	[86]
HS	Commensal (gut isolate, O9)	[87]
Plasmids		
pKM208	Encodes IPTG-inducible lambda Red recombinase; Amp^r	[88]
pKD4	Template source for kanamycin resistance cassette;Kan^r	[84]
pGEN-mcs	High retention vector with an empty multiple cloning site; Amp^r	[85]
pGEN-*neaT*^{Pnative}	pGEN-mcs containing a natively controled *neaT* variant; Amp^r	This study
pGEN-*neaT*^{Plac}	pGEN-mcs containing a *neaT* variant constitutively expressed from a leaky *lac* promoter; Amp^r	This study
Recombinant strains		
CFT073/pKM208	CFT073 with pKM208; Amp^r	This study
CFT073Δϕb0847	CFT073 ϕb0847::*kan*	[45], this study
CFT073Δ1–2	CFT073 1–2::*kan* (locus tags c0932 through c0945)	This study
CFT073Δ2–3	CFT073 2–3::*kan* (locus tags c0946 through c0962)	This study
CFT073Δ3–4	CFT073 3–4::*kan* (locus tags c0963 through c0978)	This study
CFT073Δ*neaT*	CFT073 *neaT*::*kan* (locus tag c0970)	This study
CFT073Δ*yfdK*	CFT073 *yfdK*::*kan* (locus tag c0969)	This study
CFT073Δ*Fl-D*	CFT073 *Fl-D*::*kan* (locus tags c0971 through c0978)	This study
CFT073/pGEN-mcs	CFT073 with pGEN-mcs (empty vector); Amp^r	This study
CFT073/pGEN-*neaT*^{Plac}	CFT073 with pGEN-*neaT*^{Plac}; Amp^r	This study
CFT073Δ*neaT*/pGEN-mcs	CFT073Δ*neaT* with pGEN-mcs (empty vector); Amp^r, Kan^r	This study
CFT073Δ*neaT*/pGEN-*neaT*^{Pnative}	CFT073Δ*neaT* with pGEN-*neaT*^{Pnative}; Amp^r, Kan^r	This study
CFT073Δ*neaT*/pGEN-*neaT*^{Plac}	CFT073Δ*neaT* with pGEN-*neaT*^{Plac}; Amp^r, Kan^r	This study
CFT073Δϕb0847/pGEN-mcs	CFT073Δϕb0847 with pGEN-mcs (empty vector); Amp^r, Kan^r	This study
CFT073Δϕb0847/pGEN-*neaT*^{Pnative}	CFT073Δϕb0847 with pGEN-*neaT*^{Pnative}; Amp^r, Kan^r	This study
Nissle 1917/pGEN-mcs	Nissle 1917 with pGEN-mcs (empty vector); Amp^r	This study
Nissle 1917/pGEN-*neaT*^{Pnative}	Nissle 1917 with pGEN-*neaT*^{Pnative}; Amp^r	This study
Nissle 1917/pGEN-*neaT*^{Plac}	Nissle 1917 with pGEN-*neaT*^{Plac}; Amp^r	This study
HS/pGEN-mcs	HS with pGEN-mcs (empty vector); Amp^r	This study
HS/pGEN-*neaT*^{Pnative}	HS with pGEN-*neaT*^{Pnative}; Amp^r	This study
HS/pGEN-*neaT*^{Plac}	HS with pGEN-*neaT*^{Plac}; Amp^r	This study

doi:10.1371/journal.ppat.1003175.t003

(5 mM NaCl, 0.17 mM KCl, 0.4 mM $CaCl_2$, 0.16 mM $MgSO_4$) containing 0.000016% methylene blue as an anti-fungal agent.

Infection of zebrafish embryos

One nl from each 24 h bacterial culture was pelleted, washed once with 1 ml sterile PBS (Hyclone) and re-suspended in 1 ml PBS to obtain appropriate bacterial densities for microinjection. Prior to injection, 48 hpf embryos were manually dechorionated, briefly anesthetized using 0.77 mM ethyl 3- aminobenzoate methanesulfonate salt (tricaine) (Sigma-Aldrich), and embedded in 0.8% low-melt agarose (MO BIO Laboratories) without tricaine. Approximately 1 nl of bacteria was injected directly into the pericardial cavity or the blood via the circulation valley located ventral to the yolk sac using a YOU-1 micromanipulator (Narishige), a Narishige IM-200 microinjector, and a JUN-AIR model 3-compressor setup. For each experiment, average CFU introduced per injection were determined by adding 10 drops of each inoculum into 1 ml 0.7% NaCl, which was then serially diluted and plated on Luria-Bertani (LB) agar plates. For co-challenge experiments, input doses were plated on LB agar+/−kanamycin (50 μg/ml) to determine relative numbers of the wild type and mutant strains present. After injection, embryos were carefully extracted from the agar and placed individually into wells of a 96-well microtiter plate (Nunc) containing E3 medium lacking both tricaine and methylene blue. For lethality assays, fish were examined at indicated times over the course of a 48 or 72 h period and scored for ''death'', defined here as the complete absence of heart rhythm and blood flow. Survival graphs depict total pooled results from two or more independent experiments in which groups of 10 to 20 embryos were injected. To quantify bacterial numbers during the course of co-challenge experiments, embryos were homogenized at the indicated time points in 500 μL PBS containing 0.5% Triton X-100 using a mechanical PRO 250 homogenizer (PRO Scientific). Homogenates were then serially diluted and plated on LB agar+/−kanamycin (50 μg/ml) to determine relative numbers of wild type and mutant bacteria.

Mouse infections

For co-challenge during urinary tract infection, seven- to nine-week old female CBA/J mice (Jackson Labs) mice were anesthetized using isoflurane inhalation and inoculated via transurethral catheterization with 50 µl of a 1:1 wild type to mutant bacterial suspension containing a total of 10^7 bacteria suspended in PBS. Bladders and kidneys were recovered 3 days later and each was weighed and homogenized in 1 ml containing 0.025% Triton X-100. Homogenates were serially diluted and plated on LB agar+/−kanamycin (50 µg/ml) to determine number of both wild type and mutant bacteria. Mouse experiments were repeated at least twice.

For systemic infections, female CBA/J mice (Jackson Labs) aged 6 to 8 weeks were restrained using a Universal Restrainer (Braintree Scientific, Braintree, MA) and inoculated via the tail vein over a 30 s period with a 100 µl bacterial suspension, delivering 10^6 CFU/mouse. The inoculum was prepared by re-suspending overnight cultures in PBS and diluting them to 1×10^7 CFU/ml. For co-challenges, wild type and mutant suspensions were mixed 1:1 before inoculation. Perfusion was performed on euthanized animals by cutting a small hole in the right cardiac ventricle and infusing the left ventricle slowly with 40 ml 0.9% sterile saline before organ removal. Blanching of the organs occurred with the first 20 ml of sterile saline. Excised spleens and livers were homogenized in 3 ml PBS using a mechanical homogenizer (Omni International, Marietta, GA), and homogenates were plated using an Autoplate 4000 (Spiral Biotech, Norwood, MA) onto LB agar+/−kanamycin (50 µg/ml) to differentiate wild type and mutant strains.

Statistical analysis of zebrafish and mouse infections

Kaplan-Meier survival and scatter plots were generated using GraphPad Prism 5. For Kaplan-Meier survival plots (independent challenges), the log-rank (Mantel-Cox) test was used to determine statistical differences between datasets. For competitive assays (co-challenges), numbers of wild type and mutant bacteria present in the inoculum and recovered from host tissues were determined as described above and a competitive index was calculated using the following equation where wt represents numbers wild type bacteria:

$$\text{competitive index} = \log_{10}\left[\left(\text{mutant}^{\text{input}}/\text{wt}^{\text{input}}\right)/\left(\text{mutant}^{\text{output}}/\text{wt}^{\text{output}}\right)\right]$$

Negative values obtained using the competitive index equation indicate a reduction in mutant fitness. To determine statistical significance, the Wilcoxon signed-rank test (with a hypothetical value of 0) on log-transformed competitive index values was used for co-challenges and the two-tailed Mann-Whitney statistical analysis was performed to determine significant differences between samples in non-competitive assays.

Bioinformatic analyses

Homology searches and phyletic enrichment of homologue sets. A custom database of 165 genomes and associated plasmids was assembled using the compilation of protein coding genes (.faa files downloaded from ftp://ftp.ncbi.nih.gov/genomes/Bacteria/) of each isolate listed in Table S3. BLASTp (v. 2.2.20, [56]) was used to run bidirectional protein alignments between the ϕb0847 genome and the database to identify homologues. Two sequences were considered homologous if they aligned along >50% of their lengths with an E value of $<10^{-6}$. To identify phyletic enrichment, sets of non-paralogous homologues for each ϕb0847 gene were analyzed for relative contributions made by each phylum. Then, based on the number genes in each homologue set, the same number of genomes was randomly sampled from the genome list in Table S3. In this way, we could determine the significance of the phyletic contributions to each homologue set that was observed compared to a theoretical random sampling. With custom software written in Python using SciPy, p values were generated from a Z score. Standard scores were calculated using the equation below, where x is the observed proportion contributed by a single phylum, µ is the theoretical average contribution by the same phylum (n = 1000 random samplings), and σ is the standard deviation: $z = (x-\mu)/\sigma$

Sequences used for comparisons between the GC content of *neaT* from CFT073 and homologues in other bacteria (see Figure 6C) were retrieved manually from NCBI for downstream analysis. Genome GC compositions were obtained from NCBI Genomes (http://www.ncbi.nlm.nih.gov/genomes/MICROBES/microbial_taxtree.html)

Nucleotide composition analysis. For nucleotide composition analysis, the nucleotide sequences of protein coding genes of CFT073 (.ffn files downloaded from ftp://ftp.ncbi.nih.gov/genomes/Bacteria/Escherichia_coli_CFT073_uid57915/) were used to calculate codon deviation scores and GC content using custom software written in Python with SciPy or NumPy. For codon deviation scores, genome-wide protein coding nucleotide sequences were analyzed for codon usage frequencies on a per amino acid basis. The resulting table (Table S5) was then used to determine differences between specific codon frequencies contained within a particular gene and the genome-wide frequency. The absolute values of differences in frequency were summed over a single gene to obtain the final codon deviation score. Statistical significance was determined by Z-score analysis using the genome-wide mean codon deviation score and standard deviation. Table S6 lists all deviation scores and *p* values for the CFT073 genome. GC content of genes was determined by counting the proportion of guanines and cytosines over the length of a given locus, and Z-score analysis was again implemented to determine the position of each gene within the genome-wide distribution (Table S7).

Supporting Information

Figure S1 Expression of the neaT gene in various mutant backgrounds. RNA was extracted from the indicated strains after overnight growth in M9 medium and used to generate cDNA libraries by reverse transcription (+RT). To control for genomic DNA contamination, a set of samples was prepared in parallel without reverse transcriptase (−RT). Wild type CFT073, CFT073ΔneaT, CFT073ΔyfdK, and CFT073ΔFI-D were used to determine the relative expression levels of neaT in each genetic background. Three µg of each cDNA library was used as a template for PCR amplification (30 cycles) of an internal 218 bp fragment of neaT. Equal amounts of each PCR reaction were resolved using 1% agarose gels.
(TIF)

Figure S2 Determination of *in vivo* lateral transfer of the *neaT* gene. Zebrafish were inoculated with a one-to-one mixture of wt CFT073 and CFT073ΔneaT. Infections progressed for ~12 h post-inoculation prior to homogenization and recovery of bacteria by plating on LB agar+/−kanamycin. Bacterial colonies recovered from 5 separate fish were used for colony PCR to detect presence of either the kanamycin resistance gene (lane 1 control, ~1,500 bp) or neaT (lane 2 control, 218 bp internal fragment). No double positive colonies were detected. Primers used to amplify the kanamycin gene are specific to the

priming regions of the pKD4 template plasmid. neaT was amplified using neaT RT forward/reverse (Table S8).
(TIF)

Figure S3 Plasmid-based *neaT* expression analysis. RNA was extracted from the indicated strains after overnight growth in LB broth and used to generate cDNA libraries by reverse transcription (+RT). To control for genomic DNA contamination, a set of samples was prepared in parallel without reverse transcriptase (−RT). Wild type (WT) CFT073 or HS were used to reference basal neaT message levels. CFT073ΔneaT or HS carrying pGEN-mcs (empty vector, EV), pGEN-neaT^{Pnative} (native promoter, NP), or pGEN-neaT^{Plac} (over-expressing, OE) were used to determine the relative expression levels of pGEN-neaT variants in each genetic background. Three µg of each cDNA library was used as a template for PCR amplification (28 cycles) of an internal 218 bp fragment of neaT. Equal amounts of each PCR reaction were resolved using 1% agarose gels. Graph shows average levels of neaT transcripts ± SD normalized to 16S rRNA (not shown). Data are presented relative to WT CFT073, n = 3.
(TIF)

Figure S4 Survey of clinical isolates for presence of the *neaT* gene. Various clinical E. coli isolates were surveyed for presence of the neaT gene using polymerase chain reaction. Primers used in (A) amplified a 218 bp region internal to neaT (Table S8). (B) Shows amplification of the 16s ribosomal RNA gene as a control. Isolates are described as: strain (clinical disease presentation).
(TIF)

Figure S5 *neaT* contributes to multicellular behaviors. (A) Swarm motility of wild type (wt) CFT073 and its mutant derivatives on 0.25% Eiken agar plates following overnight incubation at 37°C. (B) Complementation of swarm defect of CFT073Δ*neaT* by introduction of pGEN-*neaT*^{Plac}. The empty vector pGEN-mcs and pGEN-*neaT*^{Pnative} did not complement the Δ*neaT* mutant. (C) Swim motility of indicated CFT073 derivatives following incubations at 37°C for times indicated. Red arrows indicate advancing swim fronts and insets show magnified bright field images of the center region of each plate. (D) Images of single Nissle 1917 colonies carrying pGEN-mcs or pGEN-*neaT*^{Plac} grown for 48 h at 37°C on agar plates containing 0.001% Congo red dye to stain curli fibers. (E) Streaks of Nissle 1917 carrying pGEN-mcs, pGEN-*neaT*^{Pnative}, or pGEN-*neaT*^{Plac} grown overnight at 37°C on 1.2% LB agar containing 50 µg/ml Fluorescent Brightener 28 to visulalize cellulose production. Image was captured under ultraviolet light.
(TIF)

Figure S6 NeaT limits bacterial interactions with murine macrophages. (Left) The indicated bacterial strains were added to bone marrow derived macrophage (BMDM) monolayers at a multiplicity of infection of 10. After a 1-h incubation at 37C, total viable bacteria remaining in the wells were enumerated. (Right) Alternatively, monolayers were washed at the 1-h time point with PBS, prior to lysis, in order to determine numbers of macrophage-associated bacteria. Bars represent the means ± SD of three independent experiments performed in triplicate. *p<0.05, **p<0.01; as determined by Student's t test.
(TIF)

Table S1 Summary of results obtained from initial GI screen using different dose ranges.
(XLSX)

Table S2 Summary of inconclusive *in vitro* experiments.
(XLSX)

Table S3 List of strains contained within the custom 165 genome database.
(XLSX)

Table S4 List of strains/genomes from the 165 genome database that contain at least one *neaT* homologue.
(XLSX)

Table S5 Codon usage frequency for each amino acid based on the 5,369 protein-coding genes of CFT073.
(XLSX)

Table S6 Codon deviation score for each gene in CFT073.
(XLSX)

Table S7 GC content for each gene in CFT073.
(XLSX)

Table S8 Primers used in this study to generate recombinant strains and plasmids.
(XLSX)

Text S1 Expression of NeaT may alter bacterial group behavior.
(DOCX)

Text S2 Supporting methods used in Text S1, Figure S5 and S6.
(DOCX)

Acknowledgments

We thank Dr. Nels Elde (University of Utah) for his enlightening discussions and Dr. Kael Fischer (University of Utah) for his guidance throughout the bioinformatic analyses.

Author Contributions

Conceived and designed the experiments: TJW SRC MAM. Performed the experiments: TJW JPN SNS SRC AJL. Analyzed the data: TJW SRC MAM. Contributed reagents/materials/analysis tools: TJW JPN SNS HLTM SRC MAM. Wrote the paper: TJW JPN SRC MAM.

References

1. Ley RE, Peterson DA, Gordon JI (2006) Ecological and evolutionary forces shaping microbial diversity in the human intestine. Cell 124: 837–848.
2. Savageau MA (1983) Escherichia-Coli Habitats Cell Types and Molecular Mechanisms of Gene Control. American Naturalist 122: 732–744.
3. Walk ST, Alm EW, Calhoun LM, Mladonicky JM, Whittam TS (2007) Genetic diversity and population structure of Escherichia coli isolated from freshwater beaches. Environmental microbiology 9: 2274–2288.
4. Winfield MD, Groisman EA (2003) Role of nonhost environments in the lifestyles of Salmonella and Escherichia coli. Applied and environmental microbiology 69: 3687–3694.
5. Fricke WF, Wright MS, Lindell AH, Harkins DM, Baker-Austin C, et al. (2008) Insights into the environmental resistance gene pool from the genome sequence of the multidrug-resistant environmental isolate Escherichia coli SMS-3-5. Journal of bacteriology 190: 6779–6794.
6. Luo C, Walk ST, Gordon DM, Feldgarden M, Tiedje JM, et al. (2011) Genome sequencing of environmental Escherichia coli expands understanding of the ecology and speciation of the model bacterial species. Proceedings of the National Academy of Sciences of the United States of America 108: 7200–7205.
7. Wiles TJ, Kulesus RR, Mulvey MA (2008) Origins and virulence mechanisms of uropathogenic Escherichia coli. Experimental and molecular pathology 85: 11–19.

8. Ewers C, Janssen T, Wieler LH (2003) [Avian pathogenic Escherichia coli (APEC)]. Berliner und Munchener tierarztliche Wochenschrift 116: 381–395.
9. Shpigel NY, Elazar S, Rosenshine I (2008) Mammary pathogenic Escherichia coli. Current opinion in microbiology 11: 60–65.
10. Tan C, Xu Z, Zheng H, Liu W, Tang X, et al. (2011) Genome sequence of a porcine extraintestinal pathogenic Escherichia coli strain. Journal of bacteriology 193: 5038.
11. Carvallo FR, Debroy C, Baeza E, Hinckley L, Gilbert K, et al. (2010) Necrotizing pneumonia and pleuritis associated with extraintestinal pathogenic Escherichia coli in a tiger (Panthera tigris) cub. Journal of veterinary diagnostic investigation: official publication of the American Association of Veterinary Laboratory Diagnosticians, Inc 22: 136–140.
12. Foxman B, Brown P (2003) Epidemiology of urinary tract infections: transmission and risk factors, incidence, and costs. Infectious disease clinics of North America 17: 227–241.
13. Johnson JR, Johnston B, Clabots C, Kuskowski MA, Castanheira M (2010) Escherichia coli sequence type ST131 as the major cause of serious multidrug-resistant E. coli infections in the United States. Clinical infectious diseases: an official publication of the Infectious Diseases Society of America 51: 286–294.
14. Wiedenbeck J, Cohan FM (2011) Origins of bacterial diversity through horizontal genetic transfer and adaptation to new ecological niches. FEMS microbiology reviews 35: 957–976.
15. Stokes HW, Gillings MR (2011) Gene flow, mobile genetic elements and the recruitment of antibiotic resistance genes into Gram-negative pathogens. FEMS microbiology reviews 35: 790–819.
16. Kirschner M, Gerhart J (1998) Evolvability. Proceedings of the National Academy of Sciences of the United States of America 95: 8420–8427.
17. Pigliucci M (2008) Is evolvability evolvable? Nature reviews Genetics 9: 75–82.
18. Gogarten JP, Doolittle WF, Lawrence JG (2002) Prokaryotic evolution in light of gene transfer. Molecular biology and evolution 19: 2226–2238.
19. Hehemann JH, Correc G, Barbeyron T, Helbert W, Czjzek M, et al. (2010) Transfer of carbohydrate-active enzymes from marine bacteria to Japanese gut microbiota. Nature 464: 908–912.
20. Marchetti M, Capela D, Glew M, Cruveiller S, Chane-Woon-Ming B, et al. (2010) Experimental evolution of a plant pathogen into a legume symbiont. PLoS biology 8: e1000280.
21. Thomas CM, Nielsen KM (2005) Mechanisms of, and barriers to, horizontal gene transfer between bacteria. Nature reviews Microbiology 3: 711–721.
22. Medigue C, Rouxel T, Vigier P, Henaut A, Danchin A (1991) Evidence for horizontal gene transfer in Escherichia coli speciation. Journal of molecular biology 222: 851–856.
23. Canchaya C, Fournous G, Brussow H (2004) The impact of prophages on bacterial chromosomes. Molecular microbiology 53: 9–18.
24. Casjens S, Hendrix RW (2005) Bacteriophages and the bacterial genome. Bacterial Chromosome. Washington: Amer Soc Microbiology. pp. 39–52.
25. Dagan T, Artzy-Randrup Y, Martin W (2008) Modular networks and cumulative impact of lateral transfer in prokaryote genome evolution. Proceedings of the National Academy of Sciences of the United States of America 105: 10039–10044.
26. Welch RA, Burland V, Plunkett G, 3rd, Redford P, Roesch P, et al. (2002) Extensive mosaic structure revealed by the complete genome sequence of uropathogenic Escherichia coli. Proceedings of the National Academy of Sciences of the United States of America 99: 17020–17024.
27. Lawrence JG, Ochman H (1998) Molecular archaeology of the Escherichia coli genome. Proceedings of the National Academy of Sciences of the United States of America 95: 9413–9417.
28. Perna NT, Plunkett G, 3rd, Burland V, Mau B, Glasner JD, et al. (2001) Genome sequence of enterohaemorrhagic Escherichia coli O157:H7. Nature 409: 529–533.
29. Belda-Ferre P, Cabrera-Rubio R, Moya A, Mira A (2011) Mining virulence genes using metagenomics. PloS one 6: e24975.
30. Langille MG, Hsiao WW, Brinkman FS (2010) Detecting genomic islands using bioinformatics approaches. Nature reviews Microbiology 8: 373–382.
31. Juhas M, van der Meer JR, Gaillard M, Harding RM, Hood DW, et al. (2009) Genomic islands: tools of bacterial horizontal gene transfer and evolution. FEMS microbiology reviews 33: 376–393.
32. Touchon M, Hoede C, Tenaillon O, Barbe V, Baeriswyl S, et al. (2009) Organised genome dynamics in the Escherichia coli species results in highly diverse adaptive paths. PLoS genetics 5: e1000344.
33. Kao JS, Stucker DM, Warren JW, Mobley HL (1997) Pathogenicity island sequences of pyelonephritogenic Escherichia coli CFT073 are associated with virulent uropathogenic strains. Infection and immunity 65: 2812–2820.
34. Gal-Mor O, Finlay BB (2006) Pathogenicity islands: a molecular toolbox for bacterial virulence. Cellular microbiology 8: 1707–1719.
35. Dorman CJ (2009) Regulatory integration of horizontally-transferred genes in bacteria. Frontiers in bioscience: a journal and virtual library 14: 4103–4112.
36. Tettelin H, Masignani V, Cieslewicz MJ, Donati C, Medini D, et al. (2005) Genome analysis of multiple pathogenic isolates of Streptococcus agalactiae: implications for the microbial "pan-genome". Proceedings of the National Academy of Sciences of the United States of America 102: 13950–13955.
37. Tettelin H, Riley D, Cattuto C, Medini D (2008) Comparative genomics: the bacterial pan-genome. Current opinion in microbiology 11: 472–477.
38. Nakamura Y, Itoh T, Matsuda H, Gojobori T (2004) Biased biological functions of horizontally transferred genes in prokaryotic genomes. Nature genetics 36: 760–766.
39. Mobley HL, Green DM, Trifillis AL, Johnson DE, Chippendale GR, et al. (1990) Pyelonephritogenic Escherichia coli and killing of cultured human renal proximal tubular epithelial cells: role of hemolysin in some strains. Infection and immunity 58: 1281–1289.
40. Wiles TJ, Bower JM, Redd MJ, Mulvey MA (2009) Use of zebrafish to probe the divergent virulence potentials and toxin requirements of extraintestinal pathogenic Escherichia coli. PLoS pathogens 5: e1000697.
41. Trede NS, Langenau DM, Traver D, Look AT, Zon LI (2004) The use of zebrafish to understand immunity. Immunity 20: 367–379.
42. Li X, Wang S, Qi J, Echtenkamp SF, Chatterjee R, et al. (2007) Zebrafish peptidoglycan recognition proteins are bactericidal amidases essential for defense against bacterial infections. Immunity 27: 518–529.
43. Jault C, Pichon L, Chluba J (2004) Toll-like receptor gene family and TIR-domain adapters in Danio rerio. Molecular immunology 40: 759–771.
44. Lieschke GJ, Oates AC, Crowhurst MO, Ward AC, Layton JE (2001) Morphologic and functional characterization of granulocytes and macrophages in embryonic and adult zebrafish. Blood 98: 3087–3096.
45. Lloyd AL, Henderson TA, Vigil PD, Mobley HL (2009) Genomic islands of uropathogenic Escherichia coli contribute to virulence. Journal of bacteriology 191: 3469–3481.
46. Bower JM, Gordon-Raagas HB, Mulvey MA (2009) Conditioning of uropathogenic Escherichia coli for enhanced colonization of host. Infection and immunity 77: 2104–2112.
47. Bower JM, Mulvey MA (2006) Polyamine-mediated resistance of uropathogenic Escherichia coli to nitrosative stress. Journal of bacteriology 188: 928–933.
48. Garcia EC, Brumbaugh AR, Mobley HL (2011) Redundancy and specificity of Escherichia coli iron acquisition systems during urinary tract infection. Infection and immunity 79: 1225–1235.
49. Nilsson AS, Haggard-Ljungquist E (2007) Evolution of P2-like phages and their impact on bacterial evolution. Research in microbiology 158: 311–317.
50. Wang Z, Zhang S, Wang G, An Y (2008) Complement activity in the egg cytosol of zebrafish Danio rerio: evidence for the defense role of maternal complement components. PloS one 3: e1463.
51. Juhala RJ, Ford ME, Duda RL, Youlton A, Hatfull GF, et al. (2000) Genomic sequences of bacteriophages HK97 and HK022: pervasive genetic mosaicism in the lambdoid bacteriophages. Journal of molecular biology 299: 27–51.
52. Hendrix RW, Lawrence JG, Hatfull GF, Casjens S (2000) The origins and ongoing evolution of viruses. Trends in microbiology 8: 504–508.
53. Waldor MK, Friedman DI, Adhya SL (2005) Phages: their role in bacterial pathogenesis and biotechnology. Washington, D.C.: ASM Press. pp. 37–65.
54. Wang X, Kim Y, Ma Q, Hong SH, Pokusaeva K, et al. (2010) Cryptic prophages help bacteria cope with adverse environments. Nature communications 1: 147.
55. Smith SN, Hagan EC, Lane MC, Mobley HL (2010) Dissemination and systemic colonization of uropathogenic Escherichia coli in a murine model of bacteremia. mBio 1.
56. Altschul SF, Madden TL, Schaffer AA, Zhang J, Zhang Z, et al. (1997) Gapped BLAST and PSI-BLAST: a new generation of protein database search programs. Nucleic acids research 25: 3389–3402.
57. Papanikolaou N, Trachana K, Theodosiou T, Promponas VJ, Iliopoulos I (2009) Gene socialization: gene order, GC content and gene silencing in Salmonella. BMC genomics 10: 597.
58. Ochman H, Lawrence JG, Groisman EA (2000) Lateral gene transfer and the nature of bacterial innovation. Nature 405: 299–304.
59. Daubin V, Lerat E, Perriere G (2003) The source of laterally transferred genes in bacterial genomes. Genome biology 4: R57.
60. Kuo CH, Ochman H (2009) The fate of new bacterial genes. FEMS microbiology reviews 33: 38–43.
61. Berck S, Perret X, Quesada-Vincens D, Prome J, Broughton WJ, et al. (1999) NolL of Rhizobium sp. strain NGR234 is required for O-acetyltransferase activity. Journal of bacteriology 181: 957–964.
62. Bera A, Herbert S, Jakob A, Vollmer W, Gotz F (2005) Why are pathogenic staphylococci so lysozyme resistant? The peptidoglycan O-acetyltransferase OatA is the major determinant for lysozyme resistance of Staphylococcus aureus. Molecular microbiology 55: 778–787.
63. Yoshida Y, Yang J, Peaker PE, Kato H, Bush CA, et al. (2008) Molecular and antigenic characterization of a Streptococcus oralis coaggregation receptor polysaccharide by carbohydrate engineering in Streptococcus gordonii. The Journal of biological chemistry 283: 12654–12664.
64. Vollmer W (2008) Structural variation in the glycan strands of bacterial peptidoglycan. FEMS microbiology reviews 32: 287–306.
65. Thornton MM, Chung-Esaki HM, Irvin CB, Bortz DM, Solomon MJ, et al. (2012) Multicellularity and Antibiotic Resistance in Klebsiella pneumoniae Grown Under Bloodstream-Mimicking Fluid Dynamic Conditions. The Journal of infectious diseases 206: 588–595.
66. Lercher MJ, Pal C (2008) Integration of horizontally transferred genes into regulatory interaction networks takes many million years. Molecular biology and evolution 25: 559–567.
67. Lind PA, Andersson DI (2008) Whole-genome mutational biases in bacteria. Proceedings of the National Academy of Sciences of the United States of America 105: 17878–17883.

68. Hershberg R, Petrov DA (2010) Evidence that mutation is universally biased towards AT in bacteria. PLoS genetics 6.
69. Van Leuven JT, McCutcheon JP (2012) An AT mutational bias in the tiny GC-rich endosymbiont genome of Hodgkinia. Genome biology and evolution 4: 24–27.
70. Barker MS, Demuth JP, Wade MJ (2005) Maternal expression relaxes constraint on innovation of the anterior determinant, bicoid. PLoS genetics 1: e57.
71. Hunt BG, Ometto L, Wurm Y, Shoemaker D, Yi SV, et al. (2011) Relaxed selection is a precursor to the evolution of phenotypic plasticity. Proceedings of the National Academy of Sciences of the United States of America 108: 15936–15941.
72. Van Dyken JD, Wade MJ (2010) The genetic signature of conditional expression. Genetics 184: 557–570.
73. Whitlock MC (1996) The red queen beats the jack-of-all-trades: The limitations on the evolution of phenotypic plasticity and niche breadth. American Naturalist 148: S65–S77.
74. Waterston RH, Lindblad-Toh K, Birney E, Rogers J, Abril JF, et al. (2002) Initial sequencing and comparative analysis of the mouse genome. Nature 420: 520–562.
75. Johnson JR, Porter SB, Zhanel G, Kuskowski MA, Denamur E (2012) Virulence of Escherichia coli Clinical Isolates in a Murine Sepsis Model in Relation to Sequence Type ST131 Status, Fluoroquinolone Resistance, and Virulence Genotype. Infection and immunity.
76. Wirth T, Falush D, Lan R, Colles F, Mensa P, et al. (2006) Sex and virulence in Escherichia coli: an evolutionary perspective. Molecular microbiology 60: 1136–1151.
77. Reid SD, Herbelin CJ, Bumbaugh AC, Selander RK, Whittam TS (2000) Parallel evolution of virulence in pathogenic Escherichia coli. Nature 406: 64–67.
78. Li M, Du X, Villaruz AE, Diep BA, Wang D, et al. (2012) MRSA epidemic linked to a quickly spreading colonization and virulence determinant. Nature medicine 18: 816–819.
79. Tuller T, Girshovich Y, Sella Y, Kreimer A, Freilich S, et al. (2011) Association between translation efficiency and horizontal gene transfer within microbial communities. Nucleic acids research 39: 4743–4755.
80. Smillie CS, Smith MB, Friedman J, Cordero OX, David LA, et al. (2011) Ecology drives a global network of gene exchange connecting the human microbiome. Nature 480: 241–244.
81. Andam CP, Gogarten JP (2011) Biased gene transfer in microbial evolution. Nature reviews Microbiology 9: 543–555.
82. Mulvey MA, Lopez-Boado YS, Wilson CL, Roth R, Parks WC, et al. (1998) Induction and evasion of host defenses by type 1-piliated uropathogenic Escherichia coli. Science 282: 1494–1497.
83. Murphy KC, Campellone KG (2003) Lambda Red-mediated recombinogenic engineering of enterohemorrhagic and enteropathogenic E. coli. BMC molecular biology 4: 11.
84. Datsenko KA, Wanner BL (2000) One-step inactivation of chromosomal genes in Escherichia coli K-12 using PCR products. Proceedings of the National Academy of Sciences of the United States of America 97: 6640–6645.
85. Lane MC, Alteri CJ, Smith SN, Mobley HL (2007) Expression of flagella is coincident with uropathogenic Escherichia coli ascension to the upper urinary tract. Proceedings of the National Academy of Sciences of the United States of America 104: 16669–16674.
86. Grozdanov L, Raasch C, Schulze J, Sonnenborn U, Gottschalk G, et al. (2004) Analysis of the genome structure of the nonpathogenic probiotic Escherichia coli strain Nissle 1917. Journal of bacteriology 186: 5432–5441.
87. Rasko DA, Rosovitz MJ, Myers GS, Mongodin EF, Fricke WF, et al. (2008) The pangenome structure of Escherichia coli: comparative genomic analysis of E. coli commensal and pathogenic isolates. Journal of bacteriology 190: 6881–6893.
88. Kulesus RR, Diaz-Perez K, Slechta ES, Eto DS, Mulvey MA (2008) Impact of the RNA chaperone Hfq on the fitness and virulence potential of uropathogenic Escherichia coli. Infection and immunity 76: 3019–3026.

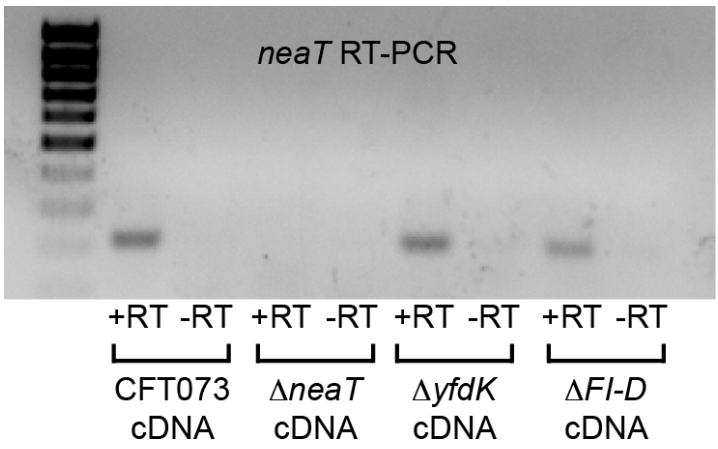

Figure A.S1. Expression of the neaT gene in various mutant backgrounds. RNA was extracted from the indicated strains after overnight growth in M9 medium and used to generate cDNA libraries by reverse transcription (+RT). To control for genomic DNA contamination, a set of samples was prepared in parallel without reverse transcriptase (−RT). Wild type CFT073, CFT073ΔneaT, CFT073ΔyfdK, and CFT073ΔFl-D were used to determine the relative expression levels of neaT in each genetic background. Three µg of each cDNA library was used as a template for PCR amplification (30 cycles) of an internal 218 bp fragment of neaT. Equal amounts of each PCR reaction were resolved using 1% agarose gels.

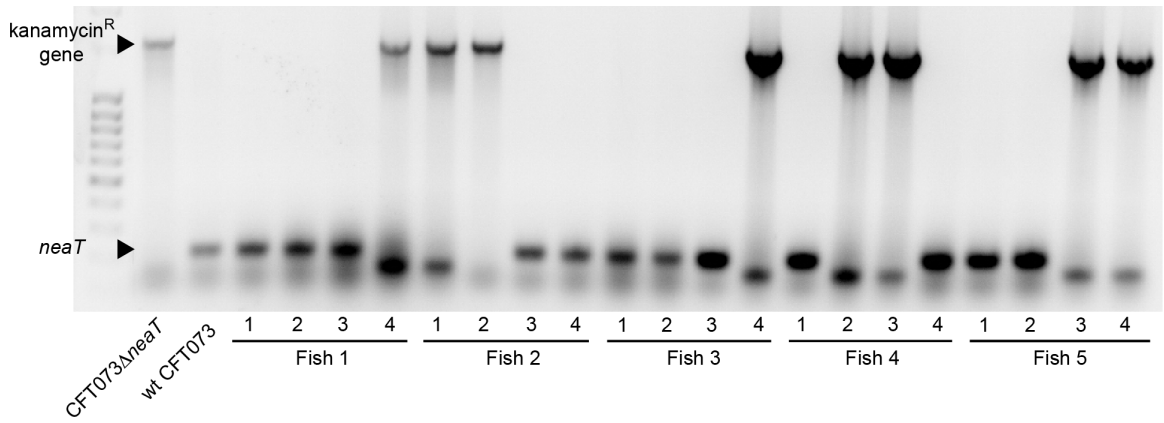

Figure A.S2. Determination of *in vivo* lateral transfer of the *neaT* gene. Zebrafish were inoculated with a one-to-one mixture of wt CFT073 and CFT073ΔneaT. Infections progressed for ~12 h postinoculation prior to homogenization and recovery of bacteria by plating on LB agar+/−kanamycin. Bacterial colonies recovered from five separate fish were used for colony PCR to detect presence of either the kanamycin resistance gene (lane 1 control, ~1,500 bp) or neaT (lane 2 control, 218 bp internal fragment). No double positive colonies were detected. Primers used to amplify the kanamycin gene are specific to the priming regions of the pKD4 template plasmid. neaT was amplified using neaT RT forward/reverse.

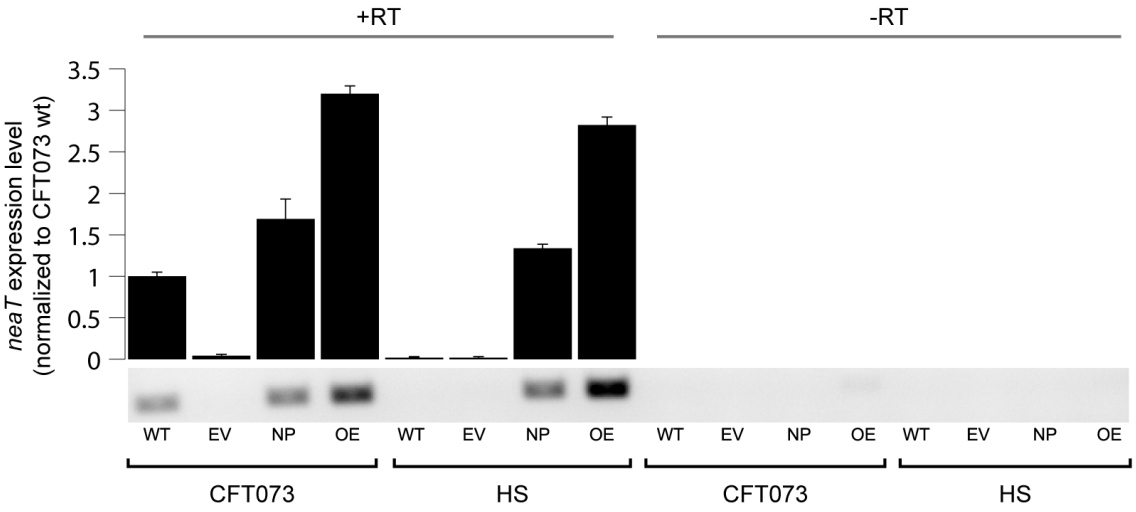

Figure A.S3. Plasmid-based *neaT* expression analysis. RNA was extracted from the indicated strains after overnight growth in LB broth and used to generate cDNA libraries by reverse transcription (+RT). To control for genomic DNA contamination, a set of samples was prepared in parallel without reverse transcriptase (−RT). Wild type (WT) CFT073 or HS were used to reference basal neaT message levels. CFT073ΔneaT or HS carrying pGEN-mcs (empty vector, EV), pGEN-neaT^{Pnative} (native promoter, NP), or pGEN-neaT^{Plac} (over-expressing, OE) were used to determine the relative expression levels of pGEN-neaT variants in each genetic background. Three µg of each cDNA library was used as a template for PCR amplification (28 cycles) of an internal 218 bp fragment of neaT. Equal amounts of each PCR reaction were resolved using 1% agarose gels. Graph shows average levels of neaT transcripts ± SD normalized to 16S rRNA (not shown). Data are presented relative to WT CFT073, n = 3.

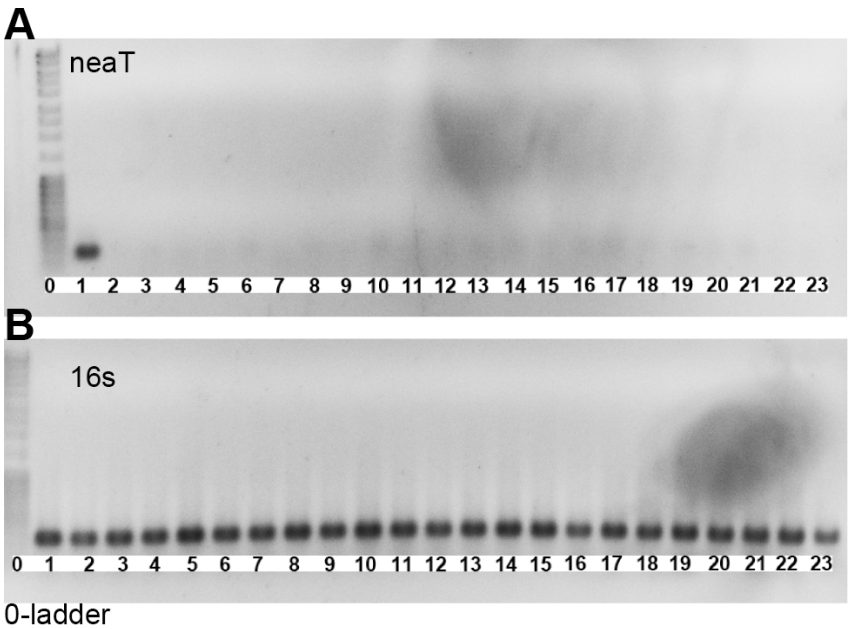

0-ladder
1-CFT073 wt (pyelonephritis)
2-CFT073Δ*neaT*
3-UTI98 (cystitis)
4-UTI45 (cystitis)
5-B212 (cystitis)
6-B217 (cystitis)
7-B220 (cystitis)
8-ARUP #1 (neonatal meningitis)
9-ARUP #2 (neonatal meningitis)
10-ATCC 35150 (0157:H7 EHEC)
11-A70 (stool)
12-A71 (stool)
13-A15 (asymptomatic bacteriuria)
14-A18 (asymptomatic bacteriuria)
15-A34 (asymptomatic bacteriuria)
16-A37 (asymptomatic bacteriuria)
17-A58 (asymptomatic bacteriuria)
18-A3 (cystitis)
19-A6 (cystitis)
20-A9 (cystitis)
21-A16 (cystitis)
22-J96 (pyelonephritis)
23-A33 (pyelonephritis)

Figure A.S4. Survey of clinical isolates for presence of the *neaT* gene. Various clinical *E. coli* isolates were surveyed for presence of the *neaT* gene using polymerase chain reaction. Primers used in (A) amplified a 218 bp region internal to neaT. (B) Shows amplification of the 16s ribosomal RNA gene as a control. Isolates are described as: strain (clinical disease presentation).

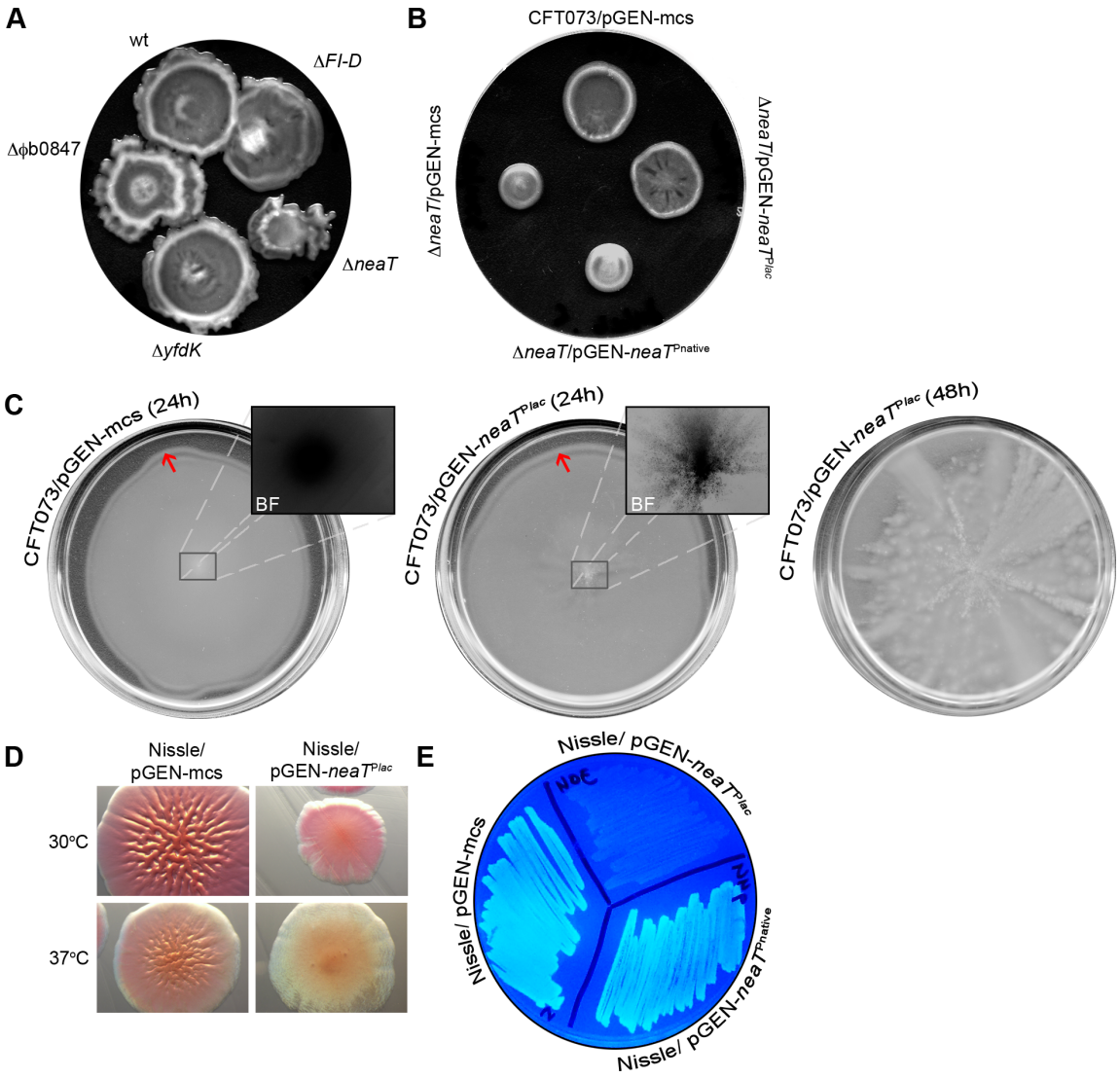

Figure A.S5. *neaT* contributes to multicellular behaviors. (A) Swarm motility of wild type (wt) CFT073 and its mutant derivatives on 0.25% Eiken agar plates following overnight incubation at 37°C. (B) Complementation of CFT073Δ*neaT* by introduction of pGEN-*neaT*^{Plac}. The empty vector pGEN-mcs and pGEN-*neaT*^{Pnative} did not complement the Δ*neaT* mutant. (C) Swim motility of indicated CFT073 derivatives following incubations at 37°C for times indicated. Red arrows indicate advancing swim fronts and insets show magnified bright field images of the center region of each plate. (D) Images of single Nissle 1917 colonies carrying pGEN-mcs or pGEN-*neaT*^{Plac} grown for 48 h at 37°C on agar plates containing 0.001% Congo red dye to stain curli fibers. (E) Streaks of Nissle 1917 carrying pGEN-mcs, pGEN-*neaT*^{Pnative}, or pGEN-*neaT*^{Plac} grown overnight at 37°C on 1.2% LB agar containing 50 µg/ml Fluorescent Brightener 28 to visulalize cellulose production. Image was captured under ultraviolet light.

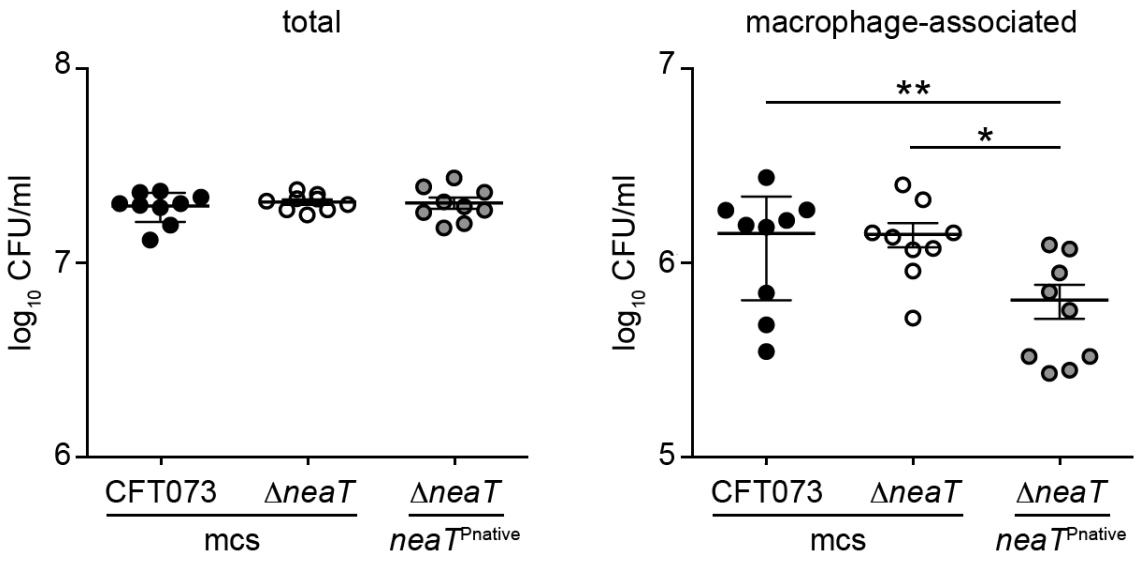

Figure A.S6. NeaT limits bacterial interactions with murine macrophages. (Left) The indicated bacterial strains were added to bone marrow derived macrophage (BMDM) monolayers at a multiplicity of infection of 10. After a 1-h incubation at 37°C, total viable bacteria remaining in the wells were enumerated. (Right) Alternatively, monolayers were washed at the 1-h time point with PBS, prior to lysis, in order to determine numbers of macrophage-associated bacteria. Bars represent the means ± SD of three independent experiments performed in triplicate. *p<0.05, **p<0.01; as determined by Student's *t* test.

APPENDIX B

THE CPX STRESS RESPONSE SYSTEM POTENTIATES THE FITNESS AND VIRULENCE OF UROPATHOGENIC *ESCHERICHIA COLI*

81, 2013, 1450-1459, doi:10.1128/IAI.01213-12

IAI Journals.ASM.org

The Cpx Stress Response System Potentiates the Fitness and Virulence of Uropathogenic *Escherichia coli*

Irina Debnath, J. Paul Norton, Amelia E. Barber, Elizabeth M. Ott, Bijaya K. Dhakal, Richard R. Kulesus, Matthew A. Mulvey

Division of Microbiology and Immunology, Pathology Department, University of Utah, Salt Lake City, Utah, USA

Strains of uropathogenic *Escherichia coli* (UPEC) are the primary cause of urinary tract infections, representing one of the most widespread and successful groups of pathogens on the planet. To colonize and persist within the urinary tract, UPEC must be able to sense and respond appropriately to environmental stresses, many of which can compromise the bacterial envelope. The Cpx two-component envelope stress response system is comprised of the inner membrane histidine kinase CpxA, the cytosolic response regulator CpxR, and the periplasmic auxiliary factor CpxP. Here, by using deletion mutants along with mouse and zebrafish infection models, we show that the Cpx system is critical to the fitness and virulence of two reference UPEC strains, the cystitis isolate UTI89 and the urosepsis isolate CFT073. Specifically, deletion of the *cpxRA* operon impaired the ability of UTI89 to colonize the murine bladder and greatly reduced the virulence of CFT073 during both systemic and localized infections within zebrafish embryos. These defects coincided with diminished host cell invasion by UTI89 and increased sensitivity of both strains to complement-mediated killing and the aminoglycoside antibiotic amikacin. Results obtained with the *cpxP* deletion mutants were more complicated, indicating variable strain-dependent and niche-specific requirements for this well-conserved auxiliary factor.

Urinary tract infections (UTIs) afflict a large proportion of the human population, representing an enormous health and financial burden worldwide (1). Most UTIs are caused by a genetically diverse group of bacteria known as uropathogenic *Escherichia coli* (UPEC). These pathogens can survive and grow within urine and the lumen of the bladder, but many can also bind and invade uroepithelial cells (2–4). Within the bladder, entry into uroepithelial cells can promote UPEC survival and persistence, rendering the pathogens protected from a variety of stresses and commonly used antibiotics (3, 5, 6). Prior to introduction into the urinary tract, UPEC likely first colonizes the host nasopharynx and gastrointestinal tract, where it does not appear to elicit any overt pathology (7–9). Within these varied host environments, and while in transit between hosts, UPEC will encounter an assorted array of stresses, including reactive nitrogen and oxygen species, nutrient limitation, shearing forces, professional phagocytes, complement and other antimicrobial compounds, competition with other microbes and, potentially, antibiotics (10–15). The ability to deal with these stresses is of paramount importance to the success of UPEC as a pathogen.

The envelope of Gram-negative bacteria interfaces with the extracellular environment, functioning as both a sensor of external conditions and as a selectively permeable physical barrier. Envelope stress response pathways are likely critical to the ability of UPEC to detect and respond to potentially fatal environmental insults during the course of infection. UPEC, as well as other *E. coli* strains, encode a number of envelope stress response systems, including sigma E (σ^E), Rcs, Psp, and the BaeSR and CpxRA two-component systems (16–19). The Cpx system is comprised of the inner membrane histidine kinase CpxA and the cytoplasmic response regulator CpxR (20–22). Autophosphorylation of CpxA in response to envelope stress results in the phosphorylation of CpxR, which then functions as a transcriptional regulator. CpxR controls the expression of protein folding and degrading factors involved in relieving envelope stress and can also regulate biofilm formation (23–26), bacterial adherence (23, 27, 28), motility and chemotaxis (29, 30), type III and type IV secretion systems (31–35) and, possibly, the synthesis of bacterial toxins (27, 36, 37). Studies using *E. coli* K-12 strains like MG1655 and MC4100 have indicated that CpxR may regulate the expression of well over 100 genes (38, 39).

In *E. coli* and other microbes, the Cpx system is subject to negative feedback through CpxP, a small CpxR-regulated periplasmic protein that can bind the sensor kinase CpxA, keeping it in an inactive state (40, 41). CpxR binding sites are situated upstream of the *cpxP* gene within a conserved 146-bp region that separates *cpxP* from the *cpxRA* operon. CpxP is the most highly inducible member of the Cpx regulon so far identified, and it has elevated expression in response to both envelope stress and entry into stationary-phase growth (40, 42). In addition to its role as a negative regulator of CpxA, CpxP also functions as an adaptor protein, interacting with subsets of misfolded periplasmic proteins and delivering them to the protease DegP for degradation (43, 44). In this process, CpxP is degraded along with its misfolded substrate, suggesting a mechanism by which bacteria can post-translationally modulate CpxP levels. By varying the amounts of CpxP within the periplasm, bacteria may be able to fine-tune the Cpx stress response, limiting inappropriate activation of CpxA in the absence of envelope stress and permitting rapid shutoff of the system once the stress is under control (20, 45).

The Cpx system appears to have a key role in regulating the virulence potential of a number of pathogens (17), including *Sal-*

Received 1 November 2012 **Returned for modification** 11 December 2012
Accepted 12 February 2013
Published ahead of print 19 February 2013
Editor: S. M. Payne
Address correspondence to Matthew A. Mulvey, mulvey@path.utah.edu.

doi:10.1128/IAI.01213-12

TABLE 1 Bacterial strains and plasmids

Strain or plasmid	Description	Source or reference(s)
Wild-type strains		
UTI89	UPEC, cystitis isolate (O18:K1:H7)	6, 95
CFT073	Urosepsis isolate (O6:K2:H1)	96
Recombinant strains		
UTI89Δ*cpxP*	UTI89 Δ*cpxP*::clm^r	This study
UTI89Δ*cpxRA*	UTI89 Δ*cpxRA*::clm^r	This study
UTI89Δ*fieF*	UTI89 Δ*fieF*::clm^r	This study
CFT073Δ*cpxP*	CFT073 Δ*cpxP*::clm^r	This study
CFT073Δ*cpxRA*	CFT073 Δ*cpxRA*::clm^r	This study
CFT073Δ*fieF*	CFT073 Δ*fieF*::clm^r	This study
Plasmids		
pKM208	IPTG-inducible Red recombinase expression plasmid, Amp^r	60
pGEN-MCS	High-retention plasmid containing empty multiple-cloning site, Amp^r	61
pJLJ41p	*cpxP* sequence with native promoter from UTI89 cloned into pGEN-MCS; Amp^r	This study
pJLJ42	*cpxRA* sequence with native promoter from UTI89 cloned into pGEN-MCS; Amp^r	This study
pNLP10-*lux*	Low-copy-number cloning vector with promoterless *luxCDABE* operon; Kan^r	39
pJW1-c*pxP*-*lux*	pNLP10 with P*cpxP*::*luxCDABE*, Kan^r	39

monella spp. (46, 47), *Legionella pneumophila* (31, 48), *Shigella* spp. (33–35), enteropathogenic *E. coli* (32, 49, 50), *Actinobacillus suis* (51), *Haemophilus ducreyi* (52, 53), *Xenorhabdus nematophila* (37, 54), and *Yersinia pseudotuberculosis* (55–57). However, direct evidence that the Cpx system can affect pathogen fitness and virulence *in vivo* within an animal host is limited to only a few studies (47, 50, 53, 54). In UPEC, the Cpx system has been examined primarily with respect to its ability to modulate the expression of P pili, filamentous adhesive organelles that can promote bacterial interactions with host kidney cells (27, 28, 58). Here, by using isogenic deletion mutants, we assessed how components of the Cpx stress response system affect the fitness and virulence of two reference UPEC isolates. Employing *in vitro* assays coupled with i*n vivo* mouse and zebrafish infection models, we demonstrate that *cpxP* and *cpxRA* can have profound and sometimes divergent effects on the pathogenic potential of UPEC.

MATERIALS AND METHODS

Bacterial strains and plasmids. The bacterial strains and plasmids used in this study are listed in Table 1. Targeted gene knockouts were created in the human cystitis isolate UTI89 and the urosepsis isolate CFT073 by using lambda Red-based homologous recombination as previously described (59, 60). Briefly, the chloramphenicol resistance cassette (clm^r) was amplified from the template plasmid pKD3 with flanking 40-bp overhangs specific for the target *cpxP* or *cpxRA* loci. PCR products were electroporated into UTI89 and CFT073 carrying the plasmid pKM208, which encodes an isopropyl-β-D-thiogalactopyranoside (IPTG)-inducible lambda Red recombinase. The *yiiP* (*fieF*) gene was knocked out by using a similar approach. Knockout strains were selected on Luria-Bertani (LB) agar plates containing chloramphenicol (20 μg/ml) and verified by PCR using the primers listed in Table 2.

Expression constructs were made using the low-copy-number plasmid pGEN-MCS and standard molecular biology techniques (61). The *cpxP* gene and the *cpxRA* operon were cloned by PCR from the UTI89 chromosome. The primers used (Table 2) to amplify each locus were designed to include 250 bp of upstream and 100 bp of downstream sequences, along with terminal PstI and SalI restriction sites. PCR products were cut using PstI and SalI and ligated into pGEN-MCS to create the CpxP and CpxRA expression constructs pJLJ41p and pJLJ42, respectively.

TABLE 2 Primers used in this study[a]

Primer	Sequence (5′–3′)
cpxP KO	
Forward	ATGCGCATAGTTACCGCTGCCGTCATGGCCT CAACGCTGGGTGTAGGCTGGAGCTGCTTC
Reverse	CTACTGGGAACGTGAGTTGCTACTACTCAATA GCTTCAACCATATGAATATCCTCCTTAG
cpxP confirmation	
Forward	CTATCGTTGAATCGCGACAG
Reverse	GGATGGTGTCTATGGCAAGG
cpxRA KO	
Forward	ATGAATAAAATCCTGTTAGTTGATGATGACC GAGAGCTGGTGTAGGCTGGAGCTGCTTC
Reverse	TTAACTCCGCTTATACAGCGGCAACCAAATC ACCAGCCGTCATATGAATATCCTCCTTAG
cpxRA confirmation	
Forward	ACTGCCAGCGTTGAGGCCATGA
Reverse	GAGTGTAGGCCTGATAAGACGCTATCAGC
fieF KO	
Forward	ATGAATCAATCTTATGGACGGCTGGTCAGTC GGGCGGCTGTGTAGGCTGGAGCTGCTTCG
Reverse	TTATGAAAGCATAGACCGTTTACCCTCCCTG GGTACGACGCATATGAATATCCTCCTTAG
fieF confirmation	
Forward	CCTTGCCATAGACACCATC
Reverse	TCAGGTCAGGCCAAATGG
pJLJ41p	
Forward (PstI)	AATCCTGCAGATTGTTTAAATACCTCCGAGGC
Reverse (SalI)	TAGAGTCGACTACCAGCGCGGCGAGAATAC
pJLJ42	
Forward (PstI)	TGCTCTGCAGTCATTTGCTCCCAAAATCTTTCT
Reverse (SalI)	GCTAGTCGACAGCGGCAAGATCGAAGATTTTT

[a] Added restriction sites underlined. KO, knockout.

Growth curves. Bacteria were grown from frozen stocks at 37°C with shaking overnight in 5 ml of LB broth or modified M9 minimal medium (6 g/liter Na_2HPO_4, 3 g/liter KH_2PO_4, 1 g/liter NH_4Cl, 0.5 g/liter NaCl, 1 mM $MgSO_4$, 0.1 mM $CaCl_2$, 0.1% glucose, 0.0025% nicotinic acid, 16.5 μg/ml thiamine, and 0.2% casein amino acids). Cultures were then diluted 1:100 into the indicated medium, and the growth of quadruplicate 200-μl samples in shaking 100-well honeycomb plates at 37°C was assessed using a Bioscreen C instrument (Growth Curves USA). For competition assays, wild-type and mutant strains diluted 1:200 were mixed at a 1-to-1 ratio in 5 ml modified M9 medium and grown with shaking at 37°C. After 2, 4, and 6 h of growth, titers of the mutant and wild-type strains were determined by plating serial dilutions on LB agar with or without chloramphenicol (to distinguish wild-type and mutant strains). Competitive indices were calculated as follows: $\log_{10}[(\text{mutant}_{\text{output}}/\text{wild-type}_{\text{output}})/(\text{mutant}_{\text{input}}/\text{wild-type}_{\text{input}})]$. Media and other reagents used in these assays were purchased from Sigma-Aldrich.

Amikacin susceptibility assays. Bacteria were grown from frozen stocks with shaking at 37°C in 5 ml modified M9 medium with or without 100 μg/ml ampicillin (used to maintain plasmids). Overnight cultures were diluted 1:100 into 1 ml modified M9 medium containing amikacin at concentrations ranging from 1 to 40 μg/ml. Each culture was then grown with shaking at 37°C for 24 h. The MIC of each strain was determined as the lowest concentration of amikacin needed to prevent growth.

***cpxP* promoter activity assays.** Bacteria carrying pNLP10-*lux* or pJW1-*cpxP-lux* were grown from frozen stocks at 37°C with shaking overnight in 5 ml modified M9 medium containing 50 μg/ml kanamycin (39). Overnight cultures were diluted 1:100 into 5 ml modified M9 medium containing 50 μg/ml kanamycin and incubated with shaking at 37°C for 4 h to reach stationary phase (optical density at 600 nm, ≈1.0). Triplicate 100-μl aliquots of each sample were then transferred into a 96-well white, opaque-walled polystyrene microplate (Dynex Technologies), and luminescence was measured immediately with a Synergy HT multidetection microplate reader (BioTek Instruments, Inc.).

Hemagglutination assays. Hemagglutination titers were determined using guinea pig red blood cells (Colorado Serum Company) as described previously (62). Bacteria used in these assays were grown statically from frozen stocks in 20 ml modified M9 medium or LB broth for 48 h at 37°C.

Mouse UTI model. Seven- to 8-week-old female CBA/J mice (Jackson Laboratory) were used, following IACUC-approved protocols as previously described (5, 63, 64). Wild-type and mutant bacterial strains were grown from frozen stocks in 20 ml static modified M9 medium for 24 h at 37°C. Prior to inoculation, bacteria were pelleted by centrifugation for 10 min at 8,000 × *g* and then resuspended in phosphate-buffered saline (PBS). Mice were anesthetized by using isoflurane inhalation and carefully inoculated by transurethral catheterization with 50 μl of a bacterial suspension containing 1×10^7 CFU. For competitive assays, wild-type UTI89 was mixed 1:1 with either the Δ*cpxP* or Δ*cpxRA* mutant prior to inoculation. For noncompetitive assays, each strain was inoculated separately. Bladders were harvested aseptically at 3 days postinoculation, weighed, and homogenized in sterile PBS containing 0.02% Triton X-100. Bacterial titers present in the input pools and in the bladder homogenates were determined by plating serial dilutions on LB agar plates. For competitive assays, LB agar plates with or without chloramphenicol (20 μg/ml) were used to distinguish the wild-type and mutant strains. Competitive indices were calculated as follows: $\log_{10}[(\text{mutant CFU inoculated}/\text{wild-type CFU inoculated})/(\text{mutant CFU recovered}/\text{wild-type CFU recovered})]$; based on this equation, values of less than 0 indicated that the wild-type strain outcompeted the mutant. Experiments were repeated two to three times, and combined data are shown.

Zebrafish infections. Zebrafish used in this study were handled in accordance with IACUC-approved protocols and following standard procedures (www.zfin.org), as previously described (65). *AB zebrafish embryos were collected from mixed egg clutches in a breeding colony that was maintained on a 14-h light/10-h dark cycle. Embryos were grown at 28.5°C in E3 medium (5 mM NaCl, 0.27 mM KCl, 0.4 mM $CaCl_2$, 0.16 mM $MgSO_4$) containing 0.000016% methylene blue as an antifungal agent. At 48 h postfertilization (hpf), embryos were manually dechorianated, briefly anesthetized with 0.77 mM ethyl 3-aminobenzoate methanesulfonate salt (Tricaine; Sigma-Aldrich), and embedded in low-melting-point agarose (Mo Bio Laboratories) without Tricaine. Agarose-embedded embryos were then transferred to E3 medium lacking methylene blue and infected individually with wild-type CFT073 or the *cpx* mutants. Bacteria were grown from frozen stocks, held static in 12 ml modified M9 medium at 37°C for 24 h. One milliliter from each culture was pelleted, washed once with 1 ml PBS, and resuspended in PBS prior to inoculation into either the pericardial cavity or circulation valley by using an Olympus SZ61 or SZX10 stereomicroscope together with a YOU-1 micromanipulator (Narishige), a Narishige IM-200 microinjector, and a JUN-AIR model 3 compressor setup. For each bacterial strain, 500 to 1,000 CFU suspended in 1 nl PBS was injected per fish. Inoculation titers were determined by adding 10 drops (1 nl each) to 1 ml 0.7% NaCl, which was then serially diluted and plated on LB agar plates. Following injection, embryos were carefully removed from the agar, placed individually into wells of a 48-well plate (Nunc) containing E3 medium, and incubated at 28.5°C. Fish viability was assessed at regular intervals for 72 h following injection by monitoring heart beats and blood flow.

Bacterial host cell association and invasion assays. Host cell association and gentamicin protection-based invasion assays were performed as previously described (66, 67). Strains used in these assays were grown at 37°C for 48 h in static LB broth to induce expression of type 1 pili. Human bladder epithelial cells, designated 5637 (HTB-9; ATCC), were grown at 37°C in 5% CO_2 using RPMI 1640 medium (Invitrogen) supplemented with 10% heat-inactivated fetal bovine serum (HyClone). Bladder cells were infected with a multiplicity of infection of ~15 bacteria per host cell.

Serum resistance assays. Frozen aliquots of pooled human sera, taken from 7 healthy volunteers by using standard protocols approved by the University of Utah Institutional Review Board, were provided by Andrew Weyrich. Care was taken to not freeze and thaw samples multiple times. Bacteria from overnight cultures grown with shaking at 37°C in modified M9 medium were pelleted by spinning at 8,000 × *g* for 5 min, washed twice, and resuspended in PBS to obtain ~1×10^6 CFU/ml. About 5×10^4 CFU of each bacterial strain was mixed individually with modified M9 medium containing 20% serum, and 200-μl aliquots of each suspension were immediately placed in a 96-well microtiter plate and incubated with gentle shaking for 2.5 h at 37°C. Plates were then placed on ice, and surviving bacteria were enumerated by plating serial dilutions on LB agar. Results were normalized to input titers. Heat-inactivated serum (treated at 55°C for 30 min) was used as a negative control.

Statistical analysis. The Mann-Whitney U test, Wilcoxon matched pair test, log-rank (Mantel-Cox) test, and Student's *t* test were performed using Prism 5.01 software (GraphPad Software). *P* values of less than 0.05 were defined as significant.

RESULTS

The Cpx system modulates UPEC resistance to amikacin. By using lambda Red-mediated linear recombination, the *cpxRA* operon and the *cpxP* gene were individually deleted from two reference UPEC strains, the cystitis isolate UTI89 and the urosepsis isolate CFT073. As the first step in our efforts to phenotypically characterize these mutants, we assessed their sensitivities to the aminoglycoside antibiotic amikacin. Previous studies showed that laboratory K-12 *E. coli* strains lacking *cpxA* or *cpxRA* have increased sensitivity to amikacin, whereas induction of the Cpx pathway or the expression of constitutively active *cpxA* mutants (*cpxA**) provides strains with improved resistance to amikacin (68–70). Resistance has been attributed to the ability of the Cpx system to activate transcription of drug exporters as well as factors that help alleviate the stress of mistranslated proteins that may

TABLE 3 Amikacin MIC assay results[a]

Strain	MIC (μg/ml)
UTI89	18
UTI89Δ*cpxRA*	6
UTI89Δ*cpxP*	28
UTI89(pGEN-MCS)	16
UTI89Δ*cpxRA*(pJLJ42)	30
UTI89Δ*cpxP*(pJLJ41p)	18
CFT073	20
CFT073Δ*cpxRA*	6
CFT073Δ*cpxP*	30
CFT073(pGEN-MCS)	20
CFT073Δ*cpxRA*(pJLJ42)	16
CFT073Δ*cpxP*(pJLJ41p)	20

[a] The assay was repeated three times and the same results were obtained.

accumulate within the bacterial envelope due to amikacin effects on ribosome activity (25, 70, 71).

In agreement with results obtained using K-12 strains (68, 69), we observed that both UTI89Δ*cpxRA* and CFT073Δ*cpxRA* were highly sensitive to amikacin relative to their wild-type counterparts, as determined by MIC assays (Table 3). Plasmid pJLJ42, which carries the *cpxRA* operon under the control of its native promoter, complemented both Δ*cpxRA* mutants, whereas the empty vector pGEN-MCS had no effect (Table 3 and unpublished observations). Deletion of *cpxP*, which leaves CpxA less repressed (40, 45), rendered UTI89 and CFT073 notably more resistant to amikacin (Table 3). Expression of recombinant *cpxP* using plasmid pJLJ41 restored the resistance of the Δ*cpxP* mutants to wild-type levels. Of note, deletion of the gene *yiiP* (*fieF*) located immediately downstream of *cpxP* did not affect the sensitivity of either UTI89 or CFT073 to amikacin (unpublished observations).

These results indicate that the Cpx response in the UPEC isolates operates, not unexpectedly, similarly to the Cpx response in K-12 strains. To further address this point, we utilized a low-copy-number reporter construct containing the *cpxP* promoter fused to a promoterless *luxCDABE* operon (39). In both CFT073 and UTI89, the deletion of *cpxRA* ablated expression of the *cpxP* reporter in early-stationary-phase cultures, whereas deletion of *cpxP* greatly enhanced expression (Fig. 1). These data parallel those reported for similar assays carried out with K-12 strains, supporting models in which CpxP functions in part as a negative regulator of Cpx activation (40, 45).

The Cpx system provides UPEC with a fitness advantage within the bladder. To address whether or not the Cpx system can affect the fitness of UPEC within the urinary tract, we utilized a well-established UTI model system, focusing on bladder colonization by the cystitis isolate UTI89. Adult female CBA/J mice were inoculated via transurethral catheterization with wild-type UTI89, UTI89Δ*cpxRA* or UTI89Δ*cpxP*, and 3 days later bacterial titers within the bladder were determined. In noncompetitive assays, in which equal numbers of the wild-type and mutant strains were inoculated separately into different mice, the Δ*cpxRA* mutant was recovered in significantly lower numbers than wild-type UTI89 (Fig. 2A). In contrast, no significant difference was observed between wild-type UTI89 and the Δ*cpxP* mutant. Similar results were obtained in competitive assays, in which the wild-type strain was mixed 1:1 with each mutant strain prior to inoculation (Fig. 2B and C). These results indicated that *cpxRA*, but not *cpxP*, is required by UTI89 to effectively colonize the bladder.

During the course of a UTI, UPEC comes across a variety of environmental stresses that can potentially limit its survival and growth within the host (10–15). These stresses include reactive nitrogen and oxygen radicals and numerous membrane-damaging substances. In LB broth and modified M9 medium, the *cpxRA* and *cpxP* deletion mutants grew normally, whether on their own in monoculture or in direct competition with the wild-type strains (Fig. 3). Likewise, no defects were observed with the Δ*cpxRA* or Δ*cpxP* mutants when challenged *in vitro* with nitrosative stress (1 mM acidified sodium nitrite), oxidative stress (0.5 or 1 M methyl viologen), or envelope stress generated by addition of 0.1% sodium dodecyl sulfate (unpublished observations). These findings indicate that deletion of *cpxRA* or *cpxP* does not alter the ability of UPEC to handle generalized stresses.

Divergent effects of the Cpx system on host cell invasion by UPEC. Effective colonization of the bladder by UPEC generally requires the expression of functional type 1 pili (63, 72–75). These filamentous adhesive organelles mediate bacterial attachment to and invasion of bladder epithelial cells, promoting the establish-

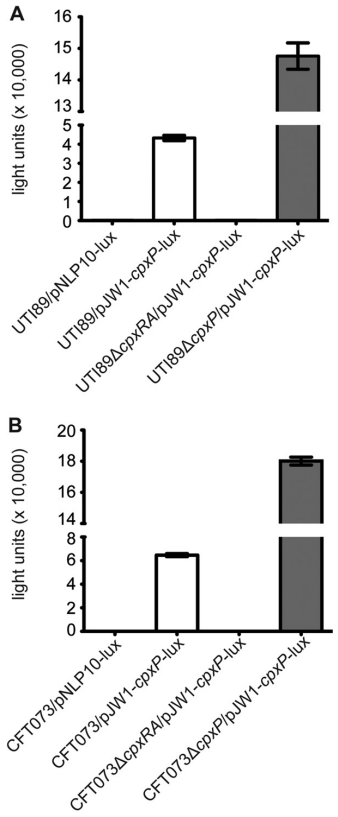

FIG 1 Deletion of *cpxP* enhances Cpx activation in both CFT073 and UTI89. Graphs indicate expression levels (± standard deviations) of the *luxCDABE* operon driven by the *cpxP* promoter in wild-type UTI89 (A) and wild-type CFT073 (B) and their mutant derivatives, following growth to early stationary phase in modified M9 medium. The pNLP1-*lux* plasmid carries a promoterless *luxCDABE* operon. Each graph shows the means ± standard errors of the means of three independent experiments performed in triplicate.

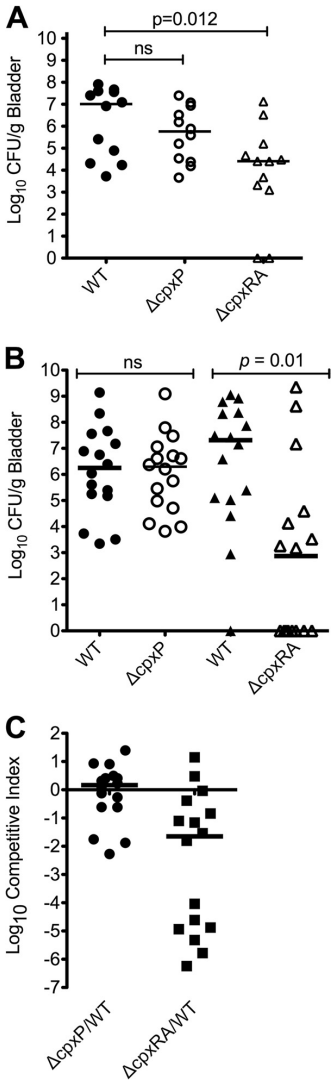

FIG 2 The Cpx system promotes UPEC fitness within the bladder. Adult female CBA/J mice were infected via catheterization with wild-type UTI89, UTI89Δ*cpxP*, or UTI89Δ*cpxRA* in noncompetitive (A) and competitive (B and C) assays. Graphs show bacterial titers present in the bladder at 3 days postinoculation. Bars denote median values for each group ($n \geq 12$ mice). The data in panel B are graphed in panel C as competitive indices. *P* values were determined using the Mann-Whitney U test (A) or Wilcoxon-matched paired signed rank test (B). ns, no significant difference.

ment and persistence of UPEC within the urinary tract (5, 6, 63, 76). In yeast agglutination assays, as well as hemagglutination assays performed using guinea pig red blood cells, we observed no overt differences in the expression of type 1 pili by the Δ*cpxRA* or Δ*cpxP* mutants relative to the wild-type UPEC isolates (unpublished observations). However, UTI89Δ*cpxRA* did show a slight, but significant (~20%), decrease in its ability to adhere to human bladder epithelial cells in culture (Fig. 4A). This reduction in adherence corresponded with a similar (~30%) decrease in host cell invasion by UTI89Δ*cpxRA*, as determined in gentamicin protection assays (Fig. 4B). These modest defects in host cell adherence and invasion could be rescued by complementation of the Δ*cpxRA* mutant with pJLJ42. In contrast to UTI89Δ*cpxRA*, the Δ*cpxP* mutant had no defect in its ability to bind bladder epithelial cells (Fig. 4A), but it was able to invade the host cells at a much higher frequency than either wild-type UTI89 or the Δ*cpxRA* mutant (Fig. 4B). Complementation of UTI89Δ*cpxP* with pJLJ42 reduced the invasion frequencies of this mutant to wild-type levels. Importantly, wild-type UTI89 and the Δ*cpxRA* and Δ*cpxP* mutants grew similarly in the cell culture medium, and all three strains were equally susceptible to killing by gentamicin at the concentration (100 μg/ml) used in these invasion assays.

Cpx components promote UPEC virulence in zebrafish. To assess effects of the Cpx system on UPEC virulence, and not fitness *per se*, we next focused on CFT073 in a zebrafish infection model that was recently developed in our laboratory (65). In this model system, bacteria are microinjected into 48-hpf zebrafish embryos via either a fluid-filled sac surrounding the heart, known as the pericardial cavity (PC), or directly into the bloodstream through the circulation valley. UPEC does not usually spread from the PC, whereas the pathogens rapidly disseminate systemically following inoculation of the bloodstream. At 48 hpf, zebrafish are dependent upon innate host defenses that include phagocytes, antimicrobial peptides, and complement—the same sort of defenses that mammalian hosts employ against UPEC (77–81). The use of zebrafish has proven to be an effective way to identify and functionally define virulence factors of relevance to UPEC and related pathogens that can colonize an assorted array of hosts and host tissues (unpublished observations and references 65 and 82).

Relative to UTI89 and many other UPEC isolates, CFT073 is especially lethal to zebrafish embryos (65). Here, we compared the lethality of wild-type CFT073 to CFT073Δ*cpxRA* and CFT073Δ*cpxP* following inoculation of 500 to 1,000 CFU of each strain individually into the PC or blood. In this infection model, increased bacterial growth correlates with decreased host survival (65). Wild-type CFT073 killed most of the zebrafish embryos within 24 h, irrespective of the site of inoculation (Fig. 5). In comparison to the wild-type strain, the virulence of both the Δ*cpxRA* and Δ*cpxP* mutants was significantly decreased. Virulence defects associated with CFT073Δ*cpxRA* and CFT073Δ*cpxP* were particularly evident following inoculation of the blood (Fig. 5B), which in general appears to be a more challenging and stressful environment than the PC (65). Wild-type CFT073 and the Δ*cpxRA* and Δ*cpxP* mutants grew similarly in modified M9 minimal medium at 28.5°C, the temperature at which the zebrafish embryos are maintained. Plasmid pJLJ42 (*cpxRA*) and pJLJ41 (*cpxP*) rescued the virulence defects associated with CFT073Δ*cpxRA* and CFT073Δ*cpxP*, respectively, but the wild-type strain carrying empty vector was attenuated, complicating interpretation of our *in vivo* complementation assays (unpublished observations).

Strain-dependent effects of Cpx components on serum resistance. Urine, like serum, contains numerous antibacterial factors, including heat-labile components of the complement system that can mediate bacterial opsonization and the formation of membrane attack complexes (14, 83–85). By modulating the composition and resilience of the bacterial envelope, we hypothesized that

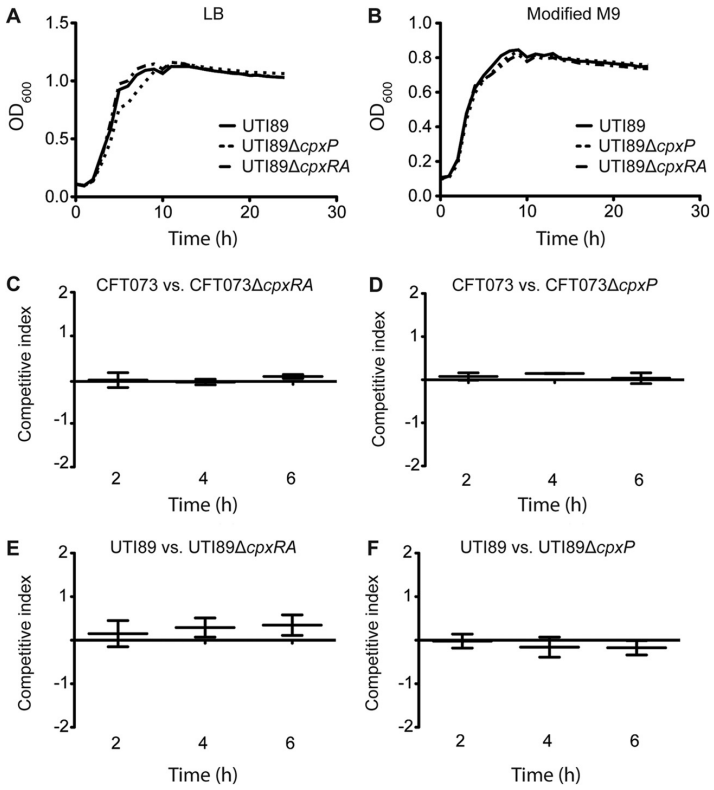

FIG 3 CFT073 and UTI89 mutants lacking either *cpxP* or *cpxRA* grow normally in LB broth and modified M9 medim. (A and B) Growth of wild-type UTI89 and associated Δ*cpxP* and Δ*cpxRA* mutants grown in LB broth (A) and modified M9 medium (B). Graphs are representative of at least three independent experiments performed in quadruplicate. (C to F) Results of competitive growth assays carried out in modified M9 medium with wild-type CFT073 and UTI89 versus isogenic Δ*cpxRA* or Δ*cpxP* mutants, as indicated. Data are presented as box-and-whiskers plots, with means ± the minimum and maximum values from three independent experiments.

the Cpx system can alter the sensitivity of UPEC to serum components. To examine this possibility, serum resistance assays were performed using wild-type UTI89 and CFT073 along with the Δ*cpxRA* and Δ*cpxP* mutants. In these assays, both UTI89Δ*cpxRA* and CFT073Δ*cpxRA* were significantly more sensitive to pooled human sera than their wild-type counterparts (Fig. 6A). UTI89Δ*cpxP* was likewise sensitive, whereas CFT073Δ*cpxP* showed no decrease in serum resistance relative to wild-type CFT073. Serum resistance defects associated with UTI89Δ*cpxRA*, CFT073Δ*cpxRA*, and UTI89Δ*cpxP* were rescued by plasmids carrying CpxRA (pJLJ42) or CpxP (pJLJ41), as appropriate (Fig. 6B). In assays that used heat-inactivated serum, which lacks functional complement, no differences were observed between the wild-type and mutant strains (Fig. 6C). Together, these data indicate that CpxRA, with strain-dependent input from CpxP, can enhance UPEC resistance to serum and, specifically, complement.

DISCUSSION

This study was aimed at delineating the impact of the Cpx envelope stress response system on the fitness and virulence of UPEC. Our results demonstrated that CpxRA and the auxiliary factor CpxP can affect the ability of UPEC to colonize distinct host environments. Employing a well-established mouse UTI model, we found that deletion of *cpxRA* limited the ability of the reference cystitis isolate UTI89 to effectively colonize the bladder, whereas deletion of *cpxP* had only modest effects. In laboratory K-12 *E. coli* strains, CpxP is not an essential regulator of the Cpx system, and instead it appears to modulate how quickly CpxA can be activated or inactivated in response to changing levels of envelope stress (20, 40, 43, 45). Within the bladder, the regulatory effects of CpxP are apparently dispensable to UTI89, at least at the 3-day time point that was analyzed. In contrast, deletion of either *cpxRA* or *cpxP* markedly attenuated the virulence of the urosepsis isolate CFT073 during both localized and systemic infections in zebrafish embryos. These data suggest that CpxP is differentially required by UPEC, depending upon strain background and the host environment. This idea was further supported by *in vitro* assays that showed that the resistance of UTI89 to complement-mediated killing was dependent upon both CpxRA and CpxP, while CFT073 required only CpxRA.

The Cpx system is intercalated within a complex web of signaling cascades and linked up with multiple biosynthetic and metabolic pathways (25, 38, 39, 41, 45, 86–88), making it difficult to

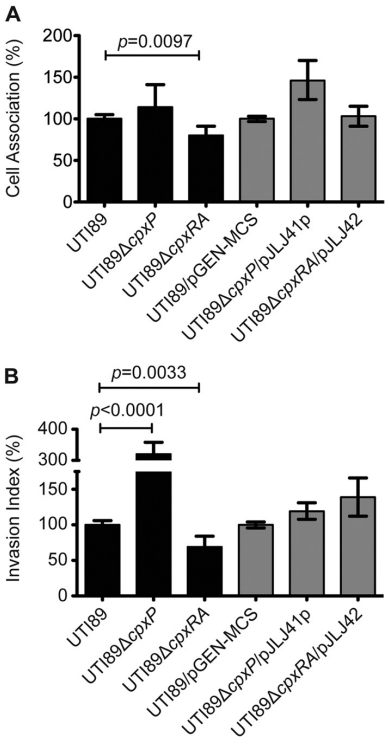

FIG 4 Cpx effects on bladder cell invasion by UTI89. Human bladder epithelial cells were infected with the indicated strains for 2 h, followed by an additional 2-h incubation in medium containing gentamicin (100 μg/ml). Graphs show the total cell-associated bacterial titers prior to addition of gentamicin (A) and for gentamicin-protected, intracellular bacteria (B). Data are expressed relative to wild-type UTI89 (black bars) or UTI89 carrying the control plasmid pGEN-MCS (gray bars) as the means ± standard errors of the means of at least three independent experiments performed in triplicate. The indicated *P* values were calculated using Student's *t* test.

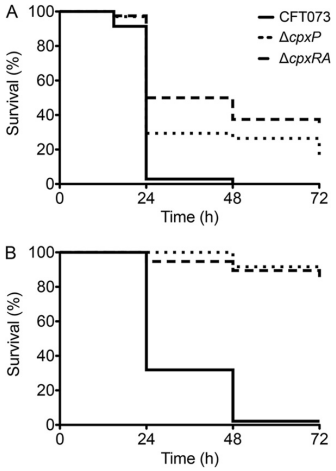

FIG 5 The Cpx system is required for full virulence of CFT073 in zebrafish embryos. The PC (A) or blood (B) of 48-hpf zebrafish embryos was inoculated with 500 to 1,000 CFU of wild-type CFT073, CFT073Δ*cpxP*, or CFT073Δ*cpxRA*, as indicated. Fish were scored for death at 0, 24, 48, and 72 h postinoculation. Data are expressed as the percent survival over time ($n \geq 17$ embryos). $P \leq 0.0008$ for the Δ*cpxP* and Δ*cpxRA* mutants versus control wild-type CFT073, as determined using Mantel-Cox log rank tests.

discern with clarity the specific mechanisms by which Cpx components moderate UPEC stress resistance and virulence phenotypes. It is clear, however, that basic regulation of the Cpx system in UPEC functions similarly to the Cpx system in nonpathogenic K-12 *E. coli* strains. In K-12 strains, CpxP regulates Cpx activation via a negative feedback loop (40), and this also appears to be the case in UPEC (Fig. 1). Furthermore, deletion of *cpxRA* rendered both UTI89 and CFT073 highly sensitive to the aminoglycoside amikacin (at 3 μg/ml), whereas deletion of *cpxP* increased amikacin resistance. These data are in agreement with work carried out in K-12 strains (68–70) and support the notion that activation of the Cpx system safeguards against aminoglycoside antibiotics. Protection is likely afforded by Cpx-mediated upregulation of proteases and other factors that alleviate envelope stress initiated by the mistranslation of inner membrane proteins in the presence of amikacin (70). Cpx activation may also heighten bacterial resistance to antibiotics via effects on the expression of drug transporters (25, 71).

The protective effects of Cpx activation are limited and will not shield against all concentrations and types of antibiotics, including the aminoglycoside gentamicin, used in our host cell invasion assays (70). This means that the slight but significant decrease in host cell invasion by UTI89Δ*cpxRA* and the elevated invasion frequencies seen with UTI89Δ*cpxP* are likely not attributable to Cpx-regulated effects on the susceptibility of UTI89 to gentamicin. Instead, the Cpx system may affect bacterial survival during or immediately after internalization or, alternatively, modulate the efficacy of the invasion process directly by affecting the surface characteristics of UPEC. The latter possibility is buoyed indirectly by observations showing that disruption of the Cpx system can alter bacterial interactions with hydrophobic abiotic surfaces (89). Of note, UPEC mutants lacking either *cpxRA* or *cpxP* were not obviously different from the wild-type strains with respect to motility, biofilm formation in microtiter plate assays, or the expression of curli or type 1 pili (unpublished observations). This indicates that many of the phenotypes commonly associated with UPEC virulence are unaffected by disruption of the Cpx system.

The reduced capacity of UTI89Δ*cpxRA* to bind and invade bladder epithelial cells may contribute to the inability of this mutant to effectively colonize the bladder. However, it is probable that additional CpxRA-regulated activities also play a role. These activities may include Cpx-mediated alterations of the bacterial envelope and peptidoglycan layer that enable bacteria to better deal with antimicrobial peptides and proteins like complement (90). The complement system can mediate bacterial opsonization and the formation of membrane attack complexes, thereby facilitating the clearance of bacteria during both localized and systemic infections (83). The strain-dependent requirement for CpxP in UPEC resistance to complement-mediated killing, as reported here (Fig. 6), highlights the individuality of UPEC isolates, which are often genetically diverse, while also raising questions regarding the functionality of highly conserved proteins like CpxP.

In addition to modulating the activity of CpxA, CpxP can func-

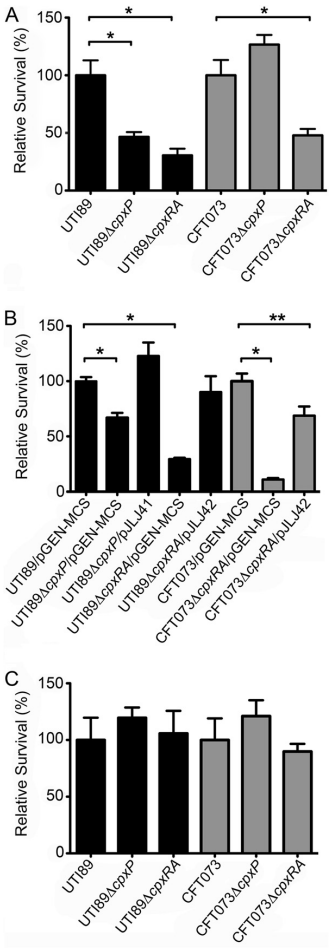

FIG 6 Cpx components have strain-dependent effects on serum resistance. About 5×10^4 CFU of wild-type UTI89 or CFT073 or their mutant derivatives were incubated at 37°C with gentle shaking in modified M9 medium containing 20% human serum (A) or 20% heat-inactivated serum (C). After 2.5 h, surviving bacteria were enumerated by plating serial dilutions. (B) Similar assays with 20% serum were performed using strains carrying plasmids pJLJ41 or pJLJ42 or the control empty vector, pGEN-MCS, as indicated. Data are presented relative to the wild-type strains as the means ± standard errors of the means of at least four independent experiments. In panel B, the control wild-type strains carried pGEN-MCS. *, $P < 0.007$; **, $P = 0.02$ (determined with Student's *t* test).

tion as a periplasmic chaperone and may act as a sensor for metal ions, like zinc and copper (43, 44, 91, 92). UTI89 is apparently more dependent upon one or more of these activities when challenged with complement, whereas CFT073 can make do without CpxP. It is feasible that structural homologues of CpxP, such as Spy and ZraP (92–94), can substitute for CpxP under specific conditions in strains like CFT073. The Cpx system is best known for its effects on the expression of periplasmic chaperones and proteases in response to envelope stress, and the misregulation of these and other factors likely contribute to the myriad defects observed with the Δ*cpxP* and Δ*cpxRA* mutants in our assays.

ACKNOWLEDGMENTS

We thank Tamara Smith in the laboratory of Andrew Weyrich (University of Utah, Department of Human Genetics) for providing the human serum samples and Travis Wiles from our laboratory for initial assistance with the serum resistance assays. We are also grateful to Jacqueline Engel for help with characterization of the *yiiP* (*fieF*) mutants and Tracy Raivio for providing plasmids pNLP10-*lux* and pJW1-*cpxP-lux*.

This work was supported by grants AI095647, AI090369, and AI088086 from the National Institute of Allergy and Infectious Diseases. A.E.B. and R.R.K. were supported by NIH Microbial Pathogenesis Training Grant T32 AI055434, while J.P.N. was supported by NIH Genetics Training Grant T32-GM007464.

REFERENCES

1. **Foxman B.** 2010. The epidemiology of urinary tract infection. Nature Rev. Urol. **7**:653–660.
2. **Dhakal BK, Kulesus RR, Mulvey MA.** 2008. Mechanisms and consequences of bladder cell invasion by uropathogenic Escherichia coli. Eur. J. Clin. Invest. **38**(Suppl. 2):2–11.
3. **Hunstad DA, Justice SS.** 2010. Intracellular lifestyles and immune evasion strategies of uropathogenic Escherichia coli. Annu. Rev. Microbiol. **64**:203–221.
4. **Jorgensen I, Seed PC.** 2012. How to make it in the urinary tract: a tutorial by Escherichia coli. PLoS Pathog. **8**:e1002907. doi:10.1371/journal.ppat.1002907.
5. **Blango MG, Mulvey MA.** 2010. Persistence of uropathogenic Escherichia coli in the face of multiple antibiotics. Antimicrob. Agents Chemother. **54**:1855–1863.
6. **Mulvey MA, Schilling JD, Hultgren SJ.** 2001. Establishment of a persistent Escherichia coli reservoir during the acute phase of a bladder infection. Infect. Immun. **69**:4572–4579.
7. **Sobel JD.** 1997. Pathogenesis of urinary tract infection. Role of host defenses. Infect. Dis. Clin. North Am. **11**:531–549.
8. **Muhldorfer I, Ziebuhr W, Hacker J.** 2001. Escherichia coli in urinary tract infections, p 1739–1748. *In* Sussman M (ed), Molecular medical microbiology. Academic Press, London, England.
9. **Smith JL, Fratamico PM, Gunther NW.** 2007. Extraintestinal pathogenic Escherichia coli. Foodborne Pathog. Dis. **4**:134–163.
10. **Ragnarsdottir B, Lutay N, Gronberg-Hernandez J, Koves B, Svanborg C.** 2011. Genetics of innate immunity and UTI susceptibility. Nat. Rev. Urol. **8**:449–468.
11. **Zasloff M.** 2007. Antimicrobial peptides, innate immunity, and the normally sterile urinary tract. J. Am. Soc. Nephrol. **18**:2810–2816.
12. **Bower JM, Gordon-Raagas HB, Mulvey MA.** 2009. Conditioning of uropathogenic Escherichia coli for enhanced colonization of host. Infect. Immun. **77**:2104–2112.
13. **Alteri CJ, Mobley HL.** 2012. Escherichia coli physiology and metabolism dictates adaptation to diverse host microenvironments. Curr. Opin. Microbiol. **15**:3–9.
14. **Li K, Feito MJ, Sacks SH, Sheerin NS.** 2006. CD46 (membrane cofactor protein) acts as a human epithelial cell receptor for internalization of opsonized uropathogenic Escherichia coli. J. Immunol. **177**:2543–2551.
15. **Mulvey MA, Schilling JD, Martinez JJ, Hultgren SJ.** 2000. Bad bugs and beleaguered bladders: interplay between uropathogenic Escherichia coli and innate host defenses. Proc. Natl. Acad. Sci. U. S. A. **97**:8829–8835.
16. **MacRitchie DM, Buelow DR, Price NL, Raivio TL.** 2008. Two-component signaling and gram negative envelope stress response systems. Adv. Exp. Med. Biol. **631**:80–110.
17. **Raivio TL.** 2005. Envelope stress responses and Gram-negative bacterial pathogenesis. Mol. Microbiol. **56**:1119–1128.
18. **Ruiz N, Silhavy TJ.** 2005. Sensing external stress: watchdogs of the Escherichia coli cell envelope. Curr. Opin. Microbiol. **8**:122–126.
19. **Joly N, Engl Jovanovic CG, Huvet M, Toni T, Sheng X, Stumpf MP, Buck M.** 2010. Managing membrane stress: the phage shock protein (Psp) response, from molecular mechanisms to physiology. FEMS Microbiol. Rev. **34**:797–827.
20. **Vogt SL, Raivio TL.** 2012. Just scratching the surface: an expanding view of the Cpx envelope stress response. FEMS Microbiol. Lett. **326**:2–11.
21. **Weber RF, Silverman PM.** 1988. The cpx proteins of Escherichia coli K12. Structure of the cpxA polypeptide as an inner membrane component. J. Mol. Biol. **203**:467–478.

22. **Dong J, Iuchi S, Kwan S, Lu Z, Lin EC.** 1993. The deduced amino-acid sequence of the cloned *cpxR* gene suggests the protein is the cognate regulator for the membrane sensor, CpxA, in a two-component signal transduction system of *Escherichia coli*. Gene **136**:227–230.
23. **Otto K, Silhavy TJ.** 2002. Surface sensing and adhesion of Escherichia coli controlled by the Cpx-signaling pathway. Proc. Natl. Acad. Sci. U. S. A. **99**:2287–2292.
24. **Prigent-Combaret C, Brombacher E, Vidal O, Ambert A, Lejeune P, Landini P, Dorel C.** 2001. Complex regulatory network controls initial adhesion and biofilm formation in Escherichia coli via regulation of the csgD gene. J. Bacteriol. **183**:7213–7223.
25. **Dorel C, Lejeune P, Rodrigue A.** 2006. The Cpx system of Escherichia coli, a strategic signaling pathway for confronting adverse conditions and for settling biofilm communities? Res. Microbiol. **157**:306–314.
26. **Dorel C, Vidal O, Prigent-Combaret C, Vallet I, Lejeune P.** 1999. Involvement of the Cpx signal transduction pathway of E. coli in biofilm formation. FEMS Microbiol. Lett. **178**:169–175.
27. **Hung DL, Raivio TL, Jones CH, Silhavy TJ, Hultgren SJ.** 2001. Cpx signaling pathway monitors biogenesis and affects assembly and expression of P pili. EMBO J. **20**:1508–1518.
28. **Hernday AD, Braaten BA, Broitman-Maduro G, Engelberts P, Low DA.** 2004. Regulation of the pap epigenetic switch by CpxAR: phosphorylated CpxR inhibits transition to the phase ON state by competition with Lrp. Mol. Cell **16**:537–547.
29. **Inoue T, Shingaki R, Hirose S, Waki K, Mori H, Fukui K.** 2007. Genome-wide screening of genes required for swarming motility in Escherichia coli K-12. J. Bacteriol. **189**:950–957.
30. **De Wulf P, Kwon O, Lin EC.** 1999. The CpxRA signal transduction system of Escherichia coli: growth-related autoactivation and control of unanticipated target operons. J. Bacteriol. **181**:6772–6778.
31. **Gal-Mor O, Segal G.** 2003. Identification of CpxR as a positive regulator of icm and dot virulence genes of Legionella pneumophila. J. Bacteriol. **185**:4908–4919.
32. **Nevesinjac AZ, Raivio TL.** 2005. The Cpx envelope stress response affects expression of the type IV bundle-forming pili of enteropathogenic Escherichia coli. J. Bacteriol. **187**:672–686.
33. **Nakayama S, Watanabe H.** 1995. Involvement of cpxA, a sensor of a two-component regulatory system, in the pH-dependent regulation of expression of Shigella sonnei virF gene. J. Bacteriol. **177**:5062–5069.
34. **Nakayama S, Watanabe H.** 1998. Identification of cpxR as a positive regulator essential for expression of the Shigella sonnei virF gene. J. Bacteriol. **180**:3522–3528.
35. **Mitobe J, Arakawa E, Watanabe H.** 2005. A sensor of the two-component system CpxA affects expression of the type III secretion system through posttranscriptional processing of InvE. J. Bacteriol. **187**:107–113.
36. **Mulvey MA.** 2002. Adhesion and entry of uropathogenic Escherichia coli. Cell. Microbiol. **4**:257–271.
37. **Herbert EE, Cowles KN, Goodrich-Blair H.** 2007. CpxRA regulates mutualism and pathogenesis in Xenorhabdus nematophila. Appl. Environ. Microbiol. **73**:7826–7836.
38. **De Wulf P, McGuire AM, Liu X, Lin EC.** 2002. Genome-wide profiling of promoter recognition by the two-component response regulator CpxR-P in Escherichia coli. J. Biol. Chem. **277**:26652–26661.
39. **Price NL, Raivio TL.** 2009. Characterization of the Cpx regulon in Escherichia coli strain MC4100. J. Bacteriol. **191**:1798–1815.
40. **Raivio TL, Popkin DL, Silhavy TJ.** 1999. The Cpx envelope stress response is controlled by amplification and feedback inhibition. J. Bacteriol. **181**:5263–5272.
41. **Hunke S, Keller R, Muller VS.** 2012. Signal integration by the Cpx-envelope stress system. FEMS Microbiol. Lett. **326**:12–22.
42. **DiGiuseppe PA, Silhavy TJ.** 2003. Signal detection and target gene induction by the CpxRA two-component system. J. Bacteriol. **185**:2432–2440.
43. **Buelow DR, Raivio TL.** 2005. Cpx signal transduction is influenced by a conserved N-terminal domain in the novel inhibitor CpxP and the periplasmic protease DegP. J. Bacteriol. **187**:6622–6630.
44. **Isaac DD, Pinkner JS, Hultgren SJ, Silhavy TJ.** 2005. The extracytoplasmic adaptor protein CpxP is degraded with substrate by DegP. Proc. Natl. Acad. Sci. U. S. A. **102**:17775–17779.
45. **Buelow DR, Raivio TL.** 2010. Three (and more) component regulatory systems: auxiliary regulators of bacterial histidine kinases. Mol. Microbiol. **75**:547–566.
46. **Leclerc GJ, Tartera C, Metcalf ES.** 1998. Environmental regulation of Salmonella typhi invasion-defective mutants. Infect. Immun. **66**:682–691.
47. **Humphreys S, Rowley G, Stevenson A, Anjum MF, Woodward MJ, Gilbert S, Kormanec J, Roberts M.** 2004. Role of the two-component regulator CpxAR in the virulence of Salmonella enterica serotype Typhimurium. Infect. Immun. **72**:4654–4661.
48. **Altman E, Segal G.** 2008. The response regulator CpxR directly regulates expression of several Legionella pneumophila icm/dot components as well as new translocated substrates. J. Bacteriol. **190**:1985–1996.
49. **MacRitchie DM, Acosta N, Raivio TL.** 2012. DegP is involved in Cpx-mediated posttranscriptional regulation of the type III secretion apparatus in enteropathogenic Escherichia coli. Infect. Immun. **80**:1766–1772.
50. **Leuko S, Raivio TL.** 2012. Mutations that impact the enteropathogenic Escherichia coli Cpx envelope stress response attenuate virulence in Galleria mellonella. Infect. Immun. **80**:3077–3085.
51. **Ojha S, Lacouture S, Gottschalk M, MacInnes JI.** 2010. Characterization of colonization-deficient mutants of Actinobacillus suis. Vet. Microbiol. **140**:122–130.
52. **Labandeira-Rey M, Brautigam CA, Hansen EJ.** 2010. Characterization of the CpxRA regulon in Haemophilus ducreyi. Infect. Immun. **78**:4779–4791.
53. **Spinola SM, Fortney KR, Baker B, Janowicz DM, Zwickl B, Katz BP, Blick RJ, Munson RS, Jr.** 2010. Activation of the CpxRA system by deletion of cpxA impairs the ability of Haemophilus ducreyi to infect humans. Infect. Immun. **78**:3898–3904.
54. **Herbert Tran EE, Goodrich-Blair H.** 2009. CpxRA contributes to Xenorhabdus nematophila virulence through regulation of lrhA and modulation of insect immunity. Appl. Environ. Microbiol. **75**:3998–4006.
55. **Liu J, Obi IR, Thanikkal EJ, Kieselbach T, Francis MS.** 2011. Phosphorylated CpxR restricts production of the RovA global regulator in Yersinia pseudotuberculosis. PLoS One **6**:e23314. doi:10.1371/journal.pone.0023314.
56. **Carlsson KE, Liu J, Edqvist PJ, Francis MS.** 2007. Influence of the Cpx extracytoplasmic-stress-responsive pathway on Yersinia sp.-eukaryotic cell contact. Infect. Immun. **75**:4386–4399.
57. **Liu J, Thanikkal EJ, Obi IR, Francis MS.** 2012. Elevated CpxR~P levels repress the Ysc-Yop type III secretion system of Yersinia pseudotuberculosis. Res. Microbiol. **163**:518–530.
58. **Jones CH, Danese PN, Pinkner JS, Silhavy TJ, Hultgren SJ.** 1997. The chaperone-assisted membrane release and folding pathway is sensed by two signal transduction systems. EMBO J. **16**:6394–6406.
59. **Datsenko KA, Wanner BL.** 2000. One-step inactivation of chromosomal genes in Escherichia coli K-12 using PCR products. Proc. Natl. Acad. Sci. U. S. A. **97**:6640–6645.
60. **Murphy KC, Campellone KG.** 2003. Lambda Red-mediated recombinogenic engineering of enterohemorrhagic and enteropathogenic E. coli. BMC Mol. Biol. **4**:11. doi:10.1186/1741-2199-4-11.
61. **Lane MC, Alteri CJ, Smith SN, Mobley HL.** 2007. Expression of flagella is coincident with uropathogenic Escherichia coli ascension to the upper urinary tract. Proc. Natl. Acad. Sci. U. S. A. **104**:16669–16674.
62. **Slonim LN, Pinkner JS, Branden CI, Hultgren SJ.** 1992. Interactive surface in the PapD chaperone cleft is conserved in pilus chaperone superfamily and essential in subunit recognition and assembly. EMBO J. **11**:4747–4756.
63. **Mulvey MA, Lopez-Boado YS, Wilson CL, Roth R, Parks WC, Heuser J, Hultgren SJ.** 1998. Induction and evasion of host defenses by type 1-piliated uropathogenic Escherichia coli. Science **282**:1494–1497.
64. **Norton JP, Mulvey MA.** 2012. Toxin-antitoxin systems are important for niche-specific colonization and stress resistance of uropathogenic Escherichia coli. PLoS Pathog. **8**:e1002954. doi:10.1371/journal.ppat.1002954.
65. **Wiles TJ, Bower JM, Redd MJ, Mulvey MA.** 2009. Use of zebrafish to probe the divergent virulence potentials and toxin requirements of extraintestinal pathogenic Escherichia coli. PLoS Pathog. **5**:e1000697. doi:10.1371/journal.ppat.1000697.
66. **Dhakal BK, Mulvey MA.** 2009. Uropathogenic Escherichia coli invades host cells via an HDAC6-modulated microtubule-dependent pathway. J. Biol. Chem. **284**:446–454.
67. **Eto DS, Gordon HB, Dhakal BK, Jones TA, Mulvey MA.** 2008. Clathrin, AP-2, and the NPXY-binding subset of alternate endocytic adaptors facilitate FimH-mediated bacterial invasion of host cells. Cell. Microbiol. **10**:2553–2567.
68. **Rainwater S, Silverman PM.** 1990. The Cpx proteins of Escherichia coli

K-12: evidence that cpxA, ecfB, ssd, and eup mutations all identify the same gene. J. Bacteriol. **172**:2456–2461.
69. **Mileykovskaya E, Dowhan W.** 1997. The Cpx two-component signal transduction pathway is activated in Escherichia coli mutant strains lacking phosphatidylethanolamine. J. Bacteriol. **179**:1029–1034.
70. **Mahoney TF, Silhavy TJ.** 18 January 2013. The Cpx stress response confers resistance to some, but not all, bactericidal antibiotics. J. Bacteriol. http://dx.doi.org/10.1128/JB02197-12.
71. **Hirakawa H, Nishino K, Hirata T, Yamaguchi A.** 2003. Comprehensive studies of drug resistance mediated by overexpression of response regulators of two-component signal transduction systems in Escherichia coli. J. Bacteriol. **185**:1851–1856.
72. **Langermann S, Palaszynski S, Barnhart M, Auguste G, Pinkner JS, Burlein J, Barren P, Koenig S, Leath S, Jones CH, Hultgren SJ.** 1997. Prevention of mucosal Escherichia coli infection by FimH-adhesin-based systemic vaccination. Science **276**:607–611.
73. **Connell I, Agace W, Klemm P, Schembri M, Marild S, Svanborg C.** 1996. Type 1 fimbrial expression enhances Escherichia coli virulence for the urinary tract. Proc. Natl. Acad. Sci. U. S. A. **93**:9827–9832.
74. **Thankavel K, Madison B, Ikeda T, Malaviya R, Shah AH, Arumugam PM, Abraham SN.** 1997. Localization of a domain in the FimH adhesin of *Escherichia coli* type 1 fimbriae capable of receptor recognition and use of a domain-specific antibody to confer protection against experimental urinary tract infection. J. Clin. Invest. **100**:1123–1136.
75. **Langermann S, Mollby R, Burlein JE, Palaszynski SR, Auguste CG, DeFusco A, Strouse R, Schenerman MA, Hultgren SJ, Pinkner JS, Winberg J, Guldevall L, Soderhall M, Ishikawa K, Normark S, Koenig S.** 2000. Vaccination with FimH adhesin protects cynomolgus monkeys from colonization and infection by uropathogenic Escherichia coli. J. Infect. Dis. **181**:774–778.
76. **Martinez JJ, Mulvey MA, Schilling JD, Pinkner JS, Hultgren SJ.** 2000. Type 1 pilus-mediated bacterial invasion of bladder epithelial cells. EMBO J. **19**:2803–2812.
77. **Trede NS, Langenau DM, Traver D, Look AT, Zon LI.** 2004. The use of zebrafish to understand immunity. Immunity **20**:367–379.
78. **Li X, Wang S, Qi J, Echtenkamp SF, Chatterjee R, Wang M, Boons GJ, Dziarski R, Gupta D.** 2007. Zebrafish peptidoglycan recognition proteins are bactericidal amidases essential for defense against bacterial infections. Immunity **27**:518–529.
79. **Jault C, Pichon L, Chluba J.** 2004. Toll-like receptor gene family and TIR-domain adapters in Danio rerio. Mol. Immunol. **40**:759–771.
80. **Lieschke GJ, Oates AC, Crowhurst MO, Ward AC, Layton JE.** 2001. Morphologic and functional characterization of granulocytes and macrophages in embryonic and adult zebrafish. Blood **98**:3087–3096.
81. **van der Vaart M, Spaink HP, Meijer AH.** 2012. Pathogen recognition and activation of the innate immune response in zebrafish. Adv. Hematol. **2012**:159807. doi:10.1155/2012/159807.
82. **Vigil PD, Wiles TJ, Engstrom MD, Prasov L, Mulvey MA, Mobley HL.** 2012. The repeat-in-toxin family member TosA mediates adherence of uropathogenic Escherichia coli and survival during bacteremia. Infect. Immun. **80**:493–505.
83. **Rus H, Cudrici C, Niculescu F.** 2005. The role of the complement system in innate immunity. Immunol. Res. **33**:103–112.
84. **Li K, Sacks SH, Sheerin NS.** 2008. The classical complement pathway plays a critical role in the opsonisation of uropathogenic Escherichia coli. Mol. Immunol. **45**:954–962.
85. **Li K, Zhou W, Hong Y, Sacks SH, Sheerin NS.** 2009. Synergy between type 1 fimbriae expression and C3 opsonisation increases internalisation of E. coli by human tubular epithelial cells. BMC Microbiol. **9**:64. doi:10.1186/1471-2180-9-64.
86. **Gerken H, Leiser OP, Bennion D, Misra R.** 2010. Involvement and necessity of the Cpx regulon in the event of aberrant beta-barrel outer membrane protein assembly. Mol. Microbiol. **75**:1033–1046.
87. **Wolfe AJ, Parikh N, Lima BP, Zemaitaitis B.** 2008. Signal integration by the two-component signal transduction response regulator CpxR. J. Bacteriol. **190**:2314–2322.
88. **Jung K, Fried L, Behr S, Heermann R.** 2012. Histidine kinases and response regulators in networks. Curr. Opin. Microbiol. **15**:118–124.
89. **Otto K, Norbeck J, Larsson T, Karlsson KA, Hermansson M.** 2001. Adhesion of type 1-fimbriated Escherichia coli to abiotic surfaces leads to altered composition of outer membrane proteins. J. Bacteriol. **183**:2445–2453.
90. **Weatherspoon-Griffin N, Zhao G, Kong W, Kong Y, Morigen, Andrews-Polymenis H, McClelland M, Shi Y.** 2011. The CpxR/CpxA two-component system up-regulates two Tat-dependent peptidoglycan amidases to confer bacterial resistance to antimicrobial peptide. J. Biol. Chem. **286**:5529–5539.
91. **Yamamoto K, Ishihama A.** 2005. Transcriptional response of Escherichia coli to external copper. Mol. Microbiol. **56**:215–227.
92. **Thede GL, Arthur DC, Edwards RA, Buelow DR, Wong JL, Raivio TL, Glover JN.** 2011. Structure of the periplasmic stress response protein CpxP. J. Bacteriol. **193**:2149–2157.
93. **Kwon E, Kim DY, Gross CA, Gross JD, Kim KK.** 2010. The crystal structure Escherichia coli Spy. Protein Sci. **19**:2252–2259.
94. **Appia-Ayme C, Hall A, Patrick E, Rajadurai S, Clarke TA, Rowley G.** 2012. ZraP is a periplasmic molecular chaperone and a repressor of the zinc-responsive two-component regulator ZraSR. Biochem. J. **442**:85–93.
95. **Chen SL, Hung CS, Xu J, Reigstad CS, Magrini V, Sabo A, Blasiar D, Bieri T, Meyer RR, Ozersky P, Armstrong JR, Fulton RS, Latreille JP, Spieth J, Hooton TM, Mardis ER, Hultgren SJ, Gordon JI.** 2006. Identification of genes subject to positive selection in uropathogenic strains of Escherichia coli: a comparative genomics approach. Proc. Natl. Acad. Sci. U. S. A. **103**:5977–5982.
96. **Welch RA, Burland V, Plunkett G, III, Redford P, Roesch P, Rasko D, Buckles EL, Liou SR, Boutin A, Hackett J, Stroud D, Mayhew GF, Rose DJ, Zhou S, Schwartz DC, Perna NT, Mobley HL, Donnenberg MS, Blattner FR.** 2002. Extensive mosaic structure revealed by the complete genome sequence of uropathogenic Escherichia coli. Proc. Natl. Acad. Sci. U. S. A. **99**:17020–17024.

APPENDIX C

URINARY TRACT INFECTIONS: CURRENT AND EMERGING MANAGEMENT STRATEGIES

Reprinted with permission from Clinical Infectious Diseases,
a journal published by Oxford University Press

Barber, A.E., Norton, J.P., Spivak, A.M., and Mulvey, M. A. Urinary tract infections: current and emerging management strategies.
Clin Infect Dis. DOI: 10.1093/cid/cit284 (2013).

INVITED ARTICLE CLINICAL PRACTICE

Ellie J. C. Goldstein, Section Editor

Urinary Tract Infections: Current and Emerging Management Strategies

Amelia E. Barber,[1] J. Paul Norton,[1] Adam M. Spivak,[2] and Matthew A. Mulvey[1]

[1]Department of Pathology, Division of Microbiology and Immunology and [2]Department of Medicine, Division of Infectious Diseases, University of Utah School of Medicine, Salt Lake City

Acute cystitis is one of the most commonly encountered bacterial infections and is responsible for substantial morbidity and high medical costs in the United States and across the globe. Though generally considered to be self-limiting and easily treated with antibiotics, urinary tract infections (UTIs) are often incompletely resolved by antibiotic therapy and frequently recur. This is in part due to the ability of uropathogenic bacteria to invade, replicate, and persist within host epithelial cells. The biological complexity of these infections combined with a dramatic rise in antibiotic-resistant pathogens highlight the need for alternative therapies. In this review we examine current management strategies for UTIs, as well as emerging treatments, including novel compounds that block bacterial interactions with the urothelium and vaccines focused on preventing both acute and recurrent infections.

Keywords. UPEC; antibiotic resistance; vaccine; cystitis; recurrent UTI.

A urinary tract infection (UTI) is defined as microbial infiltration of the otherwise sterile urinary tract and is one of the most common bacterial infections worldwide. UTIs encompass infections of the urethra (urethritis), bladder (cystitis), ureters (ureteritis), and kidney (pyelonephritis). There is an estimated annual occurrence of well over 8 million UTIs in the United States, many of which result in a visit to a physician [1]. Nearly all patients with UTI are prescribed a regimen of antibiotics, with roughly 1% of patients requiring hospitalization. The annual cost of UTI treatment in the United States is estimated at $2.14 billion [2], a value compounded by the frequency of recurrent infections. In this review we discuss the epidemiology of acute and recurrent UTIs, detail current management strategies, and explore emerging therapeutics.

Received 14 January 2013; accepted 13 April 2013.

Correspondence: Matthew A. Mulvey, PhD, University of Utah School of Medicine, 15 N Medical Dr E, #2100, Salt Lake City, UT 84112 (mulvey@path.utah.edu).

Clinical Infectious Diseases

DOI: 10.1093/cid/cit284

EPIDEMIOLOGY OF UTIs

UTIs are the most frequent bacterial infection seen in the outpatient setting: 1 in 3 women will develop a UTI requiring antibiotic treatment by age 24, and 50% experience at least 1 UTI during their lifetime [1]. The incidence of cystitis is significantly higher in women than men, likely the result of anatomic differences. Specifically, the shorter female urethra can facilitate bacterial transit from the urethral opening to the bladder. Colonization of the vaginal introitus by gastrointestinal pathogens can also increase the likelihood of urinary tract infiltration [3, 4]. Other factors, including urinary tract obstruction, incomplete voiding, and aberrant structural anatomy also predispose individuals to UTIs. Additional risk factors include prior history of UTIs, vaginal intercourse within the past 2 weeks, use of contraception with spermicide, low vaginal estrogen levels [1, 5], and individual genetic background (extensively reviewed in [6]). While a number of comorbidities increase susceptibility to UTI, the majority of UTIs occur in otherwise healthy women.

The most common bacterial cause of uncomplicated community-acquired UTI is uropathogenic *Escherichia coli* (UPEC), representing >80% of infections [1]. These

bacteria inhabit the lower intestinal tract of warm-blooded vertebrates where they lead a seemingly innocuous existence until they gain access to a niche, such as the urinary tract, where they can cause disease. Other pathogens commonly associated with uncomplicated UTI include *Staphylococcus saprophyticus*, *Klebsiella* species, *Proteus mirabilis*, and *Enterococcus faecalis* [7].

One of the more ominous issues on the horizon for bacterial infections, with UTIs being no exception, is the rise of antibiotic-resistant organisms. One especially troubling example is the heightened incidence of sequence type 131 (ST131) strains of UPEC around the world. These strains often exhibit high levels of resistance to multiple antibiotics and have undergone rapid intercontinental dispersal over the last decade [8]. ST131 strains are an increasingly common cause of community-acquired UTIs, spurring efforts to better identify and treat these resilient pathogens [8, 9]. Factors driving the global spread of ST131 strains are incompletely understood, but likely include the acquisition of antibiotic resistance genes, such as those encoding extended-spectrum β-lactamases (ESBLs), and the capacity to effectively utilize a broad range of metabolites [8, 10]. These characteristics may give ST131 strains a competitive advantage within host environments, increasing the likelihood of their dissemination within and between individuals.

RECURRENT UTIs AND INTRACELLULAR BACTERIAL RESERVOIRS

The burden of UTIs is compounded by their high rate of recurrence. Recurrent UTI (rUTI)—defined as 2 uncomplicated infections in a 6-month time period or 3 infections within a year—cause a tremendous amount of morbidity and are frustrating to patients and physicians alike [1]. Despite administration of antibiotics that seemingly clear the infection (determined by negative urine cultures), the probability that a patient will develop a second UTI within 6 months is 25%, with the chance of recurrence over a 12-month period increasing to 46%. The historical view of rUTI pathogenesis is that each recurrence represents an independent inoculation of the urinary tract. However, this model does not satisfactorily explain many (>50%, by some estimates) rUTI episodes in which the bacterial strains responsible for both the initial infection and the recurrence are genetically identical [11]. An alternative mechanism for recurrence involves the establishment of protected, intracellular bacterial reservoirs within the bladder mucosa (Figure 1).

UPEC can invade host epithelial cells, including the terminally differentiated superficial umbrella cells that line the lumen of the bladder, as well as the underlying, immature

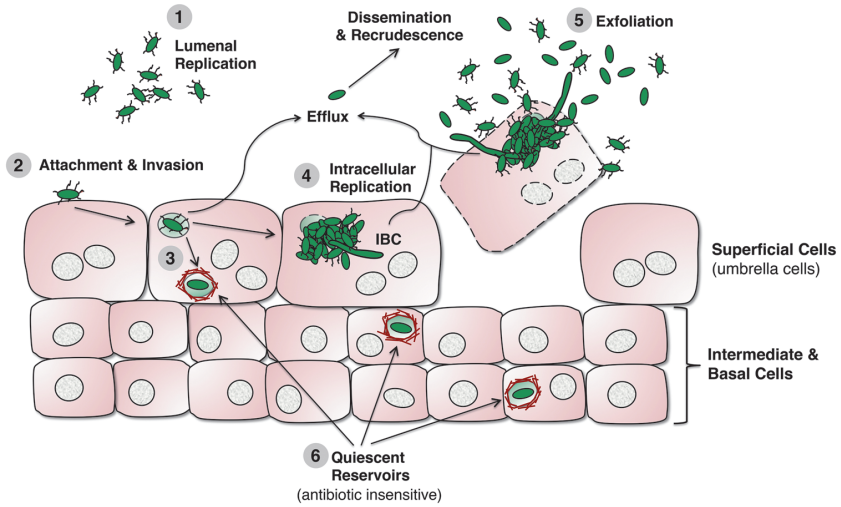

Figure 1. Events that promote the establishment and recurrence of urinary tract infection (UTI). (1) During a UTI, uropathogenic *Escherichia coli* (UPEC; green) can replicate within the lumen of the bladder or (2) attach to and invade bladder epithelial cells. (3) Following invasion, UPEC is either shuttled back out to the lumen or trafficked into late endosome-like compartments. (4) Disruption of these compartments and subsequent entry of UPEC into the host cytosol allows for rapid intracellular bacterial growth and the development of intracellular bacterial community. During these events, UPEC can acquire alternate morphologies, including the formation of long, filamentous cells that are resistant to host defenses such as neutrophils. (5) Infection can trigger the exfoliation of bladder cells, a process that aids in the elimination of adherent and internalized bacteria. The efflux of UPEC from host bladder cells, including those undergoing exfoliation, facilitates pathogen dissemination within and between hosts. (6) UPEC that remains bound within late endosome-like compartments in the urothelium can establish long-lived intracellular quiescent reservoirs that are often enmeshed within actin filaments (red) and extremely difficult to eradicate with antibiotic treatments. The resurgence of UPEC from these reservoirs can initiate recrudescent infections. Abbreviation: IBC, intracellular bacterial community.

intermediate and basal cells [12]. Within superficial bladder cells, UPEC can enter the host cytosol and rapidly multiply, forming a biofilm-like assembly known as an intracellular bacterial community (IBC) [12, 13]. The development of IBCs can enhance the ability of UPEC to establish itself within the urinary tract, building up large numbers of bacteria while sequestered away from the flow of urine and the influx of inflammatory cells and antibacterial molecules. IBCs, however, are not long-lived and will eventually disperse or be shed along with the infected host cells [14]. Indeed, the remnants of IBC-containing host cells can be detected in urine samples isolated from women seeking treatment for UTIs [3]. The efflux of UPEC from within IBCs, as well as the eventual exfoliation of the infected superficial cells, may potentiate the dissemination of UPEC both within the urinary tract and between hosts.

Rather than forming an IBC, UPEC can enter a dormant state within host epithelial cells after trafficking into membrane–bound compartments that become enmeshed within host actin filaments [12]. The quiescent nature and intracellular localization of these bacteria renders them resistant to most antibiotics and inaccessible to infiltrating neutrophils and other host defenses [13, 14]. Experimental models indicate that these quiescent intracellular UPEC reservoirs can persist for long periods in the absence of any overt clinical symptoms, even with the use of antibiotic treatments that effectively sterilize the urine [14]. Environmental signals, such as the reorganization of actin filaments that occurs as bladder cells undergo terminal differentiation, can trigger the resurgent growth of UPEC, prompting the development and dispersal of IBCs and the reinitiation of clinical symptoms. According to this model, rUTIs may in many instances be more accurately defined as recrudescent infections. These issues highlight the need for therapeutic strategies that effectively target both active and dormant stages of UTI.

CURRENT MANAGEMENT OF UTIs

Initial diagnosis of acute uncomplicated cystitis is typically based on patient medical history, taking into account past individual and family health issues, sexual activity, and current symptoms. Common indicators of acute cystitis include urinary urgency and frequency, pain when voiding (dysuria), lower abdominal discomfort, and cloudy or dark urine. The diagnosis of patients presenting with these classic symptoms may be confirmed by urinalysis showing the presence of red blood cells, high nitrite levels, and leukocyte esterase in the urine.

Although medical history and urinalysis are sufficient for the diagnosis of most uncomplicated UTIs, the gold standard for diagnosis of acute cystitis includes a bacteriological urine culture with identification of the causative agent and antimicrobial susceptibility testing. Using fresh, midstream urine, clinical confirmation of an uncomplicated UTI is classically defined as $\geq 10^5$ colony-forming units (CFU)/mL of urine. However, this definition has recently been modified based on observations that many uropathogens are capable of eliciting clinical pathology in the urinary tract even with low levels of bacteriuria [1]. Consequently, as little as 10^3 CFU/mL urine, in the presence of overt UTI symptoms, is now considered sufficient for diagnosis of acute cystitis [15]. Current recommended treatments for acute uncomplicated cystitis are described in Table 1 [1, 16].

Treatment of rUTI

For women who suffer from rUTI, low-dose antibiotic prophylaxis such as nitrofurantoin (100 mg per day), cephalexin (250 mg daily) or trimethoprim-sulfamethoxazole (40 mg/200 mg daily) can provide symptomatic relief and protection against subsequent infections [17]. For women whose UTIs are coincident with sexual activity, a single, postcoital prophylactic antibiotic can be effective in preventing infections [18]. Self-initiated antibiotics are also useful for women with frequent recurrent infections. After diagnosing themselves based on symptoms and/or a urine dipstick, they can initiate a 3-day regimen without needing to visit a physician [18].

The increasing prevalence of antibiotic-resistant uropathogens is likely to limit the effectiveness of our current antibiotic arsenal. For example, individuals who suffer from serious recurrent or chronic UTIs due to ESBL-producing ST131 strains may benefit greatly from carbapenems such as ertapenem [9], but these antibiotics are considered one of our last lines of defense and so should be used cautiously. The ongoing emergence of antibiotic-resistant strains, in conjunction with the high frequency of rUTIs, highlights the need for a better understanding of these infections and the development of new therapeutic strategies.

EMERGING THERAPIES

As noted above, many rUTIs are thought to arise from the ability of bacteria to attach to and invade the bladder mucosa, where they can form intracellular reservoirs protected from antibiotics and host defenses. As such, many emerging treatments for UTIs are aimed at blocking adhesion of bacteria to the urothelium and thereby preventing the establishment of troublesome reservoirs. Type 1 pili (or fimbriae), which are multiprotein filamentous adhesive structures encoded by virtually all UPEC isolates, are generally indispensible for colonization of the urinary tract [11]. The adhesin protein FimH, which is localized at the distal tip of each type 1 pilus, binds mannose residues on host glycoprotein receptors and allows UPEC to adhere to and invade host bladder cells [19]. Type 1 pili also promote biofilm formation and the development of IBCs [20]. Because type 1 pili are important colonization factors, the

Table 1. Common Treatment Options for Uncomplicated Cystitis

Antibiotic	Mechanism	Dosage	Notes
Nitrofurantoin monohydrate/macrocrystals	Inhibits protein, DNA, RNA, and cell wall synthesis	100 mg orally, twice daily for 5 d	Low resistance rates and risk of adverse side effects. Similar efficacy compared to a 3-d regimen of trimethoprim-sulfamethoxazole
Trimethoprim-sulfamethoxazole	Inhibits nucleic acid synthesis by folate synthesis inhibition	160 mg/800 mg (1 double-strength tablet), twice daily for 3 d	Only for use when local resistance rates do not exceed 20% and in patients who do not have sulfa drug allergies
Fosfomycin trometamol	Blocks cell wall synthesis by inactivating enolpyruvyl transferase	3 g in a single dose	Minimal resistance and risk of collateral damage. Inferior efficacy compared to other regimens
Pivmecillinam	Disrupts synthesis of cell wall by inhibiting formation of peptidoglycan cross-links	400 mg, once daily for 3–7 d	Low resistance rates and risk of adverse side effects. Not available in North America

The choice of antibiotics should be made after considering patient allergy and compliance history, local resistance rates, drug availability, and cost. Fluoroquinolones such as ciprofloxacin are highly effective and can be given if none of the recommended antimicrobials can be used. However, resistance rates to these drugs are on the rise and it is recommended that they be reserved for conditions other than acute cystitis. β-lactam antibiotics, such as amoxicillin, cefdinir, cefaclor, or cefpodoximine, in 3- to 7-day treatment regimens can be given when other recommended agents cannot be used. However, β-lactam antibiotics have inferior efficacy and a higher rate of resistance, particularly in ST131 strains. Ampicillin should not be used because it displays relatively poor efficacy in the treatment of urinary tract infections and resistance rates to ampicillin are typically high.

therapeutic potential of inhibiting the assembly or function of these adhesive organelles has received considerable attention.

Pilicides and Mannosides

The assembly of type 1 pili occurs through the chaperone-usher pathway, relying on the periplasmic chaperone FimC for the stabilization, folding, transport, and assembly of pilus subunits [21]. Small synthetic molecules known as pilicides, which are designed to target periplasmic chaperones and consequently interfere with pilus assembly, provide an attractive approach for blocking bacterial adhesion and subsequent reservoir formation. In vitro, pilicides effectively inhibit pilus biogenesis, reducing UPEC adherence to bladder epithelial cells as well as type 1 pili–dependent biofilm formation [22, 23]. The efficacy of pilicides in animal infection models has not been reported.

Researchers have also specifically targeted the FimH adhesin by use of soluble receptor analogues, or mannosides, that act as antiadhesives. These molecules bind FimH and prevent it from interacting with host receptors [24]. Recently, orally available mannoside derivatives have been developed that show great promise as therapeutics [25, 26]. In a murine UTI model, these agents work prophylactically, preventing bacterial invasion into bladder tissue [26]. They can also be used to treat established and catheter-associated infections, acting synergistically with standard antibiotic treatments to reduce UPEC titers within the urinary tract of infected mice [27].

Both mannosides and pilicides have exciting potential as future therapies for the treatment of uncomplicated cystitis and rUTI, and both types of reagents may help circumvent the rising tide of antibiotic-resistant organisms. However, one potential concern with the systemic administration of either mannosides or pilicides is potential adverse effects on commensal *E. coli* strains and other members of the intestinal microbiota, many of which also express type 1 pili [28]. Current thinking by many in the field is that use of pilicides and mannosides will likely be less disruptive than current antibiotic treatment protocols, but this supposition requires additional investigation.

Vaccinology

An alternate strategy for the prevention of recurrent and chronic UTIs is the development of systemic or mucosal vaccines. Over the past 20 years, several vaccination approaches have been explored, including the use of heat-killed whole bacteria, bacterial cell extracts, and purified UPEC-associated virulence factors as antigens. Vaccination of women using a vaginal suppository containing 10 heat-killed strains of uropathogenic bacteria showed much promise in recent years [29, 30]. This multivalent vaccine formulation, known as Solco Urovac, included 6 *E. coli* strains plus 1 strain each of *P. mirabilis*, *Morganella morganii*, *Klebsiella pneumoniae*, and *E. faecalis*. Urovac passed phase 2 clinical trials and was shown to reduce the incidence of UTI caused by *E. coli* in sexually active women

between 20 and 50 years of age with histories of rUTI [29]. Although some individual patients in the study showed increases in anti–*E. coli* antibody levels, no statistically significant differences between vaccinated and placebo control groups were detected, possibly accounting for the lack of any follow-up phase 3 trials.

Specific bacterial factors that have been targeted as vaccine candidates for UTI include the type 1 pilus–associated adhesin FimH and UPEC-associated iron acquisition systems. Like pilicides and mannosides, antibodies directed against FimH can interfere with the functionality of type 1 pili, disrupting the ability of UPEC to colonize the urinary tract. Vaccination with purified FimH coupled to its periplasmic chaperone FimC offered protection against UPEC when administered systemically in both murine and primate models of cystitis [31–33]. A similar vaccine containing a truncated version of FimH protected mice from experimentally induced cystitis when given by either intramuscular or intranasal (mucosal) inoculation, using CpG oligonucleotides as adjuvant [34].

Most bacteria require iron for survival, and while there is ample iron in the human body, it is sequestered and generally inaccessible to bacteria. Consequently, UPEC and many other pathogenic bacteria rely upon iron-chelating molecules and receptors that enable them to scavenge essential iron from the host [35]. Use of purified bacterial iron receptor proteins for vaccination against UPEC has had mixed results. Of 7 UPEC-associated iron receptors tested as vaccines in mice, 2 (IreA and LutA) provided significant protection against experimentally induced cystitis [36]. Vaccination with another iron receptor, Hma, protected against kidney infection, but not cystitis. For this analysis, the purified iron receptors were delivered intranasally after being conjugated to cholera toxin to increase antigenicity.

In total, these studies highlight both FimH and iron receptors as potentially valuable vaccine candidates that merit further investigation. However, as with mannosides and pilicides, the use of purified iron receptors, FimH, or other UPEC-associated factors as vaccines may have inadvertent effects on members of the endogenous microbiota that should be considered. In addition, the route of vaccine delivery and the types of adjuvants utilized need to be optimized for maximal efficacy in humans. While individuals prone to recurrent or chronic UTIs may benefit greatly from the development of anti-UPEC vaccines, the costs and risks of this strategy require further evaluation.

Despite these hurdles, initial success in the development of anti-UPEC vaccines has spurred the search for additional vaccine antigens. Candidate approaches, in which known virulence factors such as flagellin are targeted, continue to generate promising results [37], but less biased methods that are not necessarily reliant on our limited understanding of UTI pathogenesis may prove more fruitful. Along these lines, researchers have developed in silico approaches, known collectively as reverse vaccinology, to probe the increasingly large number of sequenced bacterial genomes for pathogen-specific, surface-localized antigens [38, 39]. These traits in a vaccine antigen should increase the efficacy of antibody responses while limiting cross-reactivity with nonpathogenic bacteria. This approach to vaccine design is encapsulated in a publicly available, Web-based system known as Vaxign (http://www.violinet.org/vaxign/). By screening for outer membrane proteins with amino acid sequences that are conserved among UPEC isolates, but absent from nonpathogenic *E. coli* strains as well as humans and mice, Vaxign identified 22 putative UPEC-specific vaccine targets [40]. Several of these are functionally undefined, and a few are known to be expressed by UPEC during UTI, but to date none have been shown to protect against cystitis. The refinement of reverse vaccinology, coupled with gene expression profiling, proteomic analyses, and emerging high-throughput genetic screens, promises to greatly enhance our ability to identify useful vaccine targets.

CONCLUSIONS

Although UTIs are often considered to be easily managed infections, they remain a huge burden for millions of individuals and our healthcare system. The increasing prevalence of antibiotic resistance among uropathogens presents a major challenge to the clinical management of UTIs. Recurrent infections, including those caused by antibiotic-sensitive pathogens, are exceptionally common and are likely attributable in part to the establishment of recalcitrant intracellular bacterial reservoirs within the bladder mucosa. Eradication of these clinically relevant reservoirs will require a better understanding of the underlying molecular mechanisms that allow for their persistence. The ongoing development of new antimicrobial approaches, such as the use of pilicides and mannosides in conjunction with antibiotics, will provide new treatment options, while the identification of new vaccine candidates and optimized vaccination protocols promises relief to individuals who suffer from recurrent or chronic UTI.

Notes

Financial support. This work was supported by the National Institutes of Health (NIH; grants AI095647, AI090369, and AI088086 to the Mulvey laboratory; NIH Microbial Pathogenesis Training Grant T32 AI055434 to A. E. B.; and NIH Genetics Training Grant T32 GM007464 to J. P. N.).

Potential conflicts of interest. All authors: No reported conflicts.

All authors have submitted the ICMJE Form for Disclosure of Potential Conflicts of Interest. Conflicts that the editors consider relevant to the content of the manuscript have been disclosed.

References

1. Dielubanza EJ, Schaeffer AJ. Urinary tract infections in women. Med Clin North Am **2011**; 95:27–41.
2. Brown P, Ki M, Foxman B. Acute pyelonephritis among adults: cost of illness and considerations for the economic evaluation of therapy. Pharmacoeconomics **2005**; 23:1123–42.
3. Rosen DA, Hooton TM, Stamm WE, Humphrey PA, Hultgren SJ. Detection of intracellular bacterial communities in human urinary tract infection. PLoS Med **2007**; 4:e329.
4. Weichhart T, Haidinger M, Horl WH, Saemann MD. Current concepts of molecular defence mechanisms operative during urinary tract infection. Eur J Clin Invest **2008**; 38(suppl 2):29–38.
5. Colgan R, Williams M, Johnson JR. Diagnosis and treatment of acute pyelonephritis in women. Am Fam Physician **2011**; 84:519–26.
6. Ragnarsdottir B, Lutay N, Gronberg-Hernandez J, Koves B, Svanborg C. Genetics of innate immunity and UTI susceptibility. Nat Rev Urol **2011**; 8:449–68.
7. Ronald A. The etiology of urinary tract infection: traditional and emerging pathogens. Am J Med **2002**; 113(suppl 1A):14S–9S.
8. Peirano G, Pitout JD. Molecular epidemiology of *Escherichia coli* producing CTX-M beta-lactamases: the worldwide emergence of clone ST131 O25:H4. Int J Antimicrob Agents **2010**; 35:316–21.
9. Pitout JD. Extraintestinal pathogenic *Escherichia coli*: an update on antimicrobial resistance, laboratory diagnosis and treatment. Expert Rev Anti Infect Ther **2012**; 10:1165–76.
10. Gibreel TM, Dodgson AR, Cheesbrough J, Bolton FJ, Fox AJ, Upton M. High metabolic potential may contribute to the success of ST131 uropathogenic *Escherichia coli*. J Clin Microbiol **2012**; 50:3202–7.
11. Bower JM, Eto DS, Mulvey MA. Covert operations of uropathogenic *Escherichia coli* within the urinary tract. Traffic **2005**; 6:18–31.
12. Eto DS, Sundsbak JL, Mulvey MA. Actin-gated intracellular growth and resurgence of uropathogenic *Escherichia coli*. Cell Microbiol **2006**; 8: 704–17.
13. Justice SS, Hung C, Theriot JA, et al. Differentiation and developmental pathways of uropathogenic *Escherichia coli* in urinary tract pathogenesis. Proc Natl Acad Sci U S A **2004**; 101:1333–8.
14. Blango MG, Mulvey MA. Persistence of uropathogenic *Escherichia coli* in the face of multiple antibiotics. Antimicrob Agents Chemother **2010**; 54:1855–63.
15. Schmiemann G, Kniehl E, Gebhardt K, Matejczyk MM, Hummers-Pradier E. The diagnosis of urinary tract infection: a systematic review. Dtsch Arztebl Int **2010**; 107:361–7.
16. Gupta K, Hooton TM, Naber KG, et al. International clinical practice guidelines for the treatment of acute uncomplicated cystitis and pyelonephritis in women: a 2010 update by the Infectious Diseases Society of America and the European Society for Microbiology and Infectious Diseases. Clin Infect Dis **2011**; 52:e103–20.
17. Foster RT Sr. Uncomplicated urinary tract infections in women. Obstet Gynecol Clin North Am **2008**; 35:235–48, viii.
18. Nickel JC. Practical management of recurrent urinary tract infections in premenopausal women. Rev Urol **2005**; 7:11–7.
19. Martinez JJ, Mulvey MA, Schilling JD, Pinkner JS, Hultgren SJ. Type 1 pilus-mediated bacterial invasion of bladder epithelial cells. EMBO J **2000**; 19:2803–12.
20. Wright KJ, Seed PC, Hultgren SJ. Development of intracellular bacterial communities of uropathogenic *Escherichia coli* depends on type 1 pili. Cell Microbiol **2007**; 9:2230–41.
21. Thanassi DG, Bliska JB, Christie PJ. Surface organelles assembled by secretion systems of gram-negative bacteria: diversity in structure and function. FEMS Microbiol Rev **2012**; 36:1046–82.
22. Pinkner JS, Remaut H, Buelens F, et al. Rationally designed small compounds inhibit pilus biogenesis in uropathogenic bacteria. Proc Natl Acad Sci U S A **2006**; 103:17897–902.
23. Chorell E, Pinkner JS, Bengtsson C, et al. Mapping pilicide anti-virulence effect in *Escherichia coli*, a comprehensive structure-activity study. Bioorg Med Chem **2012**; 20:3128–42.
24. Han Z, Pinkner JS, Ford B, et al. Structure-based drug design and optimization of mannoside bacterial FimH antagonists. J Med Chem **2010**; 53:4779–92.
25. Klein T, Abgottspon D, Wittwer M, et al. FimH antagonists for the oral treatment of urinary tract infections: from design and synthesis to in vitro and in vivo evaluation. J Med Chem **2010**; 53:8627–41.
26. Cusumano CK, Pinkner JS, Han Z, et al. Treatment and prevention of urinary tract infection with orally active FimH inhibitors. Sci Transl Med **2011**; 3:109ra15.
27. Guiton PS, Cusumano CK, Kline KA, et al. Combinatorial small-molecule therapy prevents uropathogenic *Escherichia coli* catheter-associated urinary tract infections in mice. Antimicrob Agents Chemother **2012**; 56:4738–45.
28. Buchanan K, Falkow S, Hull RA, Hull SI. Frequency among Enterobacteriaceae of the DNA sequences encoding type 1 pili. J Bacteriol **1985**; 162:799–803.
29. Hopkins WJ, Elkahwaji J, Beierle LM, Leverson GE, Uehling DT. Vaginal mucosal vaccine for recurrent urinary tract infections in women: results of a phase 2 clinical trial. J Urol **2007**; 177:1349–53; quiz 591.
30. Uehling DT, Hopkins WJ, Elkahwaji JE, Schmidt DM, Leverson GE. Phase 2 clinical trial of a vaginal mucosal vaccine for urinary tract infections. J Urol **2003**; 170:867–9.
31. Langermann S, Mollby R, Burlein JE, et al. Vaccination with FimH adhesin protects cynomolgus monkeys from colonization and infection by uropathogenic *Escherichia coli*. J Infect Dis **2000**; 181:774–8.
32. Langermann S, Palaszynski S, Barnhart M, et al. Prevention of mucosal *Escherichia coli* infection by FimH-adhesin-based systemic vaccination. Science **1997**; 276:607–11.
33. Thankavel K, Madison B, Ikeda T, et al. Localization of a domain in the FimH adhesin of *Escherichia coli* type 1 fimbriae capable of receptor recognition and use of a domain-specific antibody to confer protection against experimental urinary tract infection. J Clin Invest **1997**; 100: 1123–36.
34. Poggio TV, La Torre JL, Scodeller EA. Intranasal immunization with a recombinant truncated FimH adhesin adjuvanted with CpG oligodeoxynucleotides protects mice against uropathogenic *Escherichia coli* challenge. Can J Microbiol **2006**; 52:1093–102.
35. Wiles TJ, Kulesus RR, Mulvey MA. Origins and virulence mechanisms of uropathogenic *Escherichia coli*. Exp Mol Pathol **2008**; 85:11–9.
36. Alteri CJ, Hagan EC, Sivick KE, Smith SN, Mobley HL. Mucosal immunization with iron receptor antigens protects against urinary tract infection. PLoS Pathog **2009**; 5:e1000586.
37. Karam MR, Oloomi M, Mahdavi M, Habibi M, Bouzari S. Assessment of immune responses of the flagellin (FliC) fused to FimH adhesin of uropathogenic *Escherichia coli*. Mol Immunol **2012**; 54:32–9.
38. Sivick KE, Mobley HL. An "omics" approach to uropathogenic *Escherichia coli* vaccinology. Trends Microbiol **2009**; 17:431–2.
39. Moriel DG, Bertoldi I, Spagnuolo A, et al. Identification of protective and broadly conserved vaccine antigens from the genome of extraintestinal pathogenic *Escherichia coli*. Proc Natl Acad Sci U S A **2010**; 107: 9072–7.
40. He Y, Xiang Z, Mobley HL. Vaxign: the first Web-based vaccine design program for reverse vaccinology and applications for vaccine development. J Biomed Biotechnol **2010**; 2010:297505.